Published in final edited form as:

Chem Rev. 2017 February 08; 117(3): 2059–2107. doi:10.1021/acs.chemrev.6b00636.

Copper–Oxygen Complexes Revisited: Structures, Spectroscopy, and Reactivity

Courtney E. Elwell, **Nicole L. Gagnon**, **Benjamin D. Neisen**, **Debanjan Dhar**, **Andrew D. Spaeth**, **Gereon M. Yee**, and **William B. Tolman**

Department of Chemistry, Center for Metals in Biocatalysis, University of Minnesota, 207 Pleasant St. SE, Minneapolis, Minnesota 55455, United States

Abstract

A longstanding research goal has been to understand the nature and role of copper–oxygen intermediates within copper-containing enzymes and abiological catalysts. Synthetic chemistry has played a pivotal role in highlighting the viability of proposed intermediates and expanding the library of known copper–oxygen cores. In addition to the number of new complexes that have been synthesized since the previous reviews on this topic in this journal (Mirica, L. M.; Ottenwaelder, X.; Stack, T. D. P. *Chem. Rev.* **2004,** 104, 1013–1046 and Lewis, E. A.; Tolman, W. B. *Chem. Rev.* **2004,** 104, 1047–1076), the field has seen significant expansion in the (1) range of cores synthesized and characterized, (2) amount of mechanistic work performed, particularly in the area of organic substrate oxidation, and (3) use of computational methods for both the corroboration and prediction of proposed intermediates. The scope of this review has been limited to well-characterized examples of copper–oxygen species but seeks to provide a thorough picture of the spectroscopic characteristics and reactivity trends of the copper–oxygen cores discussed.

Graphical Abstract

ORCID

Debanjan Dhar: 0000-0002-3027-0226

Andrew D. Spaeth: 0000-0002-4265-6150

William B. Tolman: 0000-0002-2243-6409

NOTE ADDED IN PROOF

A useful review published in July, 2016, was mistakenly not included, see ref 407. Additional ideas about the nature of the active intermediate in PHM were provided in the following paper, which we had also neglected to cite, see ref 408.

Notes

The authors declare no competing financial interest.

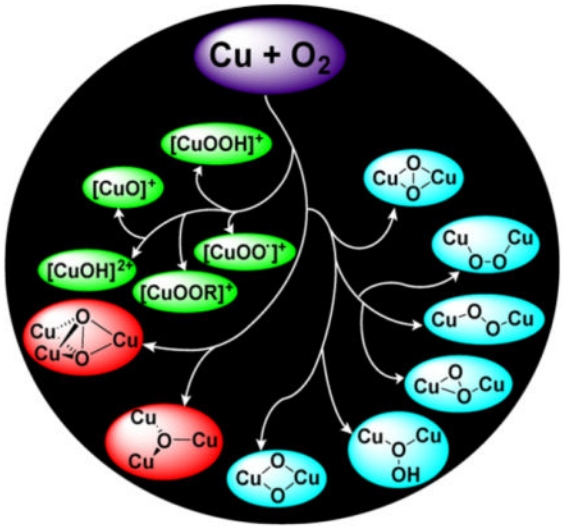

1. INTRODUCTION

Understanding how oxygenations and oxidations of organic molecules operate and developing new selective, green, and efficient methods to perform these transformations are central goals in chemical research.[1–4] Such reactions are critically important in myriad processes, including metabolism, synthesis of useful organic compounds, and energy-related conversions. Metal ions play a privileged role as oxygenation and oxidation reagents and catalysts, largely through their ability to activate O_2 and to generate structurally intriguing metal–oxygen species that can have the ability to attack even the strongest C–H bonds. Copper ions are particularly prevalent in enzymes,[5,6] heterogeneous catalysts,[7,8] and soluble reagents[9–11] that oxidize organic molecules, and they are also involved in four-electron processes that interconvert O_2 and H_2O.[12–14] A rich variety of mechanisms have been postulated for these systems, which may contain one or more copper ions that generate structurally diverse intermediates. Longstanding goals have been to comprehend these mechanisms, determine the geometries and electronic structures of the key intermediates, and unravel structure/function relationships for the catalytic centers, ultimately to enable the design of new and more selective and/or reactive oxidation catalysts.

A particularly valuable strategy for reaching these goals involves the synthesis, characterization, and detailed evaluation of the reactivity and mechanisms of reactions of discrete molecules that contain copper–oxygen moieties. In this review, we survey recent studies that use this strategy and that have provided unique and fundamental insights into possible structures, properties, and reactivities of copper–oxygen intermediates involved in oxygenation and oxidation reactions in both biological and abiological systems. As two previous comprehensive reviews on the subject were published in this journal in 2004,[15,16] we focus on work that has appeared since then, and through August 2016. The reader also is pointed to a number of more narrowly targeted but useful reviews or accounts on this subject that have appeared since 2004.[4,9,12,14,17–39]

In this section, we set the stage for discussion of the synthetic work by briefly surveying various proposals for copper–oxygen intermediates in biology and in abiological catalysts. The subsequent discussion is organized by the copper ion nuclearity of the synthetic compounds (sections 2–4). The supporting ligands and their abbreviations discussed in all the sections are provided in Charts 1, 2, 3, 4, and 5, organized according to the number and type of donors they contain.

1.1. Proposed Copper–Oxygen Intermediates in Biology

Much of the research on synthetic copper–oxygen compounds is inspired by postulates for active site intermediates and mechanisms in enzymes. A recent comprehensive review describes these enzymes and their copper-containing active sites in detail,[5] so here we only briefly summarize some of the proposed copper–oxygen motifs and key issues that have guided synthetic modeling work (Figure 1).

Monocopper species have been proposed as intermediates in hydroxylations catalyzed by dopamine and tyramine β-monooxygenases (DβM and TβM),[41–44] peptidylglycine α-hydroxylating monooxogyenase (PHM),[45,46] and the more recently characterized lytic polysaccharide monooxygenase (LPMO) (Figure 1a and b).[47–51] In DβM, TβM, and PHM, the copper coordination sphere includes two histidine imidazolyls and a methionine thioether, whereas in LPMO a histidine imidazolyl and a “histidine brace” comprising a histidine imidazolyl and the amine terminus of the peptide chain are bound to the active site metal ion. This same “histidine brace” has also been identified in particulate methane monooxygenase (pMMO).[52] For all of the monocopper systems, reaction of a Cu(I) form with O_2 is proposed to yield a copper(II)-superoxo adduct (X = $OO^{\bullet-}$).[53] Such an adduct has been characterized by X-ray crystallography in an oxygenated precatalytic PHM enzyme complex[54] and has been proposed to attack the C–H bond of substrate, primarily on the basis of kinetic data obtained for DβM and PHM.[41] The presumed product is a copper(II)-hydroperoxide (X = OOH; also written as $[CuOOH]^+$).[55,56] This latter species could also be formed from the superoxo complex by addition of a proton from the medium and an electron from a redox site. Alternatively, a copper(II)-hydroperoxide might also be capable of attacking the substrate, either directly or after O–O bond scission to yield a copper(II)-oxyl (X = $O^{\bullet}$; also written as $[CuO]^+$). Computational studies aimed at evaluating the feasibility of these intermediates and their ability to attack a substrate C–H bond have indicated that the $[CuO]^+$ unit, best described as having a triplet ground state with a Cu(II) ion weakly bonded to an O-centered radical,[17,57] is the least stable species and is the most potent oxidant.[58–61] These various ideas concerning the mechanism of substrate attack by the monocopper enzyme sites and the structures of the putative intermediates have inspired numerous attempts to synthesize complexes with the Cu–X (X = $OO^{\bullet-}$, OOH, $O^{\bullet}$) cores, and related species, and to understand their properties and reactivities (section 2).

In the coupled binuclear polyphenol oxidases (CB–PPOs, of which tyrosinase and catechol oxidase are the most studied), it is proposed that the substrate binds to the oxy form of the enzyme to generate the “peroxo” intermediate shown in Figure 1c. The μ-η^2:η^2-peroxo binding mode shown in this intermediate has been conclusively identified by X-ray crystallography in the oxy forms of the O_2 binding protein hemocyanin[62] and in tyrosinase[63]

and catechol oxidase,[64] as well as by spectroscopy in other enzymes.[65] Attack at the substrate by the (μ-η^2:η^2-peroxo)dicopper intermediate in tyrosinase is a mechanistic paradigm.[5,32,66,67] Yet, the elucidation of a facile equilibrium between (μ-η^2:η^2-peroxo)dicopper and bis(μ-oxo)dicopper cores in synthetic complexes[68,69] provides precedence for the postulate of a similar equilibrium in the CB-PPOs. Even though a bis(μ-oxo) species has not been observed in any enzyme, it may still be formed as a transient reactive intermediate, which raises a key question: which core is responsible for the electrophilic attack at the coordinated phenol substrate, in particular to result in hydroxylation of the aromatic ring? This and related questions have stimulated extensive research aimed at understanding the reactivities of complexes that contain the μ-η^2:η^2-peroxo and bis(μ-oxo) cores (section 3).

This research has also been driven by hypotheses about the involvement of the (μ-η^2:η^2-peroxo)- and bis(μ-oxo)dicopper cores in particulate methane monooxygenase (pMMO).[70–76] Other dicopper species have also been suggested (Figure 1d), in large part stimulated by the identification by X-ray crystallography and EXAFS of a dicopper site in the enzyme.[29,77–80] These species include triplet[75] or mixed-valent Cu(II)Cu(III)[72] variants of the bis(μ-oxo)dicopper core, a (μ-oxo)dicopper(II) unit akin to what has been proposed in Cu-doped zeolite catalysts (see section 1.2),[81–83] and dicopper units that incorporate a copper(II)-oxyl moiety.[77] Alternative hypotheses of mono-[84] and tricopper catalytic sites in pMMO have also been advanced, and proposals of additional tricopper reactive intermediates such as that shown in Figure 1d have been made.[85,86] In view of the tentative understanding of the nature of the pMMO active site and the mechanism(s) by which the strong C–H bond of methane is attacked, along with the significance of the reaction it catalyzes, much effort continues to be expended to develop models of the various proposed pMMO di- and tricopper active site intermediates and to evaluate their reactivity (sections 3 and 4).

Tricopper intermediates are involved in the complete 4-electron reduction of O_2 to H_2O catalyzed by the large and biologically important class of multicopper oxidases, which include laccase, ascorbate oxidase, ceruloplasmin, bilirubin oxidase, cuprous oxidase, and others.[5,40] Extensive spectroscopic and computational studies of these enzymes have led to the postulate of two key “peroxo” and “native” intermediates along the 4-electron dioxygen reduction pathway (Figure 1e).[5,40] The importance of the oxygen reduction reaction (ORR) (cf. for fuel cell applications)[87] and the novel structures proposed for the various enzyme intermediates have inspired efforts to construct multicopper model complexes, as described in section 4.

The ORR is also catalyzed by cytochrome *c* oxidase (C*c*O, a member of a broader class of heme copper oxidases), which is the terminal mitochondrial component of the respiratory chain that uses the energy supplied by the ORR to pump protons across the cellular membrane and fuel adenosine triphosphate (ATP) synthesis.[5,88,89] The binding and reduction of O_2 to H_2O by C*c*O, with avoidance of H_2O_2 production, occurs at a heterobimetallic active site comprising a heme adjacent to a copper center bound to three histidyl imidazoles, one of which is linked via a post-translational modification to a tyrosine residue. Key proposed intermediates include a peroxo species potentially coordinated to both iron and copper, as well as “P_M”, in which the O–O bond is broken and the Fe, Cu, and

tyrosine moieties are oxidized (Figure 1f). Approaches toward understanding the detailed mechanism of the ORR by C*c*O and how partial reduction to yield H_2O_2 are avoided include targeting reactive heme-copper oxygen species for synthesis and characterization as well as using electrochemical methods to evaluate catalysis in model complexes. The results of such approaches have been reviewed extensively elsewhere, so will not be described herein.[12,21,24,90–95]

In addition to the multitude of fascinating copper–oxygen motifs proposed as intermediates in enzymes, copper–oxygen species have also been hypothesized to be involved in the generation of "reactive oxygen species" (ROS) by copper complexes targeted as metallodrugs and nucleases.[96,97] In most cases, copper–oxygen intermediates have not been identified as distinct intermediates in ROS generation, but data in support of the "intermediacy of a ROS that is intimately bound to the copper center"[98] has been presented for copper bound to the amino terminal Cu(II)- and Ni(II)-binding (ATCUN) peptide motif.[99–101] The nature of such "intimately bound" ROS/copper species is not known. Copper-promoted generation of ROS has also been implicated in many neurodegenerative diseases,[102–105] but we are unaware of experimental evidence for specific copper–oxygen intermediates in these processes. Nonetheless, information gleaned from studies of synthetic copper–oxygen complexes may inform understanding of ROS generation mechanisms by a variety of copper species in a biological context.

1.2. Proposed Copper–Oxygen Intermediates in Abiological Catalysis

Copper–oxygen intermediates akin to those postulated for enzymes may also be involved in oxidations of organic substrates by synthetic catalysts.[9,10] In most cases, however, evidence for such intermediates in oxidations is sparse or nonexistent, or pathways involving aerial oxidation of Cu(I) to Cu(II) species are invoked that do not specify the nature of any copper–oxygen species involved.[106,107] We note here just a few key examples where experimental support for copper–oxygen intermediates during an oxidation reaction has been provided and/or particularly provocative hypotheses for copper–oxygen intermediates are proposed on the basis of theory.

Particular attention has been focused on the mechanism of the selective oxidation of methane to methanol by copper sites in zeolites.[81,82,108–110] An early proposal[111] invoking a bis(μ-oxo)dicopper species as being responsible for attacking the strong C–H bond of methane has been supplanted on the basis of extensive spectroscopic data by the hypothesis of a dicopper(II) species with a single oxo bridge[82,112–114] that is derived from a μ-η^2:η^2-peroxo precursor.[115] DFT calculations support the notion that the (μ-oxo)dicopper species abstracts a hydrogen atom from substrate.[112] A driving force is the formation of a strong O–H bond (calculated to be 90 kcal/mol) to yield the $[Cu_2(\mu\text{-OH})]^{2+}$ product, although the reaction step was found to be endothermic by 13.8 kcal/mol. It was further proposed that approach of methane to the oxo-bridged dicopper(II) moiety along the reaction coordinate is accompanied by changes in low-lying singly occupied molecular orbitals, essentially inducing formation of a novel mixed valent oxyl radical species with significant p orbital character on the bridging O atom oriented to facilitate hydrogen atom abstraction from the substrate (Figure 2a). The role of water in methane oxidation by Cu in zeolites has been

evaluated by experiment and theory,[114,116,117] and suggested to play multiple roles, including to change the nature of the active site structure. More recent theoretical work led to the proposal of a pathway invoking peroxo and terminal hydroxo and oxyl intermediates (Figure 2b).[83] An alternative $[Cu_3(\mu\text{-}O)_3]^{2+}$ core has been proposed in mordenite (Figure 2c).[118] While formally a mixed valent species $(Cu(III)_2Cu(II))$, the cluster was described as having all Cu(II) ions with radical character on the O atoms on the basis of DFT calculations. In contrast, a monocopper $[CuOH]^+$ species has been suggested to be the oxidant in so-called 8-membered ring zeolites.[119] Clearly, the mechanism(s) of O_2 activation and methane hydroxylation are controversial, providing much impetus for investigation of putative dicopper species through synthetic modeling approaches.

Another illustrative example of a copper-catalyzed oxidation reaction for which intriguing intermediates are proposed is the hydroxylation of benzoate derivatives (Figure 3).[120,121] DFT calculations employed to analyze this process suggested that homolytic scission of the N–O bond in a copper(II) complex of trimethylamine-*N*-oxide (TMAO) yielded a copper(II)-oxyl intermediate.[121] A concerted pathway for hydroxylation of the aromatic ring by this intermediate was found to be favored relative to a stepwise hydrogen atom abstraction/rebound process. Copper(II)-oxyl species have also been proposed in other catalytic reactions. For example, on the basis of DFT calculations such a unit has been suggested to be the active oxidant in the oxidation of alkanes by H_2O_2 catalyzed by tris(pyrazolyl)hydroborate-based copper complexes.[122] These and other examples of copper-catalyzed oxidations for which copper–oxygen species are postulated serve as yet more impetus for studies aimed at understanding the properties of copper–oxygen complexes.

2. MONOCOPPER COMPOUNDS

In this section, we focus on work reported since 2004 on preparing, characterizing, and understanding the reactivity of mononuclear copper–oxygen complexes. The discussion is divided into three parts: 1:1 $Cu:O_2$ complexes, copper(II) alkyl/hydroperoxide complexes, and high valent $[CuO]^+/[CuOH]^{2+}$ species.

2.1. 1:1 $Cu:O_2$ Complexes

Complexes comprising a copper ion bound to an O_2^{n-} unit ($n = 1$ or 2) model the initial adduct formed upon reaction of Cu(I) biosites with O_2 (Figure 4). Such complexes have been prepared by exposure of solutions of Cu(I) complexes to dioxygen or by reaction of a superoxide salt with a Cu(II) precursor, with both types of procedures typically performed at low temperatures in organic solvent. The complexes vary with respect to the way in which the O_2^{n-} unit binds (end-on, η^1, versus side-on, η^2) and the degree of electron transfer from the copper ion to the O_2 moiety, with (superoxo)copper(II) and (peroxo)copper(III) representing the two extreme formulations. In many cases, the 1:1 $Cu:O_2$ complexes are observed only as transient intermediates that convert to or interconvert rapidly with dicopper species (section 3). Key research goals have been to elucidate how supporting ligands influence the structural attributes of the 1:1 $Cu:O_2$ adducts and to understand structure/reactivity correlations (See Note Added in Proof).[123,124]

2.1.1. Structures and Properties—Prior to 2004, only three examples of isolable 1:1 Cu:O_2 complexes had been described, with two having been characterized by X-ray crystallography (**1a** and **3b**, Figure 5). Compounds **1**, **3**, and **4** exhibit side-on (η^2) binding of the O_2^{n-} fragment. Subsequently, the first X-ray crystal structure of an end-on (η^1) (superoxo)copper(II) complex was reported (**2**),[125,126] and a number of other 1:1 Cu:O_2 complexes have been described.[54,61,123,126–143] The properties of the 1:1 Cu:O_2 adducts that have been isolated to date are summarized in Tables 1 and 2 (with several reported earlier than 2004 included for purposes of comparison and discussion).[144–151]

With few exceptions, the adducts share an intense UV–vis feature ~400 nm (ε ~10^3 $M^{-1}cm^{-1}$), the irradiation into which results in enhancement of ν(O–O) and ν(Cu–O) in Raman spectra. Thus, it is assigned as an $O_2^{n-} \rightarrow$ Cu ligand to metal charge transfer (LMCT) transition. The ν(O–O) and ν(Cu– O) fall in the range of 950–1200 cm^{-1} and 430–560 cm^{-1}, respectively. In general, the complexes assigned as having endon (η^1) coordination exhibit ν(O–O) > ~1100 cm^{-1} commonly associated with superoxide, which also holds for the side-on (η^2) complexes supported by the **L39** ligands (R = *t*Bu or Ad). The low values <1000 cm^{-1} for the other η^2 complexes implicate a significantly reduced O–O bond order, but these values are higher than typically observed for metal-peroxides (~800–850 cm^{-1}).[123] The available measured (X-ray crystallography) and calculated O–O bond distances (Table 2) are consistent with the ν(O–O) differences (higher ν(O–O) = shorter O–O distance).

These and other findings suggest that the degree of electron transfer upon binding of O_2 varies, which can be understood within the context of two extreme resonance structure formulations, Cu(II)-$O_2^{-\bullet}$ versus Cu(III)-O_2^{2-}. Evaluation of the electronic structures of several of the adducts (particularly the structurally defined complexes **1**–**4**) has incorporated results from application of Badger's rule (ν(O–O)/O–O distance relationship), spectroscopy, the oxygen equilibrium isotope effect for O_2 binding, and theory.[123,138,152,153] From these studies, a bonding picture has evolved of a continuum between the extreme resonance structures with the position on the continuum being determined by the electron-donating power and denticity of the supporting ligands. For example, Badger's rule plots of O–O distance versus $1/\nu^{2/3}$ showed good correlations for experimental and calculated data for compounds with a variety of metals and O_2^{n-} binding modes, with the only exceptions being a few cases where librational motion led to underestimation of the O–O bond distance determined by X-ray crystallography (including for **1**).[123,154] The spread of data across O–O between ~1.28–1.39 Å is consistent with O_2^{n-} assignments having both integer and noninteger values of *n* between ~1–2 (i.e., continuum of values).

Complex **2** represents a paradigm for compounds formulated as η^1-Cu(II)-$O_2^{-\bullet}$ species. NMR[132] and variable-temperature variable-field MCD data[133] indicated that **2** has a triplet (S = 1) ground state, as determined similarly for the η^1-Cu(II)-$O_2^{-\bullet}$ species supported by the tren ligand **L42b**.[135] The data for **2** were analyzed and interpreted using DFT calculations, leading to a description involving two singly occupied orthogonal orbitals, one nonbonding orbital localized on the O_2^{n-} moiety (π^*_v) and the other an antibonding orbital with similar Cu and O character (d_{z^2}, Figure 6).[133] In accordance with TD-DFT calculations, the LMCT band corresponds to the transition from the highest occupied π^*_σ to the d_{z^2} orbital. More accurate quantum chemical calculations using completely renormalized coupled-cluster

theory or multiconfigurational methods led to further understanding of the biradical and multideterminental nature of the η^1-Cu(II)-$O_2^{-\bullet}$ moiety and a somewhat different orbital description.[143] An ^{18}O equilibrium isotope effect of 1.0148 was measured and noted to be larger than those reported for other η^1-O_2^{n-} adducts in hemes and cobalt compounds (1.0041–1.0066).[155,156] The results were interpreted to be consistent with weak covalency in the Cu(II)-$O_2^{-\bullet}$ interaction and increased ionic character in the valence bond description.[132]

Intriguing perturbations to the properties of **2**, as well as its reactivity (section 2.1.2), were found upon reaction with CF_3CO_2H.[134] The formation of a 1:1 adduct **2**·CF_3CO_2H was reflected by a 62 nm (3655 cm^{-1}) blue shift of the LMCT transition that was reversed by addition of base. The adduct exhibits a ν(O–O) ~30 cm^{-1} higher than **2**, which was unchanged when CF_3CO_2D was used. NMR and XAS data indicated similar triplet ground states and coordination geometries in **2** and **2**·CF_3CO_2H. Together, the experimental data and accompanying DFT calculations supported the structure for the adduct shown in Figure 7. To rationalize the finding from DFT calculations that H-bonding to the distal oxygen in this model lengthens the O–O bond and lowers ν(O–O) (opposite of experiment), it was proposed that the observed properties of the adduct arose from "the electrostatic interaction with the dipole of CF_3CO_2H and not a change in orbital covalency imparted by the hydrogen bond."[134]

The influences of hydrogen bonding on the properties of the η^1-Cu(II)-$O_2^{-\bullet}$ unit have also been explored in complexes comprising the tris(pyridylmethyl)amine (**L41a**) ligand frame. While an earlier reported X-ray structure[157] purporting to identify intramolecular hydrogen bonding to the $[CuO_2]^+$ unit in a complex of **L41l** was found to be in error,[158] complex **5** (Figure 7) was conclusively identified on the basis of UV–vis and resonance Raman spectroscopy.[130] Values of 1130 and 482 cm^{-1} for ν(O–O) and ν(Cu–O), respectively, that are greater than observed in other complexes of **L41a** derivatives were interpreted using DFT calculations to indicate hydrogen bonding to both the proximal and distal oxygen atoms of the bound superoxide ligand. Importantly, these interactions stabilize the complex sufficiently to enable spectroscopic characterization and reactivity studies (section 2.1.2).

Another η^1-Cu(II)-$O_2^{-\bullet}$ species with atypical properties is [K(18-crown-6)][(**L28a**)CuO_2] (**6**).[128] While exhibiting a ν(O–O) of 1104 cm^{-1} consistent with other η^1 superoxides, the LMCT absorption feature (assigned by TD-DFT calculations) was at 627 nm, a significantly longer wavelength than all other examples (Table 1). It is likely that the anionic nature of the complex that is reflected in nucleophilic, rather than the typical electrophilic, reactivity of the superoxide moiety (section 2.1.2) underlies the low energy of its LMCT band.

Low ν(O–O) values of 964 and 1033 cm^{-1} were observed for [Cu^{II}(**L75**)($O_2^{-\bullet}$) (NEt_3)][146] and the adduct supported by **L33**,[131] respectively, both of which were postulated to feature η^1 binding of their superoxide ligands. Reasons for these disparities from the norm are unclear, although the similarity of ν(O–O) of [Cu^{II}(**L75**)($O_2^{-\bullet}$) (NEt_3)] to those associated with some η^2 complexes could indicate that its assignment as an η^1 complex may be incorrect.

Turning next to the smaller set of complexes that exhibit η^2-coordination of the O_2^{n-} unit, it is here that ligand structural differences have been shown to most significantly influence the degree of charge transfer from the copper ion to the bound O_2^{n-} unit. These effects have been most clearly defined in comparisons between **1** versus **3** and **4**.[123,138,151] All three have singlet ground states, but clear differences in their ν(O–O) values (Table 1) and Cu K- and L-edge XAS data support a Cu(II)-$O_2^{-\bullet}$ formulation for **1** but significant Cu(III)-O_2^{2-} character for **3** and **4** along with a high degree of covalency in the metal–ligand bonding.[138] These data and accompanying theoretical calculations show that the more strongly electron-donating **L2** and **L3** ligands in **3** and **4** play a key role in stabilizing the higher metal oxidation state. Indeed, decreasing the electron donation of **L2d** by replacement of the backbone methyl groups with CF_3 units (**L2g**) prevents formation of a 1:1 Cu:O_2 adduct.[139] Other theoretical studies have examined in detail the continuum on which **1**, **3**, and **4** reside and confirm that the more strongly electron-donating ligands stabilize the singlet with Cu(III)-O_2^{2-} character.[143,153]

A unique example of a complex proposed to contain η^2-Cu(II)-$O_2^{-\bullet}$ with a triplet ground state was recently reported using the supporting ligand **L71**.[159] The assignment was based on UV–vis spectroscopy, the observation of paramagnetically broadened resonances in NMR spectra, and DFT calculations. In the absence of more definitive structural data from additional experiments (i.e., resonance Raman, X-ray crystallography, and EXAFS), however, the formulation of this complex must be regarded as tentative.

2.1.2. Reactivity—We focus on two aspects of reactivity: the process by which 1:1 Cu:O_2 adducts form and their subsequent reactions. The kinetics and thermodynamics of the oxygenation of Cu(I) complexes supported by N-donor ligands described extensively in the previous review have been augmented by more recent work[132,144,160–164] (Tables 3 and 4, which include previously published data for the systems supported by **L41a** and **L42a**).

Intriguing variations in kinetic and thermodynamic parameters for oxygenation reactions point to differences in reaction mechanisms for formation of 1:1 Cu:O_2 adducts. In a detailed comparison using a “flash and trap” method (irradiation of Cu(I)-CO complexes in the presence of O_2) of the systems supported by **L40a**, **L41a**, and **L43c** that feature identical bis(pyridylmethyl)amine units linked to variable fourth donors, positive $\Delta S^{\ddagger}_{on}$ values for **L40a** and **L43c** contrasted with a negative $\Delta S^{\ddagger}_{on}$ value for **L41a** (all in the same solvent, THF).[161] These data were interpreted to indicate divergent dissociative interchange or associative mechanisms, respectively, but with the difference not being due to the order of solvent or O_2 binding or loss. Instead, it was hypothesized that O_2 binding occurs initially in both cases but with differences in whether electron transfer from Cu(I) to O_2 (to yield Cu(II)-$O_2^{-\bullet}$ species) occurs before or after solvent dissociation. An interesting parallel was drawn between this notion and the postulated formation of a pre-equilibrium 1:1 Cu:O_2 adduct prior to O_2 release upon reaction of $O_2^{-\bullet}$ with Cu(II) complexes of **L41a** and **L45** examined by stopped-flow kinetics and competitive ^{18}O isotope effects.[165]

The kinetics and thermodynamics of O_2 binding to the Cu(I) complexes of **L41a**, **L41d**, and **L44** were compared using a direct photolysis method (photoejection of O_2 from 1:1 Cu:O_2 adducts followed by monitoring of rebinding).[160] The **L41d** and **L44** systems exhibited

similar $\Delta H^{\ddagger}_{on}$ values, but the $\Delta S^{\ddagger}_{on}$ value for the former is more negative. These findings were interpreted to indicate that the $O_{carbonyl}$ interaction is weak in the Cu(I) complex of **L41d**, with a more ordered transition state for this system due to simultaneous $O_{carbonyl}$ and O_2 coordination. A large negative $\Delta S^{\ddagger}_{on}$ value was also measured for the system supported by **L36**, which was suggested to indicate an associative mechanism involving a highly ordered/restricted transition state.[162]

The mechanism by which O_2 reacts with Cu(I) complexes supported by β-diketiminate derivatives (**L2d** and **L2e**) was elucidated through a combination of theory and low temperature stopped flow kinetics experiments.[151] A dual pathway mechanism was proposed for the reaction that yields complex **3a** (Figure 8) on the basis of the results of low-temperature stopped-flow kinetics experiments (in THF solvent) and DFT calculations. The observation of a two-term rate law (eq 1) was interpreted to indicate operation of both pathways A and B, wherein A involves direct rate-determining reaction of O_2 with the Cu(I) complex and B is a dissociative route, involving rate-determining solvolysis prior to rapid reaction with O_2. Pathway B is rendered effectively inoperative in the presence of excess nitrile, and the presence of bound nitrile in pathway A was confirmed by observation of decreases in rate as a function of *para*-substituent when *para*-X-benzonitriles (X = CH_3O, CH_3, H, F, Cl, and CN) were used (Hammett $\rho = -0.34$). Both routes operate in the absence of added nitrile, as indicated from plots of k_{obs} versus $[O_2]$ that were linear but with nonzero intercepts ($k_{obs} = k_A[O_2] + k_B$). DFT calculations corroborated this dual pathway model and provided details of the reaction trajectories and structures of transition states and intermediates.

$$\text{rate} = k_A[(\mathbf{L2})\text{Cu}(\text{CH}_3\text{CN})][\text{O}_2] + k_B[(\mathbf{L2})\text{Cu}(\text{CH}_3\text{CN})] \quad (1)$$

Finally, with respect to the overall thermodynamics of O_2 binding (Table 4), the order of binding strength is tris(2-(dimethylamino)ethyl)amine (**L42a**) > tris(2-pyridylmethyl)-amine derivatives (**L40a** ~ **L41a** ~ **L43c**) > tris-((tetramethylguanidino)(2-aminoethyl))amine (**L44**) > 1-isopropyl-5-(2-(2-pyridyl)ethyl)-1,5-diazacyclooctane (**L36**). The experimental $\Delta H°$ and $\Delta S°$ values were negative for all complexes, with the exception of $\Delta S°$ for the complex supported by **L36**, as expected for a spontaneous O_2 binding reaction where $K_{eq} > 1$ for all complexes.

Commonly, 1:1 Cu:O_2 adducts can react with an additional equivalent of Cu(I) to generate a 2:1 Cu:O_2 species (section 3). Indeed, prevention of this process has been key for the isolation and full characterization of 1:1 Cu:O_2 adducts such as **1**–**4**, with ligand steric encumbrance being a critical controlling factor. For example, the isolation of **3** and **4** stands in contrast to the formation of bis(μ-oxo)dicopper complexes when Cu(I) complexes of less hindered **L2** ligands were used, with both *ortho*-aryl substituents and backbone groups being impactful (cf. **L2f**, **L74**).[149,166] The tendency to react with an additional Cu(I) species was used purposefully to help characterize the 1:1 Cu:O_2 adduct **6** (Figure 9).[128] Treatment of **6**, prepared by reaction of a Cu(II) precursor with KO_2, with [(**L41a**)Cu(I)]OTf cleanly yielded

the (*trans*-1,2-peroxo)dicopper complex **7**, which was readily identified by its diagnostic UV–vis and resonance Raman features (section 3.2).

A hemilabile thioether ligand group enabled controlled isolation of a 1:1 Cu:O_2 adduct and subsequent conversion to a bis(μ-oxo)dicopper complex.[141] Oxygenation of the Cu(I) complex of **L74** (X = Me, Ph) yielded a side-on η^2 adduct (**8**), the properties of which were consistent with minimal interaction with the thioether group and significant Cu(III)-O_2^{2-} character, just like **3** and **4** (Figure 10). Unlike **3** and **4**, however, the binding of O_2 was reversible, and upon vigorous purging with Ar, a bis(μ-oxo)dicopper complex (**9**) formed. It was concluded on the basis of the observations, as well as DFT calculations, that the O_2 binding equilibrium involves slow dissociation of O_2 (k_{off}) and a large equilibrium constant (K_{eq}).[141] The trapping of η^2 metal-peroxo complexes was also used to prepare heterobimetallic bis(μ-oxo) complexes comprising CuNi and CuPd pairs,[167] and an analogous bis(μ-oxo) complex with a CuGe pair was prepared by oxygenation of a Cu(I)–Ge(II) complex (section 3.1.4).[168]

In general, the η^2 complexes with Cu(III)-O_2^{2-} character epitomized by complexes **3** and **4** are poor oxidants and do not react with H atom donors like phenols or O atom acceptors like PPh_3 (which simply displaces O_2 from **3a** to yield a Cu(I)-PPh_3 complex). Computational studies show that the poor oxidizing ability of these complexes may be traced to the strong electrondonating character of their supporting ligands that render reduction and protonation difficult.[123,169] Still, reaction of **3a** with [Cu(CH_3CN)$_4$]OTf in the presence of 3,5-diphenylpyrazole (pz) resulted in an unusual hydroxylation/oxidation of a ligand aryl ring (Figure 11).[170] The product was formulated on the basis of X-ray crystallography as a Cu(II)-semiquinone complex, arising from attack of some copper–oxygen intermediate (unidentified) at a ligand aryl ring and an NIH shift of one of the isopropyl groups.[171] The hydroxylation resembles one reported previously upon oxygenation of a fluorinated β-diketiminate Cu(I) complex, for which the nature of copper–oxygen intermediates was not determined.[172]

In view of the proposals that a Cu(II)-$O_2^{-\bullet}$ species is responsible for attacking a substrate C–H bond in the enzymes PHM, DβM,[58] and LPMO,[47] relevant reactivity of complexes with this unit have come under scrutiny. The putative η^2-Cu(II)-$O_2^{-\bullet}$ complex supported by **L71** converts 9,10-dihydroanthracene to anthracene, ultimately yielding a bis(μ-hydroxo)-dicopper(II) product via the presumed intermediacy of a [CuOOH]$^+$ complex.[159] Several η^1-Cu(II)-$O_2^{-\bullet}$ complexes exhibited promising reactions with C– H bonds.[130,131,137,162,173] Although unreactive with typical substrates with weak C–H bonds like 9,10-dihydroanthracene, xanthene, or 10-methyl-9,10-dihydroacridine, the η^1-Cu(II)-$O_2^{-\bullet}$ complex **5** (Figure 7) was shown to oxidize BNAH (1-benzyl-1,4-dihydronicotinamide) or BzImH (1,3-dimethyl-2,3-dihydrobenzimidazole) at −125 °C in MeTHF, yielding BNA^+ or BzIm as well as a (1,2-*trans*-peroxo)dicopper complex (Figure 12).[130] In addition, kinetic data revealed a significant KIE (12.1) when BNAD was used, with the overall reaction occurring twice as fast with BNAH than with BzImH. These data were interpreted to indicate that the reactions involve initial HAT (homolytic C–H bond cleavage) given that BNAH is a better hydrogen atom donor than BzImH.[130]

The η^1-Cu(II)-$O_2^{-\bullet}$ complex **10** supported by **L33c** decomposes to yield a Cu(II)-alkoxide resulting from intramolecular hydroxylation of a benzylic C–H bond (Figure 13).[131,162] The reaction followed first-order kinetics with a KIE of 4.1 at −65 °C, activation parameters consistent with an intramolecular process ($\Delta H^{\ddagger}$ = 4.54 ± 0.02 kcal mol^{-1}, $\Delta S^{\ddagger}$ = −53 ± 0.1 cal K^{-1} mol^{-1}), and a Hammett ρ of −0.63 were interpreted to support HAT. On the basis of results from DFT calculations, a pathway involving HAT to yield a $[CuOOH]^+$ intermediate that then "rebounds" its proximal O atom via transition state **11** was favored relative to an alternative distal oxygen transfer.[162] In further studies of the reactivity of **10**,[174] monitoring its decay in the presence of 1-electron reductants enabled estimation of its oxidation potential to be 0.19 ± 0.07 V versus SCE (acetone, 25 °C). In addition, HAT from TEMPOH was observed, but reactions with phenols yielded Cu(II)-phenolate complexes via proton transfer. With *para*-substituted triaryl phosphines [$P(Ar^Y)_3$; Y = OCH_3, H, F, Cl], O atom transfer was observed with a large Hammett ρ of −4.3 indicative of attack by a strong electrophile (either the superoxide in **10** or a derived $[CuO]^+$ species, for which no evidence was available).[174]

In a comparison of the reactivity of the η^1-Cu(II)-$O_2^{-\bullet}$ complexes supported by **L41b** and the mixed N/thioether S donor ligand **L68**, respectively, reaction of the latter at −135 °C in 4:1 MeTHF:CF_3CH_2OH with *N*-methyl-9,10-dihydroacridine or 2,6-di-*tert*-butyl-4-methoxyphenol yielded 10-methyl-9-acridone or 2,6-di-*tert*-butyl-1,4-benzoquinone, respectively. These products were not observed with the complex supported by **L41b**.[137] It was concluded that the thioether ligation in the complex of **L68**, which models that found in the enzymes PHM and DβM, enhances the oxidizing power of the coordinated superoxide ligand, supporting a similar role for the methionine ligand in the biological systems.

Augmenting the examples noted above of η^1-Cu(II)-$O_2^{-\bullet}$ complexes performing HAT from weak O–H bonds are a number of other explorations of similar reactions. Complexes supported by electron-donating TMPA derivatives, **L41b** and **L41c**, and **L44** react rapidly with phenols and mechanistic studies have provided key insights.[127,136,175] The Cu(II)-$O_2^{-\bullet}$ complexes supported by **L41b** and **L44** convert *para*-MeO-2,6-di-*tert*-butylphenol to a mixture of the corresponding quinone, hydroperoxide, and radical (in boxes, Figure 14); only quinones are formed from 2,6-di-*tert*-butylphenol and 2,4,6-tri-*tert*butylphenol. [136,175] For the case of **L44**, an alkoxide complex arising from intramolecular hydroxylation of a ligand methyl group is observed, which was proposed to result from reaction of the $[CuOOH]^+$ species derived from initial HAT from the weak phenol (or TEMPOH) O–H bond (this reaction is discussed in section 2.2).[175] In a detailed study of the **L41c** system with a range of phenols,[127] two pathways were identified, a 2-electron oxidation of *para*-X-2,6-di-*tert*-butylphenols to the quinone and a 4-electron oxidation of 2,4,6-trialkyl-substituted phenols to the quinone, presumably via loss of alkene. On the basis of kinetic data, a common mechanism involving initial HAT to yield a phenoxyl radical was proposed, with an additional reaction of the radical with another equivalent of the Cu(II)-$O_2^{-\bullet}$ complex yielding intermediate **12** at low temperature (Figure 14). For X = alkoxy (illustrated for methoxy), subsequent hydrolysis yields the product quinone, whereas for X = alkyl (illustrated for *tert*-butyl), alkene loss is the major route toward the quinone product, both of which occur upon warming/workup.[127]

In contrast to the above examples, the reactions of η^1-Cu(II)-$O_2^{-\bullet}$ complexes supported by **L28a** and **L42b** do not readily abstract H atoms from phenols.[129,128] The low observed reactivity of the **L42b** complex with hydroxylamine and phenols (in acetone at −90 °C) was ascribed to poor access of substrate due to the hydrophobic steric encumbrance of the supporting ligand.[129] For the complex supported by **L28a**, reaction with alkyl-substituted phenols was not observed, while deprotonation of nitrophenol was observed, consistent with the nucleophilic/basic character of the anionic complex.[128]

Finally, we note that 1:1 Cu:O_2 adducts have been proposed as intermediates in catalytic reductions of O_2 to H_2O_2 or H_2O.[176–178] For example, in a study of the influence of added cations on 2-versus 4-electron reductions of O_2, the η^1-Cu(II)-$O_2^{-\bullet}$ complexes supported by **L41a** or **L35a** were postulated to be reduced by Fc* or Me_2Fc, respectively, in the presence of Sc^{3+} to yield a Cu(II) intermediate and ScO_2^+, thus driving the reaction to yield peroxide instead of water.[176]

2.2. [CuOOR]$^+$ Complexes

The [CuOOR]$^+$ unit has been suggested as a key intermediate in catalytic oxidations by O_2 or ROOH (R = H, alkyl, or acyl). In the following subsections, we discuss the syntheses and mechanisms of the formation of [CuOOR]$^+$ species, their properties, and their reactivity.

2.2.1. Syntheses and Mechanism(s) of Formation—The (hydroperoxo)copper(II) unit proposed to be an active oxidant in enzymes may be accessed by the routes outlined in Figure 15. One path involves a 1:1 Cu:O_2 adduct reacting with a proton and an electron, either via separate steps or through PCET or hydrogen atom transfer from substrate.[175] This route directly models the way the [CuOOH]$^+$ moiety is thought to be generated in biology. Alternative syntheses to [CuOOR]$^+$ (R = H, alkyl, or acyl) involve treatment of copper(I) or copper(II) precursors with H_2O_2 or ROOH either in the presence or absence of base.[179–194] The following examples are illustrative and include the few cases where mechanisms have been examined experimentally.

The formation of a [CuOOH]$^+$ intermediate via the PCET pathway shown in Figure 15 was implicated in mechanistic studies of the 2-electron reduction of O_2 to H_2O_2 by ferrocene (Fc) or 1,1′-dimethylferrocene (Me_2Fc) by [(**L45**)Cu]$^{2+}$ in the presence of $HClO_4$ in acetone.[195] In this study encompassing detailed kinetic experiments, the rate of formation of the intermediate [(**L45**)CuOOH]$^+$ was found to be temperature-independent, which was rationalized by postulating that the negative ΔH for the binding of O_2 to [(**L45**)Cu]$^+$ (formed rapidly by reduction of the Cu(II) precursor by Fc or Me_2Fc) is approximately the same as $\Delta H^{\ddagger}$ for the rate-determining PCET reaction of the 1:1 Cu:O_2 adduct; this equivalence explains the observed activationless conversion. It is noteworthy that a closely related system, [(**L41a**)Cu]$^{2+}$, with one less –CH_2– in the ligand backbone, exhibits quite different behavior, such that 1-electron reduction to the Cu(I) form is rate-determining, binuclear 2:1 Cu:O_2 intermediates are involved (section 3), and O_2 undergoes 4-electron reduction to H_2O.[178]

In another study, kinetics experiments and DFT calculations were used to monitor the reaction of H_2O_2 in the presence of NEt_3 with Cu(II)-solvato (S) complexes of the tridentate

ligands **L35b** and **L35c**.[179] Saturation kinetics were observed and interpreted to indicate rapid equilibrium formation of $HOO^{-}Et_3NH^{+}$ (K), which then formed an initial $[CuOOH]^{+}$ complex (k_1, Figure 16). Conversion of this initial complex to a second $[CuOOH]^{+}$ species with the hydroperoxide now in the equatorial position was proposed. An alternative hypothesis also consistent with the kinetic data involves loss of a proton and conversion of the –OOH ligand to a η^2-peroxide. However, DFT calculations do not support this alternative hypothesis. This work complements a previous study using less sterically encumbered **L38a** in which analogous saturation kinetics were observed and similarly interpreted, but characterization of the $[CuOOH]^{+}$ product(s) was hindered by subsequent formation of (μ-η^2:η^2-peroxo)dicopper(II) species.[196]

Another unusual route to a $[CuOOH]^{+}$ complex was proposed that involves reaction of a Cu(I) complex with H_2O_2 in the absence of added base.[188] Specifically, reaction of a Cu(I) complex supported by the ligand **L41h** with 1.5 equiv of H_2O_2 at −90 °C in acetone yielded 1 equiv. H_2O and [(**L41h**)$CuOOH]^{+}$, which is stabilized by intramolecular hydrogen bonding. To rationalize this result, and in particular the observed stoichiometry, a Fenton-like reaction to yield a copper-oxyl, $[CuO]^{+}$ (section 2.3), was proposed (Figure 17). It was suggested that this species is then trapped by the Cu(I) precursor to yield a (μ-oxo)dicopper(II) complex, which reacts with H_2O_2 to yield the $[CuOOH]^{+}$ product. An alternative pathway was also considered, whereby reaction of the Cu(I) complex with H_2O_2 yields hydroxyl radical and a (hydroxo)-copper(II) complex, which then affords the peroxo product upon reaction with H_2O_2.

A unique route to an alkylperoxide complex was reported involving reaction of copper(II) complexes of ligands **L18** with H_2O_2 in acetone (Figure 18).[180,184] An acetone molecule is functionalized to yield the novel species **13**, the characterization of which is described below (section 2.2.2). The 2-hydroxy-2-peroxypropane ligand was formed in an analogous way upon reaction of an iron(II) complex with H_2O_2 in acetone.[197] When the reactions of the copper(II) complexes of **L18** with H_2O_2 or cumene hydroperoxide[185] were performed in nitrile solvents, simple $[CuOOR]^{+}$ (R = H or cumyl) complexes formed instead, highlighting a drastic solvent effect on the course of the synthesis.

The reaction of cumene hydroperoxide with a Cu(I) precursor supported by the highly sterically hindered ligand **L42c** results in the generation of a complex (**18**) with a $[CuOOR]^{+}$ moiety and an anilino radical ligand (Figure 19).[194] A mechanism for formation of this unusual product was proposed involving initial generation of a $[Cu^{I}OOR]$ complex featuring a protonated aniline arm (**15**) and hydrogen bonding from an N–H to the bound peroxide. Heterolytic O–O bond scission and release of ROH would generate the copper(II)-hydroxide (**17**), either stepwise via a copper-oxyl intermediate (**16**) that then undergoes H atom tautomerization or in concerted fashion. Substitution of the hydroxide in **17** by cumene hydroperoxide would yield the final product (**18**).

2.2.2. Structures and Properties—Only two complexes with the $[CuOOR]^{+}$ unit have been characterized by X-ray crystallography; their structures are drawn in Figure 20.[198,199] The X-ray structures shown in Figure 20 show similar η^1 coordination of the hydro- and alkylperoxo ligands, respectively, and identical O–O distances of 1.460(6) Å consistent with

a peroxide formulation.[37,199] A key difference is the presence of two hydrogen-bonding interactions in the **L41e** complex (**19**) from the amide substituent N–H groups to the proximal oxygen of the peroxide. As noted below (section 2.2.3), these interactions influence the properties and reactivity of the $[CuOOH]^+$ unit.

Other $[CuOOR]^+$ complexes have been identified and characterized via a multitude of spectroscopic techniques (Table 5).[175,179–195,200–210] Notably, these complexes show a diagnostic UV–vis feature at ~350 nm assigned as a peroxide→ Cu(II) ligand-to-metal charge transfer (LMCT) transition. In general, this absorption is observed at higher energy and intensity for R = H than for R = alkyl. Excitation into the LMCT band with resonance Raman spectroscopy allows for observation of O-isotope sensitive Cu–O and O–O vibrations. Typically, values of ν(Cu–O) ~550 cm^{-1} and ν(O–O) ~850 cm^{-1} are observed, with additional vibrational modes observed for $[CuOOR]^+$ (R = alkyl), including C–C–C and O–C–C stretches. These complexes typically exhibit EPR signals characteristic for Cu(II) sites (data not shown).

An illustrative example is the identification of complex **18** as a $[CuOOR]^+$ species with a bound anilino radical that is based on (a) UV–vis and resonance Raman data typical for the $[CuOOR]^+$ moiety and (b) the observation of ligand vibrations associated with the anilino radical in resonance Raman spectra.[194] These assignments were confirmed through comparison to spectra obtained using ligand deuteration on the anilino rings and DFT calculations. The complex is EPR silent, consistent with antiferromagnetic coupling between the radical and the Cu(II) ion.

2.2.3. Reactivity—Variability in the reactivity of $[CuOOR]^+$ complexes has been observed, with some being stable only at low temperature and prone to decomposition upon warming and/or reactions with exogenous substrates and others being quite robust and unreactive. In addition, the reaction pathways are sensitive to the nature of the supporting ligand and the solvent.

Examples of stable, relatively unreactive $[CuOOR]^+$ complexes include those supported by the ligands **L35b**–**c**,[179] **L42a** (R = H or *Cm*),[190] **L19** (R = H),[183] and **L41e** (R = H).[198] DFT calculations aimed at evaluating the reactivity of [(**L19**)-CuOOH]$^+$ for epoxidation of ethylene revealed a high reaction barrier for O–O bond homolysis consistent with experimental observations (i.e., 40.2 kcal/mol for O–O bond homolysis).[183] The stability of the **L41e** complex **19** (Figure 20 and Figure 21) was attributed to a combination of hydrogen bonds from the amido NH groups to the proximal O atom of the bound hydroperoxo ligand and steric shielding by the *tert*-butyl substituents.[198,211] From a comparative survey of the properties of $[CuOOH]^+$ complexes supported by a series of **L41** derivatives with differing hydrogen bonding capabilities and steric influences, it was concluded that hydrogen bonding to the proximal oxygen is correlated with a lower energy peroxo → Cu(II) LMCT transition, higher ν(O–O), lower ν(Cu–O), and slower rates of decomposition. These results are consistent with the hydrogen bond interaction causing a weakening of the Cu– O bond and a strengthening of the O–O bond that is broken in the decomposition process.[37] Conversely, a $[CuOOH]^+$ complex supported by **L43a** (**21**, Figure 21) was proposed to

feature hydrogen bonding to the distal O atom, and it was found to decompose faster than an analog supported by **L43b** (**22**) that lacked this distal interaction (Figure 21).[37,207]

Hydrogen bonding from a secondary amine group to the proximal O atom in a $[CuOOH]^+$ complex of **L41h** (**23**, Figure 22) also inhibits N-dealkylation reactions (see below) as well as reactions with exogenous substrates.[188] Interestingly, this complex forms a (*trans*-1,2-peroxo)dicopper(II) species upon warming (Figure 22). In addition, it yields 1 equiv. H_2O_2 upon treatment with $HClO_4$, a reaction that can be reversed by subsequent addition of Et_3N over multiple cycles. Hydrogen bonding was also postulated to stabilize a $[CuOOH]^+$ complex of **L70b**, here involving the hydroperoxo O–H interacting with a ligand phenoxide O atom.[193] This complex was proposed to be an intermediate in the catalytic oxidations of cyclohexane and toluene by H_2O_2 in the presence of HNO_3.

Intramolecular hydroxylation of supporting ligand aryl groups was observed upon decay of several $[CuOOR]^+$ complexes. [180,181,184] Warming of the $[CuOOH]^+$ complex **24** supported by **L41f** in acetone from −80 °C to room temperature followed by aqueous workup yielded the phenol shown in Figure 23a, which was labeled with ^{18}O when $H_2{}^{18}O_2$ was used.[181] The involvement of a bis(μ-oxo)dicopper species was ruled out by independent synthesis of such a species from a Cu(I) complex of **L41f** and O_2 and determination that it did not yield hydroxylated ligand. Mechanisms involving either direct attack at the aryl group of the hydroperoxo moiety or O–O bond homolysis to yield a reactive copper-oxyl were proposed.

Intramolecular aryl group hydroxylation was also observed upon warming of the 2-hydroxy-2-peroxypropane complex **13** (Figures 18 and 23b).[180,184] The final product was the phenoxide complex **26** (Figure 23b), which was isolated and characterized by X-ray crystallography.[180] The reaction followed first-order kinetics to yield an intermediate **25**, and studies of the series with X = NO_2, Cl, H, Me, OMe gave a Hammett $\rho = -2.2$ consistent with electrophilic attack at the aryl group. The KIE for the perdeuterated aryl analog was negligible (0.9 ± 0.02). The structure of **25** shown in Figure 23b was proposed on the basis of the combined experimental data and DFT calculations, and the indicated mechanism involving general acid–base catalysis by $HNEt_3^+$ and its conjugate (used in the synthesis of **13**) was suggested. The analog of **13** lacking the aryl substituents (i.e., complex supported by **L18a**) decomposed to yield a Cu(II)-acetate complex, in which one of the O atoms in the acetate ligand was shown to derive from H_2O_2 (determined from isotopic labeling). A mechanism was proposed on the basis of DFT calculations involving tautomerization of the 2-hydroxy-2-peroxypropane ligand, a Baeyer–Villiger-type 1,2-methyl shift, and hydrolysis of the resulting ester complex (Figure 24).[184]

The $[CuOOR]^+$ unit has also been implicated as an oxidant of pendant *N*-alkyl amine groups,[175,182,186,187,189] including N-dealkylations that model the function of PHM.[41] In one set of studies,[182,186,189] the warming and subsequent demetalation of $[CuOOH]^+$ complexes supported by **L41g** and **L41i**–**k** yielded unperturbed ligand, mono-N-dealkylated ligand, and the respective aldehyde as predominant products (>40% yield each), with smaller amounts of overoxidized coproducts (Figure 25). An intermediate copper(II)-alkoxide complex **28** was identified by ESI-MS,[182,186] the O atom of which derived from the H_2O_2 used to prepare the $[CuOOH]^+$ unit according to the results of isotope labeling

experiments. Initial mechanistic hypotheses invoked O–O bond homolysis of the $[CuOOH]^+$ complex to yield a reactive $[CuO]^+$ species that cleaves the weak C–H bond adjacent to the amine N atom to yield an iminium radical cation. Subsequent "rebound" would yield the alkoxide intermediate, which upon aqueous workup decomposes to the N-dealkylated amine and the aldehyde. Indirect support for the initial O–O bond homolysis route included the observations that (a) N-dealkylation did not occur to the same extent when bis(μ-oxo)dicopper species of the same ligands were examined (ruling out such species as potential intermediates) and (b) the same alkoxide intermediate **28** was observed upon treatment of Cu(I) precursors of the intact ligand with PhIO. In addition, ESI-MS evidence consistent with the $[CuO]^+$ intermediate was obtained.

A similar pathway was proposed to rationalize the formation of the copper(II)-alkoxide **30** upon reaction of the 1:1 Cu:O_2 adduct **2** with phenols or TEMPOH (Figure 26).[175] In these reactions, the 1:1 Cu:O_2 adduct abstracts an H atom from the phenol or TEMPOH to generate a $[CuOOH]^+$ complex **29**, that then was proposed to undergo the O–O bond homolysis process. Supporting evidence included observation of the same alkoxide complex **30** upon treatment of a Cu(II) precursor with H_2O_2 (consistent with a $[CuOOH]^+$ intermediate) or reaction of a Cu(I) precursor with PhIO (consistent with a copper-oxyl intermediate). A DFT study proposed a 15 kcal/mol barrier for abstraction of the H atom of the methyl group of the amine by the distal O atom of the $[CuOOH]^+$ complex, with concomitant O–O bond scission.[212]

These mechanistic hypotheses for N-dealkylation reactions of $[CuOOH]^+$ complexes have been called into question in more recent work.[189] In a detailed mechanistic investigation of the system (**27**, Figure 25), with R = *para*-X-phenyl (X = Cl, H, and OMe), DFT calculations revealed high-energy barriers (27–34 kcal/mol) inconsistent with measured reaction rates for mechanisms involving (a) direct HAT by the distal oxygen (like that proposed for **2**), (b) prior O–O bond homolysis to yield a copper-oxyl, or (c) a pathway involving concerted Cu–O bond homolysis and HAT (to give Cu(I) and H_2O_2). Upon deuteration of the ligand, no KIE was observed, further arguing against the direct HAT pathway. Instead, a mechanism involving Cu–O bond homolysis to yield Cu(I) and the hydroperoxyl radical was proposed, which was found to have a reasonably low barrier of 14.8 kcal/mol (Figure 27). Subsequent Fenton-like chemistry involving reaction of the Cu(I) complex with H_2O_2 was suggested to yield a Cu(II)-hydroxide and hydroxyl radical. HAT by this radical followed by "rebound" from the Cu(II)-hydroxide would afford the requisite carbinolamine that undergoes N-dealkylation.

Evidence in favor of O–O bond homolysis in a $[CuOOR]^+$ (R = $C(Me)_2Ph$) complex was observed in **31** (Figure 28).[185] Decomposition yielded a bis(hydroxo)dicopper(II) complex and acetophenone. Oxidation of exogenous substrates 10-methyl-9,10-dihydroacridine or 1,4-cyclohexadiene was observed, with a large KIE of 19.2 at −40 °C for the 9,9-dideuterated derivative of the former indicating rate-determining C–H(D) attack. In the presence of the radical trap, 5,5-dimethyl-1-pyrroline-*N*-oxide (DMPO), hydroxylation to yield a complex assigned as **32** occurred. Acetophenone was a coproduct in all of the reactions. A stepwise mechanism involving rapid pre-equilibrium formation of a $[CuO]^+$

species **33** (K_{eq}) followed by HAT or radical trapping steps was proposed, although it was noted that the kinetic data are also consistent with a concerted process.

Heterolytic O–O bond scission was implicated in reactions of Cu(I) complexes of **L18a** (**34**) and **L69** (**35**) with cumyl hydroperoxide (Figure 29).[191,192] In both systems, the reaction proceeded to give cumyl alcohol (CmOH) as the predominant product (90–98%), with only minor amounts of acetophenone observed. These results are consistent with 2-electron reduction of the peroxide moiety. However, the stoichiometry for the reactions involving the two ligands differed; for **34**, a 2:1 Cu:HOOR stoichiometry was observed (50% yield of CmOH), whereas for **35**, the yield of CmOH was ~100% (1:1 Cu:HOOR stoichiometry). In addition, upon workup of the reaction with **35**, the sulfoxide form of the ligand was isolated. Presumably, and on the basis of analogy to results for a dicopper(I) complex (section 3), the pathway for **34** involves dicopper intermediates [1 electron from each Cu(I)]. For **35**, a mechanism involving formation of a $[CuOOR]^+$ intermediate was proposed, with the second necessary electron coming from the sulfur donor to give the intermediate **36**. Subsequent heterolytic cleavage of the O–O bond generates CmOH and the Cu(I) complex **38** of the sulfoxide, possibly via the intermediacy of a species such as **37**. It is worth noting that heterolytic O–O bond scission and involvement of a ligand donor atom was also observed for **15** (Figure 19).[194]

The unusual $[CuOOR]^+$ radical complex **18**[194] (Figure 19) cleanly oxidized various *para*-substituted benzylic alcohols to benzaldehydes (substituents: OMe, Me, F, Cl) in a 2-electron process reminiscent of the copper(II)-phenoxyl unit in galactose oxidase (GAO)[213] and model complexes.[214,215] In the presence of excess substrate, the reaction followed pseudo first-order kinetics, and a Hammett plot of the second-order rate constants had a ρ value of -0.42 ± 0.08, similar to that reported for GAO (-0.09 ± 0.32).[216] On the basis of this similarity to the enzyme, a mechanism was proposed involving substitution of the peroxide ligand by the alcohol (to yield ROOH), followed by intramolecular HAT by the anilino radical (vs the phenoxyl radical in GAO).

Finally, in chemistry relevant to biomolecule oxidation by reactive nitrogen species,[217] the $[CuOOH]^+$ complex **23** (Figure 22) supported by **L41h** was found to react with NO according to eq 2.[201] A Cu(I)-peroxynitrite complex was postulated as an intermediate, with support coming from observation of nitration of 2,4-di-*tert*-butylphenol after treatment of **23** with the phenol followed by addition of NO. The finding of N_2O as a coproduct in the reaction of **23** with NO was rationalized by proposing disproportionation of NO by a Cu(I) intermediate(s).

$$2[CuOOH]^+ + 4NO \rightarrow 2[Cu^{II}(NO_3^-)]^+ + H_2O + N_2O(g) \quad (2)$$

2.3. $[CuO]^+$ and $[CuOH]^{2+}$ Species

Of the monocopper–oxygen intermediates proposed to be involved in catalytic oxidations, species which contain the $[CuO]^+$ unit ("copper-oxyl" species) have proven to be

particularly elusive. Proposals for the intermediacy of such species in reactions of copper complexes in solution go back more than two decades.[120,218,219] Yet, while a number of computational studies have probed their properties and led to proposals that intermediates of this type are potent oxidants, such species have only been observed experimentally in the gas phase and only indirect evidence exists for their involvement in homogeneous systems. Examples of such cases involving reactions of $[CuOOR]^+$ complexes were discussed in section 2.2. The following discussion will briefly summarize the computational predictions concerning the properties of the $[CuO]^+$ moiety and some other experimental examples that hint at the involvement of the $[CuO]^+$ unit in homogeneous oxidation reactions. The discussion will then shift toward recent examples of $[CuOH]^{2+}$ species, which may be considered to be the conjugate acid of the $[CuO]^+$ moiety and have also been suggested as relevant species in biological oxidations.

2.3.1. $[CuO]^+$—Numerous computational studies have evaluated the $[CuO]^+$ unit within gas-phase ions,[57,61,220–226] a protein environment,[17,59] and complexes in solution.[121,122,227,228] Detailed evaluation of the bare $[CuO]^+$ ion supports a triplet ground state with the configuration $(1\sigma)^2(2\sigma)^2(1\pi_x)^2(1\pi_y)^2(1\delta)^4(3\sigma^*)^2(2\pi_x^*)^1(2\pi_y^*)^1(4\sigma^*)^0$ [Figure 30 (left)],[57,220,222] which has been noted to be analogous to the $^3\Sigma_g^-$ ground state of dioxygen.[229] But rather than having biradical spin density equally distributed between the two atoms like in O_2, in $[CuO]^+$ the singly occupied $2\pi^*$ orbitals have predominant oxygen p character, as reflected by the spin densities of 1.68 on O and 0.32 on Cu.[222] Analogous triplet ground states were found for the $[CuO]^+$ unit in various ligand environments, albeit sometimes with different orbital descriptions. For example, in the distorted trigonal bipyramidal environment of the PHM active site, one electron occupies what is essentially a nonbonding p_x (O) orbital and the other occupies a σ-type molecular orbital comprising antibonding d_z^2 (Cu) and p_z (O) orbitals [Figure 30 (right)]. This situation has been contrasted with the much more strongly bonding interactions involved in the $Fe^{IV}O$ unit.[17] Indeed, the Cu–O bond in $[CuO]^+$ is weak, as reflected in low bond dissociation energies determined from experiment (31.1 ± 2.8 kcal/mol)[230] and theory (~25 kcal/mol).[57]

Consistent with its biradical character and a weak Cu–O bond, the $[CuO]^+$ unit by itself, or in ligated form, has been predicted to be highly reactive. As noted previously (section 1), computations predict that reaction barriers for substrate attack by $[CuO]^+$ in enzymes such as DβM,[59,60] PHM,[17,46] or LPMO[61] are significantly lower than that for other intermediates such as 1:1 $Cu:O_2$ adducts or $[CuOOH]^+$. Similar predictions have been made for synthetic systems.[183] Additionally, the product O–H bonds formed in HAT reactions mediated by these species are generally strong (~90–99 kcal mol^{-1} in some cases).[227] Experiments have shown that in the gas phase, the ion $[(phen)CuO]^+$ attacks a variety of hydrocarbon C–H bonds[221,231] and the even more reactive $[CuO]^+$ ion readily attacks the strong C–H bond of methane.[222,223,231] Full discussion of this extensive work is beyond the scope of this review, which focuses primarily on complexes in condensed phase. We note here, however, that a key feature of many of these reactions is spin-inversion from the triplet potential energy surface to the singlet surface, which generally occurs after the initial oxidation step (either HAT or O atom transfer).[59,183,226] The subsequent steps in these reactions (either radical rebound in the case of the HAT reactions or ring closure in the case of epoxidation reactions)

generally involve the one electron reduction from copper(II) to copper(I). The reduction is more favorable for the singlet state than the triplet state which is why spin-inversion generally happens after the initial oxidation step but before the second transition state.

Postulates of $[CuO]^+$ as an intermediate in reactions of $[CuOOR]^+$ complexes were discussed in section 2.2, where it was noted that most supporting evidence is indirect (with the exception of ESI-MS data for the reaction of **28** with PhIO).[186] Another example drawing inspiration from nonheme iron enzymes[232–234] involved the reaction of copper(I)-α-ketocarboxylate complexes (**39**) supported by **L17** with O_2 (Figure 31).[228] Demetalation and workup of the reaction mixtures revealed that aromatic hydroxylation of the ligand had taken place. DFT calculations predicted a pathway involving nucleophilic attack on the α-ketocarboxylate ligand by a 1:1 $Cu:O_2$ intermediate followed by decarboxylation. The resulting peracid species can then attack the ring directly via a very "oxolike" peracid transition state ["TS-peracid", path (b)] or form a $[CuO]^+$ type intermediate that then attacks the ring ["TS-oxo", path (a)]. The latter was found to be the more kinetically favorable pathway. In line with other studies, theory indicated that the $[CuO]^+$ species in path (a) has a triplet ground state and that spin crossover from the triplet to the singlet potential energy surfaces should be efficient.[235]

In a more direct attempt to access a $[CuO]^+$ complex, a set of Cu(I) complexes of bidentate N-donor ligands were treated with oxo transfer reagents Me_3NO, pyridinium *N*-oxides, or PhIO.[236] In several cases, stable Cu(I)-*N*-oxide adducts formed, attesting to the energetic cost of accessing a $[CuO]^+$ species. With ligand **L2d**, a bis(μ-oxo)dicopper complex was generated in the reaction with Me_3NO, which might have derived from dimerization of a $[CuO]^+$ precursor. However, alternative pathways such as that involving dimerization of a Me_3NO adduct followed by amine loss could not be ruled out.

2.3.2. $[CuOH]^{2+}$ Complexes—Protonation of the $[CuO]^+$ unit would yield a $[CuOH]^{2+}$ core, which may be envisioned as a (hydroxo)copper(III) species that could exhibit significant reactivity with C–H bonds. Such species **40**–**43** (Figure 32) have been prepared using strongly electron-donating dicarboxamido ligands,[237–239] which are related to other amide-containing ligands that had been used previously to stabilize Cu(III) complexes.[240–244] These complexes were prepared by 1-electron oxidation of $[CuOH]^+$ precursors and were formulated as Cu(III) compounds on the basis of X-ray absorption spectroscopy, EPR spectroscopy, and TD-DFT analysis of UV–vis spectra. Key spectroscopic features for the $[CuOH]^{2+}$ core include (a) an X-ray absorption edge energy ~1.7 eV higher than that of the precursor Cu(II) complex and average Cu–O(N) distances shorter by ~0.1 Å than the Cu(II) precursor by EXAFS, (b) EPR silence consistent with a $S = 0$ Cu(III) formulation, and (c) identification of the intense absorption feature ~500–570 nm assigned by TD-DFT calculations as a ligand-to-metal charge transfer transition from the π system of the flanking aryl rings to the $[CuOH]^{2+}$ core for **40**–**43**.

In the initial report describing **40**, high rates for H atom abstraction from 9,10-dihydroanthracene (DHA) were found (i.e., $k = 1.1(1)\ M^{-1}\ s^{-1}$ at −80 °C).[237] The products observed were anthracene and the corresponding complex with a $[Cu(OH_2)]^{2+}$ core. Kinetic studies using deuterated substrate revealed a high H/D KIE of 40 at −60 °C, clearly

reflecting C– H bond scission in the rate-determining step and suggestive of a significant tunneling contribution. Since this first report, more detailed studies of the properties and reactivities of **40**, **42**, and **43** were performed.[238,239] The differing degrees of electron donation by the ligands across the series were reflected in spectroscopic properties and oxidation potential differences. For example, a 400 mV range in $E_{1/2}$ values for the Cu^{III}/Cu^{II} redox couple was observed [**43** (−260 mV) < **40** (−74 mV) < **42** (+124 mV), all versus Fc^+/Fc in 1,2-difluorobenzene (DFB)]. The redox behavior is inversely correlated to the basicity of the hydroxide in the Cu(II) precursors, which spans a range of ~4 p*K*a units (16–20), and together these effects result in the formation of strong O–H bonds in the aquo complexes that are products of HAT reactions (bond dissociation enthalpies (BDEs) = 88–91 kcal mol^{-1}; **43** < **40** < **42**).[238,239] The complexes **40**, **42**, and **43** attack substrates with C–H bond enthalpies ranging from 76 (DHA) to 99 kcal/mol (cyclohexane). A plot of the log of the second-order rate constants (*k*) versus the difference in BDEs between the substrate C–H bonds and the product aquo complex O–H bonds was linear (Figure 33), indicating a common HAT mechanism across the series of substrates and complexes. The results are also consistent with a rate-dependence on the thermodynamic driving forces, in line with results observed for PCET reactions of other metal oxo/hydroxo compounds.[245,246] In computations evaluating the pathway of the reactions with DHA, transition state structures were defined and significant corrections to account for proton tunneling were necessary to obtain activation parameters that agreed with experimental values.

More recently, stopped-flow kinetics studies of the fast reactions of **40** and **42** with a range of *para*-substituted phenols were performed (*para*-substituents X = NMe_2, OMe, Me, H, Cl, NO_2, and CF_3).[247] The data were interpreted to indicate that concerted PCET occurred across the series, except for the most acidic case (X = NO_2), for which a pathway involving proton transfer prior to electron transfer (PT/ET) was implicated. Importantly, the high reactivity of **40**–**43** with C–H and O–H bonds provides key precedence for the notion that the $[CuOH]^{2+}$ unit could be involved in copper-catalyzed oxidations and might be a more viable intermediate than the more elusive $[CuO]^+$ core.[31]

3. DICOPPER COMPOUNDS

As noted in section 1, dicopper–oxygen species have been identified as intermediates in the CB-PPO enzymes such as tyrosinase and catechol oxidase and have been under intense discussion as possible reactive species in pMMO (Figure 1, panels c and d). Most commonly, 2:1 $Cu:O_2$ complexes have been prepared by reaction of Cu(I) complexes with O_2 at low temperature, via trapping of an initially formed 1:1 Cu/O_2 adduct by an additional Cu(I) center. Multiple isomeric structures for 2:1 $Cu:O_2$ complexes are possible (Figure 34). Of these, the (*trans*-1,2-peroxo), (μ-η^2:η^2-peroxo), and bis(μ-oxo)dicopper cores are the most well-studied, and their diagnostic spectroscopic properties, structural features, and typical reactivity patterns have been well-documented in previous reviews.[15,16,32,34,66,248,249] More recent work on complexes with these cores, other ones shown in Figure 34, and additional moieties comprising single oxo, hydroxo, and hydroperoxo bridges are described below.

3.1. (μ-η^2:η^2-Peroxo)- and Bis(μ-oxo)dicopper Complexes

In view of the evidence that the (μ-η^2:η^2-peroxo)- and bis(μ-oxo)dicopper cores can readily interconvert, any discussion of the reactivity of one must acknowledge the possible involvement of the other. Nonetheless, the respective cores are differentially stabilized as a result of ligand structural and other influences, such that, in many cases, one or the other is observed as the sole or predominant product of oxygenations of Cu(I) complexes. Thus, in the following discussion we consider complexes of each core in turn and then turn to new insights into the factors that affect their interconversions.

3.1.1. Reactivity of (μ-η^2:η^2-Peroxo)dicopper Complexes—Since 2004, several new (μ-η^2:η^2-peroxo)dicopper complexes have been identified and their reactivity examined, with a particular view toward understanding the details of aromatic hydroxylation relevant to tyrosinase function.[32] An especially stable (μ-η^2:η^2-peroxo)dicopper complex was prepared using the extremely hindered ligand **L20c** ($t_{1/2}$ = 14 h in MeOH, 9.6 days in aqueous Na_2HPO_4), and its X-ray crystal structure was determined (Figure 35).[250] It exhibits a high ν(O–O) of 773 cm^{-1} indicative of a strong O–O bond and as a result of the high degree of steric bulk of the supporting ligand does not coexist with a bis(μ-oxo)dicopper isomer, like the system supported by **L20b** comprising *i*Pr rather than *t*Bu ligand substituents.[68,69] The complex effects the catalytic aerobic oxidation of 3,5-di-*tert*-butylcatechol to 3,5-di-*tert*-butylquinone and oxidation of benzyl alcohol to benzaldehyde.

Reaction of the Cu(I) complex of **L1a** with O_2 rapidly yielded a (μ-η^2:η^2-peroxo)dicopper complex **44** identified on the basis of UV–vis and resonance Raman spectroscopy and EXAFS (Figure 36).[251,252] Formation of the product followed first-order kinetics, indicative of rate-determining generation of a 1:1 Cu:O_2 complex followed by rapid trapping by an additional Cu(I) precursor. Subtle but clear differences in spectroscopic properties among the various complexes **44** with variable counteranions (X) were traced to different counteranion interactions with the dicopper core. It is noteworthy that the formation of **44** only using **L1a** contrasts with the generation of a mixture of (μ-η^2:η^2-peroxo)- and bis(μ-oxo)dicopper complexes when the N-methylated variant **L1b** was used. Preferential stabilization of the μ-η^2:η^2-peroxo complex by the weaker σ-donating 2° amine ligands in **L1a** was suggested as a rationale for this difference.

Importantly, unlike what is typically seen for bis(μ-oxo)-dicopper compounds, **44** did not abstract an H atom from 2,4-di-*tert*-butylphenol. Moreover, in a reaction directly relevant to tyrosinase function, treatment of **44** with 2,4-di-*tert*-butylphenolate followed by warming of the reaction mixture results in the formation of a 1:1 mixture of catechol and quinone (Figure 36).[251,252] When the reaction was performed at −125 °C, a long-lived (~3 h) intermediate formed which was identified on the basis of UV–vis and resonance Raman spectroscopy and DFT computations as **45**, a bis(μ-oxo)dicopper complex in which the phenolate has displaced an arm of **L1a** to bind in an equatorial position.[253] Compound **45** decays via first-order kinetics to an intermediate proposed to be the catecholate adduct **46**. Consistent with an electrophilic aromatic substitution pathway, the rate of decay was slowed by electron-withdrawing substituents on the phenolate (Hammett ρ = −2.2) and an inverse 2° kinetic isotope effect was observed upon deuteration at the (hydroxylated) ortho position.

Protonation then yields the final products, (semiquinonato)Cu(II) (**47**) and (aquo)Cu(I) (**48**) complexes. This work demonstrated that a pathway involving isomerization of the (μ-η^2:η^2-peroxo)- to a bis(μ-oxo)dicopper species that then attacks bound deprotonated substrate is a viable mechanism that may also occur in tyrosinase.[251–253] This reactivity has been effectively exploited in effecting catalytic oxidations of alcohols and phenols.[254–256]

Assembly of the (μ-η^2:η^2-peroxo)dicopper core using simple monodentate ligands has been accomplished[257–259] by performing synthetic reactions at very low temperature (−125 to −145 °C). This research builds upon earlier work performed under different conditions that did not allow for conclusive identification of the product (Figure 37).[260,261] The (μ-η^2:η^2-peroxo)dicopper core was formed in reactions of simple $[(Im)_3Cu(I)]^+$ (Im = 2- or 4,5-alkyl-substituted imidazoles) complexes with O_2 in 2-MeTHF at −125 °C.[257] The resulting (μ-η^2:η^2-peroxo)dicopper complexes **49** ligated only by the indicated monodentate imidazoles are stable at −125 °C but decay upon warming ($t_{1/2}$ = 25 min at −105 °C). These species are highly reactive with sodium phenolates which yield predominantly catechols and lesser amounts of quinones (hydrogen atom abstraction not observed) without an observable intermediate. Addition of excess **L42a** to the (μ-η^2:η^2-peroxo)dicopper complex supported by 1,2-dimethylimidazole at −125 °C yields the (*trans*-1,2-peroxo)dicopper complex **50** bound by **L42a**, a ligand-exchange process ("core capture")[259] with precedent in copper–oxygen chemistry[261] that here also involves isomerization of the Cu_2O_2 unit. In more recent work,[258] the previous failure to observe a (μ-η^2:η^2-peroxo)dicopper complex using 1- or 4-methylimidazole or unsubstituted imidazole was obviated by an alternate synthesis involving reaction of the known[262] bis(μ-oxo)dicopper complex **51** of tetramethylpropylenediamine (**L10a**) with an excess of the imidazole at −145 °C, a temperature attained by using a 4:1 2-MeTHF:THF eutectic mixture as solvent. Addition of 4 equiv of sodium 15-crown-5,2-*tert*-butyl-4-cyano phenolate to the resulting (μ-η^2:η^2-peroxo)dicopper complex **49** at −145 °C yielded a phenolate-bound bis(μ-oxo)dicopper species akin to **45** (Figure 36), but here in a more biomimetic and sterically unencumbered ligand environment comprising imidazoles coordinating via their Nτ positions.

A relatively stable (μ-η^2:η^2-peroxo)dicopper complex ($t_{1/2}$ ~ 30 min at room temperature) prepared using **L37** as supporting ligand was found to convert exogenous phenolates to catechols.[263] Kinetics of the stoichiometric reactions of sodium phenolates revealed saturation behavior interpreted to indicate a pre-equilibrium binding step, with studies of phenolate substituent effects on the rate constant giving a Hammett ρ of −0.99. More complicated phenols such as estrone or 8-hydroxyquinoline are also hydroxylated. The stability of the (μ-η^2:η^2-peroxo)dicopper complex enabled its use as a hydroxylation catalyst, with 25 equiv *p*-methoxyphenol and 50 equiv NEt_3 as well as 10 equiv of quinone formed in 1 h and 15 equiv formed in 24 h. A similar type of reactivity is also observed for copper complexes supported by **L15** which effects catalytic conversion of 2,4-di-*tert*-butylphenol to the corresponding quinone in the presence of trimethylamine with a turnover number of 22.[264] Additionally other similar ligand frameworks comprising **L9**, **L46**, **L16a**, or **L16b** have also been used to promote similar catalytic oxidations.[265–267]

Oxygenation of a dicopper(I) complex of the hexadentate ligand **L58c** in acetone at −80 °C yields a UV–vis spectrum consistent with the formation of a (μ-η^2:η^2-peroxo)dicopper

complex (**52**, Figure 38).[268] The kinetics and thermodynamics of O_2 binding to form this complex were determined and comparisons to those previously reported for other analogous systems of xylyl-bridged hexadentate dinucleating ligands were drawn.[269,270] Importantly, unlike those systems that decayed to give products resulting from intramolecular hydroxylation of the bridging xylyl group, decomposition of **52** yielded a bis(μ-hydroxo)dicopper product with no xylyl hydroxylation observed. Reaction of **52** with sodium phenolates resulted in hydroxylation to yield catechols, and the observed saturation kinetics for the reactions were interpreted to indicate weak preequilibrium binding of the phenolate ($\Delta H^{\circ} = -1.9 \pm 0.1$ kcal mol^{-1}, $\Delta S^{\circ} = -2.1 \pm 1.5$ cal K^{-1} mol^{-1}) prior to rate-determining electrophilic attack (supported by Hammett $\rho = -1.8$). No evidence for bis(μ-oxo)dicopper core formation was observed, suggesting that in this system the μ-η^2:η^2-peroxo unit is responsible for the phenolate hydroxylation. In a separate study, **52** was shown to effect the oxidation of thioanisole to the sulfoxide.[271] The reaction is slow, however [$k = (12 \pm 1) \times 10^{-5}$ s^{-1}], so the more reactive system supported by **L58a**[272,273] was examined. Catalytic sulfoxidation was observed upon treatment of a dicopper(II) complex of **L58a** with reductant and O_2, and it was proposed that a reactive intermediate **53** was involved (Figure 38). In a more recent study using **L58d**, which employs chiral alkyl substituents on the benzimidazole instead of the achiral methyl group in **L58a**, the corresponding copper complexes were used to affect stereoselective oxidation reactions of enantiomeric mixtures of catechols and thioansioles.[274]

In contrast to what was observed for the system supported by **L58c**, oxygenation of dicopper(I) complexes of dinucleating ligands featuring aromatic bridges often results in hydroxylation of those bridges, as originally described for xylyl complexes (Figure 39).[275,276] In several cases, no oxygenated intermediate was observed,[181,277] and in some of these instances a (μ-η^2:η^2-peroxo)dicopper species was proposed on the basis of precedent or DFT calculations.[278,279] In other cases, a (μ-η^2:η^2-peroxo)-dicopper was observed by spectroscopy and insights into the kinetics and thermodynamics of its formation and/or intramolecular hydroxylation reactivity were attained.[280–282] For example, kinetic studies of the oxygenation and subsequent intramolecular hydroxylation reactions of Cu(I) complexes of **L58g** and **L58h** and the asymmetric ligand **L50a** were performed.[280] A low $\Delta H^{\ddagger}$ for the oxygenation of the **L58g** and **L58h** complexes was rationalized by postulating a left-lying pre-equilibrium formation of a 1:1 Cu:O_2 adduct [i.e., $Cu^{I}Cu^{II}(O_2^{-})$ species] that slowly evolved to a (μ-η^2:η^2-peroxo)dicopper complex (Figure 40). Both the rates of oxygenation and the intramolecular hydroxylation increased as the ligand was rendered more electron-donating (**L58h** > **L58g** > **L58f**). Slow ligand hydroxylation for the system supported by **L50a** was proposed to reflect "a less than ideal proximity or orientation of the complex's electrophilic peroxo group toward the arene *pi* system."

In another study of a related system supported by **L58i** (Figure 39, R_3 = Me; R = H, OMe, *t*Bu, NO_2), the (μ-η^2:η^2-peroxo)dicopper intermediate **54**, implicated in the hydroxylation of the bridging arene ring to yield **55**, was detected by UV–vis and resonance Raman spectroscopy.[281] Once again, a Hammett ρ value of −1.9 was observed, consistent with electrophilic attack at the ring and in agreement with the value measured for tyrosinase. DFT calculations benchmarked by Cu L-edge XAS for R = NO_2 corroborated this conclusion (via

comparison to the bis(μ-oxo)dicopper complex of **L1a**).[282,283] The computationally proposed mechanism involves transfer of π electrons from the bridging arene to the peroxo σ^* orbital and O–O bond scission in the key reaction step, rather than prior isomerization to a bis(μ-oxo)dicopper isomer. In novel transformations for the (μ-η^2:η^2-peroxo)dicopper moiety, for R = H, trapping of **54** by excess styrene and solvent THF was observed to compete with intramolecular hydroxylation, to yield styrene oxide or 2-hydroxy-THF, respectively. In addition, the (μ-η^2:η^2-peroxo)dicopper core has been implicated in hydrogen atom abstractions, reactions that are unusual for this type of core. This reactivity has been seen for a range of substrates with C–H bond dissociation enthalpies between 75 and 92 kcal/mol, with key evidence being a linear log k vs C–H bond BDE plot and large H/D kinetic isotope effects.[282] Additional studies focused on variation of *para*-substituents on the pyridine rings with the same ligand backbone, revealing that the rate of O_2 binding increases with increasing electron-donation.[280] Radical chemistry was implicated in reactions of several other (μ-η^2:η^2-peroxo)dicopper complexes.[284–287] Conclusive evidence for the formation of a (μ-η^2:η^2-peroxo)dicopper complex upon reaction of a Cu(I) complex of **L8** ligands was reported on the basis of UV–vis and resonance Raman spectroscopy, XAS, magnetic susceptibility measurements, and DFT calculations.[284] Hydrogen atom abstraction without hydroxylation was observed upon reaction of the complex with R = *t*Bu with 2,4-di-*tert*-butylphenol.

Radical coupling of phenols was observed for the (μ-η^2:η^2-peroxo)dicopper complex of **L52**, which was characterized by UV–vis spectroscopy and XAS.[285] Spectroscopic evidence indicated that peroxo complexes of ill-defined structure formed upon reaction of Cu(II) complexes of **L32** and **L51a-c** with H_2O_2 in water,[286] and trapping experiments suggested that hydroxyl radicals formed upon their decay that were implicated in DNA cleavage reactions.[287]

A mechanistic study probed the involvement of the (μ-η^2:η^2-peroxo)dicopper complex (**58**) of **L51a** in the catalytic reduction of O_2 to H_2O by a Cu(II) complex (**56**) using decamethylferrocene (Fc*) and CF_3CO_2H as reductant and proton source, respectively (Figure 41).[288] The proposed mechanism involves rapid electron transfer from Fc* to **56** to yield the dicopper(I) complex **57**, the kinetics of which were analyzed by Marcus theory. Subsequent oxygenation of **57** yields **58**, a known reaction.[289] The rate of reduction of **58** by Fc* is unaffected by CF_3CO_2H, supporting the stepwise reduction/protonation sequence. Because of the possibility of rapid equilibration of **58** with a bis(μ-oxo)dicopper isomer **59**, the possibility that reduction/protonation occurs from **59** was examined. Analysis of activation parameters for reduction of **58** involving comparison to those obtained for the bis(μ-oxo)-dicopper complex of **L18a** (see below) led to the conclusion that direct reduction of **58** occurred.

3.1.2. Reactivity of Bis(μ-oxo)dicopper Complexes—With the aim of understanding the effects of supporting ligands on the properties of the bis(μ-oxo)dicopper core and accessing accurate and functional models of purported biological intermediates, new examples of bis(μ-oxo)dicopper complexes have been prepared and their reactivity probed. One approach has centered on using ever-simpler and less sterically encumbered N-donor

supporting ligands, with the goal of enhancing reactivity of this core with exogenous substrates and better mimicking the putative active site of pMMO that features the "histidine brace" (Figure 1d). In a systematic study building upon earlier work,[290,291] a set of *N*-peralkylated diamine ligands (**L6a**–**e**, **L1d**–**f**), as well as tridentate polyazacyclononane ligands (**L20a** and **L84**), studied for comparative purposes, were used to prepare nine different bis(μ-oxo)dicopper complexes by reacting monocopper(I) starting complexes with dioxygen in various solvents.[292] The formulations of the products were confirmed by EPR, UV–vis, and resonance Raman spectroscopy, as well as an X-ray structure in one case (supported by **L6c**; Figure 42). Among the key findings was that the rate of oxygenation of the Cu(I) complex of **L6d** was ~300 times slower than others with methyl substituents. This was interpreted to indicate an associative mechanism for initial 1:1 Cu:O_2 adduct formation that is slowed by the larger ethyl groups in **L6d**. The least hindered complex of **L6c** was the most stable, a discovery that was noted to have positive implications for future studies of reactivity with external substrates that might have greater access to the bis(μ-oxo)dicopper core if smaller supporting ligands were used.

Support for this idea came from studies of the system supported by *N*,N,N′,N′-tetramethylethylenediamine (**L1c**).[293] It had been found previously that oxygenation of the Cu(I) complex of this sterically unencumbered ligand yielded a bis(μ-oxo)tricopper(II,II,III) complex arising from reaction of an initially formed bis(μ-oxo)dicopper intermediate with a [(**L1c**)-Cu(I)]$^+$ moiety.[291,294] By performing the oxygenation at low concentrations of Cu(I) (<2 mM), the dinuclear complex was prepared preferentially (Figure 43). Importantly, the complex was found to be particularly stable toward decomposition, enabling the oxidation of benzyl alcohol to benzaldehyde, a new reaction for bis(μ-oxo)complexes supported by *N*-peralkylated diamines.

Even less sterically hindered complexes comprising primary amine donors were then targeted, a key goal being to model the RNH_2 coordination found in the proposed active site of pMMO. Direct oxygenation of Cu(I) complexes of primary amines failed to yield isolable products, so the "core capture" method was used as described in section 3.1.1.[295,296] Thus, the bis(μ-oxo)dicopper complex (**51**) of **L10a** was prepared by reaction of a Cu(I) precursor with O_2, and then this complex was treated with another ligand (2 equiv) at −125 °C to rapidly yield new bis(μ-oxo)dicopper products **61**–**63** (Figure 44). The shown thermodynamic stability order was determined through mixing experiments and DFT calculations. The stabilization of the complexes by primary amine and histamine ligands arises from stronger metal–ligand interactions, as reflected by blue-shifted LMCT features in UV–vis spectra caused by higher energies of acceptor orbitals. These strengthened interactions were proposed to arise not from greater ligand basicity but from decreased hindrance that facilitates shorter metal–ligand bonds. The histamine ligation in **62** and **63** is notable with respect to its similarity to the histidine brace in the proposed active sites of pMMO and LPMO. Compounds **61**–**63** were found to be capable of HAT from substrates with weak C–H bonds (74–76 kcal/mol) even at −125 °C, with steric accessibility to the bis(μ-oxo)dicopper core being key for substrate access.

The involvement of a bis(μ-oxo)dicopper unit in catalytic oxidations has been proposed in both homogeneous[297] and heterogeneous systems.[298] Oxygenation of solutions of Cu(I)

complexes of β-diketiminate ligands **L2a** and **L2b** or treatment of the corresponding Cu(II)-acetato complexes with H_2O_2/NEt_3 afforded bis(μ-oxo)dicopper complexes as shown by UV–vis and resonance Raman spectroscopy. Oxidation of cyclohexane (2.5 M) to cyclohexanol (~20% yield) and cyclohexanone (~6% yield) was effected by the Cu(II)-acetato complexes (0.83 mM) and H_2O_2 (83 mM). Catalysis did not proceed when ligands with Me groups in the position adjacent to the N-donors were used (**L2c** and **L2h**), and with these ligands bis(μ-oxo)dicopper complexes were not formed upon treatment with H_2O_2/NEt_3, presumably for precedented steric reasons.[149] These results were interpreted to support a mechanistic hypothesis that the bis(μ-oxo)dicopper core (activated by the electron-withdrawing ligand substituents) was responsible for attacking the cyclohexane substrate.

Catalytic oxidation of toluene to benzaldehyde was performed by a Cu(II) complex of ligand **L34** immobilized within the nanochannels of functionalized mesoporous silica nanoparticles. [298] The involvement of a bis(μ-oxo)dicopper complex was inferred on the basis of the results of experiments wherein the immobilized complex was first reduced by ascorbate and then exposed to O_2. UV–vis spectroscopy and XAS data were consistent with formation of a bis(μ-oxo)dicopper core. Confinement of this core and O_2 within the nanoparticles was argued to be critical for the high levels of catalytic activity observed in what was determined by kinetics to be a consecutive process: toluene → benzyl alcohol → benzaldehyde.

The catalytic reduction of O_2 to H_2O by Fc* and CF_3CO_2H was examined using a Cu(II) complex of **L18a** (**64**), and a mechanism involving initial reduction to a Cu(I) species that then reacts with O_2 to yield a bis(μ-oxo)dicopper core (**65**) was proposed (Figure 45).[288] Consistent with this pathway, reaction of the independently prepared bis(μ-oxo)dicopper complex with Fc* occurred rapidly upon mixing at a rate that was not influenced by added CF_3CO_2H.

Using a ligand that incorporates elements of previously studied systems comprising bis[2-(pyridin-2-yl)ethyl]amine derivatives and amines, a hybrid ligand **L24** was used to prepare a bis(μ-oxo)dicopper complex.[299] This product was identified by UV–vis spectroscopy and found to generate radicals or derived coupling products upon reaction with phenols.

In work following up to the previously reported discovery that oxygenation of a Cu(I) complex of **L5** leads to hydroxylation of its appended arene group via the intermediacy of a bis(μ-oxo)dicopper complex,[300] DFT calculations of this system and studies of a related and synthetically more readily accessible ligand **L7** were performed.[301] Oxygenation of a Cu(I) complex of **L7** also resulted in arene hydroxylation, with subsequent hydrolysis yielding aldehydes as the final products (Figure 46). The formation of a bis(μ-oxo)dicopper intermediate was supported by the observation of an optical absorption at 400 nm in low-temperature stopped-flow kinetic experiments. Importantly, within the context of the viability of bis(μ-oxo)dicopper core as an oxidant capable of tyrosinase activity, DFT calculations supported rapid conversion of an initially formed (μ-η^2:η^2-peroxo)dicopper complex to the more stable bis(μ-oxo)dicopper isomer, which then performed the electrophilic attack at the arene.

In a related strategy, the appended phenol in ligand **L80a** was oxidized to a quinone upon reaction of its Cu(I) complex with O_2.[302] The same quinone product was formed upon oxygenation of the Cu(I) complex of **L80b**, supporting initial catechol formation in the overall reaction of **L80a**. By analogy to the finding that the system supported by a ligand analog comprising a phenyl (**L18b**–**f**) instead of a phenol appendage yields a bis(μ-oxo)dicopper complex, a similar intermediate was invoked, with support from DFT calculations (Figure 47).

The diimine ligand **L11**,[303] bis(guanidine) ligands **L14** and **L13**,[304,305] and the hybrid guanidine-amine ligand **L27**[306] were found to support formation of bis(μ-oxo)dicopper complexes upon oxygenation of Cu(I) precursors. The complex supported by **L14** decayed to yield alkoxo-bridged products derived from hydroxylation of ligand methyl groups.[305] A comparison of the reactivity of the bis(μ-oxo)dicopper complexes **66, 67**, and **51** supported by **L14**, **L27**, and **L10a**,[262] respectively, with 2,4-di*tert*-butylphenol and -phenolate revealed intriguing differences (Figure 48). Complex **66** was unreactive, **51** gave radical coupling products upon reaction with both the phenol and phenolate, and **67** coupled 2,4-di-*tert*-butylphenol and hydroxylated 2,4-di-*tert*-butylphenolate. These results were rationalized by invoking the greater basicity and stronger σ-donating power of the guanidate. With two such guanidate groups in **66**, stabilization of the bis(μ-oxo)dicopper core is sufficient to shut down oxidative reactivity, whereas in the hybrid ligand system **67**, this effect is attenuated and both radical and hydroxylation reactions are observed. As in other systems that hydroxylate phenolates, saturation kinetics were observed, consistent with association of the phenolate to the bis(μ-oxo)dicopper core prior to electrophilic attack. It is also noteworthy that the reactions of **51**, **66**, and **67** with 2 equiv. $FcCO_2H$ (an electron and proton donor) results in conversion to a bis(μ-hydroxo)-dicopper(II) complex, with an intermediate (unobserved) (μ-oxo)(μ-hydroxo)Cu(II)Cu(III) complex proposed on the basis of DFT calculations.[306]

Identification of a bis(μ-oxo)dicopper intermediate that decays via hydroxylation of a bridging aryl unit in a dinucleating ligand was reported for the system supported by **L47**.[307] This finding stands in contrast to the more common observation of (μ-η^2:η^2-peroxo)dicopper intermediates with related xylylbridged ligands (see section 3.1.1). A related hydroxylation where an unobserved bis(μ-oxo)dicopper species is a possible intermediate has been reported.[308] It is noteworthy that in addition to attacking its bridging aryl unit, the bis(μ-oxo)-dicopper complex of **L47** also reacts with 2,4-di-*tert*-butylphenolate to give both radical coupling and ring hydroxylation products (catechol plus trace quinone).[307]

A different xylyl-bridged dinucleating ligand was found to support formation of a bis(μ-oxo)dicopper complex that hydroxylates phenolates.[39,309,310] Comparison of the reactivity of dicopper(I) complexes of ligands **L57** and **L48** revealed different behavior, wherein only **L48** supported formation of a copper–oxygen intermediate, identified as **68** on the basis of UV–vis and resonance Raman spectroscopy (Figure 49).[309] Treatment of **68** with various *para*-substituted phenolates resulted in clean catechol formation (with no complications from intramolecular arene hydroxylation), and in the case of the reaction with *p*-chlorophenolate performed at −95 °C, the bis(μ-oxo)dicopper phenolate adduct **69** was identified as an

intermediate by resonance Raman spectroscopy.[310] The properties and key kinetic parameters for the decay of **69** (i.e., Hammett $\rho = -1.9$) are similar to those reported for **45** supported by **L1a** (Figure 36), corroborating their similar structures.

Finally, we note that an earlier report of the synthesis of a bis(μ-oxo)dicopper complex supported by **L23a**,[311] an open chain analog of the **L20** framework, was followed by a low-temperature stopped-flow study of the kinetics of its formation.[164] A comparison to a series of other related oxygenations revealed the reaction of the Cu(I) complex of **L23a** to be significantly faster, as illustrated by a k_{on} for the initial binding step for **L23a** being ~10^7 greater than for **L20b**.[68,269]

3.1.3. Interconversions of (μ-η^2:η^2-Peroxo)- and Bis(μ-oxo)dicopper Cores—

Since 2004, a number of studies have further examined the factors that influence the relative stabilities of these isomeric cores and the possible interconversions between them. The roles of ligand structural variations on the reactivity of Cu(I) complexes of a large set of pyridylamine ligands have been examined particularly extensively over several decades and the results reviewed.[312,313] In work reported after 2004, the ligand **L38b** was used to draw comparisons with the properties and O_2 reactivity of previously studied Cu(I) complexes of **L38a** and **L38c** (illustrated for R = CH_2CH_2Ph in Figure 50).[314] The Cu(I) complex of **L38b** exhibited an oxidation potential and rate of reaction with O_2 intermediate between those of **L38a** and **L38c**. Upon oxygenation it yielded a (μ-η^2:η^2-peroxo)dicopper complex like that formed using **L38a**[315,316] but with a weaker O–O bond as reflected by a lower ν(O–O) ($\Delta\nu$ = ~20 cm^{-1}). This result contrasts with the formation of a bis(μ-oxo)dicopper complex that had been reported previously using **L38c**.[317] Thus, the 6-methyl substituents reduce the electron-donating power of the ligand framework that **L38b** and **L38c** share, apparently by weakening the Cu–N(pyridine) bonds through steric repulsions, thus inhibiting O–O bond scission. Related steric effects caused by quinolyl groups also led oxygenation of the Cu(I) complex of **L35b** to yield a (μ-η^2:η^2-peroxo)dicopper complex.[318]

Building upon previous work probing solvent effects on the (μ-η^2:η^2-peroxo)/bis(μ-oxo)dicopper equilibrium,[69,291] this equilibrium was examined in detail as a function of solvent for the system involving **L21a**.[319] The operation of a rapid equilibrium between the two isomers supported by **L21a** was confirmed by low-temperature stopped-flow kinetics. UV–vis and resonance Raman spectra showed the proportion of bis(μ-oxo)dicopper isomer formed followed the order CH_2Cl_2 < Et_2O ~ acetone < THF, consistent with greater stabilization of this isomer by more strongly coordinating solvents. Low-frequency features associated with Cu–N_{eq} and Cu---Cu modes in resonance Raman spectra for the (μ-η^2:η^2-peroxo)dicopper isomer shifted as a function of solvent similarly, but the Cu_2O_2 core vibration of the bis(μ-oxo)dicopper core was invariant. These results were interpreted to indicate that the solvent coordinates to the (μ-η^2:η^2-peroxo)dicopper core, but how the overall thermodynamics favoring the other isomer are influenced by the solvent remained unclear.

Electronic effects on the equilibrium were examined in a subsequent comparative study of the series **L21** (R = NMe_2, OMe, H, and Cl).[320] Varying the *para* substituents had negligible effects on the oxidation potentials of their Cu(I) complexes and on the ν(C–O) stretches in

their Cu(I)-carbonyl complexes, but the bis(μ-oxo):(μ-η^2:η^2-peroxo) ratio formed upon oxygenation of the Cu(I) complexes was significantly influenced (in contrast to more minor effects on that ratio reported previously for the **L32** system).[321,322] Thus, this ratio increased as the supporting ligand became more electron-donating, consistent with enhanced stabilization of the more oxidized copper sites in the bis(μ-oxo)dicopper core (Figure 51). This trend was seen using both noncoordinating CH_2Cl_2 and coordinating THF as solvent, but for CH_2Cl_2, it was attenuated for R = OMe, H, and Cl, such that the proportions of the (μ-η^2:η^2-peroxo)dicopper isomer were increased in that solvent. Only the bis(μ-oxo)dicopper isomer was seen for R = NMe_2 using either solvent, indicating that the solvent effects are secondary to the electronic ones propagated by the *para* substituents on the ligand.

In the above study, enhanced electron donation by the supporting ligand results in reductive cleavage of the O–O bond, which has been postulated to occur via "backbonding" into the μ-η^2:η^2-peroxo σ* orbital. Weakening of the O–O bond without such reductive bond scission was defined in an X-ray structure of the (μ-η^2:η^2-peroxo)dicopper complex of **L23b**,[323] which had been shown previously to have a low ν(O–O) of 721 cm^{-1}.[324] A long O–O bond of 1.540(5) Å was measured, and EXAFS and resonance Raman data confirmed that no bis(μ-oxo)dicopper isomer was present, ruling out compositional disorder as the reason for observation of the long O–O distance. This observation was rationalized using DFT calculations by invoking a *trans*-influence of the supporting ligand that "decreases the O_2^{2-} π^*_σ-to-Cu charge transfer (which) results in more electron density in the π antibonding orbitals of the peroxide and thus the weaker O–O bond,"[323] a process distinct from the backbonding to the σ* orbital that induces formation of the bis(μ-oxo) dicopper core.

A detailed study of the reactivity of the mixture of (μ-η^2:η^2-peroxo) and bis(μ-oxo)dicopper complexes supported by **L32** (R = H, MeO, and Me_2N) provided insights into redox behavior, mechanisms of attack at various exogenous substrates, and mechanisms of PCET reactions.[325] Among the findings was the discovery that for reactions with exogenous substrates like THF or dimethylaniline, pre-equilibrium binding of substrate occurs prior to oxidation. Using the mechanistic probes *N*-cyclopropyl-*N*-methylaniline (CMA) and (*p*-methoxyphenyl)-2,2-dimethylpropanol (MDP), it was concluded that the systems supported by **L32** (R = H, MeO) reacted by a CPET (concerted proton electron transfer) pathway, whereas for R = NMe_2, a consecutive ET/PT (electron transfer/proton transfer) mechanism is followed. Complicating the interpretation of the results of these studies is the presence of an equilibrium between (μ-η^2:η^2-peroxo)- and bis(μ-oxo)dicopper isomers, either or both of which may be the reactant in each case.

Subtle ligand geometric factors had significant effects on the course of oxygenations of Cu(I) complexes of the ligand series **L22**, **L26**, **L29**, and **L33**, including on the ratios of (μ-η^2:η^2-peroxo)- and bis(μ-oxo)dicopper isomers (Figure 52).[326] The Cu(I) complex of the 6-membered ring ligand **L26** was reactive with O_2, however an intermediate was not observed. The complex with the 7-membered ring **L29** yielded a bis(μ-oxo)dicopper core, the complex with the 8-membered ring **L33** formed a 1:1 Cu:O_2 adduct, and the complex of the noncyclic ligand **L22** yielded a mixture of (μ-η^2:η^2-peroxo)- and bis(μ-oxo)dicopper products. These differences were rationalized using electrochemical data and analysis of X-ray crystal

structures of the Cu(I) complexes. Bite angle and Cu–N distance constraints associated with the macrocycles in **L26**, **L29**, and **L33** were deemed responsible for the observed Cu(I)/O_2 reactivity. While **L33** and **L22** contain similar propyl linkers between ligand N-donors, the rigidity of the former prevented attainment of proper geometries to support (μ-η^2:η^2-peroxo)- or bis(μ-oxo)dicopper isomers, while flexibility in the latter enabled formation of both cores as a mixture. In another example of subtle ligand geometry changes influencing the stability of these isomers, DFT calculations indicated that simply changing one methylene linker in **L49a** to an ethyl linker (**L49b**) shifted the preference for formation of a bis(μ-oxo)dicopper complex to the (μ-η^2:η^2-peroxo)dicopper congener. [327]

In addition to solvent and ligand electronic, steric, and geometric influences, counterions also were found to affect the relative stability of the (μ-η^2:η^2-peroxo)- or bis(μ-oxo)dicopper cores.[328] Oxygenation of the complex [(**L10b**)Cu(CH_3CN)]X in THF, CH_2Cl_2, or acetone yielded an equilibrating mixture of the two cores, the ratio of which depended on the identity of X. With a relatively noncoordinating anion such as SbF_6^-, the bis(μ-oxo)dicopper isomer is favored. More basic anions like $CH_3SO_3^-$ or $PhCO_2^-$ favor the (μ-η^2:η^2-peroxo)dicopper form, with titration data for the most basic ones indicating association of one anion per dicopper complex. EXAFS supported by DFT calculations indicated bidentate bridging coordination of the anion to the syn axial positions of the (μ-η^2:η^2-peroxo)dicopper unit, thus rationalizing stabilization relative to its bis(μ-oxo)dicopper isomer. Analogous stabilization of a (μ-η^2:η^2-peroxo)dicopper core was proposed in a study of decarboxylation of α-ketocarboxylates, where binding of benzoylformate or benzoate were proposed to convert the bis(μ-oxo)dicopper complex of **L10a** to the carboxylate-bridged (μ-η^2:η^2-peroxo)-dicopper unit.[329]

The presence of an appropriate thioether appendage on a diamine ligand was found to change the preference for formation of the respective $[Cu_2O_2]^{2+}$ cores (Figure 53).[330] Thus, oxygenation of a Cu(I) complex of **L73** proceeds similarly to that of **L10a**[262] to give a bis(μ-oxo)dicopper complex, whereas the alkylthioether group in **L72** induces generation of a (μ-η^2:η^2-peroxo)dicopper core through metal coordination (thus acting as a tridentate ligand analogous to **L23b**,[324] which gives the same isomer). Previous studies of the O_2 reactions with Cu(I) complexes of ligands similar to **L72** and **L73**, but with pyridyl arms (**L76** and **L77**), resulted in sulfoxidations with no copper–oxygen intermediates observed.[331]

Predicting the relative stability of the (μ-η^2:η^2-peroxo) and bis(μ-oxo)dicopper cores by theory has been pursued by many investigators but with widely varying results as a function of methodology used. A full elaboration of these difficulties is beyond the scope of the current discussion, so we point the interested reader to two insightful and comprehensive discussions.[332,333]

3.1.4. Heterobinuclear Bis(μ-oxo) Complexes—In efforts to expand the pallet of bi(μ-oxo)dimetal complexes with the aim of discovering new reactivity of potential relevance to catalytic oxidations, several synthetic strategies toward such species containing a copper ion have been pursued.[167,168,334–336] In one approach, a 1:1 metal/O_2 adduct was mixed with a second metal reagent (Figures 54 and 55).[167,334–336] Thus, reaction of the 1:1 Cu:O_2 adduct **3a** (see Figure 5) with Ni(I) complex **70** (**L81**) generated a mixture of **71** (major) and **72**

(minor) (Figure 54), formulated as having the indicated isomeric cores on the basis of UV–vis, EPR, and resonance Raman spectroscopy [ν(O–O) and $[CuNi(\mu\text{-}O)_2]^{2+}$ core vibration at 847 and 625 cm^{-1}, respectively].[167] An opposite route was taken in preparing compounds **73a**–**h** and **74**, whereby a 1:1 M:O_2 adduct [for example, M = $(Ph_3P)_2Pd$ or Pt,[334] or (**L2d**)Ni[335]] was treated with a Cu(I) complex of ligands **L23c**, **L2d**, **L10a**, **L6a**, or **L20b** (Figure 55). UV–vis and resonance Raman data supported the indicated formulations of the products (Table 6), with additional XAS/EXAFS and computational results provided for **74** (Cu–Ni = 2.81 Å).[335]

Reactivity distinct from that typical of bis(μ-oxo)dicopper complexes was seen in several studies of the heterobimetallic complexes. For example, $[NH_4][PF_6]$ protonated **73b** (ESIMS), while reaction with CO_2 led to a $(PPh_3)_2Pt_{II}$–CO_3 adduct. No reaction of **73a**–**h** was observed with DHA, thioanisole, or 1-decene, but a coupled biphenol was observed upon treatment with 2,4-di-*tert*-butylphenol.[334] Taken together, the reactivity of compounds **73a**–**h** is indicative of nucleophilic character that contrasts with what is generally seen for bis(μ-oxo)dicopper complexes but is in line with the norm for bis(μ-oxo)diplatinum complexes.[337,338] Studies of **74** also show its O atoms to act as nucleophiles.[336] Thus, reaction of **74** with benzoyl chloride led to formation of benzoic acid, and examination of the kinetics of the reactions with a series of *para*-substituted benzoyl chlorides revealed a Hammett ρ = 2.5. On the other hand, examination of the kinetics of the reactions of **74** with phenols showed for R = H on the supporting ligand **L23c**, HAT occurred like what was seen for the bis(μ-oxo)dicopper species. For R = Me, both HAT and PCET mechanisms were followed depending on the phenol, highlighting the subtle effect ligand substituents can have on mechanisms of reactions with exogenous substrates.

In a different synthetic route to heterobimetallic complexes, oxygenation of Cu(I)–Ge(II) complexes **76** and **77** was explored (Figure 56).[168] For the system **76** ligated by $N(SiMe_3)_2^-$ ligands, UV–vis and resonance Raman spectroscopy indicated that **75** was produced (Table 6). The analogous complexes supported by **L2d** and **L4c** were also prepared by reaction of the corresponding transient 1:1 Cu:O_2 adduct with $Ge[N(SiMe_3)_2]_2$. Reaction of **77** with O_2 proceeded differently, giving products indicative of loss of the Ge(II) fragment and formation of a transient 1:1 Cu:O_2 adduct. In support of this formulation for the transient species, reaction with $Ge[N\text{-}(SiMe_3)_2]_2$ yielded **75**.

3.2. Other Peroxo Complexes

3.2.1. (1,2-Peroxo)dicopper Complexes—Ever since the report in 1988 of the first X-ray structure of a Cu/O_2 complex that showed it to be a (*trans*-1,2-peroxo)dicopper(II) species,[339] many examples of this type of core have been characterized, including by X-ray crystallography.[145,340] Key spectroscopic properties of such complexes, mostly reported since 2004, are presented in Table 7.[128,144,200,341–346] They have in common the typical, previously analyzed[347] signatures comprising (1) peroxide $\pi^* \rightarrow$ Cu(II) *d* LMCT features at 530–550 nm (~10,000 M^{-1} cm^{-1}) and 600 nm (sh) and (2) characteristic resonance Raman stretching frequencies for ν(O–O) and ν(Cu–O) at ~800–850 cm^{-1} and ~550 cm^{-1}, respectively. Slight variations evaluated through detailed comparisons with the parent **L41a** system have provided insights into geometric differences or donor atom effects. For

example, in **78** (**L67**), respective ν(O–O) and ν(Cu–O) values were found to be 10 and 16 cm^{-1} lower than those for the **L41a** complex (Figure 57). These shifts were interpreted to indicate increased electron donation by the thioether donor in **L67** that reduces peroxide-to-Cu π^* donation, weakening both the Cu–O and O–O bonds.[342] Similar arguments were used to rationalize why **L82** is a weaker donor than **L67**.[343] The relative absorption intensities for the complexes supported by the thioether-containing ligands **L82** and **L67** are inverted (extinction coefficient at ~610 nm greater than that at ~550 nm) relative to the more typical pattern (extinction coefficient at ~550 nm greater than that at ~610 nm), which was attributed to a geometric distortion toward square pyramidal in the thioether donor cases that inverts the energy order of the π^*_σ and π^*_v orbitals.[342,343] A similar geometric distortion was invoked to explain weaker Cu–O and O–O bonding in the (*trans*-1,2-peroxo)dicopper complex of **L40a**.[344]

In general, (*trans*-1,2-peroxo)dicopper compounds are supported by tetradentate ligands, which typically inhibit adoption of coordination numbers >5 and thus prevent formation of (μ-η^2:η^2-peroxo)- or bis(μ-oxo)dicopper cores. Yet, different cores can be accessed through variation of ligand steric influences or donor types. Thus, while oxygenation of the Cu(I) complex of **L82** yielded a (*trans*-1,2-peroxo)dicopper complex, replacement of the thioether S with an ether O (**L78b**) resulted in formation of a bis(μ-oxo)dicopper core.[343] The bis(pyridylmethyl)amine derivatives **L30** and **L38d** are similarly divergent in their oxygenation chemistry, with the former yielding a (*trans*-1,2-peroxo)dicopper core proposed to involve anisole O coordination to the metal ions and the latter yielding a bis(μ-oxo)dicopper complex because of the noncoordinating nature of the benzyl group.[348] A comparison of a series of derivatives of **L41a** that are modified at the 6-position of one pyridyl arm showed that for R = Me, a (*trans*-1,2-peroxo)-dicopper core forms, but if that substituent is more sterically encumbered (i.e., R = aryl or secondary amine), a bis(μ-oxo)dicopper complex is favored (Figure 58).[341] These findings were rationalized by positing that the large substituent weakens the Cu–N interaction with the substituted pyridyl donor, favoring the lower coordination number typical for bis-(pyridylmethyl)amine ligands suitable for bis(μ-oxo)dicopper complex formation.[317] Differences in steric effects also were proposed to underlie the different course of oxygenations of Cu(I) complexes of bispidine derivatives **L31a** and **L31b**; only 1:1 Cu:O_2 adduct formation was seen for **L31b**, whereas **L31a** supported a (*trans*-1,2-peroxo)dicopper complex.[200]

An equilibrium between (*trans*-1,2-peroxo)- and bis(μ-oxo)dicopper cores was reported,[345] with possible implications for understanding novel reactivity ascribed to the former.[346] Following previous studies of the oxygenation of [(**L40d**)Cu]-PF_6 in EtCN,[349,350] it was found that oxygenation of its $B(C_6F_5)_4^-$ salt in THF initially yielded UV–vis spectra consistent with (*trans*-1,2-peroxo)dicopper species but then evolved to a final spectrum that also contained features indicative of the bis(μ-oxo)dicopper core. The presence of two sets of ν(O–O) and ν(Cu–O) stretching frequencies (in addition to the Cu_2O_2 mode at 584 cm^{-1}) was attributed to the presence of two (*trans*-1,2-peroxo)dicopper isomers differing with respect to the disposition of the **L40d** ligands (C_1 vs C_i symmetry species; Figure 59). Kinetic and thermodynamic parameters for the equilibrium were reported. Inspired by the finding of this equilibrium, it was suggested on the basis of DFT calculations that a bis(μ-

oxo)dicopper isomer might also be energetically accessible for another system previously reported to yield a (*trans*-1,2-peroxo)dicopper complex. This complex supported by **L60** had been found to bind and hydroxylate exogenous phenolates in what was cited to be a novel reactivity for the typically nucleophilic (*trans*-1,2-peroxo)dicopper core.[346] It was proposed that a bis(μ-oxo)dicopper isomer was energetically inaccessible; however, this was challenged using the calibrated DFT method, which suggests that the phenolate oxidation might actually be performed by a bis(μ-oxo)dicopper isomer.[345]

In recent studies of the reactivity of (*trans*-1,2-peroxo)-dicopper complexes supported by **L30**[348] or **L42a**,[340] oxidation of toluene to predominantly benzaldehyde was observed. It was noted, however,[348] that the involvement of other copper–oxygen intermediates could not be ruled out. Protonation of the (*trans*-1,2-peroxo)dicopper core typically results in formation of H_2O_2[344,351] but can also yield a (1,1-hydroperoxo)dicopper species (see section 3.3).

Inspired by a theoretical analysis of the mechanism of formation of the (μ-η^2:η^2-peroxo)dicopper core in hemocyanin, [352] a (*cis*-1,2-peroxo)dicopper moiety was targeted for synthesis and characterization.[38,353,354] In accordance with the computations, the process of formation of the antiferromagnetically coupled singlet (μ-η^2:η^2-peroxo)dicopper unit from triplet O_2 and two Cu(I) ions requires an initial activation event followed by intersystem crossing. This initial activation was proposed to involve an electron transfer from each Cu(I) ion into orthogonal O_2 π^* orbitals to lead to a triplet (1,2-peroxo)dicopper unit. The first example of a (*cis*-1,2-peroxo)-dicopper complex was prepared using the pyrazolate-bridged ligand **L65a** (Figure 60).[353] The X-ray structure of the stable complex **79** revealed *cis* binding of the peroxide ligand with a Cu–O–O–Cu torsion angle of 65.2°. A sodium ion binds to the peroxide in the crystals and in solution. Detailed characterization by spectroscopy and magnetism studies indicated weak binding of the peroxide to the two Cu(II) ions (ν(Cu–O) = 437 cm^{-1}, ν(O–O) = 799 cm^{-1}) that are only weakly antiferromagnetically coupled ($-2J$ = 144 cm^{-1}). This weak coupling was ascribed to the torsion angle intermediate between the extremes expected for strong antiferromagnetic (0°) or ferromagnetic coupling (90°). With the aim of driving the geometry toward that which would favor a triplet ground state, ligand **L65b** featuring an additional methylene linker was examined.[354] Indeed, the resulting (1,2-peroxo)dicopper complex **80** exhibited a shorter Cu–Cu separation of 3.68 Å and a 104.5° torsion angle (thus, denoted as a *"trans"* geometry) and a triplet ground state arising from noninteracting orthogonal magnetic orbitals (Figure 60). Thus, complex **80** represents a unique model of the intermediate species proposed along the pathway of O_2 activation by hemocyanin and related enzymes.

3.2.2. (1,1-Hydroperoxo)dicopper Complexes—Several dicopper complexes featuring 1,1-hydroperoxo ligands have been prepared, typically via protonation of a (peroxo)dicopper precursor or reaction of a Cu(II) complex with H_2O_2.[355–359] For those complexes characterized since 2004, spectroscopic data are presented in Table 8; X-ray crystal structures of complexes **81** and **82** (Figure 61) were determined. Common features include intense UV–vis absorptions assigned as LMCT transitions at ~350–400 nm, ν(O–O) ~860–890 cm^{-1} that are higher than typically seen for (peroxo)dicopper complexes (*vide infra*), and EPR data indicative of weak antiferromagnetic coupling between the Cu(II) ions.

The synthesis of **82** is notable insofar as it is a unique case where protonation of a (peroxo)dicopper species (**80**) to generate a (1,1-hydroperoxo)dicopper complex is reversible.[359] The protonation of **80** to yield **82** proceeded without a detectable intermediate (stopped-flow, −20 °C) and was readily reversed by treatment with 1,8-diazabicyclo-undec-7-ene (DBU). The pK_a for **82** in CH_3CN was determined to be 22.2 ± 0.3.

Several examples of hydroxylation reactions have been observed for (1,1-hydroperoxo)dicopper complexes. The (1,1-hydroperoxo)dicopper complex resulting from reaction of the dicopper(I) complex of **L54** with O_2 was found to react with the nitrile solvent to yield an aldehyde and cyanide (found as a bridging ligand in a tetracopper(II) product).[355] A mechanism involving hydroxylation of the α-C–H bond of the nitrile by the hydroperoxo moiety was proposed. In a separate report, the same (1,1-hydroperoxo)dicopper complex was implicated in the oxidation of guanine in reactions with DNA.[360] Intramolecular hydroxylation of a ligand arm methylene group was observed for complex **81** upon its decomposition in the solid state.[357] A (1,1-hydroperoxo)dicopper complex was identified at low temperature as an intermediate in the double hydroxylation of the bridging arene in **L58b** upon reaction of its dicopper(II) complex with H_2O_2,[358] a reaction reminiscent of an earlier report of the system supported by **L49a**.[361]

(1,1-Hydroperoxo)dicopper complexes have also been implicated in dioxygen reduction reactions, with mechanistic differences seen under different reaction conditions.[362,363] Catalytic 2-electron reduction of O_2 to H_2O_2 was observed upon reaction of **83** with HOTf and Fc* in acetone, but 4-electron reduction of O_2 to H_2O occurred when $HClO_4$ was used with Fc* or weaker reductants such as Fc (Figure 62). Mechanistic studies led to the proposal that when the stronger acid $HClO_4$ is used, protonation of both the hydroxide and the phenoxide occurs, resulting in decomplexation of the latter and more facile reduction of the dicopper(I) intermediate (less powerful reductant needed). The weaker acid HOTf does not protonate the phenoxide bridge, making reduction more thermodynamically difficult. Importantly, in both cases a (1,1-hydroperoxo)dicopper intermediate is involved; but with HOTf, protonation and loss of H_2O_2 occurs (2-electron reduction pathway), whereas with $HClO_4$, PCET reductive cleavage of the hydroperoxide is favored (4-electron reduction pathway).

3.2.3. (μ-η^1:η^2-Peroxo)dicopper Complexes—Two examples of this binding mode have been proposed as products of oxygenation of dicopper(I) complexes of pentadentate ligands **L63** and **L64** (see Figure 34).[364,365] Unfortunately, confirmation of this unusual bonding mode via X-ray crystallography has not been reported, and the UV–vis, resonance Raman, and EPR spectroscopic data for these complexes do not differ significantly from that typical for (1,2-peroxo)dicopper complexes. Still, it is reasonable to suggest that the bis(pyridylmethyl)amine fragment in **L63** and **L64** would favor η^2 coordination, and precedent exists for other metal ions for (μ-η^1:η^2-peroxo) coordination (Figure 63).[352,364,365]

3.3. Mono(μ-oxo/hydroxo)dicopper Complexes

Inspired by the various postulates of oxo-and hydroxo-bridged dicopper cores as intermediates in catalytic oxidations by pMMO and Cu-doped zeolites (section 1), significant recent effort has been focused on understanding the properties of synthetic analogs. The relatively few synthetic complexes with (μ-oxo)dicopper(II) cores have been reviewed recently.[29] Thus, herein, we only briefly survey selected examples. In early work, complexes **84**,[29,366] **85**,[367] **86**,[368–370] and **87**[218,371] supported by mononucleating ligands were prepared (Figure 64), with their formulations indicated by spectroscopy and their accessibility from multiple routes described (cf. reactions of Cu(I) complexes with O_2, PhIO, and/or NO). An X-ray crystal structure was reported for **85**, but interpretation was hindered by disorder involving the chemically inequivalent O atoms in the core.[367] In general, the oxo ligands in these complexes are nucleophilic, readily protonated, and transferable to oxophilic substrates like PPh_3. (μ-Oxo)dicopper(II) units were also identified in the complexes **88** (postulated, but not identified conclusively), [372,373,374] **89**, and **90** (Figure 65).[375] Complex **89** was characterized by X-ray crystallography, but charge balance considerations led to the postulate that the crystals contained a 1:1 mixture of **89** and its protonated (μ-hydroxo)dicopper(II) congener. Complex **90** was characterized by ^{1}H NMR spectroscopy, EXAFS, and ESI-MS, and was EPR silent. EXAFS and DFT calculations show a Cu–Cu distance of 2.91 and 2.844 Å, respectively. In addition to converting Ph_3P to Ph_3PO, **90** also oxidizes di-*tert*-butylphenol to yield products of radical coupling and further oxidation (quinone and 2,4,7,9-tetra-*tert*-butyloxepino[2,3-*b*]-benzofuran). Reaction of **91** with O_2 or PhIO at low temperature also yielded (μ-oxo)dicopper-(II) units, although as a mixture of intramolecular, dimeric, and oligomeric species.[376]

While dicopper(II) complexes with hydroxide bridges are common,[377] higher valent examples relevant to proposed pMMO or Cu-zeolite intermediates have only been examined recently.[378,379] The structurally defined dicopper(II) complexes **92** and **93** (Figure 66) were oxidized by 1-electron to yield species formulated as Cu(II)Cu(III) complexes on the basis of spectroscopic data. Both complexes exhibited axial EPR spectra consistent with a localized mixed-valent ground state, with additional support provided by DFT calculations. Subtle differences in the UV–vis data were interpreted to indicate Robin-Day[380] class II behavior for **93**.[379] For the complex derived from **92**, an additional 1-electron oxidation was proposed to yield a dicopper(III) species on the basis of Cu K-edge XAS and UV–vis redox titration results.[378] DFT calculations supported retention of the hydroxo bridges in the oxidized complexes.

4. TRICOPPER COMPOUNDS

Interest in the properties of tricopper–oxygen complexes has been stimulated by the role such species play in the reduction of O_2 to H_2O by the multicopper oxidases (MCOs) and by the postulate of tricopper species as active intermediates in pMMO. With respect to the MCOs, particular attention has been paid to identifying the so-called *"*peroxo*"* and *"*native*"* intermediates in these enzymes through spectroscopy, as described in several reviews (Figure 1e).[5,6,381] Importantly, detailed studies of relevant tricopper-oxgyen compounds have provided fundamental information useful for delineation of the structures of these

enzyme intermediates.[382] In addition, the controversial postulate of a tricopper active site in pMMO[76,86] has stimulated intriguing studies of the biological reactivity of tricopper complexes with C–H bonds.

4.1. Bis(*μ*-oxo)tricopper Complexes

Since the first report of the $[Cu_3O_2]^{3+}$ core in complexes supported by **L6a**[294] and others described in the previous review,[383,384] two other examples have been identified.[385,386] In one case, oxygenation of a Cu(I) complex of a sterically unencumbered **L4a** with O_2 generated a novel neutral complex proposed to contain the $[Cu_3O_2]^{3+}$ core on the basis of UV–vis and EPR spectroscopy (signal indicative of an S = 1 ground state), ESI-MS, and a 3:1 Cu:O_2 reaction stoichiometry.[385] Decreased electrophilic reactivity relative to other examples and the observation of oxidation of PPh_3 to $OPPh_3$ were traced to the overall neutral charge of the complex and the strong electron-donating characteristics of the **L4a** supporting ligands.

In a second example, ligands comprising bis(pyridylmethyl)-amine (**L61a**) or mono(pyridylmethyl)amine (**L61b**) chelates were preorganized to bind three Cu(I) ions by Y(III) binding to a heptadentate **L61** donor set (Figure 67).[386] Low-temperature oxygenation at low concentrations (0.05 mM) yielded $[Cu_3O_2]^{3+}$ cores as indicated by UV–vis spectroscopy and the Cu:O_2 stoichiometry. These findings contrast with the results of oxygenations of Cu(I) complexes of simple N-donor analogs, highlighting the key role of the ligand preorganization of the Ytemplate in driving the formation of the tricopper unit. The complexes were not reactive with 2,4-di-*tert*-butylphenol or DHA, but HAT was seen from TEMPOH and oxygen atom transfer was seen to PPh_3.

4.2. Other Tricopper–Oxygen Complexes

Numerous unsuccessful attempts to prepare tricopper–oxygen intermediates via oxygenation reactions of tricopper(I) complexes supported by multidentate ligands have been reported, with the formation of stable tricopper(II) motifs or undesired dicopper–oxygen units being common outcomes. [278,387,388] In addition, many examples of trinuclear copper(II) complexes have been characterized, with particular interest focused on their use as catalysts for hydrocarbon oxidations.[389–395] A full discussion of such complexes is beyond the scope of the current review. Instead, we focus on select examples of complexes of particular relevance or use in understanding the nature of the *“*native*”* and *“*peroxo*”* intermediates in MCOs or the active center in pMMO.

While oxygenation of the Cu(I) complexes of **L1a** at low temperature yielded the peroxo complex **44** (Figure 36), reaction of [(**L1a**)Cu(CH_3CN)]X (X = ClO_4^-) with O_2 at room temperature yielded the tris(hydroxo)tricopper complex **94** that models a proposed structure for the native intermediate in MCOs (Figure 68).[396] For X = $CF_3SO_3^-$, or when excess (Bu_4N)(CF_3SO_3) was added to **94**, a bis(hydroxo)dicopper complex **95** formed instead, and the preference for the species formed was traced to hydrogen bonding and ion-pairing interactions in both the solid state and THF solution. Complex **94** exhibited spin-frustration and interesting magnetic properties that were examined in detail using variable-field magnetic circular dichroism and EPR spectroscopy.[397] Subsequent detailed comparisons

were made between the properties of **94** and those of an alternative structure for the native intermediate,[398,399] namely a (μ_3-oxo)tricopper cluster which lacked additional bridging ligands.[400] It was concluded that the properties of the (μ_3-oxo)tricopper cluster best matched those of the native intermediate; the driving force for the formation of the stable (μ_3-oxo)tricopper core was shown to be critical for the overall O_2 reduction process catalyzed by the enzymes.[399]

Various tricopper complexes supported by ligands **L79a**–**f** have been shown to participate in the catalytic oxidations of hydrocarbons,[374,401,402] including the conversion of methane to methanol.[403] These results have been cited in favor of the proposition that the active site of pMMO contains a tricopper cluster.[86] A general mechanism for dioxygen activation by tricopper(I) complexes of these ligands has been proposed which involves initial formation of a (peroxo)dicopper intermediate (**96**) that undergoes O–O bond scission to yield a highly reactive mixed-valent species **97** (Figure 69). DFT calculations led to the suggestion of a mechanism for substrate oxidation by this intermediate involving "singlet oxene transfer."[85] While a provocative proposal, such a pathway remains speculative because intermediate **97** has not been identified definitively by experiment. Within this context, we note the identification of a $[Cu_3(\mu\text{-}O)_3]^{2+}$ core that hydroxylates methane in the zeolite mordenite (Figure 2).[118]

5. SUMMARY AND CONCLUSIONS

Since the publication of the previous articles published in this journal on this subject in 2004,[15,16] significant further advances have been made in our understanding of the nature of copper–oxygen complexes relevant to catalytic intermediates. New motifs have been discovered, including heterbimetallic bis(μ-oxo), $[CuOH]^{2+}$, (*cis*-1,2-peroxo)dicopper, and mixed-valent (μ-hydroxo)dicopper(II,III) cores. In addition, as described above, new examples of previously known cores have been characterized with variable supporting ligands, including simple ones like imidazoles, which more closely mimic biological donors. Moreover, new insights into the reactivity of a variety of copper–oxygen species have been obtained that have changed the way we think about their role in catalytic oxidations.

No doubt, the field has matured and the questions being addressed are ever more focused on details of spectroscopy and mechanism. Many important challenges remain, however, that continue to stimulate research. For example, while identified in the gas phase and evaluated by theory, complexes with the $[CuO]^+$ core have yet to be isolated and characterized. Postulates of novel copper-containing structures as active species in important oxidations, such as the hydroxylation of methane or the oxidative cleavage of DNA (by the ATCUN motif, for example),[98] await unequivocal verification. Indeed, the nature of the oxidant in LPMO and pMMO remains a mystery, and efforts continue to be made to synthesize and characterize relevant compounds that are capable of attacking strong C–H bonds at rapid rates, such as those with oxo/hydroxo bridges between copper ions at various oxidation levels. New catalytic oxidations using copper compounds as catalysts continue to be discovered, but firm identification of intermediates and mechanisms often is lacking. Examples span oxidations of water[404,405] and hydrocarbons,[406] reactions of particularly keen interest, because of their relevance to energy transformations. The need to understand

how such reactions proceed provides ample impetus for further study using approaches like those described herein that involve the clever use of supporting ligands to enable the detailed characterization of novel copper–oxygen compounds.

Acknowledgments

We thank all the co-workers and collaborators who contributed to the work cited in this review. Financial support for this work was provided by the National Institutes of Health (R37GM47365).

ABBREVIATIONS

ATCUN	amino terminal Cu(II)- and Ni(II)-binding
ATP	adenosine triphosphate
BDE	bond dissociation enthalpy
BNAH	1-benzyl-1,4-dihydronicotinamide
BzIm	1,3-dimethyl-2,3-dihydrobenzimidazole
CB-PPO	coupled binuclear polyphenol oxidases
C*c*O	cytochrome *c* oxidase
Cm	cumyl
CMA	*N*-cyclopropyl-*N*-methylamine
CPET	concerted proton electron transfer
D*β*M	dopamine *β*-monooxygenase
DBU	1,8-diazabicyclo-undec-7-ene
DFB	1,2-difluorobenzene
DFT	density functional theory
DHA	9,10-dihydroanthracene
DMPO	5,5-dimethyl-1-pyrroline *N*-oxide
DNA	deoxyribonucleic acid
EPR	electron paramagnetic resonance
ESI-MS	electrospray ionization-mass spectrometry
EXAFS	extended X-ray absorption fine structure
Fc	ferrocene
Fc*	decamethylferrocene
GAO	galactose oxidase

Gly	glycine
HAT	hydrogen atom transfer
HIPT	3,5-bis(2,4,6-triisopropylphenyl)phenyl
His	histidine
Im	imidazole
KIE	kinetic isotope effect
LMCT	ligand-to-metal charge transfer
LPMO	lytic polysaccharide monooxygenase
MCD	magnetic circular dichroism
MCO	multicopper oxidase
MDP	(*p*-methoxyphenyl)-2,2-dimethylpropanol
Met	methionine
MO	molecular orbital
NIH	National Institutes of Health
NMR	nuclear magnetic resonance
ORR	oxygen reduction reaction
OTf	trifluoromethanesulfonate
PCET	proton-coupled electron transfer
Phen	phenanthroline
PHM	peptidylglycine α-hydroxylating monooxygenase
pMMO	particulate methane monooxygenase
PT/ET	proton transfer/electron transfer
pz	3,5-diphenylpyrazole
ROS	reactive oxygen species
RT	room temperature
SCE	standard calomel electrode
TβM	tyramine β-monooxygenase
TD-DFT	time dependent-density functional theory
TEMPO	2,2,6,6-tetramethyl-1-piperidinyloxy radical

THF	tetrahydrofuran
TIPT	3,5-bis(2,6-diisopropylphenyl)phenyl
TMAO	trimethylamine-*N*-oxide
TMPA	tris(2-methylpyridyl)amine
TS	transition state
UV–vis	ultraviolet–visible
XAS	X-ray absorption spectroscopy
ZSM	zeolite socony mobile

References

1. Punniyamurthy T, Velusamy S, Iqbal J. Recent Advances in Transition Metal Catalyzed Oxidation of Organic Substrates with Molecular Oxygen. Chem Rev. 2005; 105:2329–2364. [PubMed: 15941216]
2. Newhouse T, Baran PS. If C-H Bonds Could Talk: Selective CH Bond Oxidation. Angew Chem, Int Ed. 2011; 50:3362–3374.
3. Wencel-Delord J, Droge T, Liu F, Glorius F. Towards mild metal-catalyzed C-H bond activation. Chem Soc Rev. 2011; 40:4740–4761. [PubMed: 21666903]
4. Yee, GM., Tolman, WB. Transition Metal Complexes and the Activation of Dioxygen. In: Kroneck, PMH.Sosa Torres, ME.Sigel, A.Sigel, H., Sigel, RKO., editors. Sustaining Life on Planet Earth: Metalloenzymes Mastering Dioxygen and Other Chewy Gases. Vol. 15. Springer; Cham, Switzerland: 2015. p. 131-204.Metal Ions in Life Sciences Series
5. Solomon EI, Heppner DE, Johnston EM, Ginsbach JW, Cirera J, Qayyum M, Kieber-Emmons MT, Kjaergaard CH, Hadt RG, Tian L. Copper Active Sites in Biology. Chem Rev. 2014; 114:3659–3853. [PubMed: 24588098]
6. Solomon EI, Sarangi R, Woertink JS, Augustine AJ, Yoon J, Ghosh S. O_2 and N_2O Activation by Bi-, Tri-, and Tetranuclear Cu Clusters in Biology. Acc Chem Res. 2007; 40:581–591. [PubMed: 17472331]
7. Ali ME, Rahman MM, Sarkar SM, Hamid SBA. Heterogeneous Metal Catalysts for Oxidation Reactions. J Nanomater. 2014; 2014:1–23.
8. Ren Y, Wang M, Chen X, Yue B, He H. Heterogeneous Catalysis of Polyoxometalate Based Organic–Inorganic Hybrids. Materials. 2015; 8:1545–1567. [PubMed: 28788017]
9. van der Vlugt, JI., Meyer, F. Homogeneous Copper-Catalyzed Oxidations. In: Meyer, F., Limberg, C., editors. Organometallic Oxidation Catalysis. Vol. 22. Springer-Verlag; Berlin: 2007. p. 191-240.Topics in Organometallic Chemistry Series
10. Allen SE, Walvoord RR, Padilla-Salinas R, Kozlowski MC. Aerobic Copper-Catalyzed Organic Reactions. Chem Rev. 2013; 113:6234–6458. [PubMed: 23786461]
11. Ryland BL, Stahl SS. Practical Aerobic Oxidations of Alcohols and Amines with Homogeneous Copper/TEMPO and Related Catalyst Systems. Angew Chem, Int Ed. 2014; 53:8824–8838.
12. Hematian S, Garcia-Bosch I, Karlin KD. Synthetic Heme/Copper Assemblies: Toward an Understanding of Cytochrome *c* Oxidase Interactions with Dioxygen and Nitrogen Oxides. Acc Chem Res. 2015; 48:2462–2474. [PubMed: 26244814]
13. Thorseth MA, Tornow CE, Tse ECM, Gewirth AA. Cu Complexes that Catalyze the Oxygen Reduction Reaction. Coord Chem Rev. 2013; 257:130–139.
14. Singh A, Spiccia L. Water Oxidation Catalysts Based on Abundant 1st Row Transition Metals. Coord Chem Rev. 2013; 257:2607–2622.

15. Mirica LM, Ottenwaelder X, Stack TDP. Structure and Spectroscopy of Copper–Dioxygen Complexes. Chem Rev. 2004; 104:1013–1046. [PubMed: 14871148]
16. Lewis EA, Tolman WB. Reactivity of Dioxygen–Copper Systems. Chem Rev. 2004; 104:1047–1076. [PubMed: 14871149]
17. Decker A, Solomon EI. Dioxygen Activation by Copper, Heme and Non-Heme Iron Enzymes: Comparison of Electronic Structures and Reactivities. Curr Opin Chem Biol. 2005; 9:152–163. [PubMed: 15811799]
18. De A, Mandal S, Mukherjee R. Modeling Tyrosinase Activity. Effect of Ligand Topology on Aromatic Ring Hydroxylation: An Overview. J Inorg Biochem. 2008; 102:1170–1189. [PubMed: 18336914]
19. Smirnov VV, Brinkley DW, Lanci MP, Karlin KD, Roth JP. Probing Metal-Mediated O_2 Activation in Chemical and Biological System. J Mol Catal A: Chem. 2006; 251:100–107.
20. Tolman WB. Using Synthetic Chemistry to Understand Copper Protein Active Sites: A Personal Perspective. JBIC, J Biol Inorg Chem. 2006; 11:261–271. [PubMed: 16447049]
21. Itoh S. Mononuclear copper active-oxygen complexes. Curr Opin Chem Biol. 2006; 10:115–122. [PubMed: 16504568]
22. Chufán EE, Puiu SC, Karlin KD. Heme–Copper/Dioxygen Adduct Formation, Properties, and Reactivity. Acc Chem Res. 2007; 40:563–572. [PubMed: 17550225]
23. Hatcher LQ, Karlin KD. Ligand Influences in Copper-Dioxygen Complex-Formation and Substrate Oxidations. Adv Inorg Chem. 2006; 58:131–184.
24. Collman JP, Decreau RA. Functional Biomimetic Models for the Active Site in the Respiratory Enzyme Cytochrome *c* Oxidase. Chem Commun. 2008:5065–5076.
25. Que L Jr, Tolman WB. Biologically Inspired Oxidation Catalysis. Nature. 2008; 455:333–340. [PubMed: 18800132]
26. Karlin, KD.Itoh, S., Rokita, S., editors. Copper-Oxygen Chemistry. Wiley Series of Reactive Intermediates in Chemistry and Biology. Vol. 4. John Wiley & Sons, Inc; Hoboken, NJ: 2011.
27. Solomon EI, Ginsbach JW, Heppner DE, Kieber-Emmons MT, Kjaergaard CH, Smeets PJ, Tian L, Woertink JS. Copper Dioxygen (Bio)inorganic Chemistry. Faraday Discuss. 2011; 148:11–39. [PubMed: 21322475]
28. Ray K, Heims F, Pfaff FF. Terminal Oxo and Imido Transition-Metal Complexes of Groups 9–11. Eur J Inorg Chem. 2013; 2013:3784–3807.
29. Haack P, Limberg C. Molecular Cu_{II}-O-Cu_{II} Complexes: Still Waters Run Deep. Angew Chem, Int Ed. 2014; 53:4282–4293.
30. Sala X, Maji S, Bofill R, García-Antón J, Escriche L, Llobet A. Molecular Water Oxidation Mechanisms Followed by Transition Metals: State of the Art. Acc Chem Res. 2014; 47:504–516. [PubMed: 24328498]
31. Gagnon N, Tolman WB. $[CuO]^+$ and $[CuOH]^{2+}$ Complexes: Intermediates in Oxidation Catalysis? Acc Chem Res. 2015; 48:2126–2131. [PubMed: 26075312]
32. Rolff M, Schottenheim J, Tuczek F. Monooxygenation of External Phenolic Substrates in Small-Molecule Dicopper Complexes: Implications on the Reaction Mechanism of Tyrosinase. J Coord Chem. 2010; 63:2382–2399.
33. Koval IA, Gamez P, Belle C, Selmeczi K, Reedijk J. Synthetic Models of the Active Site of Catechol Oxidase: Mechanistic Studies. Chem Soc Rev. 2006; 35:814–840. [PubMed: 16936929]
34. Rolff M, Schottenheim J, Decker H, Tuczek F. Copper–O_2 Reactivity of Tyrosinase Models Towards External Monophenolic Substrates: Molecular Mechanism and Comparison with the Enzyme. Chem Soc Rev. 2011; 40:4077–4098. [PubMed: 21416076]
35. Lee JY, Karlin KD. Elaboration of Copper–Oxygen Mediated C–H Activation Chemistry in Consideration of Future Fuel and Feedstock Generation. Curr Opin Chem Biol. 2015; 25:184–193. [PubMed: 25756327]
36. Ray K, Heims F, Schwalbe M, Nam W. High-Valent Metal-Oxo Intermediates in Energy Demanding Processes: From Dioxygen Reduction to Water Splitting. Curr Opin Chem Biol. 2015; 25:159–171. [PubMed: 25703840]

37. Yamaguchi S, Masuda H. Basic Approach to Development of Environment-Friendly Oxidation Catalyst Materials. Mononuclear Hydroperoxo Copper(II) Complexes. Sci Technol Adv Mater. 2005; 6:34–47.
38. Dalle KE, Meyer F. Modelling Binuclear Metallobiosites: Insights from Pyrazole-Supported Biomimetic and Bioinspired Complexes. Eur J Inorg Chem. 2015; 2015:3391–3405.
39. Serrano-Plana J, Garcia-Bosch I, Company A, Costas M. Structural and Reactivity Models for Copper Oxygenases: Cooperative Effects and Novel Reactivities. Acc Chem Res. 2015; 48:2397–2406. [PubMed: 26207342]
40. Li J, Farrokhnia M, Rulíšek L, Ryde U. Catalytic Cycle of Multicopper Oxidases Studied by Combined Quantum- and Molecular-Mechanical Free-Energy Perturbation Methods. J Phys Chem B. 2015; 119:8268–8284. [PubMed: 26039490]
41. Klinman JP. The Copper-Enzyme Family of Dopamine β-Monooxygenase and Peptidylglycine α-Hydroxylating Monooxygenase: Resolving the Chemical Pathway for Substrate Hydroxylation. J Biol Chem. 2006; 281:3013–3016. [PubMed: 16301310]
42. Hess CR, Wu Z, Ng A, Gray EE, McGuirl MA, Klinman JP. Hydroxylase Activity of Met471Cys Tyramine β-Monooxygenase. J Am Chem Soc. 2008; 130:11939–11944. [PubMed: 18710228]
43. Hess C, Klinman J, Blackburn N. The Copper Centers of Tyramine β-Monooxygenase and its Catalytic-Site Methionine Variants: An X-ray Absorption Study. JBIC, J Biol Inorg Chem. 2010; 15:1195–1207. [PubMed: 20544364]
44. Vendelboe TV, Harris P, Zhao Y, Walter TS, Harlos K, El Omari K, Christensen HEM. The crystal structure of human dopamine β-hydroxylase at 2. 9 Å resolution. Science Advances. 2016; 2:1–10.
45. Chufán EE, Prigge ST, Siebert X, Eipper BA, Mains RE, Amzel LM. Differential Reactivity between Two Copper Sites in Peptidylglycine α-Hydroxylating Monooxygenase. J Am Chem Soc. 2010; 132:15565–15572. [PubMed: 20958070]
46. Rudzka K, Moreno DM, Eipper B, Mains R, Estrin DA, Amzel LM. Coordination of Peroxide to the CuM Center of Peptidylglycine α-Hydroxylating Monooxygenase (PHM): Structural and Computational Study. JBIC, J Biol Inorg Chem. 2013; 18:223–232. [PubMed: 23247335]
47. Hemsworth GR, Davies GJ, Walton PH. Recent Insights Into Copper-Containing Lytic Polysaccharide Mono-Oxygenases. Curr Opin Struct Biol. 2013; 23:660–668. [PubMed: 23769965]
48. Kjaergaard CH, Qayyum MF, Wong SD, Xu F, Hemsworth GR, Walton DJ, Young NA, Davies GJ, Walton PH, Johansen KS, Hodgson KO, Hedman B, Solomon EI. Spectroscopic and computational insight into the activation of O_2 by the mononuclear Cu center in polysaccharide monooxygenases. Proc Natl Acad Sci U S A. 2014; 111:8797–8802. [PubMed: 24889637]
49. Gudmundsson M, Kim S, Wu M, Ishida T, Momeni MH, Vaaje-Kolstad G, Lundberg D, Royant A, Ståhlberg J, Eijsink VGH, et al. Structural and Electronic Snapshots during the Transition from a Cu(II) to Cu(I) Metal Center of a Lytic Polysaccharide Monooxygenase by X-ray Photoreduction. J Biol Chem. 2014; 289:18782–18792. [PubMed: 24828494]
50. Hemsworth GR, Henrissat B, Davies GJ, Walton PH. Discovery and Characterization of a New Family of Lytic Polysaccharide Monooxygenases. Nat Chem Biol. 2013; 10:122–126. [PubMed: 24362702]
51. Lo Leggio L, Simmons TJ, Poulsen JCN, Frandsen KEH, Hemsworth GR, Stringer MA, von Freiesleben P, Tovborg M, Johansen KS, De Maria L, et al. Structure and Boosting Activity of a Starch-Degrading Lytic Polysaccharide Monooxygenase. Nat Commun. 2015; 6:5961–5969. [PubMed: 25608804]
52. Culpepper MA, Rosenzweig AC. Architecture and Active Site of Particulate Methane Monooxygenase. Crit Rev Biochem Mol Biol. 2012; 47:483–492. [PubMed: 22725967]
53. Bollinger JM Jr, Krebs C. Enzymatic C–H Activation by Metal–Superoxo Intermediates. Curr Opin Chem Biol. 2007; 11:151–158. [PubMed: 17374503]
54. Prigge ST, Eipper BA, Mains RE, Amzel LM. Dioxygen Binds End-On to Mononuclear Copper in a Precatalytic Enzyme Complex. Science. 2004; 304:864–867. [PubMed: 15131304]
55. Chen P, Bell J, Eipper BA, Solomon EI. Oxygen Activation by the Noncoupled Binuclear Copper Site in Peptidylglycine α-Hydroxylating Monooxygenase. Spectroscopic Definition of the Resting

Sites and the Putative Cu_{II}^{M}–OOH Intermediate. Biochemistry. 2004; 43:5735–5747. [PubMed: 15134448]

56. Meliá C, Ferrer S, Řezáč J, Parisel O, Reinaud O, Moliner V, de la Lande A. Investigation of the Hydroxylation Mechanism of Noncoupled Copper Oxygenases by Ab Initio Molecular Dynamics Simulations. Chem - Eur J. 2013; 19:17328–17337. [PubMed: 24259416]
57. Rezabal E, Gauss J, Matxain JM, Berger R, Diefenbach M, Holthausen MC. Quantum Chemical Assessment of the Binding Energy of CuO^+ J Chem Phys. 2011; 134:064304-1–064304-13. [PubMed: 21322677]
58. Chen P, Solomon EI. O_2 activation by Binuclear Cu Sites: Noncoupled Versus Exchange Coupled Reaction Mechanisms. Proc Natl Acad Sci U S A. 2004; 101:13105–13110. [PubMed: 15340147]
59. Kamachi T, Kihara N, Shiota Y, Yoshizawa K. Computational Exploration of the Catalytic Mechanism of Dopamine β-Monooxygenase: Modeling of Its Mononuclear Copper Active Sites. Inorg Chem. 2005; 44:4226–4236. [PubMed: 15934751]
60. Yoshizawa K, Kihara N, Kamachi T, Shiota Y. Catalytic Mechanism of Dopamine β-Monooxygenase Mediated by Cu(III)-Oxo. Inorg Chem. 2006; 45:3034–3041. [PubMed: 16562959]
61. Kim S, Ståhlberg J, Sandgren M, Paton RS, Beckham GT. Quantum Mechanical Calculations Suggest that Lytic Polysaccharide Monooxygenases Use a Copper-Oxyl, Oxygen-Rebound Mechanism. Proc Natl Acad Sci U S A. 2014; 111:149–154. [PubMed: 24344312]
62. Magnus KA, Ton-That H, Carpenter JE. Recent Structural Work on the Oxygen Transport Protein Hemocyanin. Chem Rev. 1994; 94:727–735.
63. Matoba Y, Kumagai T, Yamamoto A, Yoshitsu H, Sugiyama M. Crystallographic Evidence That the Dinuclear Copper Center of Tyrosinase Is Flexible during Catalysis. J Biol Chem. 2006; 281:8981–8990. [PubMed: 16436386]
64. Gerdemann C, Eicken C, Krebs B. The Crystal Structure of Catechol Oxidase: New Insight into the Function of Type-3 Copper Proteins. Acc Chem Res. 2002; 35:183–191. [PubMed: 11900522]
65. Ginsbach JW, Kieber-Emmons MT, Nomoto R, Noguchi A, Ohnishi Y, Solomon EI. Structure/Function Correlations Among Coupled Binuclear Copper Proteins Through Spectroscopic and Reactivity Studies of NspF. Proc Natl Acad Sci U S A. 2012; 109:10793–10797. [PubMed: 22711806]
66. Decker H, Schweikardt T, Nillius D, Salzbrunn U, Jaenicke E, Tuczek F. Similar Enzyme Activation and Catalysis in Hemocyanins and Tyrosinases. Gene. 2007; 398:183–191. [PubMed: 17566671]
67. Inoue T, Shiota Y, Yoshizawa K. Quantum Chemical Approach to the Mechanism for the Biological Conversion of Tyrosine to Dopaquinone. J Am Chem Soc. 2008; 130:16890–16897. [PubMed: 19007228]
68. Halfen JA, Mahapatra S, Wilkinson EC, Kaderli S, Young VG, Que L, Zuberbuhler AD, Tolman WB. Reversible Cleavage and Formation of the Dioxygen O-O Bond Within a Dicopper Complex. Science. 1996; 271:1397–1400. [PubMed: 8596910]
69. Cahoy J, Holland PL, Tolman WB. Experimental Studies of the Interconversion of μ-η^2: η^2-Peroxo- and Bis(μ-oxo)dicopper Complexes. Inorg Chem. 1999; 38:2161–2168. [PubMed: 11671001]
70. Himes RA, Karlin KD. Copper–Dioxygen Complex Mediated C–H Bond Oxygenation: Relevance for Particulate Methane Monooxygenase (pMMO). Curr Opin Chem Biol. 2009; 13:119–131. [PubMed: 19286415]
71. Culpepper MA, Cutsail GE, Hoffman BM, Rosenzweig AC. Evidence for Oxygen Binding at the Active Site of Particulate Methane Monooxygenase. J Am Chem Soc. 2012; 134:7640–7643. [PubMed: 22540911]
72. Yoshizawa K, Shiota Y. Conversion of Methane to Methanol at the Mononuclear and Dinuclear Copper Sites of Particulate Methane Monooxygenase (pMMO): A DFT and QM/MM Study. J Am Chem Soc. 2006; 128:9873–9881. [PubMed: 16866545]
73. Shiota Y, Yoshizawa K. Comparison of the Reactivity of Bis(μ-oxo)$Cu^{II}Cu^{III}$ and $Cu^{III}Cu^{III}$ Species to Methane. Inorg Chem. 2009; 48:838–845. [PubMed: 19113938]

74. Itoyama S, Doitomi K, Kamachi T, Shiota Y, Yoshizawa K. Possible Peroxo State of the Dicopper Site of Particulate Methane Monooxygenase from Combined Quantum Mechanics and Molecular Mechanics Calculations. Inorg Chem. 2016; 55:2771–2775. [PubMed: 26918461]
75. Da Silva JCS, Pennifold RCR, Harvey JN, Rocha WR. A Radical Rebound Mechanism for the Methane Oxidation Reaction Promoted by the Dicopper Center of a pMMO Enzyme: A Computational Perspective. Dalton Trans. 2016; 45:2492–2504. [PubMed: 26697968]
76. Sirajuddin S, Rosenzweig AC. Enzymatic Oxidation of Methane. Biochemistry. 2015; 54:2283–2294. [PubMed: 25806595]
77. Balasubramanian R, Rosenzweig AC. Structural and Mechanistic Insights into Methane Oxidation by Particulate Methane Monooxygenase. Acc Chem Res. 2007; 40:573–580. [PubMed: 17444606]
78. Balasubramanian R, Smith SM, Rawat S, Yatsunyk LA, Stemmler TL, Rosenzweig AC. Oxidation of Methane by a Biological Dicopper Centre. Nature. 2010; 465:115–119. [PubMed: 20410881]
79. Smith SM, Rawat S, Telser J, Hoffman BM, Stemmler TL, Rosenzweig AC. Crystal Structure and Characterization of Particulate Methane Monooxygenase from Methylocystis species Strain M. Biochemistry. 2011; 50:10231–10240. [PubMed: 22013879]
80. Rosenzweig AC, Sazinsky MH. Structural Insights into Dioxygen-Activating Copper Enzymes. Curr Opin Struct Biol. 2006; 16:729–735. [PubMed: 17011183]
81. Vanelderen P, Vancauwenbergh J, Sels BF, Schoonheydt RA. Coordination Chemistry and Reactivity of Copper in Zeolites. Coord Chem Rev. 2013; 257:483–494.
82. Vanelderen P, Hadt RG, Smeets PJ, Solomon EI, Schoonheydt RA, Sels BF. Cu-ZSM-5: A Biomimetic Inorganic Model for Methane Oxidation. J Catal. 2011; 284:157–164. [PubMed: 23487537]
83. Yumura T, Hirose Y, Wakasugi T, Kuroda Y, Kobayashi H. Roles of Water Molecules in Modulating the Reactivity of Dioxygen-Bound Cu-ZSM-5 toward Methane: A Theoretical Prediction. ACS Catal. 2016; 6:2487–2495.
84. Lawton TJ, Rosenzweig AC. Methane-Oxidizing Enzymes: An Upstream Problem in Biological Gas-to-Liquids Conversion. J Am Chem Soc. 2016; 138:9327–9340. [PubMed: 27366961]
85. Chen PPY, Chan SI. Theoretical Modeling of the Hydroxylation of Methane as Mediated by the Particulate Methane Monooxygenase. J Inorg Biochem. 2006; 100:801–809. [PubMed: 16494948]
86. Chan SI, Yu SSF. Controlled Oxidation of Hydrocarbons by the Membrane-Bound Methane Monooxygenase: The Case for a Tricopper Cluster. Acc Chem Res. 2008; 41:969–979. [PubMed: 18605740]
87. Shao M, Chang Q, Dodelet JP, Chenitz R. Recent Advances in Electrocatalysts for Oxygen Reduction Reaction. Chem Rev. 2016; 116:3594–3657. [PubMed: 26886420]
88. Yoshikawa S, Shimada A. Reaction Mechanism of Cytochrome *c* Oxidase. Chem Rev. 2015; 115:1936–1989. [PubMed: 25603498]
89. Kaila VRI, Verkhovsky MI, Wikström M. Proton-Coupled Electron Transfer in Cytochrome Oxidase. Chem Rev. 2010; 110:7062–7081. [PubMed: 21053971]
90. Kim E, Chufán EE, Kamaraj K, Karlin KD. Synthetic Models for Heme–Copper Oxidases. Chem Rev (Washington, DC, U S). 2004; 104:1077–1134.
91. Karlin KD, Kim E. Ligand Influences in Heme–Copper O_2-Chemistry as Synthetic Models for Cytochrome *c* Oxidase. Chem Lett. 2004; 33:1226–1231.
92. Decreau RA, Collman JP, Hosseini A. Electrochemical Applications. How Click Chemistry Brought Biomimetic Models to the Next Level: Electrocatalysis Under Controlled Rate of Electron Transfer. Chem Soc Rev. 2010; 39:1291–1301. [PubMed: 20349534]
93. Collman JP, Boulatov R, Sunderland CJ, Fu L. Functional Analogues of Cytochrome *c* Oxidase, Myoglobin, and Hemoglobin. Chem Rev. 2004; 104:561–588. [PubMed: 14871135]
94. Collman JP, Ghosh S. Recent Applications of a Synthetic Model of Cytochrome *c* Oxidase: Beyond Functional Modeling. Inorg Chem. 2010; 49:5798–5810. [PubMed: 20527796]
95. Chatterjee S, Sengupta K, Hematian S, Karlin KD, Dey A. Electrocatalytic O_2-Reduction by Synthetic Cytochrome *c* Oxidase Mimics: Identification of a "Bridging Peroxo" Intermediate Involved in Facile $4e^-/4H^+$ O_2-Reduction. J Am Chem Soc. 2015; 137:12897–12905. [PubMed: 26419806]

96. Wende C, Lüdtke C, Kulak N. Copper Complexes of NDonor Ligands as Artificial Nucleases. Eur J Inorg Chem. 2014; 2014:2597–2612.

97. Tegoni M, Valensin D, Toso L, Remelli M. Copper Chelators: Chemical Properties and Biomedical Applications. Curr Med Chem. 2014; 21:3785–3818. [PubMed: 24934357]

98. Jin Y, Cowan JA. DNA Cleavage by Copper–ATCUN Complexes. Factors Influencing Cleavage Mechanism and Linearization of dsDNA. J Am Chem Soc. 2005; 127:8408–8415. [PubMed: 15941274]

99. Harford C, Sarkar B. Amino Terminal Cu(II)- and Ni(II)-Binding (ATCUN) Motif of Proteins and Peptides: Metal Binding, DNA Cleavage, and Other Properties. Acc Chem Res. 1997; 30:123–130.

100. Yu Z, Han M, Cowan JA. Toward the Design of a Catalytic Metallodrug: Selective Cleavage of G-Quadruplex Telomeric DNA by an Anticancer Copper–Acridine–ATCUN Complex. Angew Chem, Int Ed. 2015; 54:1901–1905.

101. Joyner JC, Reichfield J, Cowan JA. Factors Influencing the DNA Nuclease Activity of Iron, Cobalt, Nickel, and Copper Chelates. J Am Chem Soc. 2011; 133:15613–15626. [PubMed: 21815680]

102. Gaggelli E, Kozlowski H, Valensin D, Valensin G. Copper Homeostasis and Neurodegenerative Disorders (Alzheimer's, Prion, and Parkinson's Diseases and Amyotrophic Lateral Sclerosis). Chem Rev. 2006; 106:1995–2044. [PubMed: 16771441]

103. Barnham KJ, Bush AI. Metals in Alzheimer's and Parkinson's Diseases. Curr Opin Chem Biol. 2008; 12:222–228. [PubMed: 18342639]

104. Hureau C, Faller P. Aβ-mediated ROS Production by Cu Ions: Structural Insights, Mechanisms and Relevance to Alzheimer's Disease. Biochimie. 2009; 91:1212–1217. [PubMed: 19332103]

105. Barnham KJ, Bush AI. Biological Metals and Metal-Targeting Compounds in Major Neurodegenerative Diseases. Chem Soc Rev. 2014; 43:6727–6749. [PubMed: 25099276]

106. McCann SD, Stahl SS. Mechanism of Copper/Azodicarboxylate-Catalyzed Aerobic Alcohol Oxidation: Evidence for Uncooperative Catalysis. J Am Chem Soc. 2016; 138:199–206. [PubMed: 26694091]

107. Tsang ASK, Kapat A, Schoenebeck F. Factors That Control C–C Cleavage versus C–H Bond Hydroxylation in Copper-Catalyzed Oxidations of Ketones with O_2. J Am Chem Soc. 2016; 138:518–526. [PubMed: 26675262]

108. Alayon EMC, Nachtegaal M, Ranocchiari M, van Bokhoven JA. Catalytic Conversion of Methane to Methanol Using Cu-Zeolites. Chimia. 2012; 66:668–674. [PubMed: 23211724]

109. Tomkins P, Mansouri A, Bozbag SE, Krumeich F, Park MB, Alayon EMC, Ranocchiari M, van Bokhoven JA. Isothermal Cyclic Conversion of Methane into Methanol over Copper-Exchanged Zeolite at Low Temperature. Angew Chem, Int Ed. 2016; 55:5467–5471.

110. Himes RA, Karlin KD. A New Copper-Oxo Player in Methane Oxidation. Proc Natl Acad Sci U S A. 2009; 106:18877–18878. [PubMed: 19889982]

111. Groothaert MH, Smeets PJ, Sels BF, Jacobs PA, Schoonheydt RA. Selective Oxidation of Methane by the Bis(μ-oxo)dicopper Core Stabilized on ZSM-5 and Mordenite Zeolites. J Am Chem Soc. 2005; 127:1394–1395. [PubMed: 15686370]

112. Woertink JS, Smeets PJ, Groothaert MH, Vance MA, Sels BF, Schoonheydt RA, Solomon EI. A $[Cu_2O]^{2+}$ Core in Cu-ZSM-5, the Active Site in the Oxidation of Methane to Methanol. Proc Natl Acad Sci U S A. 2009; 106:18908–18913. [PubMed: 19864626]

113. Vanelderen P, Snyder BER, Tsai ML, Hadt RG, Vancauwenbergh J, Coussens O, Schoonheydt RA, Sels BF, Solomon EI. Spectroscopic Definition of the Copper Active Sites in Mordenite: Selective Methane Oxidation. J Am Chem Soc. 2015; 137:6383–6392. [PubMed: 25914019]

114. Alayon EMC, Nachtegaal M, Bodi A, Ranocchiari M, van Bokhoven JA. Bis(μ-oxo) Versus Mono(μ-oxo)dicopper Cores in a Zeolite for Converting Methane to Methanol: an in situ XAS and DFT Investigation. Phys Chem Chem Phys. 2015; 17:7681–7693. [PubMed: 25732559]

115. Smeets PJ, Hadt RG, Woertink JS, Vanelderen P, Schoonheydt RA, Sels BF, Solomon EI. Oxygen Precursor to the Reactive Intermediate in Methanol Synthesis by Cu-ZSM-5. J Am Chem Soc. 2010; 132:14736–14738. [PubMed: 20923156]

116. Alayon EM, Nachtegaal M, Ranocchiari M, van Bokhoven JA. Catalytic Conversion of Methane to Methanol over Cu–mordenite. Chem Commun. 2012; 48:404–406.

117. Alayon EMC, Nachtegaal M, Bodi A, van Bokhoven JA. Reaction Conditions of Methane-to-Methanol Conversion Affect the Structure of Active Copper Sites. ACS Catal. 2014; 4:16–22.
118. Grundner S, Markovits MAC, Li G, Tromp M, Pidko EA, Hensen EJM, Jentys A, Sanchez-Sanchez M, Lercher JA. Single-site Trinuclear Copper Oxygen Clusters in Mordenite for Selective Conversion of Methane to Methanol. Nat Commun. 2015; 6:7546. [PubMed: 26109507]
119. Kulkarni AR, Zhao ZJ, Siahrostami S, Nørskov JK, Studt F. Monocopper Active Site for Partial Methane Oxidation in Cu-Exchanged 8MR Zeolites. ACS Catal. 2016; 6:6531–6536.
120. Reinaud O, Capdevielle P, Maumy M. Copper(II) Mediated Aromatic Hydroxylation by Trimethylamine N-oxide. J Chem Soc, Chem Commun. 1990:566–568.
121. Comba P, Knoppe S, Martin B, Rajaraman G, Rolli C, Shapiro B, Stork T. Copper(II)-Mediated Aromatic ortho-Hydroxylation: A Hybrid DFT and Ab Initio Exploration. Chem - Eur J. 2008; 14:344–357. [PubMed: 17907133]
122. Conde A, Vilella L, Balcells D, Diaz-Requejo MM, Lledos A, Perez PJ. Introducing Copper as Catalyst for Oxidative Alkane Dehydrogenation. J Am Chem Soc. 2013; 135:3887–3896. [PubMed: 23409843]
123. Cramer CJ, Tolman WB. Mononuclear CuO_2 complexes: Geometries, Spectroscopic Properties, Electronic Structures, and Reactivity. Acc Chem Res. 2007; 40:601–608. [PubMed: 17458929]
124. Itoh S. Developing Mononuclear Copper–Active-Oxygen Complexes Relevant to Reactive Intermediates of Biological Oxidation Reactions. Acc Chem Res. 2015; 48:2066–2074. [PubMed: 26086527]
125. Schatz M, Raab V, Foxon SP, Brehm G, Schneider S, Reiher M, Holthausen MC, Sundermeyer J, Schindler S. Combined Spectroscopic and Theoretical Evidence for a Persistent End-On Copper Superoxo Complex. Angew Chem, Int Ed. 2004; 43:4360–4363.
126. Würtele C, Gaoutchenova E, Harms K, Holthausen MC, Sundermeyer J, Schindler S. Crystallographic Characterization of a Synthetic 1:1 End-On Copper Dioxygen Adduct Complex. Angew Chem, Int Ed. 2006; 45:3867–3869.
127. Lee JY, Peterson RL, Ohkubo K, Garcia-Bosch I, Himes RA, Woertink J, Moore CD, Solomon EI, Fukuzumi S, Karlin KD. Mechanistic Insights into the Oxidation of Substituted Phenols via Hydrogen Atom Abstraction by a Cupric–Superoxo Complex. J Am Chem Soc. 2014; 136:9925–9937. [PubMed: 24953129]
128. Donoghue PJ, Gupta AK, Boyce DW, Cramer CJ, Tolman WB. An Anionic, Tetragonal Copper(II) Superoxide Complex. J Am Chem Soc. 2010; 132:15869–15871. [PubMed: 20977226]
129. Kobayashi Y, Ohkubo K, Nomura T, Kubo M, Fujieda N, Sugimoto H, Fukuzumi S, Goto K, Ogura T, Itoh S. Copper(I)-Dioxygen Reactivity in a Sterically Demanding Tripodal Tetradentate tren Ligand: Formation and Reactivity of a Mononuclear Copper(II) End-On Superoxo Complex. Eur J Inorg Chem. 2012; 2012:4574–4578.
130. Peterson RL, Himes RA, Kotani H, Suenobu T, Tian L, Siegler MA, Solomon EI, Fukuzumi S, Karlin KD. Cupric Superoxo-Mediated Intermolecular C–H Activation Chemistry. J Am Chem Soc. 2011; 133:1702–1705. [PubMed: 21265534]
131. Kunishita A, Kubo M, Sugimoto H, Ogura T, Sato K, Takui T, Itoh S. Mononuclear Copper(II)–Superoxo Complexes that Mimic the Structure and Reactivity of the Active Centers of PHM and DβM. J Am Chem Soc. 2009; 131:2788–2789. [PubMed: 19209864]
132. Lanci MP, Smirnov VV, Cramer CJ, Gauchenova EV, Sundermeyer J, Roth JP. Isotopic Probing of Molecular Oxygen Activation at Copper(I) Sites. J Am Chem Soc. 2007; 129:14697–14709. [PubMed: 17960903]
133. Woertink JS, Tian L, Maiti D, Lucas HR, Himes RA, Karlin KD, Neese F, Würtele C, Holthausen MC, Bill E, et al. Spectroscopic and Computational Studies of an End-on Bound Superoxo-Cu(II) Complex: Geometric and Electronic Factors That Determine the Ground State. Inorg Chem. 2010; 49:9450–9459. [PubMed: 20857998]
134. Peterson RL, Ginsbach JW, Cowley RE, Qayyum MF, Himes RA, Siegler MA, Moore CD, Hedman B, Hodgson KO, Fukuzumi S, et al. Stepwise Protonation and Electron-Transfer

Reduction of a Primary Copper-Dioxygen Adduct. J Am Chem Soc. 2013; 135:16454–16467. [PubMed: 24164682]

135. Ginsbach JW, Peterson RL, Cowley RE, Karlin KD, Solomon EI. Correlation of the Electronic and Geometric Structures in Mononuclear Copper(II) Superoxide Complexes. Inorg Chem. 2013; 52:12872–12874. [PubMed: 24164429]
136. Maiti D, Fry HC, Woertink JS, Vance MA, Solomon EI, Karlin KD. A 1:1 Copper–Dioxygen Adduct is an End-on Bound Superoxo Copper(II) Complex which Undergoes Oxygenation Reactions with Phenols. J Am Chem Soc. 2007; 129:264–265. [PubMed: 17212392]
137. Kim S, Lee JY, Cowley RE, Ginsbach JW, Siegler MA, Solomon EI, Karlin KD. A N_3S(thioether)-Ligated Cu^{II}-Superoxo with Enhanced Reactivity. J Am Chem Soc. 2015; 137:2796–2799. [PubMed: 25697226]
138. Sarangi R, Aboelella N, Fujisawa K, Tolman WB, Hedman B, Hodgson KO, Solomon EI. X-ray Absorption Edge Spectroscopy and Computational Studies on $LCuO_2$ Species: Superoxide–Cu^{II} versus Peroxide–Cu^{III} Bonding. J Am Chem Soc. 2006; 128:8286–8296. [PubMed: 16787093]
139. Hill LMR, Gherman BF, Aboelella NW, Cramer CJ, Tolman WB. Electronic Tuning of β-Diketiminate Ligands with Fluorinated Substituents: Effects on the O_2-Reactivity of Mononuclear Cu(I) Complexes. Dalton Trans. 2006:4944–4953. [PubMed: 17047744]
140. Reynolds AM, Gherman BF, Cramer CJ, Tolman WB. Characterization of a 1:1 Cu-O_2 Adduct Supported by an Anilido Imine ligand. Inorg Chem. 2005; 44:6989–6997. [PubMed: 16180861]
141. Aboelella NW, Gherman BF, Hill LMR, York JT, Holm N, Young VG, Cramer CJ, Tolman WB. Effects of Thioether Substituents on the O_2 reactivity of β-Diketiminate-Cu(I) complexes: Probing the Role of the Methionine Ligand in Copper Monooxygenases. J Am Chem Soc. 2006; 128:3445–3458. [PubMed: 16522125]
142. Kjaergaard CH, Qayyum MF, Wong SD, Xu F, Hemsworth GR, Walton DJ, Young NA, Davies GJ, Walton PH, Johansen KS, et al. Spectroscopic and Computational Insight into the Activation of O_2 by the Mononuclear Cu Center in Polysaccharide Monooxygenases. Proc Natl Acad Sci U S A. 2014; 111:8797–8802. [PubMed: 24889637]
143. Cramer CJ, Gour JR, Kinal A, Wloch M, Piecuch P, Shahi ARM, Gagliardi L. Stereoelectronic Effects on Molecular Geometries and State-Energy Splittings of Ligated Monocopper Dioxygen Complexes. J Phys Chem A. 2008; 112:3754–3767. [PubMed: 18341313]
144. Weitzer M, Schindler S, Brehm G, Schneider S, Hörmann E, Jung B, Kaderli S, Zuberbühler AD. Reversible Binding of Dioxygen by the Copper(I) Complex with Tris(2-dimethylaminoethyl)amine (Me_6tren) Ligand. Inorg Chem. 2003; 42:1800–1806. [PubMed: 12639112]
145. Komiyama K, Furutachi H, Nagatomo S, Hashimoto A, Hayashi H, Fujinami S, Suzuki M, Kitagawa T. Dioxygen Reactivity of Copper(I) Complexes with Tetradentate Tripodal Ligands Having Aliphatic Nitrogen Donors: Synthesis, Structures, and Properties of Peroxo and Superoxo Complexes. Bull Chem Soc Jpn. 2004; 77:59–72.
146. Chaudhuri P, Hess M, Weyhermüller T, Wieghardt K. Aerobic Oxidation of Primary Alcohols by a New Mononuclear Cu^{II}-Radical Catalyst. Angew Chem, Int Ed. 1999; 38:1095–1098.
147. Fujisawa K, Tanaka M, Moro-oka Y, Kitajima N. A Monomeric Side-On Superoxocopper(II) Complex: Cu(O_2) (HB(3-*t*Bu-5-*i*Prpz)$_3$. J Am Chem Soc. 1994; 116:12079–12080.
148. Chen P, Root DE, Campochiaro C, Fujisawa K, Solomon EI. Spectroscopic and Electronic Structure Studies of the Diamagnetic Side-On Cu^{II}-Superoxo Complex Cu(O_2)[HB(3-R-5-*i*Prpz)$_3$]: Anti-ferromagnetic Coupling versus Covalent Delocalization. J Am Chem Soc. 2003; 125:466–474. [PubMed: 12517160]
149. Spencer DJE, Aboelella NW, Reynolds AM, Holland PL, Tolman WB. β-Diketiminate Ligand Backbone Structural Effects on Cu(I)/O_2 Reactivity: Unique Copper-Superoxo and Bis(μ-oxo) Complexes. J Am Chem Soc. 2002; 124:2108–2809. [PubMed: 11878952]
150. Aboelella NW, Lewis EA, Reynolds AM, Brennessel WW, Cramer CJ, Tolman WB. Snapshots of Dioxygen Activation by Copper: The Structure of a 1:1 Cu/O_2 Adduct and Its Use in Syntheses of Asymmetric Bis(μ-oxo) Complexes. J Am Chem Soc. 2002; 124:10660–10661. [PubMed: 12207513]

151. Aboelella NW, Kryatov SV, Gherman BF, Brennessel WW, Young VG, Sarangi R, Rybak-Akimova EV, Hodgson KO, Hedman B, Solomon EI, et al. Dioxygen Activation at a Single Copper Site: Structure, Bonding, and Mechanism of Formation of 1:1 Cu–O_2 Adducts. J Am Chem Soc. 2004; 126:16896–16911. [PubMed: 15612729]
152. Pantazis DA, McGrady JE. On the Nature of the Bonding in 1:1 Adducts of O_2. Inorg Chem. 2003; 42:7734–7736. [PubMed: 14632488]
153. Gherman BF, Cramer CJ. Modeling the Peroxide/Superoxide Continuum in 1:1 Side-on Adducts of O_2 with Cu. Inorg Chem. 2004; 43:7281–7283. [PubMed: 15530076]
154. Cramer CJ, Tolman WB, Theopold KH, Rheingold AL. Variable Character of O-O and M-O Bonding in Side-on (η^2) 1:1 Metal Complexes of O_2. Proc Natl Acad Sci U S A. 2003; 100:3635–3640. [PubMed: 12634422]
155. Lanci MP, Roth JP. Oxygen Isotope Effects upon Reversible O_2-Binding Reactions: Characterizing Mononuclear Superoxide and Peroxide Structures. J Am Chem Soc. 2006; 128:16006–16007. [PubMed: 17165732]
156. Tian G, Klinman JP. Discrimination Between ^{16}O and ^{18}O in Oxygen Binding to the Reversible Oxygen Carriers Hemoglobin, Myoglobin, Hemerythrin, and Hemocyanin: A New Probe for Oxygen Binding and Reductive Activation by Proteins. J Am Chem Soc. 1993; 115:8891–8897.
157. Harata M, Jitsukawa K, Masuda H, Einaga H. A Structurally Characterized Mononuclear Copper(II)-Superoxo Complex. J Am Chem Soc. 1994; 116:10817–10818.
158. Berreau LM, Mahapatra S, Halfen JA, Young VG, Tolman WB. Independent Synthesis and Structural Characterization of a Mononuclear Copper–Hydroxide Complex Previously Assigned as a Copper–Superoxide Species. Inorg Chem. 1996; 35:6339–6342.
159. Sanchez-Eguia BN, Flores-Alamo M, Orio M, Castillo I. Side-on Cupric-Superoxo Triplet Complexes as Competent Agents for H-abstraction Relevant to the Active Site of PHM. Chem Commun. 2015; 51:11134–11137.
160. Saracini C, Liakos DG, Zapata Rivera JE, Neese F, Meyer GJ, Karlin KD. Excitation Wavelength Dependent O_2 Release from Copper(II)–Superoxide Compounds: Laser Flash-Photolysis Experiments and Theoretical Studies. J Am Chem Soc. 2014; 136:1260–1263. [PubMed: 24428309]
161. Lucas HR, Meyer GJ, Karlin KD. CO and O_2 Binding to Pseudo-tetradentate Ligand–Copper(I) Complexes with a Variable NDonor Moiety: Kinetic/Thermodynamic Investigation Reveals Ligand-Induced Changes in Reaction Mechanism. J Am Chem Soc. 2010; 132:12927–12940. [PubMed: 20726586]
162. Kunishita A, Ertem MZ, Okubo Y, Tano T, Sugimoto H, Ohkubo K, Fujieda N, Fukuzumi S, Cramer CJ, Itoh S. Active Site Models for the Cu_A Site of Peptidylglycine α-Hydroxylating Monooxygenase and Dopamine β-Monooxygenase. Inorg Chem. 2012; 51:9465–9480. [PubMed: 22908844]
163. Fry HC, Scaltrito DV, Karlin KD, Meyer GJ. The Rate of O_2 and CO Binding to a Copper Complex, Determined by a "Flashand-Trap" Technique, Exceeds that for Hemes. J Am Chem Soc. 2003; 125:11866–11871. [PubMed: 14505408]
164. Astner J, Weitzer M, Foxon SP, Schindler S, Heinemann FW, Mukherjee J, Gupta R, Mahadevan V, Mukherjee R. Syntheses, Characterization, and Reactivity of Copper Complexes with Tridentate N-Donor Ligands. Inorg Chim Acta. 2008; 361:279–292.
165. Smirnov VV, Roth JP. Evidence for Cu–O_2 Intermediates in Superoxide Oxidations by Biomimetic Copper(II) Complexes. J Am Chem Soc. 2006; 128:3683–3695. [PubMed: 16536541]
166. Spencer DJE, Reynolds AM, Holland PL, Jazdzewski BA, Duboc-Toia C, Le Pape L, Yokota S, Tachi Y, Itoh S, Tolman WB. Copper Chemistry of β-Diketiminate Ligands: Monomer/Dimer Equilibria and a New Class of Bis(μ-oxo)dicopper Compounds. Inorg Chem. 2002; 41:6307–6321. [PubMed: 12444774]
167. Aboelella NW, York JT, Reynolds AM, Fujita K, Kinsinger CR, Cramer CJ, Riordan CG, Tolman WB. Mixed Metal Bis(μ-oxo) complexes with $[CuM(\mu\text{-}O)_2]^{n+}$ (M = Ni(III) or Pd(II)) cores. Chem Commun. 2004:1716–1717.

168. York JT, Young VG, Tolman WB. Heterobimetallic Activation of Dioxygen: Characterization and Reactivity of Novel Cu(I)-Ge(II) Complexes. Inorg Chem. 2006; 45:4191–4198. [PubMed: 16676981]

169. Gherman BF, Heppner DE, Tolman WB, Cramer CJ. Models for Dioxygen Activation by the Cu^{B} Site of Dopamine β-Monooxygenase and Peptidylglycine α-Hydroxylating Monooxygenase. JBIC, J Biol Inorg Chem. 2006; 11:197–205. [PubMed: 16344970]

170. Reynolds AM, Lewis EA, Aboelella NW, Tolman WB. Reactivity of a 1:1 Copper-Oxygen Complex: Isolation of a Cu(II)-*o*-Iminosemiquinonato Species. Chem Commun. 2005:2014–2016.

171. Karlin KD, Cohen BI, Jacobson RR, Zubieta J. Dioxygen-Copper Reactivity: Hydroxylation-Induced Methyl Migration in a Copper Monooxygenase Model System. J Am Chem Soc. 1987; 109:6194–6196.

172. Laitar DS, Mathison CJN, Davis WM, Sadighi JP. Copper(I) Complexes of a Heavily Fluorinated β-Diketiminate Ligand: Synthesis, Electronic Properties, and Intramolecular Aerobic Hydroxylation. Inorg Chem. 2003; 42:7354–7356. [PubMed: 14606823]

173. Sterckx H, De Houwer J, Mensch C, Caretti I, Tehrani KA, Herrebout WA, Van Doorslaer S, Maes BUW. Mechanism of the Cu^{II}-catalyzed benzylic oxygenation of (aryl)(heteroaryl)methanes with oxygen. Chem Sci. 2016; 7:346–357.

174. Tano T, Okubo Y, Kunishita A, Kubo M, Sugimoto H, Fujieda N, Ogura T, Itoh S. Redox Properties of a Mononuclear Copper(II)-Superoxide Complex. Inorg Chem. 2013; 52:10431–10437. [PubMed: 24004030]

175. Maiti D, Lee DH, Gaoutchenova K, Würtele C, Holthausen MC, Narducci Sarjeant AA, Sundermeyer J, Schindler S, Karlin KD. Reactions of a Copper(II) Superoxo Complex Lead to C–H and O–H Substrate Oxygenation: Modeling Copper-Monooxygenase C–H Hydroxylation. Angew Chem, Int Ed. 2008; 47:82–85.

176. Kakuda S, Rolle CJ, Ohkubo K, Siegler MA, Karlin KD, Fukuzumi S. Lewis Acid-Induced Change from Four-to Two-Electron Reduction of Dioxygen Catalyzed by Copper Complexes Using Scandium Triflate. J Am Chem Soc. 2015; 137:3330–3337. [PubMed: 25659416]

177. McCrory CCL, Ottenwaelder X, Stack TDP, Chidsey CED. Kinetic and Mechanistic Studies of the Electrocatalytic Reduction of O_2 to H_2O with Mononuclear Cu Complexes of Substituted 1,10-Phenanthrolines. J Phys Chem A. 2007; 111:12641–12650. [PubMed: 18076134]

178. Fukuzumi S, Kotani H, Lucas HR, Doi K, Suenobu T, Peterson RL, Karlin KD. Mononuclear Copper Complex-Catalyzed Four-Electron Reduction of Oxygen. J Am Chem Soc. 2010; 132:6874–6875. [PubMed: 20443560]

179. Osako T, Nagatomo S, Kitagawa T, Cramer C, Itoh S. Kinetics and DFT Studies on the Reaction of Copper(II) Complexes and H_2O_2. JBIC, J Biol Inorg Chem. 2005; 10:581–590. [PubMed: 16133201]

180. Kunishita A, Teraoka J, Scanlon JD, Matsumoto T, Suzuki M, Cramer CJ, Itoh S. Aromatic Hydroxylation Reactivity of a Mononuclear Cu(II)–Alkylperoxo Complex. J Am Chem Soc. 2007; 129:7248–7249. [PubMed: 17503824]

181. Mandal S, Mukherjee R. A New Tyrosinase Model with 1,3-Bis[(2-dimethylaminoethyl)iminomethyl]benzene: Binuclear Copper-(I) and Phenoxo/Hydroxo-Bridged Dicopper(II) Complexes. Inorg Chim Acta. 2006; 359:4019–4026.

182. Maiti D, Narducci Sarjeant AA, Karlin KD. Copper(II)–Hydroperoxo Complex Induced Oxidative N-Dealkylation Chemistry. J Am Chem Soc. 2007; 129:6720–6721. [PubMed: 17474748]

183. Kamachi T, Lee YM, Nishimi T, Cho J, Yoshizawa K, Nam W. Combined Experimental and Theoretical Approach To Understand the Reactivity of a Mononuclear Cu(II)–Hydroperoxo Complex in Oxygenation Reactions. J Phys Chem A. 2008; 112:13102–13108. [PubMed: 18991428]

184. Kunishita A, Scanlon JD, Ishimaru H, Honda K, Ogura T, Suzuki M, Cramer CJ, Itoh S. Reactions of Copper(II)-H_2O_2 Adducts Supported by Tridentate Bis(2-pyridylmethyl)amine Ligands: Sensitivity to Solvent and Variations in Ligand Substitution. Inorg Chem. 2008; 47:8222–8232. [PubMed: 18698765]

185. Kunishita A, Ishimaru H, Nakashima S, Ogura T, Itoh S. Reactivity of Mononuclear Alkylperoxo Copper(II) Complex. O–O Bond Cleavage and C–H Bond Activation. J Am Chem Soc. 2008; 130:4244–4245. [PubMed: 18335943]

186. Maiti D, Narducci Sarjeant AA, Karlin KD. Copper–Hydroperoxo-Mediated N-Debenzylation Chemistry Mimicking Aspects of Copper Monooxygenases. Inorg Chem. 2008; 47:8736–8747. [PubMed: 18783212]

187. Chaloner L, Askari MS, Kutteh A, Schindler S, Ottenwaelder X. Formation and Reactivity of a Biomimetic Hydroperoxocopper(II) Cryptate. Eur J Inorg Chem. 2011; 2011:4204–4211.

188. Kim S, Saracini C, Siegler MA, Drichko N, Karlin KD. Coordination Chemistry and Reactivity of a Cupric Hydroperoxide Species Featuring a Proximal H-Bonding Substituent. Inorg Chem. 2012; 51:12603–12605. [PubMed: 23153187]

189. Kim S, Ginsbach JW, Lee JY, Peterson RL, Liu JJ, Siegler MA, Sarjeant AA, Solomon EI, Karlin KD. Amine Oxidative N-Dealkylation via Cupric Hydroperoxide Cu-OOH Homolytic Cleavage Followed by Site-Specific Fenton Chemistry. J Am Chem Soc. 2015; 137:2867–2874. [PubMed: 25706825]

190. Choi YJ, Cho KB, Kubo M, Ogura T, Karlin KD, Cho J, Nam W. Spectroscopic and Computational Characterization of $Cu^{II}OOR$ (R = H or cumyl) Complexes Bearing a Me_6tren Ligand. Dalton Trans. 2011; 40:2234–2241. [PubMed: 21258722]

191. Tano T, Sugimoto H, Fujieda N, Itoh S. Heterolytic Alkyl Hydroperoxide O–O Bond Cleavage by Copper(I) Complexes. Eur J Inorg Chem. 2012; 2012:4099–4103.

192. Tano T, Mieda K, Sugimoto H, Ogura T, Itoh S. A Copper Complex Supported by an N_2S-Tridentate Ligand Inducing Efficient Heterolytic O–O Bond Cleavage of Alkylhydroperoxide. Dalton Trans. 2014; 43:4871–4877. [PubMed: 24492382]

193. Biswas S, Dutta A, Debnath M, Dolai M, Das KK, Ali M. A Novel Thermally Stable Hydroperoxo-Copper(II) Complex in a $Cu(N_2O_2)$ Chromophore of a Potential N_4O_2 Donor Schiff Base Ligand: Synthesis, Structure and Catalytic Studies. Dalton Trans. 2013; 42:13210–13219. [PubMed: 23884097]

194. Paria S, Ohta T, Morimoto Y, Ogura T, Sugimoto H, Fujieda N, Goto K, Asano K, Suzuki T, Itoh S. Generation, Characterization, and Reactivity of a Cu^{II}–Alkylperoxide/Anilino Radical Complex: Insight into the O–O Bond Cleavage Mechanism. J Am Chem Soc. 2015; 137:10870–10873. [PubMed: 26291639]

195. Das D, Lee YM, Ohkubo K, Nam W, Karlin KD, Fukuzumi S. Temperature-Independent Catalytic Two-Electron Reduction of Dioxygen by Ferrocenes with a Copper(II) Tris[2-(2-pyridyl)ethyl]amine Catalyst in the Presence of Perchloric Acid. J Am Chem Soc. 2013; 135:2825–2834. [PubMed: 23394287]

196. Osako T, Nagatomo S, Tachi Y, Kitagawa T, Itoh S. Low-Temperature Stopped-Flow Studies on the Reactions of Copper(II) Complexes and H_2O_2: The First Detection of a Mononuclear Copper(II)–Peroxo Intermediate. Angew Chem, Int Ed. 2002; 41:4325–4328.

197. Payeras, AMi, Ho, RYN., Fujita, M., Que, L, Jr. The Reaction of $[Fe^{II}(tpa)]$ with H_2O_2 in Acetonitrile and Acetone–Distinct Intermediates and Yet Similar Catalysis. Chem - Eur J. 2004; 10:4944–4953. [PubMed: 15372680]

198. Wada A, Harata M, Hasegawa K, Jitsukawa K, Masuda H, Mukai M, Kitagawa T, Einaga H. Structural and Spectroscopic Characterization of a Mononuclear Hydroperoxo–Copper(II) Complex with Tripodal Pyridylamine Ligands. Angew Chem, Int Ed. 1998; 37:798–799.

199. Kitajima N, Katayama T, Fujisawa K, Iwata Y, Morooka Y. Synthesis, Molecular Structure, and Reactivity of (Alkylperoxo)copper-(II) Complex. J Am Chem Soc. 1993; 115:7872–7873.

200. Comba P, Haaf C, Helmle S, Karlin KD, Pandian S, Waleska A. Dioxygen Reactivity of New Bispidine-Copper Complexes. Inorg Chem. 2012; 51:2841–2851. [PubMed: 22332786]

201. Kim S, Siegler MA, Karlin KD. Peroxynitrite Chemistry Derived from Nitric Oxide Reaction with a Cu(II)-OOH Species and a Copper Mediated NO Reductive Coupling Reaction. Chem Commun (Cambridge, U K). 2014; 50:2844–2846.

202. Park GY, Lee JY, Himes RA, Thomas GS, Blackburn NJ, Karlin KD. Copper–Peptide Complex Structure and Reactivity When Found in Conserved His-X_{aa}-His Sequences. J Am Chem Soc. 2014; 136:12532–12535. [PubMed: 25171435]

203. Ohta T, Tachiyama T, Yoshizawa K, Yamabe T. Synthesis, Structure, and Catalytic Function of a Disulfide-Bridged Dicopper(I) Complex. Tetrahedron Lett. 2000; 41:2581–2585.
204. Fujii T, Naito A, Yamaguchi S, Wada A, Funahashi Y, Jitsukawa K, Nagatomo S, Kitagawa T, Masuda H. Construction of a Square-Planar Hydroperoxo-Copper(II) Complex Inducing a Higher Catalytic Reactivity. Chem Commun. 2003:2700–2701.
205. Fujii T, Yamaguchi S, Funahashi Y, Ozawa T, Tosha T, Kitagawa T, Masuda H. Mononuclear Copper(II)-Hydroperoxo Complex Derived from Reaction of Copper(I) Complex with Dioxygen as a Model of DβM and PHM. Chem Commun. 2006:4428–4430.
206. Ohtsu H, Itoh S, Nagatomo S, Kitagawa T, Ogo S, Watanabe Y, Fukuzumi S. Characterization of Imidazolate-Bridged Dinuclear and Mononuclear Hydroperoxo Complexes. Inorg Chem. 2001; 40:3200–3207. [PubMed: 11399193]
207. Yamaguchi S, Nagatomo S, Kitagawa T, Funahashi Y, Ozawa T, Jitsukawa K, Masuda H. Copper Hydroperoxo Species Activated by Hydrogen-Bonding Interaction with Its Distal Oxygen. Inorg Chem. 2003; 42:6968–6970. [PubMed: 14577757]
208. Chen P, Fujisawa K, Solomon EI. Spectroscopic and Theoretical Studies of Mononuclear Copper(II) Alkyl- and Hydroperoxo Complexes: Electronic Structure Contributions to Reactivity. J Am Chem Soc. 2000; 122:10177–10193.
209. Kodera M, Kita T, Miura I, Nakayama N, Kawata T, Kano K, Hirota S. Hydroperoxo–Copper(II) Complex Stabilized by N_3S-Type Ligand Having a Phenyl Thioether. J Am Chem Soc. 2001; 123:7715–7716. [PubMed: 11481001]
210. Sanyal I, Ghosh P, Karlin KD. Mononuclear Copper(II)-Acylperoxo Complexes. Inorg Chem. 1995; 34:3050–3056.
211. Yamaguchi S, Wada A, Nagatomo S, Kitagawa T, Jitsukawa K, Masuda H. Thermal Stability of Mononuclear Hydroperoxocopper(II) Species, Effects of Hydrogen Bonding and Hydrophobic Field. Chem Lett. 2004; 33:1556–1557.
212. Poater A, Cavallo L. Probing the Mechanism of O_2 Activation by a Copper(I) Biomimetic Complex of a C-H Hydroxylating Copper Monooxygenase. Inorg Chem. 2009; 48:4062–4066. [PubMed: 19331376]
213. Whittaker JW. Free Radical Catalysis by Galactose Oxidase. Chem Rev. 2003; 103:2347–2363. [PubMed: 12797833]
214. Jazdzewski BA, Tolman WB. Understanding the Copper-Phenoxyl Radical Array in Galactose Oxidase: Contributions from Synthetic Modeling Studies. Coord Chem Rev. 2000; 200–202:633–685.
215. Itoh S, Taki M, Fukuzumi S. Active Site Models for Galactose Oxidase and Related Enyzmes. Coord Chem Rev. 2000; 198:3–20.
216. Whittaker MM, Whittaker JW. Catalytic Reaction Profile for Alcohol Oxidation by Galactose Oxidase. Biochemistry. 2001; 40:7140–7148. [PubMed: 11401560]
217. Pacher P, Beckman JS, Liaudet L. Nitric Oxide and Peroxynitrite in Health and Disease. Physiol Rev. 2007; 87:315–424. [PubMed: 17237348]
218. Kitajima N, Koda T, Iwata Y, Moro-oka Y. Reaction Aspects of a μ-Peroxo Binuclear Copper(II) Complex. J Am Chem Soc. 1990; 112:8833–8839.
219. Réglier M, Amadeï E, Tadayoni R, Waegell B. Pyridine Nucleus Hydroxylation with Copper Oxygenase Models. J Chem Soc, Chem Commun. 1989:447–450.
220. Fiedler A, Schröeder D, Shaik S, Schwarz H. Electronic Structures and Gas-Phase Reactivities of Cationic Late-Transition-Metal Oxides. J Am Chem Soc. 1994; 116:10734–10741.
221. Schröder D, Holthausen MC, Schwarz H. Radical-Like Activation of Alkanes by the Ligated Copper Oxide Cation (Phenanthroline)CuO^+ J Phys Chem B. 2004; 108:14407–14416.
222. Dietl N, van der Linde C, Schlangen M, Beyer MK, Schwarz H. Diatomic $[CuO]^+$ and Its Role in the Spin-Selective Hydrogen- and Oxygen-Atom Transfers in the Thermal Activation of Methane. Angew Chem, Int Ed. 2011; 50:4966–4969.
223. Dietl N, Schlangen M, Schwarz H. Thermal Hydrogen-Atom Transfer from Methane: The Role of Radicals and Spin States in Oxo-Cluster Chemistry. Angew Chem, Int Ed. 2012; 51:5544–5555.

224. Rijs NJ, Weiske T, Schlangen M, Schwarz H. On Divorcing Isomers, Dissecting Reactivity, and Resolving Mechanisms of Propane C-H and aryl C-X (X = halogen) Bond Activations Mediated by a Ligated Copper(III) Oxo Complex. Chem Phys Lett. 2014; 608:408–424.
225. Schwarz H. Thermal Hydrogen-Atom Transfer from Methane: A Mechanistic Exercise. Chem Phys Lett. 2015; 629:91–101.
226. Yoshizawa, K. Methane Hydroxylation by First Row Transition Metal Oxides. Computational Modeling for Homogeneous and Enzymatic Catalysis: A Knowledge-Base for Designing Efficient Catalysts. Morokuma, K., Musaev, DG., editors. Wiley-VCH; Weinheim, Germany: 2008. p. 317-335.
227. Gherman BF, Tolman WB, Cramer CJ. Characterization of the Structure and Reactivity of Monocopper-Oxygen Complexes Supported by β-Diketiminate and Anilido-Imine Ligands. J Comput Chem. 2006; 27:1950–1961. [PubMed: 17019721]
228. Hong S, Huber SM, Gagliardi L, Cramer CC, Tolman WB. Copper(I)-α-Ketocarboxylate Complexes: Characterization and O_2 Reactions That Yield Copper-Oxygen Intermediates Capable of Hydroxylating Arenes. J Am Chem Soc. 2007; 129:14190–14192. [PubMed: 17958429]
229. Shaik S, Danovich D, Fiedler A, Schröder D, Schwarz H. Two-State Reactivity in Organometallic Gas-Phase Ion Chemistry. Helv Chim Acta. 1995; 78:1393–1407.
230. Rodgers MT, Walker B, Armentrout PB. Reactions of Cu^+(^{1}S and ^{3}D) with O_2, CO, CO_2, N_2, NO, N_2O, and NO_2 Studied by Guided Ion Beam Mass Spectrometry. Int J Mass Spectrom. 1999; 182–183:99–120.
231. Rijs NJ, González-Navarrete P, Schlangen M, Schwarz H. Penetrating the Elusive Mechanism of Copper-Mediated Fluoromethylation in the Presence of Oxygen through the Gas-Phase Reactivity of Well-Defined $[LCuO]^+$ Complexes with Fluoromethanes $(CH_{(4-n)}F_n$, n = 1–3. J Am Chem Soc. 2016; 138(9):3125–3135. [PubMed: 26859159]
232. Costas M, Mehn MP, Jensen MP, Que L Jr. Dioxygen Activation at Mononuclear Nonheme Iron Active Sites: Enzymes Models and Intermediates. Chem Rev. 2004; 104:939–986. [PubMed: 14871146]
233. Abu-Omar MM, Loaiza A, Hontzeas N. Reaction Mechanisms of Mononuclear Non-Heme Iron Oxygenases. Chem Rev. 2005; 105:2227–2252. [PubMed: 15941213]
234. Purpero V, Moran GR. The Diverse and Pervasive Chemistries of the α-keto Acid Dependent Enzymes. JBIC, J Biol Inorg Chem. 2007; 12:587–601. [PubMed: 17431691]
235. Huber SM, Ertem MZ, Aquilante F, Gagliardi L, Tolman WB, Cramer CJ. Generating Cu^{II}-Oxyl/Cu^{III}-Oxo Species from Cu^I-α-Ketocarboxylate Complexes and O_2: In Silico Studies on Ligand Effects and C-H-Activation Reactivity. Chem - Eur J. 2009; 15:4886–4895. [PubMed: 19322769]
236. Hong S, Gupta AK, Tolman WB. Intermediates in Reactions of Copper(I) Complexes with N-Oxides: From the Formation of Stable Adducts to Oxo Transfer. Inorg Chem. 2009; 48:6323–6325. [PubMed: 19425587]
237. Donoghue PJ, Tehranchi J, Cramer CJ, Sarangi R, Solomon EI, Tolman WB. Rapid C–H Bond Activation by a Monocopper(III)–Hydroxide Complex. J Am Chem Soc. 2011; 133:17602–17605. [PubMed: 22004091]
238. Dhar D, Tolman WB. Hydrogen Atom Abstraction from Hydrocarbons by a Copper(III)-Hydroxide Complex. J Am Chem Soc. 2015; 137:1322–1329. [PubMed: 25581555]
239. Dhar D, Yee GM, Spaeth AD, Boyce DW, Zhang H, Dereli B, Cramer CJ, Tolman WB. Perturbing the Copper(III)-Hydroxide Unit through Ligand Structural Variation. J Am Chem Soc. 2016; 138:356–368. [PubMed: 26693733]
240. Anson FC, Collins TJ, Richmond TG, Santarsiero BD, Toth JE, Treco BGRT. Highly Stabilized Copper(III) Complexes. J Am Chem Soc. 1987; 109:2974–2979.
241. McDonald MR, Fredericks FC, Margerum DW. Characterization of Copper(III)–Tetrapeptide Complexes with Histidine as the Third Residue. Inorg Chem. 1997; 36:3119–3124. [PubMed: 11669966]

242. Youngblood MP, Margerum DW. Reaction Entropies of Copper(III,II) Peptide and Nickel(III,II) Peptide Redox Couples and the Role of Axial Solvent Coordination. Inorg Chem. 1980; 19:3068–3072.
243. Burke SK, Xu Y, Margerum DW. Cu(II)Gly_2HisGly Oxidation by H_2O_2/Ascorbic Acid to the Cu(III) Complex and Its Subsequent Decay to Alkene Peptides. Inorg Chem. 2003; 42:5807–5817. [PubMed: 12971748]
244. Diaddario LL, Robinson WR, Margerum DW. Crystal and Molecular Structure of the Copper(III)-Tripeptide Complex of Tri-α-Aminoisobutyric Acid. Inorg Chem. 1983; 22:1021–1025.
245. Warren JJ, Tronic TA, Mayer JM. Thermochemistry of Proton-Coupled Electron Transfer Reagents and its Implications. Chem Rev. 2010; 110:6961–7001. [PubMed: 20925411]
246. Mayer JM. Understanding Hydrogen Atom Transfer: From Bond Strengths to Marcus Theory. Acc Chem Res. 2011; 44:36–46. [PubMed: 20977224]
247. Dhar D, Yee GM, Markle TF, Mayer JM, Tolman WB. Reactivity of the Copper(III)-Hydroxide Unit with Phenols. Chem Sci. 2017; published online. doi: 10.1039/C6SC03039D
248. Rolff M, Tuczek F. How Do Copper Enzymes Hydroxylate Aliphatic Substrates? Recent Insights from the Chemistry of Model Systems. Angew Chem, Int Ed. 2008; 47:2344–2347.
249. Decker H, Schweikardt T, Tuczek F. The First Crystal Structure of Tyrosinase: All Questions Answered? Angew Chem, Int Ed. 2006; 45:4546–4550.
250. Karahalis GJ, Thangavel A, Chica B, Bacsa J, Dyer RB, Scarborough CC. Synthesis and Catalytic Reactivity of a Dicopper(II) μ-η^2:η^2-Peroxo Species Supported by 1,4,7-Tri-*tert*-butyl-1,4,7-triazacyclononane. Inorg Chem. 2016; 55:1102–1107. [PubMed: 26789550]
251. Mirica LM, Vance M, Rudd DJ, Hedman B, Hodgson KO, Solomon EI, Stack TDP. Tyrosinase Reactivity in a Model Complex: An Alternative Hydroxylation Mechanism. Science. 2005; 308:1890–1892. [PubMed: 15976297]
252. Mirica LM, Rudd DJ, Vance MA, Solomon EI, Hodgson KO, Hedman B, Stack TDP. μ-η^2:η^2-Peroxodicopper-(II) Complex with a Secondary Diamine Ligand: A Functional Model of Tyrosinase. J Am Chem Soc. 2006; 128:2654–2665. [PubMed: 16492052]
253. Op't Holt BT, Vance MA, Mirica LM, Heppner DE, Stack TDP, Solomon EI. Reaction Coordinate of a Functional Model of Tyrosinase: Spectroscopic and Computational Characterization. J Am Chem Soc. 2009; 131:6421–6438. [PubMed: 19368383]
254. Xu B, Lumb JP, Arndtsen BA. A TEMPO-Free Copper-Catalyzed Aerobic Oxidation of Alcohols. Angew Chem, Int Ed. 2015; 54:4208–4211.
255. Esguerra KVN, Fall Y, Lumb JP. A Biomimetic Catalytic Aerobic Functionalization of Phenols. Angew Chem, Int Ed. 2014; 53:5877–5881.
256. Esguerra KVN, Lumb JP. Adapting Melanogenesis to a Regioselective C–H Functionalization of Phenols. Synlett. 2015; 26:2731–2738.
257. Citek C, Lyons CT, Wasinger EC, Stack TDP. Self-Assembly of the Oxy-Tyrosinase Core and the Fundamental Components of Phenolic Hydroxylation. Nat Chem. 2012; 4:317–322. [PubMed: 22437718]
258. Chiang L, Keown W, Citek C, Wasinger EC, Stack TDP. Simplest Monodentate Imidazole Stabilization of the oxy-Tyrosinase Cu_2O_2 Core: Phenolate Hydroxylation through a Cu^{III} Intermediate. Angew Chem, Int Ed. 2016; 55:10453–10457.
259. Citek C, Herres-Pawlis S, Stack TDP. Low Temperature Syntheses and Reactivity of Cu_2O_2 Active-Site Models. Acc Chem Res. 2015; 48:2424–2433. [PubMed: 26230113]
260. Sanyal I, Strange RW, Blackburn NJ, Karlin KD. Formation of a Copper-Dioxygen Complex (Cu_2-O_2)Using Simple Imidazole Ligands. J Am Chem Soc. 1991; 113:4692–4693.
261. Sanyal I, Karlin KD, Strange RW, Blackburn NJ. Chemistry and Structural Studies on the Dioxygen-Binding Copper-1,2-Dimethylimidazole System. J Am Chem Soc. 1993; 115:11259–11270.
262. Mahadevan V, DuBois JL, Hedman B, Hodgson KO, Stack TDP. Exogenous Substrate Reactivity with a $[Cu(III)_2O_2]^{2+}$ Core: Structural Implications. J Am Chem Soc. 1999; 121:5583–5584.
263. Hoffmann A, Citek C, Binder S, Goos A, Ruebhausen M, Troeppner O, Ivanović-Burmazović I, Wasinger EC, Stack TDP, Herres-Pawlis S. Catalytic Phenol Hydroxylation with Dioxygen:

Extension of the Tyrosinase Mechanism beyond the Protein Matrix. Angew Chem, Int Ed. 2013; 52:5398–5401.

264. Schottenheim J, Fateeva N, Thimm W, Krahmer J, Tuczek F. Catalytic Conversion of Monophenols to *Ortho*-Quinones in a Tyrosinase-Like Fashion: Towards More Biomimetic and More Efficient Model Systems. Z Anorg Allg Chem. 2013; 639:1491–1497.
265. Hamann JN, Tuczek F. New Catalytic Model Systems of Tyrosinase: Fine Tuning of the Reactivity with Pyrazole-Based NDonor Ligands. Chem Commun. 2014; 50:2298–2300.
266. Rolff M, Schottenheim J, Peters G, Tuczek F. The First Catalytic Tyrosinase Model System Based on a Mononuclear Copper(I) Complex: Kinetics and Mechanism. Angew Chem, Int Ed. 2010; 49:6438–6442.
267. Schottenheim J, Gernert C, Herzigkeit B, Krahmer J, Tuczek F. Catalytic Models of Tyrosinase: Reactivity Differences between Systems Based on Mono- and Binucleating Ligands. Eur J Inorg Chem. 2015; 2015:3501–3511.
268. Palavicini S, Granata A, Monzani E, Casella L. Hydroxylation of Phenolic Compounds by a Peroxodicopper(II) Complex: Further Insight into the Mechanism of Tyrosinase. J Am Chem Soc. 2005; 127:18031–18036. [PubMed: 16366554]
269. Mahapatra S, Kaderli S, Llobet A, Neuhold YM, Palanché T, Halfen JA, Young VG Jr, Kaden TA, Que L Jr, Zuberbühler AD, Tolman WB. Binucleating Ligand Structural Effects on (μ-Peroxo)- and Bis(μ-oxo)dicopper Complex Formation and Decay: Competition Between Arene Hydroxylation and Aliphatic C-H Bond Activation. Inorg Chem. 1997; 36:6343–6356.
270. Becker M, Schindler S, Karlin KD, Kaden TA, Kaderli S, Palanché T, Zuberbühler AD. Intramolecular Ligand Dydroxylation: Mechanistic High-Pressure Studies on the Reaction of a Dinuclear Copper(I) Complex with Dioxygen. Inorg Chem. 1999; 38:1989–1995. [PubMed: 11670976]
271. Gamba I, Palavicini S, Monzani E, Casella L. Catalytic Sulfoxidation by Dinuclear Copper Complexes. Chem - Eur J. 2009; 15:12932–12936. [PubMed: 19876984]
272. Battaini G, Casella L, Gullotti M, Monzani E, Nardin G, Perotti A, Randaccio L, Santagostini L, Heinemann FW, Schindler S. Structure and Reactivity Studies on Dinuclear Copper Complexes of the Ligand α,α'-Bis{bis[1-(1′-methyl-2′-benzimidazolyl)methyl]amino}-*m*-xylene. Eur J Inorg Chem. 2003; 2003:1197–1205.
273. Granata A, Monzani E, Casella L. Mechanistic Insight into the Catechol Oxidase Activity by a Biomimetic Dinuclear Copper Complex. JBIC, J Biol Inorg Chem. 2004; 9:903–913. [PubMed: 15449133]
274. Perrone ML, Lo Presti E, Dell'Acqua S, Monzani E, Santagostini L, Casella L. Synthesis, Characterization, and Stereoselective Oxidations of the Dinuclear Copper(II) Complex Derived from a Chiral Diamino-*m*-xylenetetra(benzimidazole) Ligand. Eur J Inorg Chem. 2015; 2015:3493–3500.
275. Karlin KD, Hayes JC, Gultneh Y, Cruse RW, McKown JW, Hutchinson JP, Zubieta J. Copper-Mediated Hydroxylation of an Arene: Model System for the Action of Copper Monooxygenases. Structures of a Binuclear Cu(I) Complex and Its Oxygenated Product. J Am Chem Soc. 1984; 106:2121–2128.
276. Pidcock E, Obias HV, Zhang CX, Karlin KD, Solomon EI. Investigation of the Reactive Oxygen Intermediate in An Arene Hydroxylation Reation Performed by Xylyl-Bridged Binuclear Copper Complexes. J Am Chem Soc. 1998; 120:7841–7847.
277. Foxon SP, Utz D, Astner J, Schindler S, Thaler F, Heinemann FW, Liehr G, Mukherjee J, Balamurugan V, Ghosh D, et al. Reaction Behaviour of Dinuclear Copper(I) Complexes with *m*-Xylyl-Based Ligands Towards Dioxygen. Dalton Trans. 2004:2321–2328. [PubMed: 15278125]
278. Ohi H, Tachi Y, Itoh S. Modeling the Mononuclear, Dinuclear, and Trinuclear Copper(I) Reaction Centers of Copper Proteins Using Pyridylalkylamine Ligands Connected to 1,3,5-Triethylbenzene Spacer. Inorg Chem. 2006; 45:10825–10835. [PubMed: 17173442]
279. Sander O, Henβ A, Näther C, Würtele C, Holthausen MC, Schindler S, Tuczek F. Aromatic Hydroxylation in a Copper Bis(imine) Complex Mediated by a μ-η^2:η^2 Peroxo Dicopper Core: A Mechanistic Scenario. Chem - Eur J. 2008; 14:9714–9729. [PubMed: 18785680]

280. Karlin KD, Zhang CX, Rheingold AL, Galliker B, Kaderli S, Zuberbühler AD. Reversible Dioxygen Binding and Arene Hydroxylation Reactions: Kinetic and Thermodynamic Studies Involving Ligand Electronic and Structural Variations. Inorg Chim Acta. 2012; 389:138–150.

281. Matsumoto T, Furutachi H, Kobino M, Tomii M, Nagatomo S, Tosha T, Osako T, Fujinami S, Itoh S, Kitagawa T, et al. Intramolecular Arene Hydroxylation versus Intermolecular Olefin Epoxidation by (μ-η^2:η^2-Peroxo)dicopper(II) Complex Supported by Dinucleating Ligand. J Am Chem Soc. 2006; 128:3874–3875. [PubMed: 16551071]

282. Matsumoto T, Ohkubo K, Honda K, Yazawa A, Furutachi H, Fujinami S, Fukuzumi S, Suzuki M. Aliphatic C-H Bond Activation Initiated by a (μ-η^2:η^2-Peroxo)dicopper(II) Complex in Comparison with Cumylperoxyl Radical. J Am Chem Soc. 2009; 131:9258–9267. [PubMed: 19530656]

283. Qayyum MF, Sarangi R, Fujisawa K, Stack TDP, Karlin KD, Hodgson KO, Hedman B, Solomon EI. L-Edge X-ray Absorption Spectroscopy and DFT Calculations on Cu_2O_2 Species: Direct Electrophilic Aromatic Attack by Side-on Peroxo Bridged Dicopper(II) Complexes. J Am Chem Soc. 2013; 135:17417–17431. [PubMed: 24102191]

284. Walli A, Dechert S, Bauer M, Demeshko S, Meyer F. BOX Ligands in Biomimetic Copper-Mediated Dioxygen Activation: A Hemocyanin Model. Eur J Inorg Chem. 2014; 2014:4660–4676.

285. Sprakel VSI, Feiters MC, Meyer-Klaucke W, Klopstra M, Brinksma J, Feringa BL, Karlin KD, Nolte RJM. Oxygen Binding and Activation by the Complexes of PY2- and TPA-appended Diphenylglycoluril Receptors with Copper and Other Metals. Dalton Trans. 2005:3522–3534. [PubMed: 16234934]

286. Zhu Q, Lian Y, Thyagarajan S, Rokita SE, Karlin KD, Blough NV. Hydrogen Peroxide and Dioxygen Activation by Dinuclear Copper Complexes in Aqueous Solution: Hydroxyl Radical Production Initiated by Internal Electron Transfer. J Am Chem Soc. 2008; 130:6304–6305. [PubMed: 18433125]

287. Thyagarajan S, Murthy NN, Narducci Sarjeant AA, Karlin KD, Rokita SE. Selective DNA Strand Scission with Binuclear Copper Complexes: Implications for an Active Cu_2O_2 Species. J Am Chem Soc. 2006; 128:7003–7008. [PubMed: 16719480]

288. Tahsini L, Kotani H, Lee YM, Cho J, Nam W, Karlin KD, Fukuzumi S. Electron-Transfer Reduction of Dinuclear Copper Peroxo and Bis-μ-oxo Complexes Leading to the Catalytic Four-Electron Reduction of Dioxygen to Water. Chem - Eur J. 2012; 18:1084–1093. [PubMed: 22237962]

289. Karlin KD, Tyeklar Z, Farooq A, Haka MS, Ghosh P, Cruse RW, Gultneh Y, Hayes JC, Toscano PJ, Zubieta J. Dioxygen-Copper Reactivity and Functional Modeling of Hemocyanins. Reversible Binding of O_2 and Carbon Monoxide to Dicopper(I) Complexes $[Cu^I_2(L)]^{2+}$ (L = dinucleating ligand) and the Structure of a Bis(carbonyl) Adduct, $[Cu^I_2(L)\ (CO)_2]^{2+}$ Inorg Chem. 1992; 31:1436–1451.

290. Mahadevan V, Hou Z, Cole AP, Root DE, Lal TK, Solomon EI, Stack TDP. Irreversible Reduction of Dioxygen by Simple Peralkylated Diamine-Copper(I) Complexes: Characterization and Thermal Stability of a $[Cu_2(\mu\text{-}O)_2]^{2+}$ Core. J Am Chem Soc. 1997; 119:11996–11997.

291. Stack TDP. Complexity with Simplicity: a Steric Continuum of Chelating Diamines with Copper(I) and Dioxygen. Dalton Trans. 2003:1881–1889.

292. Cole AP, Mahadevan V, Mirica LM, Ottenwaelder X, Stack TDP. Bis(μ-oxo)dicopper(III) Complexes of a Homologous Series of Simple Peralkylated 1,2-Diamines: Steric Modulation of Structure, Stability, and Reactivity. Inorg Chem. 2005; 44:7345–7364. [PubMed: 16212361]

293. Kang P, Bobyr E, Dustman J, Hodgson KO, Hedman B, Solomon EI, Stack TDP. Bis(μ-oxo) Dicopper(III) Species of the Simplest Peralkylated Diamine: Enhanced Reactivity toward Exogenous Substrates. Inorg Chem. 2010; 49:11030–11038. [PubMed: 21028910]

294. Cole AP, Root DE, Mukherjee P, Solomon EI, Stack TDP. A Trinuclear Intermediate in the Copper-Mediated Reduction of O_2: Four Electrons from Three Coppers. Science. 1996; 273:1848–1850. [PubMed: 8791587]

295. Citek C, Lin BL, Phelps TE, Wasinger EC, Stack TDP. Primary Amine Stabilization of a Dicopper(III) Bis(μ-oxo) Species: Modeling the Ligation in pMMO. J Am Chem Soc. 2014; 136:14405–14408. [PubMed: 25268334]

296. Citek C, Gary JB, Wasinger EC, Stack TDP. Chemical Plausibility of Cu(III) with Biological Ligation in pMMO. J Am Chem Soc. 2015; 137:6991–6994. [PubMed: 26020834]

297. Shimokawa C, Teraoka J, Tachi Y, Itoh S. A Functional Model for pMMO (Particulate Methane Monooxygenase): Hydroxylation of Alkanes with H_2O_2 Catalyzed by β-Diketiminatocopper(II) Complexes. J Inorg Biochem. 2006; 100:1118–1127. [PubMed: 16584781]

298. Liu CC, Lin TS, Chan SI, Mou CY. A Room Temperature Catalyst for Toluene Aliphatic C-H Bond Oxidation: Tripodal Tridentate Copper Complex Immobilized in Mesoporous Silica. J Catal. 2015; 322:139–151.

299. Mandal S, De A, Mukherjee R. Formation of $\{Cu^{III}_2(\mu\text{-}O)_2\}^{2+}$ Core Due to Dioxygen Reactivity of a Copper(I) Complex Supported by a New Hybrid Tridentate Ligand: Reaction with Exogenous Substrates. Chem Biodiversity. 2008; 5:1594–1608.

300. Holland PL, Rodgers KR, Tolman WB. Is the Bis(μ-oxo)dicopper Core Capable of Hydroxylating an Arene? Angew Chem, Int Ed. 1999; 38:1139–1142.

301. Becker J, Gupta P, Angersbach F, Tuczek F, Näther C, Holthausen MC, Schindler S. Selective Aromatic Hydroxylation with Dioxygen and Simple Copper Imine Complexes. Chem - Eur J. 2015; 21:11735–11744. [PubMed: 26088961]

302. Hamann JN, Rolff M, Tuczek F. Monooxygenation of an Appended Phenol in a Model System of Tyrosinase: Implications on the Enzymatic Reaction Mechanism. Dalton Trans. 2015; 44:3251–3258. [PubMed: 25597816]

303. Petrovic D, Hill LMR, Jones PG, Tolman WB, Tamm M. Synthesis and Reactivity of Copper(I) Complexes with an Ethylene-Bridged Bis(imidazolin-2-imine) Ligand. Dalton Trans. 2008:887–894. [PubMed: 18259621]

304. Herres S, Heuwing AJ, Florke U, Schneider J, Henkel G. Hydroxylation of a Methyl Group: Synthesis of $[Cu_2(btmmO)_2I]^+$ and of $[Cu_2(btmmO)_2]^{2+}$ Containing the Novel Ligand Bis-(trimethylmethoxy)guanidino Propane (btmmO) by Copper-Assisted Oxygen Activation. Inorg Chim Acta. 2005; 358:1089–1095.

305. Herres-Pawlis S, Flörke U, Henkel G. Tuning of Copper(I)–Dioxygen Reactivity by Bis(guanidine) Ligands. Eur J Inorg Chem. 2005; 2005:3815–3824.

306. Herres-Pawlis S, Verma P, Haase R, Kang P, Lyons CT, Wasinger EC, Floerke U, Henkel G, Stack TDP. Phenolate Hydroxylation in a Bis(μ-oxo)dicopper(III) Complex: Lessons from the Guanidine/Amine Series. J Am Chem Soc. 2009; 131:1154–1169. [PubMed: 19119846]

307. Mandal S, Mukherjee J, Lloret F, Mukherjee R. Modeling Tyrosinase and Catecholase Activity Using New *m*-Xylyl-Based Ligands with Bidentate Alkylamine Terminal Coordination. Inorg Chem. 2012; 51:13148–13161. [PubMed: 23194383]

308. Martínez-Calvo M, Vázquez López M, Pedrido R, González-Noya AM, Bermejo MR, Monzani E, Casella L, Sorace L. Endogenous Arene Hydroxylation Promoted by Copper(I) Cluster Helicates. Chem - Eur J. 2010; 16:14175–14180. [PubMed: 20967897]

309. Company A, Lamata D, Poater A, Solà M, Rybak-Akimova EV, Que L, Fontrodona X, Parella T, Llobet A, Costas M. O_2 Chemistry of Dicopper Complexes with Alkyltriamine Ligands. Comparing Synergistic Effects on O_2 Binding. Inorg Chem. 2006; 45:5239–5241. [PubMed: 16813375]

310. Company A, Palavicini S, Garcia-Bosch I, Mas-Ballesté R, Que L, Rybak-Akimova EV, Casella L, Ribas X, Costas M. Tyrosinase-Like Reactivity in a $Cu^{III}_2(\mu\text{-}O)_2$ Species. Chem - Eur J. 2008; 14:3535–3538. [PubMed: 18348133]

311. Schindler S. Reactivity of Copper(I) Complexes Towards Dioxygen. Eur J Inorg Chem. 2000; 2000:2311–2326.

312. Hatcher LQ, Karlin KD. Oxidant Types in Copper-Dioxygen Chemistry: The Ligand Coordination Defines the Cu_n-O_2 Structure and Subsequent Reactivity. JBIC, J Biol Inorg Chem. 2004; 9:669–683. [PubMed: 15311336]

313. Itoh S, Tachi Y. Structure and O_2-Reactivity of Copper(I) Complexes Supported by Pyridylalkylamine Ligands. Dalton Trans. 2006:4531–4538. [PubMed: 17016563]

314. Osako T, Terada S, Tosha T, Nagatomo S, Furutachi H, Fujinami S, Kitagawa T, Suzuki M, Itoh S. Structure and Dioxygen-Reactivity of Copper(I) Complexes Supported by Bis(6-

methylpyridin-2-ylmethyl)amine Tridentate Ligands. Dalton Trans. 2005:3514–3521. [PubMed: 16234933]

315. Karlin KD, Haka MS, Cruse RW, Meyer GJ, Farooq A, Gultneh Y, Hayes JC, Zubieta J. Dioxygen-Copper Reactivity. Models for hemocyanin: Reversible O_2 and CO Binding to Structurally Characterized Dicopper(I) Complexes Containing Hydrocarbon-Linked Bis[2-(2-pyridyl)ethyl]amine Units. J Am Chem Soc. 1988; 110:1196–1207.
316. Itoh S, Kumei H, Taki M, Nagatomo S, Kitagawa T, Fukuzumi S. Oxygenation of Phenols to Catechols by A (μ-η^2:η^2-Peroxo)dicopper(II) Complex: Mechanistic Insight into the Phenolase Activity of Tyrosinase. J Am Chem Soc. 2001; 123:6708–6709. [PubMed: 11439064]
317. Osako T, Ueno Y, Tachi Y, Itoh S. Structures and Redox Reactivities of Copper Complexes of (2-Pyridyl)alkylamine Ligands. Effects of the Alkyl Linker Chain Length. Inorg Chem. 2003; 42:8087–8097. [PubMed: 14632530]
318. Kunishita A, Osako T, Tachi Y, Teraoka J, Itoh S. Syntheses, Structures, and O_2 Reactivities of Copper(I) Complexes with Bis(2-pyridylmethyl)amine and Bis(2-quinolylmethyl)amine Tridentate Ligands. Bull Chem Soc Jpn. 2006; 79:1729–1741.
319. Liang HC, Henson MJ, Hatcher LQ, Vance MA, Zhang CX, Lahti D, Kaderli S, Sommer RD, Rheingold AL, Zuberbühler AD, et al. Solvent Effects on the Conversion of Dicopper(II) μ-η^2:η^2-Peroxo to Bis-μ-oxo Dicopper(III) Complexes: Direct Probing of the Solvent Interaction. Inorg Chem. 2004; 43:4115–4117. [PubMed: 15236520]
320. Hatcher LQ, Vance MA, Narducci Sarjeant AA, Solomon EI, Karlin KD. Copper–Dioxygen Adducts and the Sideon Peroxo Dicopper(II)/Bis(μ-oxo) Dicopper(III) Equilibrium: Significant Ligand Electronic Effects. Inorg Chem. 2006; 45:3004–3013. [PubMed: 16562956]
321. Zhang CX, Liang HC, Kim E-i, Shearer J, Helton ME, Kim E, Kaderli S, Incarvito CD, Zuberbühler AD, Rheingold AL, Karlin KD. Tuning Copper–Dioxygen Reactivity and Exogenous Substrate Oxidations via Alterations in Ligand Electronics. J Am Chem Soc. 2003; 125:634–635. [PubMed: 12526654]
322. Henson MJ, Vance MA, Zhang CX, Liang HC, Karlin KD, Solomon EI. Resonance Raman Investigation of Equatorial Ligand Donor Effects on the $Cu_2O_2^{2+}$ Core in End-On and Side-On μ-Peroxo-Dicopper(II) and Bis-μ-oxo-Dicopper(III) Complexes. J Am Chem Soc. 2003; 125:5186–5192. [PubMed: 12708870]
323. Park GY, Qayyum MF, Woertink J, Hodgson KO, Hedman B, Narducci Sarjeant AA, Solomon EI, Karlin KD. Geometric and Electronic Structure of $[\{Cu(MeAN)\}_2(\mu\text{-}\eta^2\text{:}\eta^2(O_2^{2-}))]^{2+}$ with an Unusually Long O–O Bond: O–O Bond Weakening vs. Activation for Reductive Cleavage. J Am Chem Soc. 2012; 134:8513–8524. [PubMed: 22571744]
324. Liang HC, Zhang CX, Henson MJ, Sommer RD, Hatwell KR, Kaderli S, Zuberbühler AD, Rheingold AL, Solomon EI, Karlin KD. Contrasting Copper–Dioxygen Chemistry Arising from Alike Tridentate Alkyltriamine Copper(I) Complexes. J Am Chem Soc. 2002; 124:4170–4171. [PubMed: 11960420]
325. Shearer J, Zhang CX, Zakharov LN, Rheingold AL, Karlin KD. Substrate Oxidation by Copper–Dioxygen Adducts: Mechanistic Considerations. J Am Chem Soc. 2005; 127:5469–5483. [PubMed: 15826184]
326. Abe T, Morimoto Y, Tano T, Mieda K, Sugimoto H, Fujieda N, Ogura T, Itoh S. Geometric Control of Nuclearity in Copper(I)/Dioxygen Chemistry. Inorg Chem. 2014; 53:8786–8794. [PubMed: 25101861]
327. Sander O, Näther C, Tuczek F. Chiral Dicopper Complexes with a Doubly Asymmetric Ligand as Models for the Tyrosinase Active Site: Synthesis, Structure, O_2-Reactivity and Comparison with Their Symmetric Analogs. Z Anorg Allg Chem. 2009; 635:1123–1133.
328. Ottenwaelder X, Rudd DJ, Corbett MC, Hodgson KO, Hedman B, Stack TDP. Reversible O-O Bond Cleavage in Copper-Dioxygen Isomers: Impact of Anion Basicity. J Am Chem Soc. 2006; 128:9268–9269. [PubMed: 16848427]
329. Gupta AK, Tolman WB. Copper/α-Ketocarboxylate Chemistry With Supporting Peralkylated Diamines: Reactivity of Copper(I) Complexes and Dicopper-Oxygen Intermediates. Inorg Chem. 2010; 49:3531–3539. [PubMed: 20218646]

330. Park GY, Lee Y, Lee DH, Woertink JS, Narducci Sarjeant AA, Solomon EI, Karlin KD. Thioether S-ligation in a Side-On μ-η^2:η^2-Peroxodicopper(II) Complex. Chem Commun. 2010; 46:91–93.
331. Lee Y, Lee DH, Narducci Sarjeant AA, Zakharov LN, Rheingold AL, Karlin KD. Thioether Sulfur Oxygenation from O_2 or H_2O_2 Reactivity of Copper Complexes with Tridentate N_2S thioether Ligands. Inorg Chem. 2006; 45:10098–10107. [PubMed: 17140215]
332. Lewin JL, Heppner DE, Cramer CJ. Validation of Density Functional Modeling Protocols on Experimental Bis(μ-oxo)/μ-η^2:η^2-Peroxo Dicopper Equilibria. JBIC, J Biol Inorg Chem. 2007; 12:1221–1234. [PubMed: 17710449]
333. Liakos DG, Neese F. Interplay of Correlation and Relativistic Effects in Correlated Calculations on Transition-Metal Complexes: The $(Cu_2O_2)^{2+}$ Core Revisited. J Chem Theory Comput. 2011; 7:1511–1523. [PubMed: 26610142]
334. York JT, Llobet A, Cramer CJ, Tolman WB. Heterobimetallic Dioxygen Activation: Synthesis and Reactivity of Mixed Cu–Pd and Cu–Pt Bis(μ-oxo) Complexes. J Am Chem Soc. 2007; 129:7990–7999. [PubMed: 17550254]
335. Kundu S, Pfaff FF, Miceli E, Zaharieva I, Herwig C, Yao S, Farquhar ER, Kuhlmann U, Bill E, Hildebrandt P, et al. A High-Valent Heterobimetallic $[Cu^{III}(\mu\text{-}O)_2Ni^{III}]^{2+}$ Core with Nucleophilic Oxo Groups. Angew Chem, Int Ed. 2013; 52:5622–5626.
336. Kundu S, Miceli E, Farquhar ER, Ray K. Mechanism of Phenol Oxidation by Heterodinuclear Ni Cu Bis(μ-oxo) Complexes Involving Nucleophilic Oxo Groups. Dalton Trans. 2014; 43:4264–4267. [PubMed: 24362244]
337. Sharp PR. Oxo and Imido Ligands in Late Transition Metal Chemistry. J Chem Soc, Dalton Trans. 2000:2647–2657.
338. Li JJ, Li W, Sharp PR. Phosphine-Based Platinum(II) Hydroxo and Oxo Complexes. Inorg Chem. 1996; 35:604–613.
339. Jacobson RR, Tyeklár Z, Farooq A, Karlin KD, Liu S, Zubieta J. A Copper-Oxygen (Cu_2-O_2) Complex. Crystal Structure and Characterization of a Reversible Dioxygen Binding System. J Am Chem Soc. 1988; 110:3690–3692.
340. Würtele C, Sander O, Lutz V, Waitz T, Tuczek F, Schindler S. Aliphatic C–H Bond Oxidation of Toluene Using Copper Peroxo Complexes That Are Stable at Room Temperature. J Am Chem Soc. 2009; 131:7544–7545. [PubMed: 19441813]
341. Maiti D, Woertink JS, Narducci Sarjeant AA, Solomon EI, Karlin KD. Copper Dioxygen Adducts: Formation of Bis(μ-oxo)dicopper(III) versus (μ-1,2)Peroxodicopper(II) Complexes with Small Changes in One Pyridyl-Ligand Substituent. Inorg Chem. 2008; 47:3787–3800. [PubMed: 18396862]
342. Hatcher LQ, Lee DH, Vance MA, Milligan AE, Sarangi R, Hodgson KO, Hedman B, Solomon EI, Karlin KD. Dioxygen Reactivity of a Copper(I) Complex with a N_3S Thioether Chelate; Peroxo–Dicopper(II) Formation Including Sulfur-Ligation. Inorg Chem. 2006; 45:10055–10057. [PubMed: 17140210]
343. Lee Y, Lee DH, Park GY, Lucas HR, Narducci Sarjeant AA, Kieber-Emmons MT, Vance MA, Milligan AE, Solomon EI, Karlin KD. Sulfur Donor Atom Effects on Copper(I)/O_2 Chemistry with Thioanisole Containing Tetradentate N_3S Ligand Leading to μ-1,2-Peroxo-Dicopper(II) Species. Inorg Chem. 2010; 49:8873–8885. [PubMed: 20822156]
344. Lee Y, Park GY, Lucas HR, Vajda PL, Kamaraj K, Vance MA, Milligan AE, Woertink JS, Siegler MA, Narducci Sarjeant AA, et al. Copper(I)/O_2 Chemistry with Imidazole Containing Tripodal Tetradentate Ligands Leading to μ-1,2-Peroxo–Dicopper(II) Species. Inorg Chem. 2009; 48:11297–11309. [PubMed: 19886646]
345. Kieber-Emmons MT, Ginsbach JW, Wick PK, Lucas HR, Helton ME, Lucchese B, Suzuki M, Zuberbühler AD, Karlin KD, Solomon EI. Observation of a $Cu^{II}_2(\mu$-1,2-peroxo)/$Cu^{III}_2(\mu$-oxo)$_2$ Equilibrium and its Implications for Copper–Dioxygen Reactivity. Angew Chem, Int Ed. 2014; 53:4935–4939.
346. Garcia-Bosch I, Company A, Frisch JR, Torrent-Sucarrat M, Cardellach M, Gamba I, Güell M, Casella L, Que L, Ribas X, et al. O_2 Activation and Selective Phenolate *ortho* Hydroxylation by an Unsymmetric Dicopper μ-η^1:η^1-Peroxido Complex. Angew Chem, Int Ed. 2010; 49:2406–2409.

347. Baldwin MJ, Ross PK, Pate JE, Tyeklar Z, Karlin KD, Solomon EI. Spectroscopic and Theoretical Studies of End-On Peroxide-Bridged Coupled Binuclear Copper(II) Model Complex of Relevance to the Active Sites in Hemocyanin and Tyrosinase. J Am Chem Soc. 1991; 113:8671–8679.

348. Lucas HR, Li L, Sarjeant AAN, Vance MA, Solomon EI, Karlin KD. Toluene and Ethylbenzene Aliphatic C–H Bond Oxidations Initiated by a Dicopper(II)-μ-1,2-Peroxo Complex. J Am Chem Soc. 2009; 131:3230–3245. [PubMed: 19216527]

349. Wei N, Murthy NN, Chen Q, Zubieta J, Karlin KD. Copper(I)/Dioxygen Reactivity of Mononuclear Complexes with Pyridyl and Quinolyl Tripodal Tetradentate Ligands: Reversible Formation of Cu:O_2 = 1:1 and 2:1 Adducts. Inorg Chem. 1994; 33:1953–1965.

350. Karlin KD, Wei N, Jung B, Kaderli S, Niklaus P, Zuberbuehler AD. Kinetics and Thermodynamics of Formation of Copper-Dioxygen Adducts: Oxygenation of Mononuclear Copper(I) Complexes Containing Tripodal Tetradentate Ligands. J Am Chem Soc. 1993; 115:9506–9514.

351. Paul PP, Tyeklár Z, Jacobson RR, Karlin KD. Reactivity Patterns and Comparisons in Three Classes of Synthetic Copper-Dioxygen {Cu_2-O_2}Complexes: Implication for Structure and Biological Relevance. J Am Chem Soc. 1991; 113:5322–5332.

352. Metz M, Solomon EI. Dioxygen Binding to Deoxyhemocyanin: Electronic Structure and Mechanism of the Spin-Forbidden Two-Electron Reduction of O_2. J Am Chem Soc. 2001; 123:4938–4950. [PubMed: 11457321]

353. Dalle KE, Gruene T, Dechert S, Demeshko S, Meyer F. Weakly Coupled Biologically Relevant $Cu^{II}_2(\mu\text{-}\eta^1\text{:}\eta^1\text{-}O_2)$ cis-Peroxo Adduct that Binds Side-On to Additional Metal Ions. J Am Chem Soc. 2014; 136:7428–7434. [PubMed: 24766458]

354. Kindermann N, Bill E, Dechert S, Demeshko S, Reijerse EJ, Meyer F. A Ferromagnetically Coupled (S = 1) Peroxodicopper(II) Complex. Angew Chem, Int Ed. 2015; 54:1738–1743.

355. Li L, Narducci Sarjeant AA, Vance MA, Zakharov LN, Rheingold AL, Solomon EI, Karlin KD. Exogenous Nitrile Substrate Hydroxylation by a New Dicopper-Hydroperoxide Complex. J Am Chem Soc. 2005; 127:15360–15361. [PubMed: 16262386]

356. Teramae S, Osako T, Nagatomo S, Kitagawa T, Fukuzumi S, Itoh S. Dinuclear Copper-Dioxygen Intermediates Supported by Polyamine Ligands. J Inorg Biochem. 2004; 98:746–757. [PubMed: 15134920]

357. Itoh K, Hayashi H, Furutachi H, Matsumoto T, Nagatomo S, Tosha T, Terada S, Fujinami S, Suzuki M, Kitagawa T. Synthesis and Reactivity of a (μ-1,1-Hydroperoxo)(μ-hydroxo)-dicopper(II) Complex: Ligand Hydroxylation by a Bridging Hydroperoxo Ligand. J Am Chem Soc. 2005; 127:5212–5223. [PubMed: 15810857]

358. Battaini G, Monzani E, Perotti A, Para C, Casella L, Santagostini L, Gullotti M, Dillinger R, Näther C, Tuczek F. A Double Arene Hydroxylation Mediated by Dicopper(II)–Hydroperoxide Species. J Am Chem Soc. 2003; 125:4185–4198. [PubMed: 12670241]

359. Kindermann N, Dechert S, Demeshko S, Meyer F. Proton-Induced, Reversible Interconversion of a μ-1,2-Peroxo and a μ-1,1-Hydroperoxo Dicopper(II) Complex. J Am Chem Soc. 2015; 137:8002–8005. [PubMed: 26061290]

360. Li L, Murthy NN, Telser J, Zakharov LN, Yap GPA, Rheingold AL, Karlin KD, Rokita SE. Targeted Guanine Oxidation by a Dinuclear Copper(II) Complex at Single Stranded/Double Stranded DNA Junctions. Inorg Chem. 2006; 45:7144–7159. [PubMed: 16933915]

361. Cruse RW, Kaderli S, Meyer CJ, Zuberbühler AD, Karlin KD. Copper-Mediated Hydroxylation of an Arene: Kinetics and Mechanism of the Reaction of a Dicopper(II) *m*-Xylyl-Containing Complex with H_2O_2 to Yield a Phenoxodicopper(II) Complex. J Am Chem Soc. 1988; 110:5020–5024.

362. Fukuzumi S, Tahsini L, Lee YM, Ohkubo K, Nam W, Karlin KD. Factors That Control Catalytic Two-versus Four-Electron Reduction of Dioxygen by Copper Complexes. J Am Chem Soc. 2012; 134:7025–7035. [PubMed: 22462521]

363. Das D, Lee YM, Ohkubo K, Nam W, Karlin KD, Fukuzumi S. Acid-Induced Mechanism Change and Overpotential Decrease in Dioxygen Reduction Catalysis with a Dinuclear Copper Complex. J Am Chem Soc. 2013; 135:4018–4026. [PubMed: 23442145]

364. Tachi Y, Aita K, Teramae S, Tani F, Naruta Y, Fukuzumi S, Itoh S. Dicopper–Dioxygen Complex Supported by Asymmetric Pentapyridine Dinucleating Ligand. Inorg Chem. 2004; 43:4558–4560. [PubMed: 15257580]

365. Tachi Y, Matsukawa Y, Teraoka J, Itoh S. A Stable Cu_2O_2 Complex Supported by an Asymmetric Dinucleating Pentapyridine Ligand Involving an Amide Linkage. Chem Lett. 2009; 38:202–203.

366. Davies G, El-Sayed MA, Henary M. Stoichiometry and Kinetics of the Low-Temperature Oxidation of $L_2Cu_2Cl_2$ (L = *N*,N,N′,N′-Tetraethylethylenediamine) by Dioxygen in Methylene Chloride and Properties of the Peroxocopper Products. Inorg Chem. 1987; 26:3266–3273.

367. Chaudhuri P, Ventur D, Wieghardt K, Peters EM, Peters K, Simon A. Preparation, Magnetism, and Crystal Structures of the Tautomers $[LCu(\mu_2\text{-}OH)_2CuL](ClO_4)^2$ (Blue) and $[LCu(\mu_2\text{-}OH_2)\text{-}(\mu_2\text{-}O)CuL](ClO_4)^2$ (Green): μ-Aqua-μ-oxo vs. Di-μ-hydroxo Linkage. Angew Chem, Int Ed Engl. 1985; 24:57–59.

368. Karlin KD, Gultneh Y, Hayes JC, Zubieta J. Copper(I)-Dioxygen Reactivity. 2. Reaction of a Three-Coordinate Copper(I) Complex with Dioxygen, with Evidence for a Binuclear Oxo-Copper(II) Species: Structural Characterization of a Parallel-Planar Dihydroxo-Bridged Dimer. Inorg Chem. 1984; 23:519–521.

369. Sanyal I, Mahroof-Tahir M, Nasir MS, Ghosh P, Cohen BI, Gultneh Y, Cruse RW, Farooq A, Karlin KD. Reactions of Dioxygen (O_2) with Mononuclear Copper(I) Complexes: Temperature-Dependent Formation of Peroxo- or Oxo- (and Dihydroxo-) Bridged Dicopper(II) Complexes. Inorg Chem. 1992; 31:4322–4332.

370. Obias HV, Lin Y, Murthy NN, Pidcock E, Solomon EI, Ralle M, Blackburn NJ, Neuhold YM, Zuberbühler AD, Karlin KD. Peroxo-, Oxo-, and Hydroxo-Bridged Dicopper Complexes: Observation of Exogenous Hydrocarbon Substrate Oxidation. J Am Chem Soc. 1998; 120:12960–12961.

371. Kitajima N, Koda T, Moro-oka Y. Synthesis of a Novel μ-oxo Binuclear Copper(II) Complex Ligated by Hydrotris(3,5-dimethyl-1-pyrazolyl)borate. Chem Lett. 1988; 17:347–350.

372. Lee DH, Murthy NN, Karlin KD. Copper(I)/Dioxygen Reactivity with Dinuclear Compounds: Catalytic Oxygenation and Oxo-Transfer to a Ketone. Inorg Chem. 1996; 35:804–805. [PubMed: 11666248]

373. Lee DH, Murthy NN, Karlin KD. Copper-Dioxygen Reactivity Using Dinucleating Ligands with Activated Methylene or Ketone Function. Bull Chem Soc Jpn. 2007; 80:732–742.

374. Maji S, Lee JCM, Lu YJ, Chen CL, Hung MC, Chen PPY, Yu SSF, Chan SI. Dioxygen Activation of a Trinuclear $Cu^ICu^ICu^I$ Cluster Capable of Mediating Facile Oxidation of Organic Substrates: Competition between O-Atom Transfer and Abortive Intercomplex Reduction. Chem - Eur J. 2012; 18:3955–3968. [PubMed: 22354807]

375. Haack P, Kärgel A, Greco C, Dokic J, Braun B, Pfaff FF, Mebs S, Ray K, Limberg C. Access to a Cu^{II}–O–Cu^{II} Motif: Spectroscopic Properties, Solution Structure, and Reactivity. J Am Chem Soc. 2013; 135:16148–16160. [PubMed: 24134722]

376. Haack P, Limberg C, Ray K, Braun B, Kuhlmann U, Hildebrandt P, Herwig C. Dinuclear Copper Complexes Based on Parallel β-Diiminato Binding Sites and their Reactions with O_2: Evidence for a Cu–O–Cu Entity. Inorg Chem. 2011; 50:2133–2142. [PubMed: 21341784]

377. Melník M. Study of the Relation Between the Structural Data and Magnetic nteraction in Oxo-Bridged Binuclear Copper(II) Compounds. Coord Chem Rev. 1982; 42:259–293.

378. Halvagar MR, Solntsev PV, Lim H, Hedman B, Hodgson KO, Solomon EI, Cramer CJ, Tolman WB. Hydroxo-Bridged Dicopper(II,III) and -(III,III) Complexes: Models for Putative Intermediates in Oxidation Catalysis. J Am Chem Soc. 2014; 136:7269–7272. [PubMed: 24821432]

379. Isaac JA, Gennarini F, Lopez I, Thibon-Pourret A, David R, Gellon G, Gennaro B, Philouze C, Meyer F, Demeshko S, et al. Room-Temperature Characterization of a Mixed-Valent μ-Hydroxodicopper(II,III) Complex. Inorg Chem. 2016; 55:8263–8266. [PubMed: 27518211]

380. Robin, MB., Day, P. Mixed Valence Chemistry-A Survey and Classification. In: Emeléus, HJ., Sharpe, AG., editors. Advanced Inorganic Chemistry and Radiochemistry. Vol. 10. Academic Press; 1968. p. 247-422.

381. Solomon EI. Dioxygen Binding, Activation, and Reduction to H_2O by Cu Enzymes. Inorg Chem. 2016; 55:6364–6375. [PubMed: 27299802]
382. Yoon J, Solomon EI. Electronic Structures of Exchange Coupled Trigonal Trimeric Cu(II) Complexes: Spin Frustration, Antisymmetric Exchange, Pseudo-A Terms, and their Relation to O_2 Activation in the Multicopper Oxidases. Coord Chem Rev. 2007; 251:379–400.
383. Itoh S, Fukuzumi S. Dioxygen Activation by Copper Complexes. Mechanistic Insights into Copper Monooxygenases and Copper Oxidases. Bull Chem Soc Jpn. 2002; 75:2081–2095.
384. Machonkin T, Mukherjee P, Henson M, Stack TDP, Solomon EI. The EPR Spectrum of a Cu(II/II/III) Cluster: Anisotropic Exchange in a Bent Cu(II)O_2 Core. Inorg Chim Acta. 2002; 341:39–44.
385. Gupta AK, Tolman WB. Cu(I)/O_2 Chemistry Using a β-Diketiminate Supporting Ligand Derived from N,N-Dimethylhydrazine: A $[Cu_3O_2]^{3+}$ Complex with Novel Reactivity. Inorg Chem. 2012; 51:1881–1888. [PubMed: 22268598]
386. Lionetti D, Day MW, Agapie T. Metal-Templated Ligand Architectures for Trinuclear Chemistry: Tricopper Complexes and Their O_2 Reactivity. Chem Sci. 2013; 4:785–790. [PubMed: 23539341]
387. Maiti D, Woertink JS, Ghiladi RA, Solomon EI, Karlin KD. Molecular Oxygen and Sulfur Reactivity of a Cyclotriveratrylene Derived Trinuclear Copper(I) Complex. Inorg Chem. 2009; 48:8342–8356. and references cited therein. [PubMed: 19663454]
388. Tsui EY, Day MW, Agapie T. Trinucleating Copper: Synthesis and Magnetostructural Characterization of Complexes Supported by a Hexapyridyl 1,3,5-Triarylbenzene Ligand. Angew Chem, Int Ed. 2011; 50:1668–1672. and references cited therein.
389. Kirillov, AM., Kirillova, MV., Pombeiro, AJL. Homogeneous Multicopper Catalysts for Oxidation and Hydrocarboxylation of Alkanes. In: van Eldik, R., Colin, DH., editors. Advances in Inorganic Chemistry. Vol. 65. Academic Press; 2013. p. 1-31.
390. Kirillov AM, Kirillova MV, Pombeiro AJL. Multicopper omplexes and Coordination Polymers for Mild Oxidative Functionalization of Alkanes. Coord Chem Rev. 2012; 256:2741–2759.
391. Mutti FG, Zoppellaro G, Gullotti M, Santagostini L, Pagliarin R, Andersson KK, Casella L. Biomimetic Modelling of Copper Enzymes: Synthesis, Characterization, EPR Analysis and Enantioselective Catalytic Oxidations by a New Chiral Trinuclear Copper(II) Complex. Eur J Inorg Chem. 2009; 2009:554–566.
392. Mutti FG, Gullotti M, Casella L, Santagostini L, Pagliarin R, Andersson KK, Iozzi MF, Zoppellaro G. A New Chiral, Poly-Imidazole N_8-Ligand and the Related Di- and Tri-Copper(II) Complexes: Synthesis, Theoretical Modelling, Spectroscopic Properties, and Biomimetic Stereoselective Oxidations. Dalton Trans. 2011; 40:5436–5457. [PubMed: 21298193]
393. Gullotti M, Santagostini L, Pagliarin R, Granata A, Casella L. Synthesis and Characterization of New Chiral Octadentate Nitrogen Ligands and Related Copper(II) Complexes as Catalysts for Stereoselective Oxidation of Catechols. J Mol Catal A: Chem. 2005; 235:271–284.
394. Mimmi MC, Gullotti M, Santagostini L, Saladino A, Casella L, Monzani E, Pagliarin R. Stereoselective Catalytic Oxidations of Biomimetic Copper Complexes with a Chiral Trinucleating Ligand Derived from 1,1-Binaphthalene. J Mol Catal A: Chem. 2003; 204–205:381–389.
395. Mimmi MC, Gullotti M, Santagostini L, Battaini G, Monzani E, Pagliarin R, Zoppellaro G, Casella L. Models for Biological Trinuclear Copper Clusters. Characterization and Enantioselective Catalytic Oxidation of Catechols by the Copper(II) Complexes of a Chiral Ligand Derived from (*S*)-(–)-1,1′-Binaphthyl-2,2′-diamine. Dalton Trans. 2004:2192–2201. [PubMed: 15249957]
396. Mirica LM, Stack TDP. A Tris(μ-hydroxy)tricopper(II) Complex as a Model of the Native Intermediate in Laccase and Its Relationship to a Binuclear Analogue. Inorg Chem. 2005; 44:2131–2133. [PubMed: 15792444]
397. Yoon J, Mirica LM, Stack TDP, Solomon EI. Spectroscopic Demonstration of a Large Antisymmetric Exchange Contribution to the Spin-Frustrated Ground State of a D_3 Symmetric Hydroxy-Bridged Trinuclear Cu(II) Complex: Ground-to-Excited State Superexchange Pathways. J Am Chem Soc. 2004; 126:12586–12595. [PubMed: 15453791]

398. Yoon J, Solomon EI. Ground-State Electronic and Magnetic Properties of a μ_3-Oxo-Bridged Trinuclear Cu(II) Complex: Correlation to the Native Intermediate of the Multicopper Oxidases. Inorg Chem. 2005; 44:8076–8086. [PubMed: 16241158]

399. Yoon J, Mirica LM, Stack TDP, Solomon EI. Variable-Temperature, Variable-Field Magnetic Circular Dichroism Studies of Tris-Hydroxy- and μ_3-Oxo-Bridged Trinuclear Cu(II) Complexes: Evaluation of Proposed Structures of the Native Intermediate of the Multicopper Oxidases. J Am Chem Soc. 2005; 127:13680–13693. [PubMed: 16190734]

400. Suh MP, Han MY, Lee JH, Min KS, Hyeon C. One- Pot Template Synthesis and Properties of a Molecular Bowl: Dodecaaza Macrotetracycle with μ_3-Oxo and μ_3-Hydroxo Tricopper- (II) Cores. J Am Chem Soc. 1998; 120:3819–3820.

401. Chen PPY, Yang RBG, Lee JCM, Chan SI. Facile OAtom Insertion into C-C and C-H bonds by a Trinuclear Copper Complex Designed to Harness a Singlet Oxene. Proc Natl Acad Sci U S A. 2007; 104:14570–14575. [PubMed: 17804786]

402. Chan SI, Chien CYC, Yu CSC, Nagababu P, Maji S, Chen PPY. Efficient Catalytic Oxidation of Hydrocarbons Mediated by Tricopper Clusters Under Mild Conditions. J Catal. 2012; 293:186–194.

403. Chan SI, Lu YJ, Nagababu P, Maji S, Hung MC, Lee MM, Hsu IJ, Minh PD, Lai JCH, Ng KY, et al. Efficient Oxidation of Methane to Methanol by Dioxygen Mediated by Tricopper Clusters. Angew Chem, Int Ed. 2013; 52:3731–3735.

404. Barnett SM, Goldberg KI, Mayer JM. A Soluble Copper–Bipyridine Water-Oxidation Electrocatalyst. Nat Chem. 2012; 4:498–502. [PubMed: 22614386]

405. Du J, Chen Z, Ye S, Wiley BJ, Meyer TJ. Copper as a Robust and Transparent Electrocatalyst for Water Oxidation. Angew Chem, Int Ed. 2015; 54:2073–2078.

406. A recent example: Garcia-Bosch I, Siegler MA. Copper- Catalyzed Oxidation of Alkanes with H_2O_2 under a Fenton-like Regime. Angew Chem, Int Ed. 2016; 55:12873–12876.

407. Liu JJ, Diaz DE, Quist DA, Karlin KD. Copper(I)-Dioxygen Adducts and Copper Enzyme Mechanisms. Isr J Chem. 2016; 56:738–755.

408. Abad E, Rommel JB, Kastner J. Reaction mechanism of the bicopper enzyme peptidylglycine alpha-hydroxylating monooxygenase. J Biol Chem. 2014; 289:13726–13738. [PubMed: 24668808]

Biographies

Courtney E. Elwell grew up in upstate New York and obtained her B.S. in Chemistry from Union College (Schenectady, NY) in 2014. There she worked under the direction of Laurie A. Tyler in the synthesis of thiazole-derived copper complexes and the study of their biological activity with DNA and serum proteins. She is currently a doctoral candidate advised by William B. Tolman at the University of Minnesota working on the synthesis of ligand frameworks that demonstrate how electronics and overall charge influence reactivity of monocopper and dicopper-oxygen cores.

Nicole L. Gagnon grew up in Lino Lakes, MN, and received a B.A. degree from the College of St. Benedict, MN, in 2010 under the guidance of Dr. Richard White. During her undergraduate work, she studied the simultaneous determination of partition coefficient and acid-dissociation constant of benzoic acid in water. After studying at the University of Arizona, she joined the laboratory of W. B. Tolman at the University of Minnesota in 2012. She is currently a Ph.D. candidate working on the synthesis of dicopper-hydroxide complexes for C–H bond activation using a naphthyridine-based ligand.

Benjamin D. Neisen received his B.S. in chemistry and biochemistry from the University of Minnesota–Duluth in 2011. While there, he studied ferrocene-substituted porphyrin systems

under Professor Viktor Nemykin. He then moved to the University of Minnesota–Twin Cities where he earned his M.S. in chemistry and is now a chemistry Ph.D. candidate performing research under Professor William B. Tolman studying the synthesis and reactivity of high valent copper-oxygen species.

Debanjan Dhar grew up in Kolkata, India. After the completion of his B.Sc. in Chemistry from Presidency College, Kolkata, in 2009, he moved to Indian Institute of Technology Kanpur, India, to pursue a M.Sc. in Chemistry. While in Kanpur he carried out research under the supervision of R. N. Mukherjee, where he worked on the chemistry of metal complexes of redox non-innocent ligand frameworks. He joined the Department of Chemistry, University of Minnesota, as a graduate student in 2012, where he is currently working under the guidance of William B. Tolman. His current research focus is on the chemistry of mononuclear copper-oxygen complexes and their role in C–H bond activation.

Andrew D. Spaeth grew up in Kenosha, WI. He received his B.S. from Michigan Technological University working with B. Török and E. Urnezius. He pursued graduate studies with M. V. Barybin at the University of Kansas and obtained a Ph.D. in 2014, focusing on linear azulenic organometallics. He is currently a postdoctoral research associate with William B. Tolman at the University of Minnesota. His research interests are at the intersection of computational and experimental inorganic chemistry of biological significance.

Gereon M. Yee, hailing from northern California, attended Santa Rosa Junior college before transferring to UC Davis, where he received his B.S. in chemistry in 2010. There he did undergraduate research in inorganic chemistry with Louise Berben before moving to the University of Minnesota to pursue a Ph.D. under the advisement of William B. Tolman. In 2013, he received his M.S. in chemistry, and currently, he is a 5th year Ph.D. candidate studying the effects of ligand modification on the HAT reactivity of mononuclear copper(III)-hydroxide complexes.

William B. Tolman obtained a B.A. degree from Wesleyan University, CT, in 1983, and a Ph.D. from the University of California, Berkeley, in 1987. He then was a postdoctoral associate at the Massachusetts Institute of Technology (1987–1990). Appointed as Assistant Professor in the Department of Chemistry at the University of Minnesota in 1990, he is now Distinguished McKnight University Professor. He is a member of the Centers for Metals in Biocatalysis and Sustainable Polymers and has served as Chair of the Department of Chemistry since 2009. He has received the Searle Scholars, NSF National Young Investigator, Camille & Henry Dreyfus Foundation Teacher-Scholar, and Alfred P. Sloan Foundation Awards, the Buck-Whitney Medal from the American Chemical Society (ACS), a Research Award from the Humboldt Foundation, and the 2017 ACS Award for Distinguished Service in the Advancement of Inorganic Chemistry. He is a Fellow of the American Association for the Advancement of Science and the American Chemical Society. He served as Associate Editor (2009–2012) and now as Editor-in-Chief of the ACS journal Inorganic Chemistry (from 2013 to present), sits on a number of governing and advisory boards, and was Chair of the Gordon Research Conferences on Inorganic Reaction

Mechanisms (2005) and Metals in Biology (2011). Research in his group focuses on synthetic bioinorganic and organometallic/polymer chemistry.

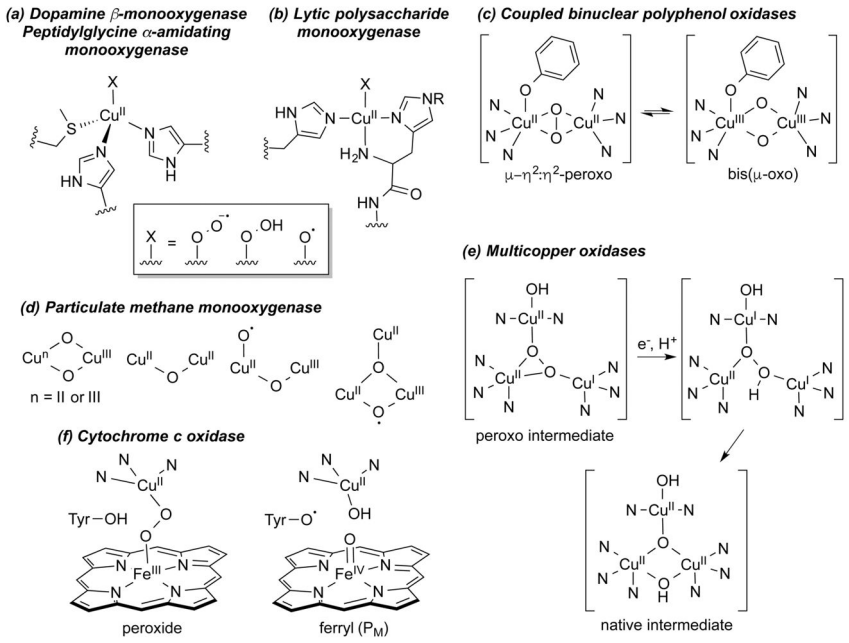

Figure 1.

Proposed copper–oxygen intermediates involved in the reactions of the indicated enzymes. (a) and (b) Superoxo, hydroperoxo, and oxyl intermediates proposed for the monocopper sites in the indicated enzymes, R = H or Me. (c) Possible equilibrium between putative substrate-bound intermediates, either of which could undergo electrophilic attack at the substrate to yield a catecholate species in the monooxygenase reaction of coupled binuclear polyphenol oxidases such as tyrosinase (N indicates nitrogen donor atom of histidine imidazoles). (d) Selected copper–oxygen intermediates speculated to be responsible for C–H bond attack of substrate by particulate methane monooxygenase. (e) Selected tricopper intermediates proposed for reduction of O_2 to H_2O by the multicopper oxidases.[40] The proximate type 1 Cu electron transfer center is not shown. (f) Two key intermediates proposed for reduction of O_2 to H_2O by the Fe–Cu core of cytochrome *c* oxidase.

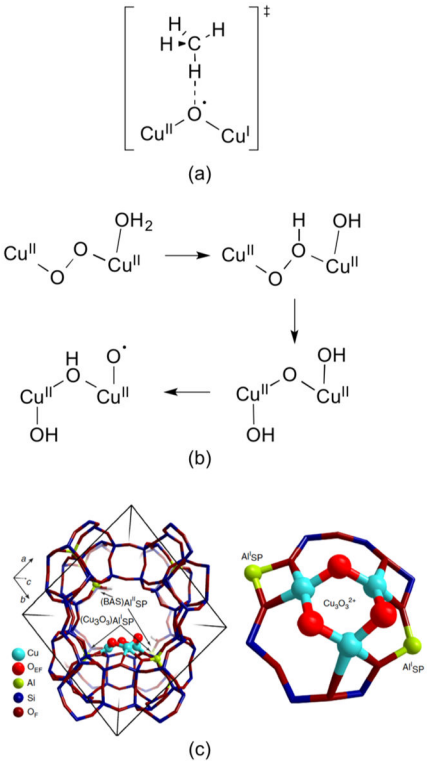

Figure 2.

(a) Proposed transition state for hydrogen atom abstraction from methane by the (μ-oxo)dicopper core of Cu-ZSM-5 (ref 112). (b) Alternative O_2 activation pathway calculated by DFT for Cu-ZSM-5 (ref 115). (c) Structure and location of $[Cu_3(\mu\text{-}O)_3]^{2+}$ core in mordenite. Reprinted with permission from ref 118. Copyright 2015 Nature Publishing Group.

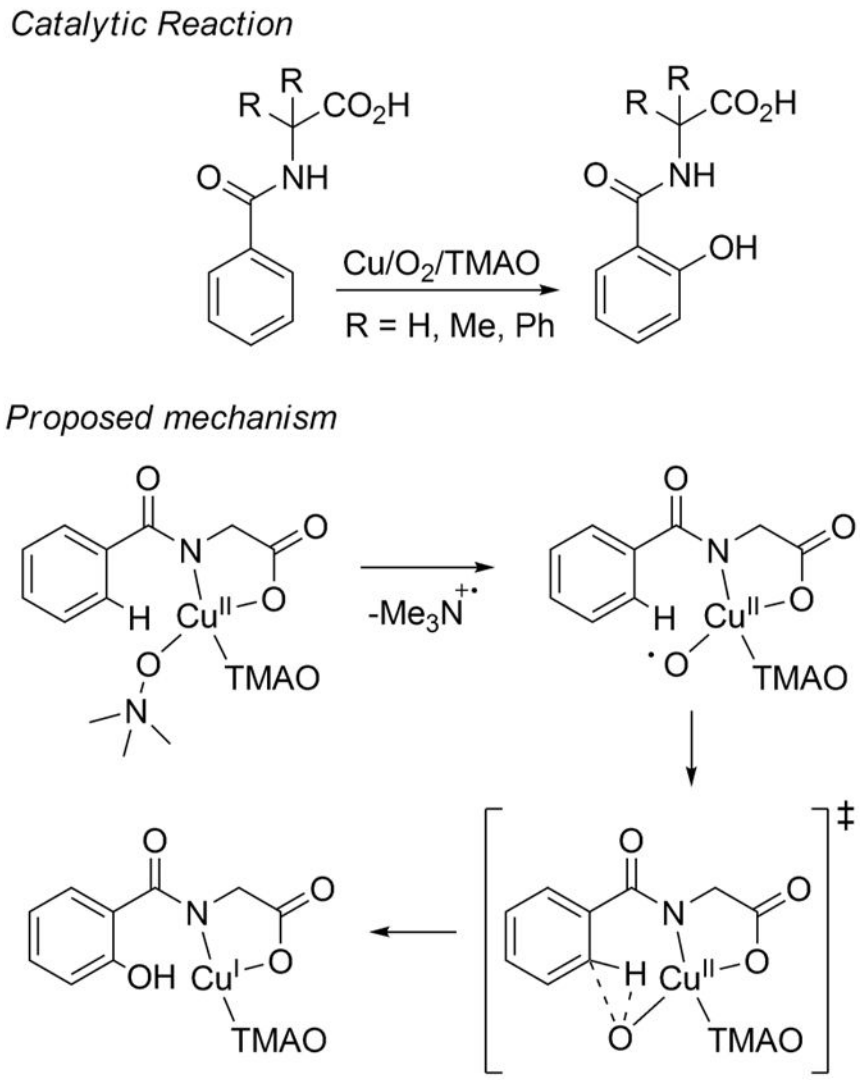

Figure 3.

Overall catalytic reaction and proposed mechanism for the hydroxylation of benzoate derivatives (TMAO is trimethylamine-*N*-oxide) (ref 121).

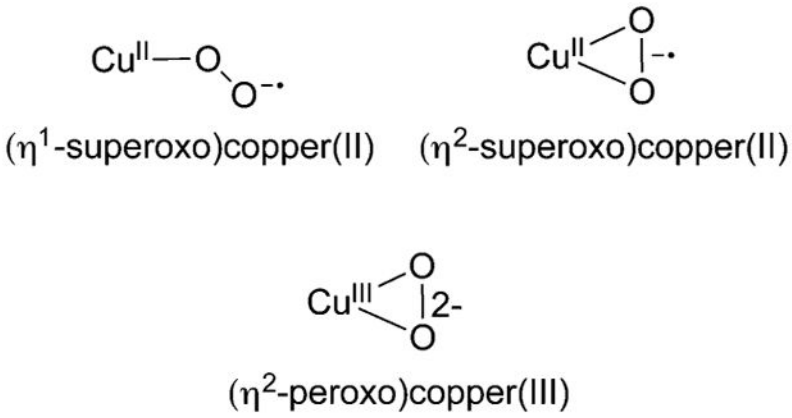

Figure 4.
1:1 Cu:O_2 core structures.

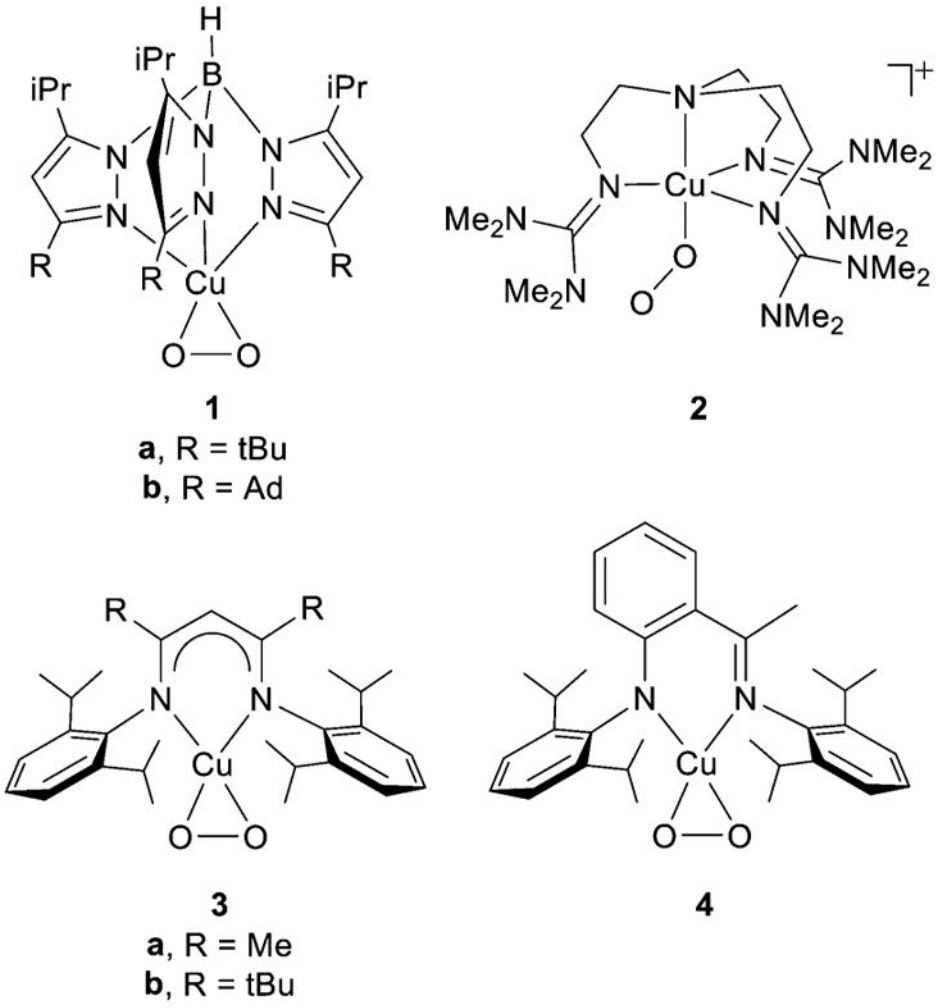

Figure 5.

1:1 Cu:O_2 adducts defined by X-ray crystallography, supported by ligands **L39a,b** (**1a,b**), **L44** (**2**), **L2d,e** (**3a,b**), or **L3b** (**4**). Reprinted from ref 123. Copyright 2007 American Chemical Society.

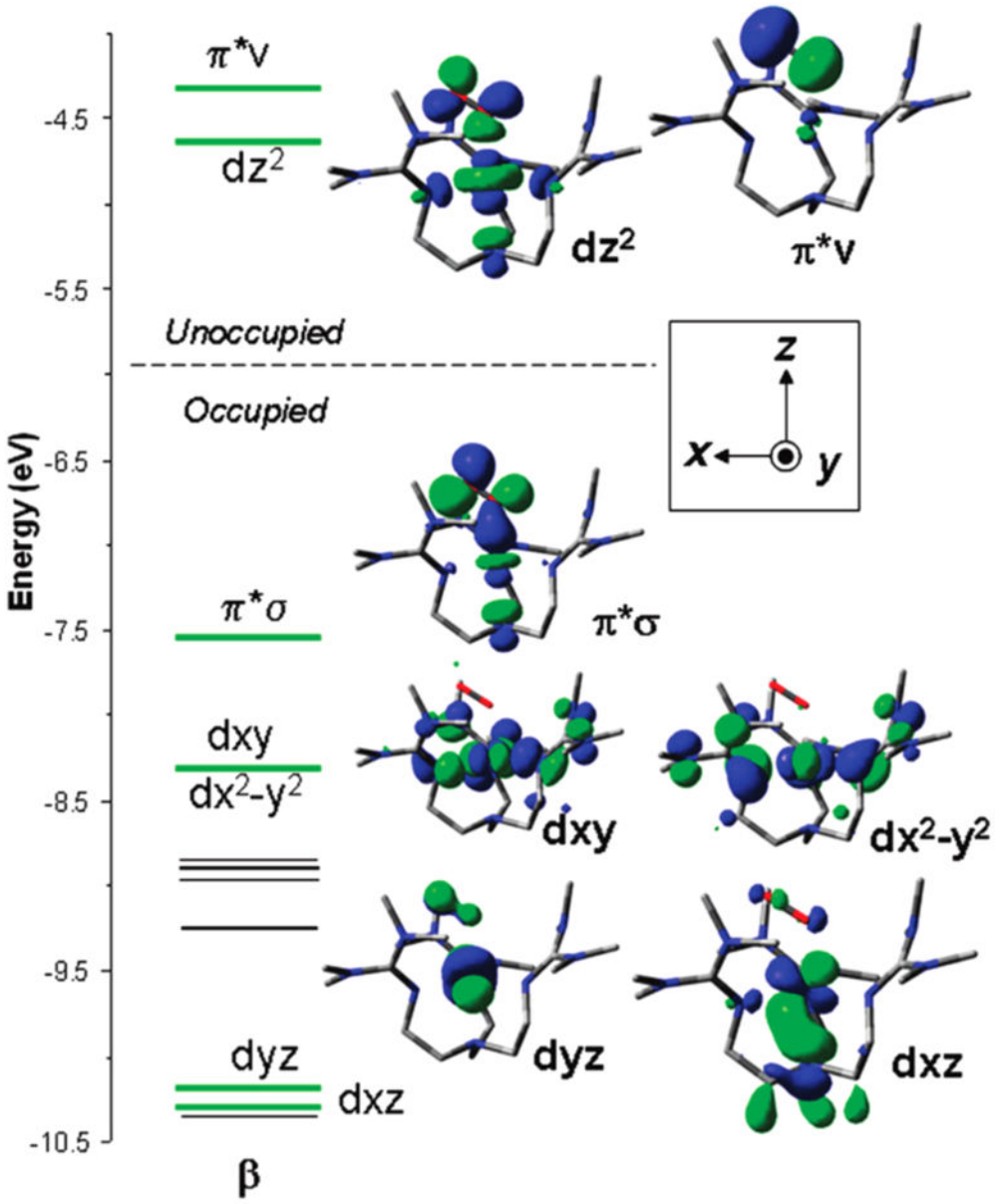

Figure 6.
DFT calculated spin down (β) MO diagram of **2**. Reprinted from ref 133. Copyright 2010 American Chemical Society.

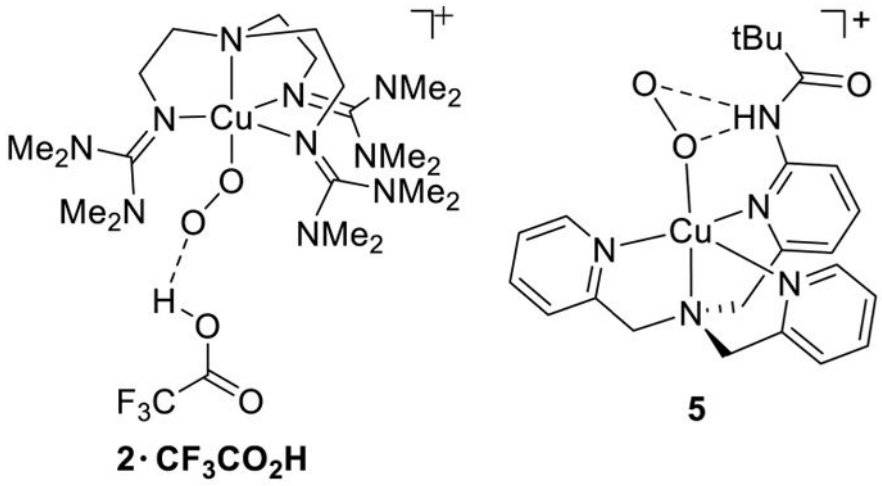

Figure 7.

Proposed hydrogen bonding interactions in **2**·CF_3CO_2H and **5** (refs 134 and 130) supported by ligands **L44** and **L41d**, respectively.

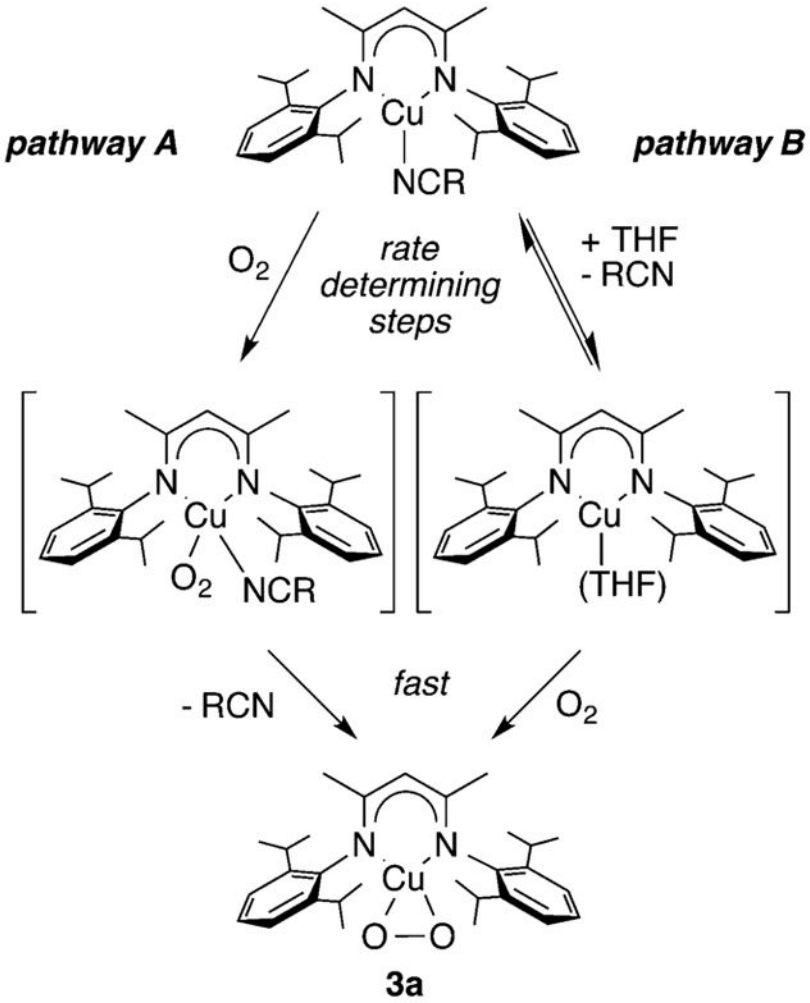

Figure 8.

Proposed dual pathway for the oxygenation reaction resulting in formation of complex **3a**. Adapted from ref 151.

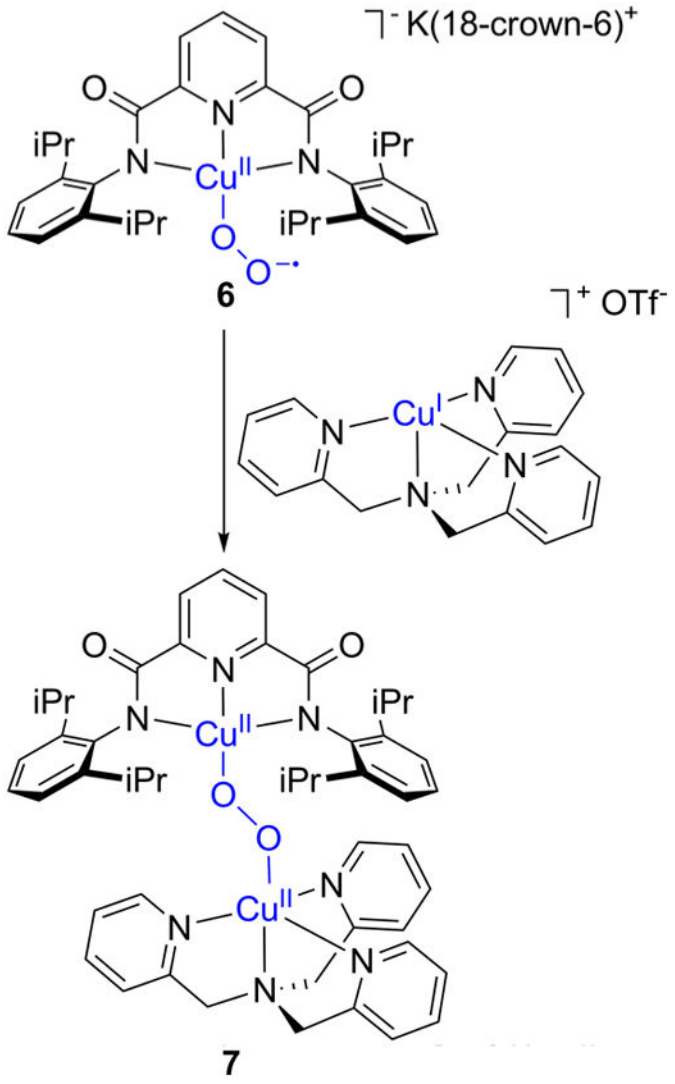

Figure 9.

Reaction of a 1:1 Cu:O_2 adduct (**6**, supported by ligand **L28a**) with a Cu(I) complex to yield a (*trans*-1,2-peroxo)dicopper complex (**7**; ref 128).

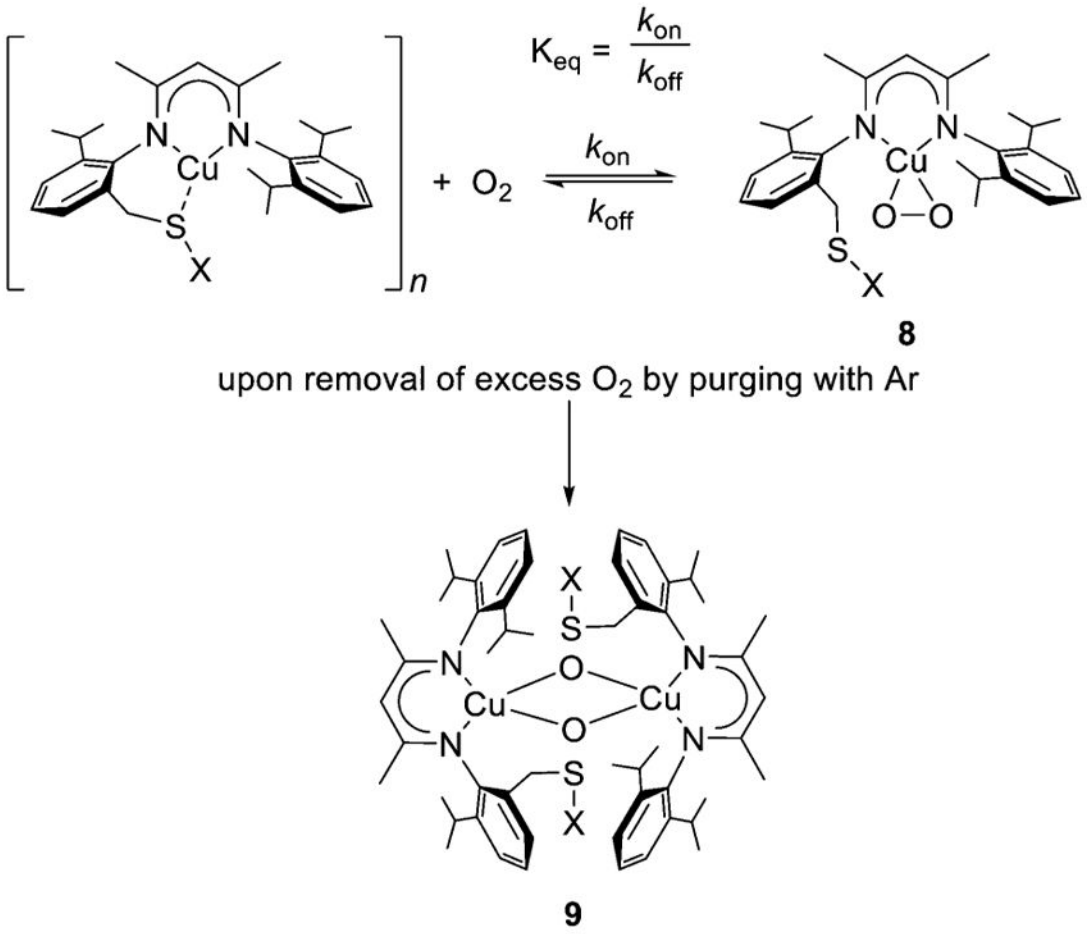

Figure 10.

Reversible O_2 binding to yield 1:1 Cu:O_2 adduct **8** (supported by **L74**, X = Me or Ph) and its conversion to a bis(μ-oxo)dicopper complex **9**. Adapted from ref 141.

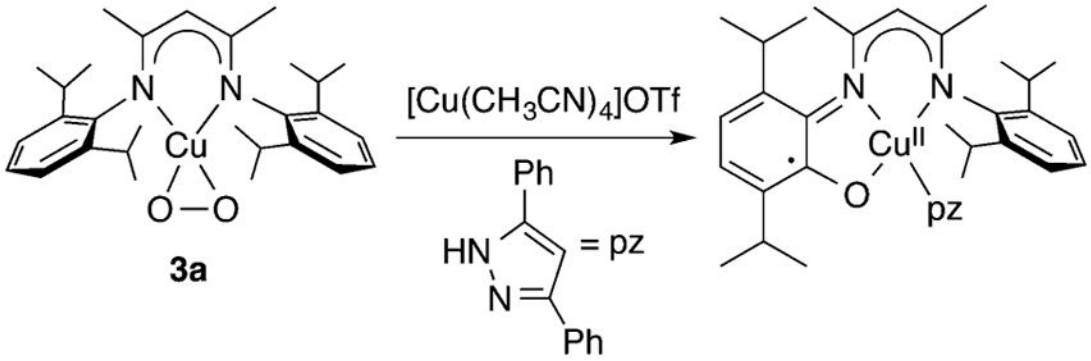

Figure 11.
Intramolecular aryl ring hydroxylation/oxidation reaction of **3a** (ref 170).

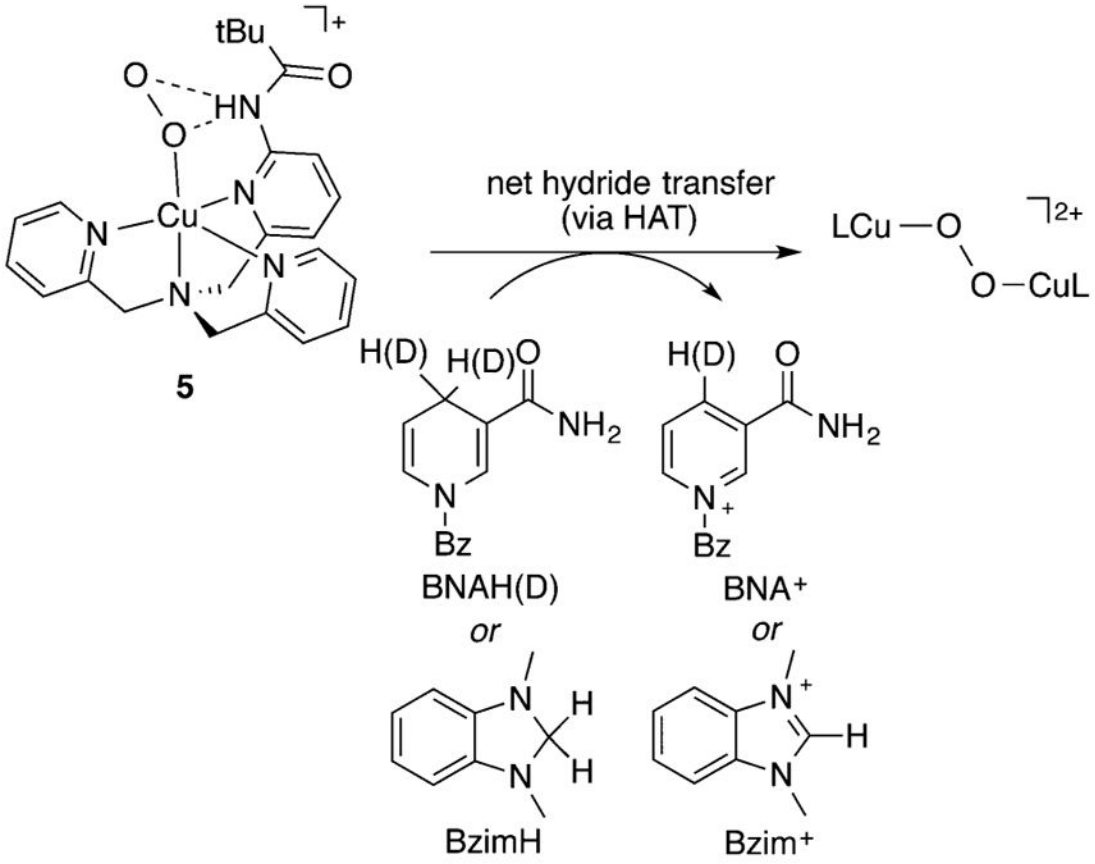

Figure 12.
Reactivity of **5** with hydride donors, proposed to involve initial HAT (ref 130).

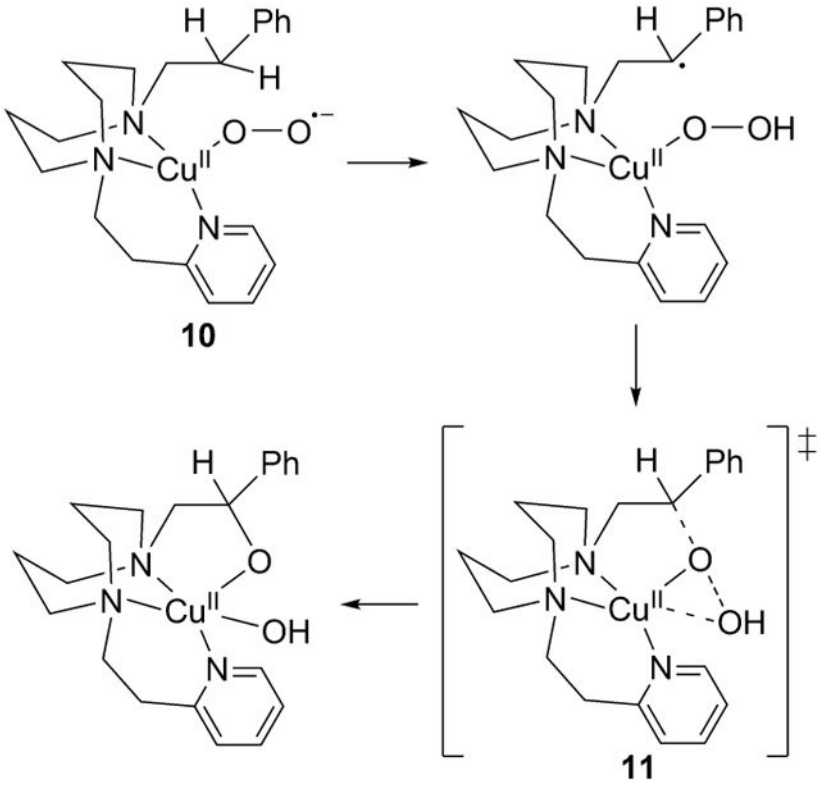

Figure 13.
Proposed mechanism for intramolecular hydroxylation by **10** (supported by **L33c**, refs 131 and 162).

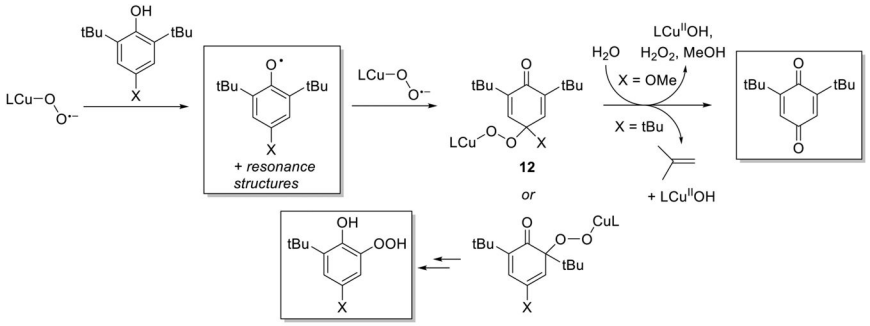

Figure 14.

Proposed pathways for the generation of oxidized products (in boxes) from the reaction of Cu(II)-$O_2^{-\bullet}$ complexes supported by L (**L41b** and **L41c**; similar products formed for **L44**) (refs 127, 136, and 175).

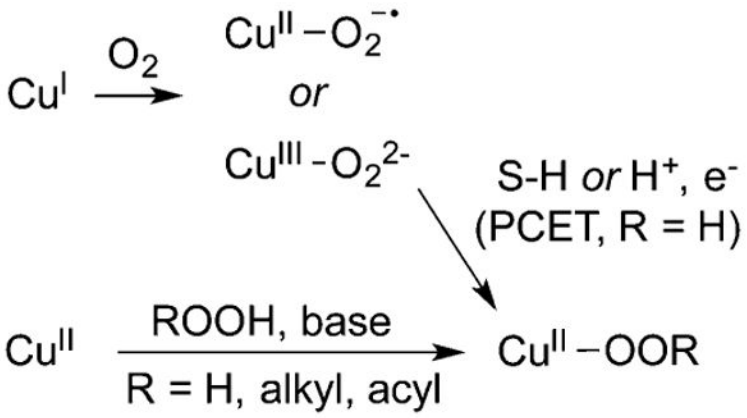

Figure 15.
Routes by which $[CuOOR]^+$ (R = H, alkyl, or acyl) complexes may be generated. S–H = substrate C–H or O–H bond. Supporting ligands not shown.

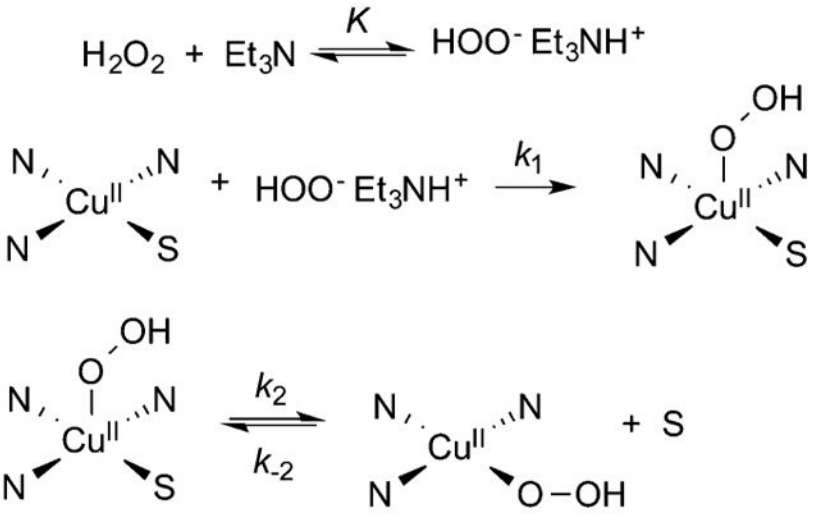

Figure 16.

Proposed mechanism for generation of $[CuOOH]^+$ complexes supported by ligand **L35b** and **L35c**. Only the donor N atoms of the supporting ligand are shown; S = solvent molecule (ref 179).

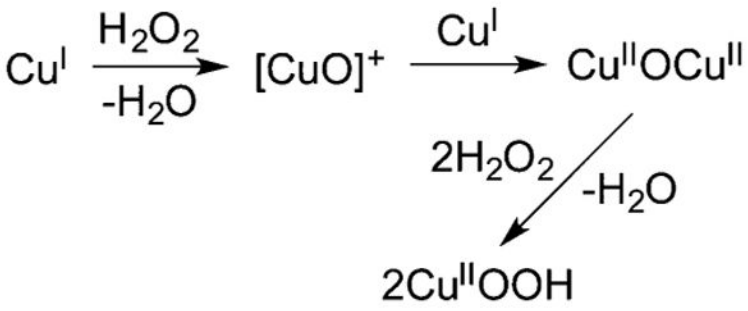

Figure 17.

Proposed mechanism for generation of $[CuOOH]^+$ complexes supported by ligand **L41h** (ligand not shown; ref 188).

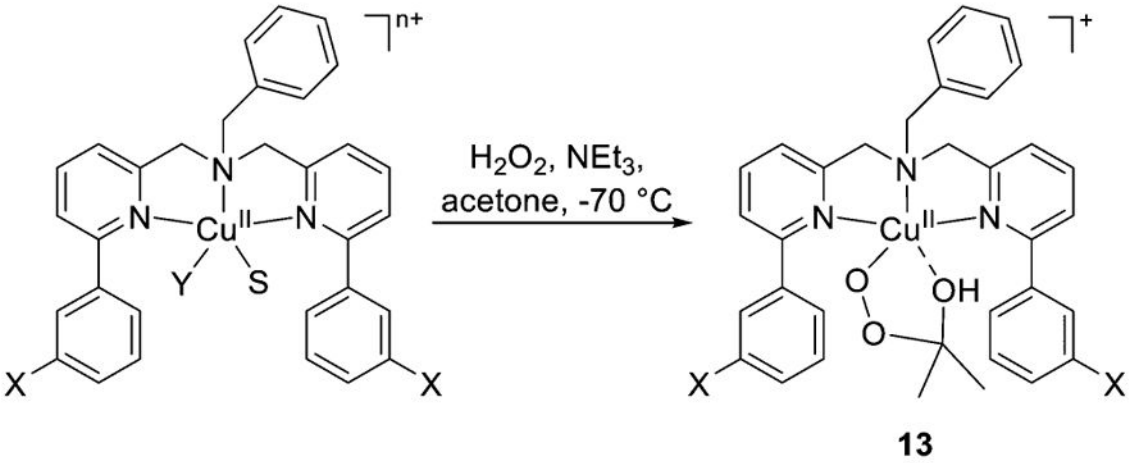

13

Figure 18.

Generation of alkylperoxide complexes supported by **L18** via functionalization of acetone solvent. Y = ClO_4^- or H_2O; S = MeCN or H_2O; X = NO_2, Cl, H, Me, OMe; n = 1 or 2, depending on Y (refs 180, 184, and 185).

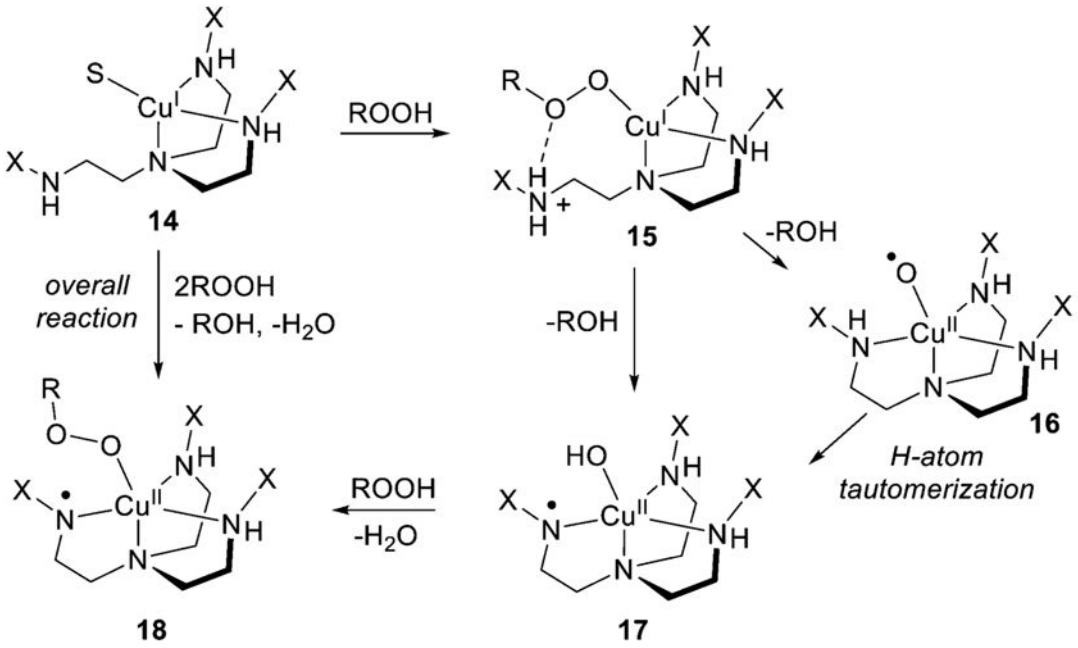

Figure 19.

Proposed mechanism for the generation of **18** from reaction of cumene hydroperoxide with the Cu(I) complex (**14**) of **L42c** (X = TIPT), R = dimethylbenzyl (cumyl), S = CH_3CN (ref 195).

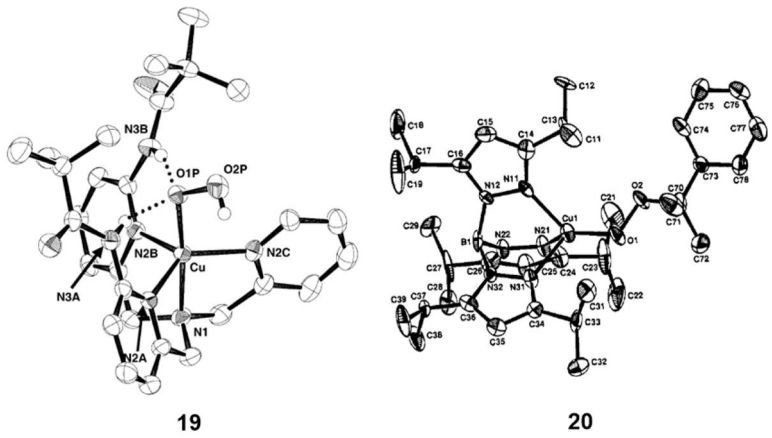

Figure 20.

X-ray structures of the $[CuOOH]^+$ complex of **L41e** (**19**), also drawn in Figure 21), and the $[CuOOCm]^+$ (*Cm* = cumyl) complex of **L39c** (**20**). Selected interatomic distances (Å): (**19**) Cu–O, 1.888(4); O–O, 1.460(6) (**20**) Cu–O, 1.816(4); O–O, 1.460(6). (**19**) Reprinted from ref 37. Copyright 2005 Elsevier. (**20**) Reprinted from ref 199. Copyright 1993 American Chemical Society.

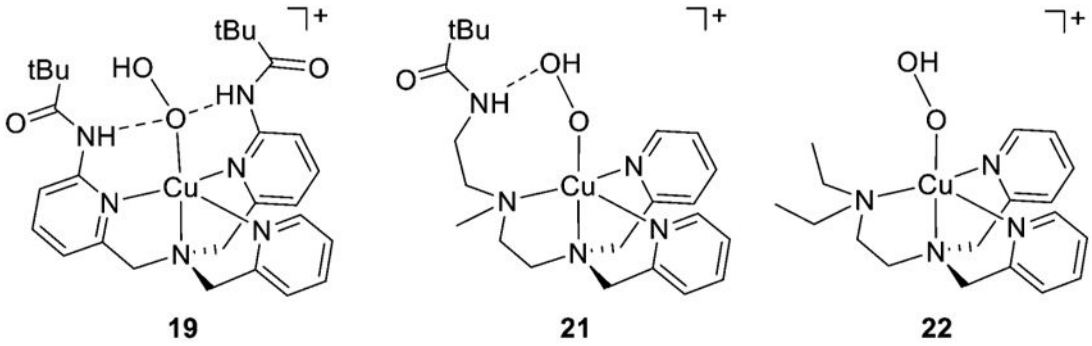

Figure 21.

$[CuOOH]^+$ complexes illustrating hydrogen bonding to the proximal O atom (**19**, supported by **L41e**) (refs 198 and 211), distal O atom (**21**, supported by **L43a**; ref 207), and with no hydrogen bonding (**22**, supported by **L43b**; ref 207).

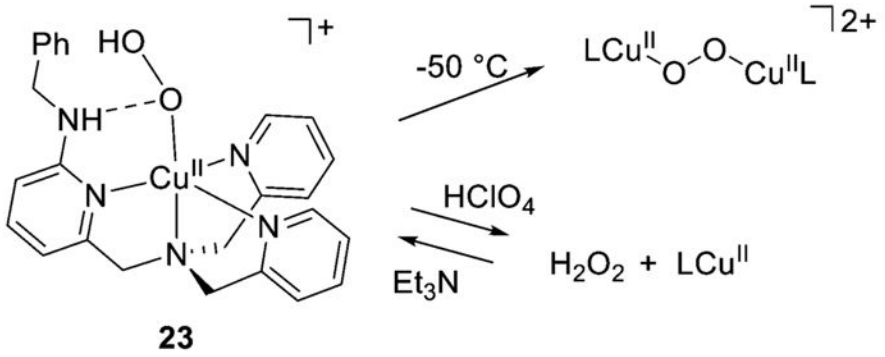

Figure 22.
Reactivity of $[CuOOH]^+$ complex **23** (L = **L41h**) (refs 188 and 193).

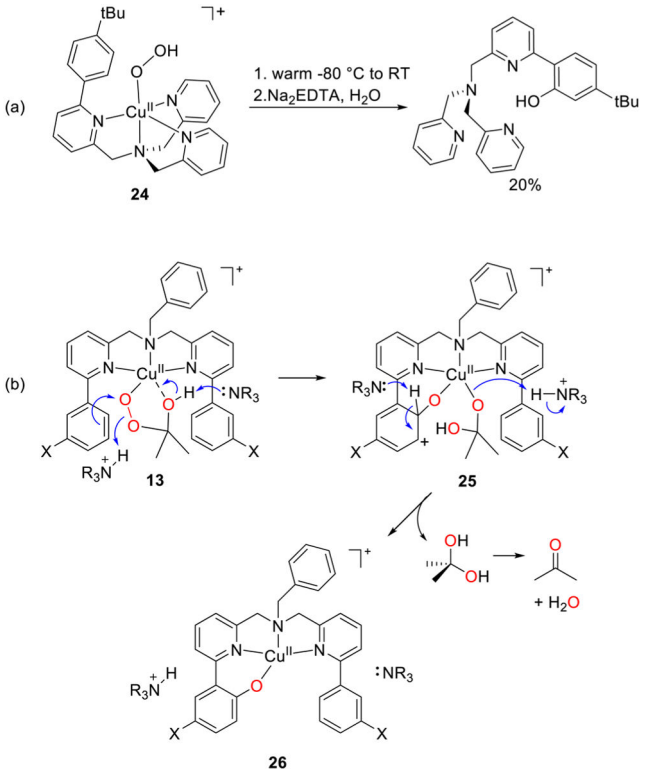

Figure 23.

Aryl group hydroxylations by $[CuOOR]^+$ complexes. (a) Reaction of complex **24** supported by **L41f** (ref 181). (b) Reaction of 2-hydroxy-2-peroxypropane complexes **13**, highlighting the proposed mechanism. X = NO_2, Cl, H, Me, OMe (refs 180 and 184).

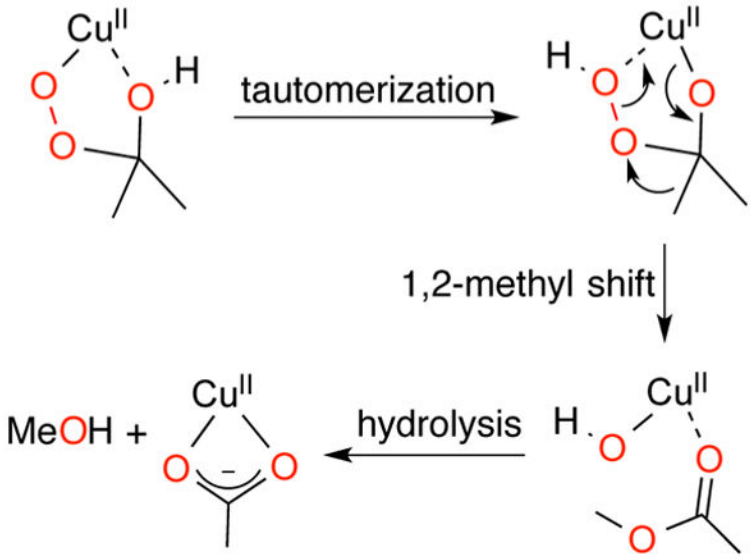

Figure 24.

Proposed mechanism for the conversion of the 2-hydroxy-2-peroxypropane complex of **L18a** to a Cu(II)-acetate complex (ref 184).

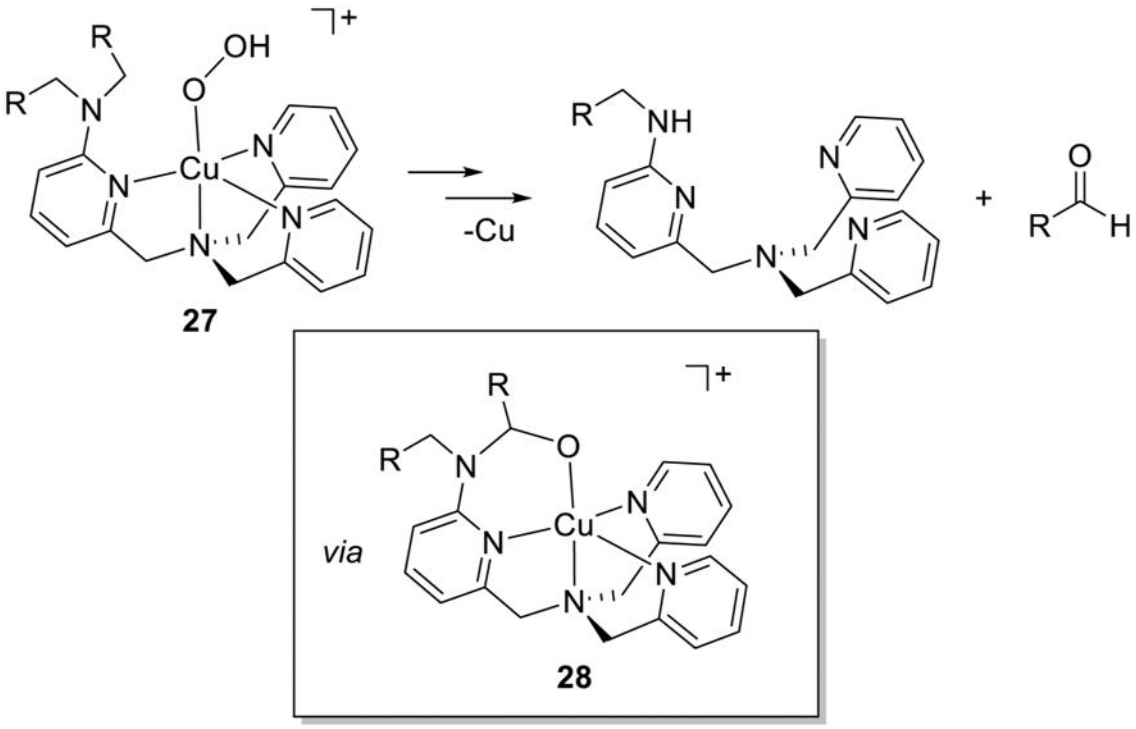

Figure 25.

N-dealkylation reactions of complexes (**27**) of **L41g** (R = H) and **L41i**–**k** (R = aryl) (refs 182, 186, and 189).

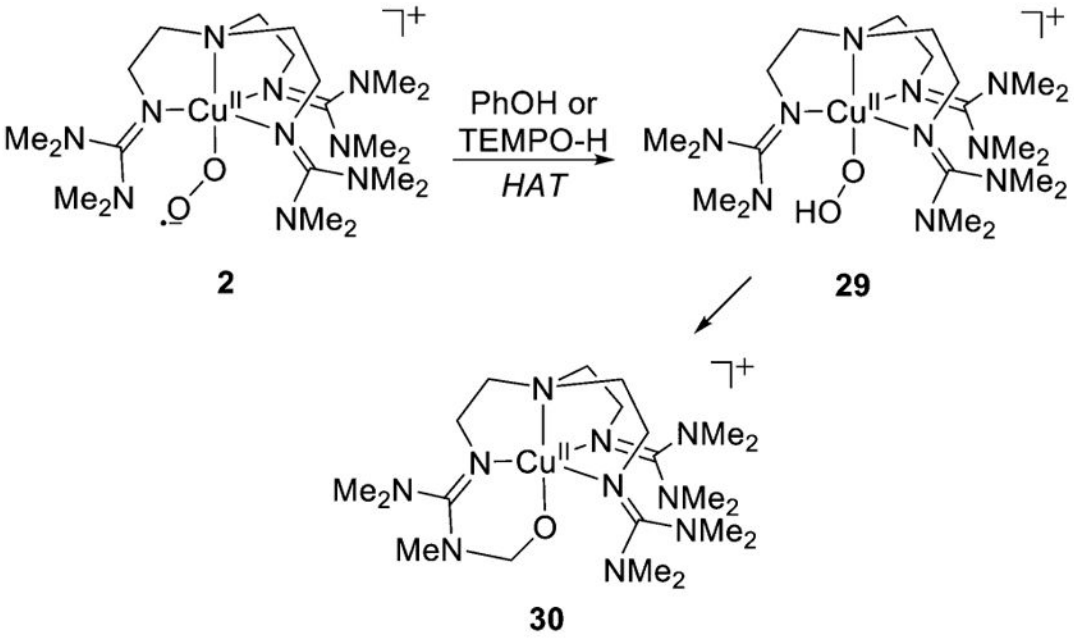

Figure 26.

Proposed conversion of 1:1 Cu:O_2 complex **2** to copper(II)-alkoxide **30** upon reaction with H atom donor reagents (ref 175).

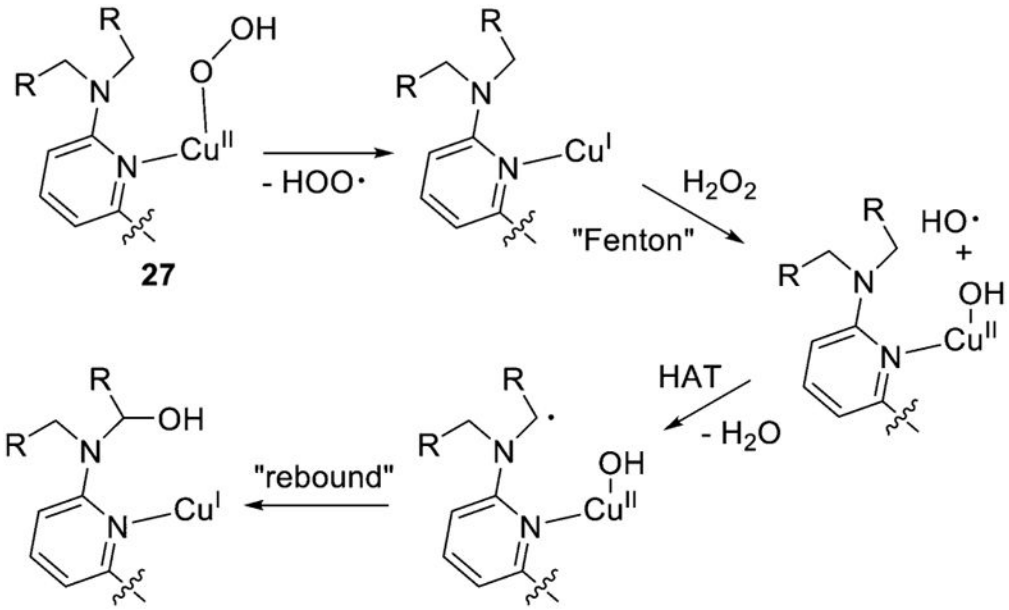

Figure 27.

Hypothesized mechanism for N-dealkylation of **27**, with only the attacked arm of the **L41i–k** ligand shown. All copper species have an overall charge of +1 (ref 189).

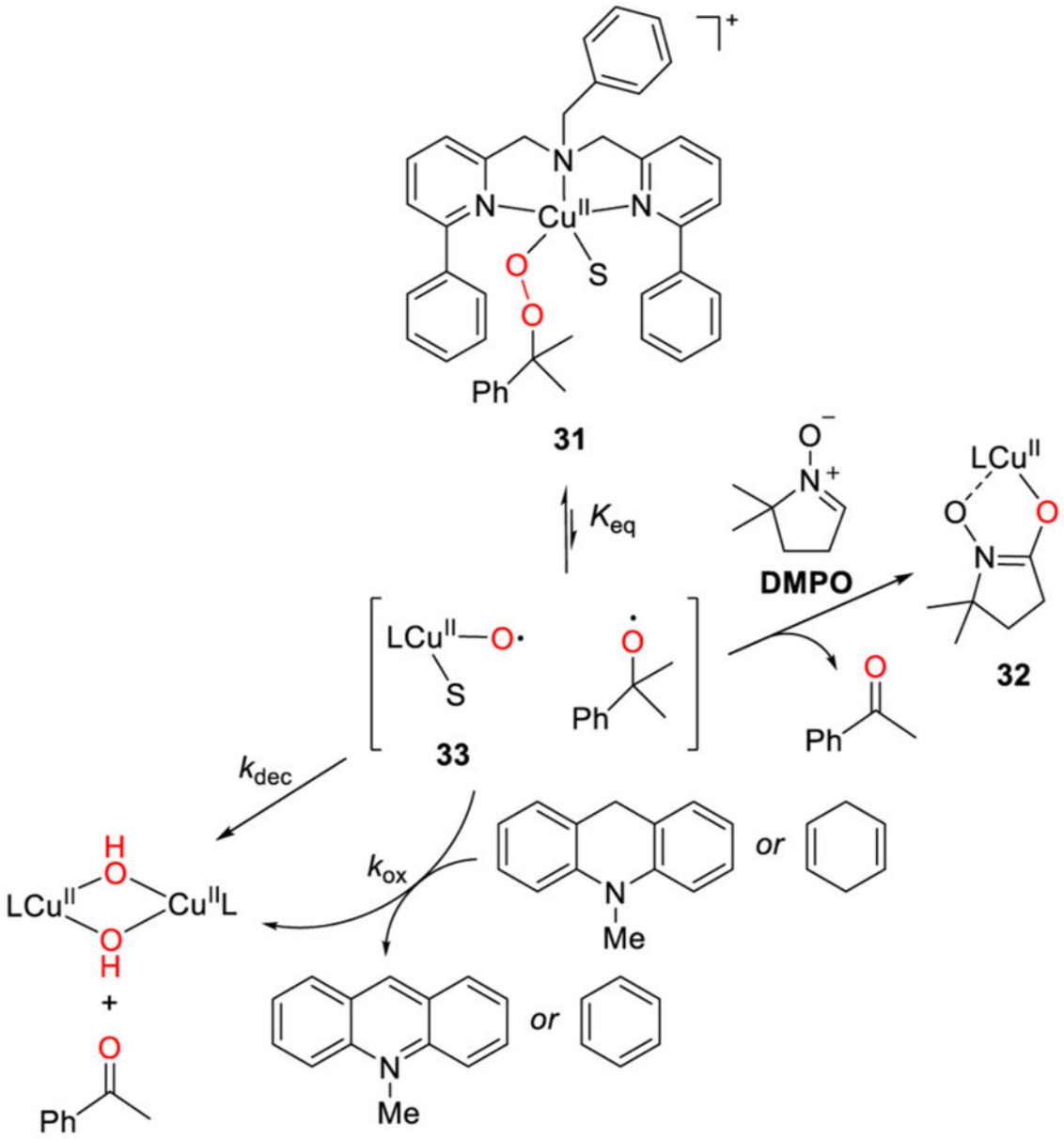

Figure 28.
Reactivity of $[CuOOR]^+$ (R = *Cm*) complex **31** with proposed mechanism involving O–O bond homolysis (ref 185).

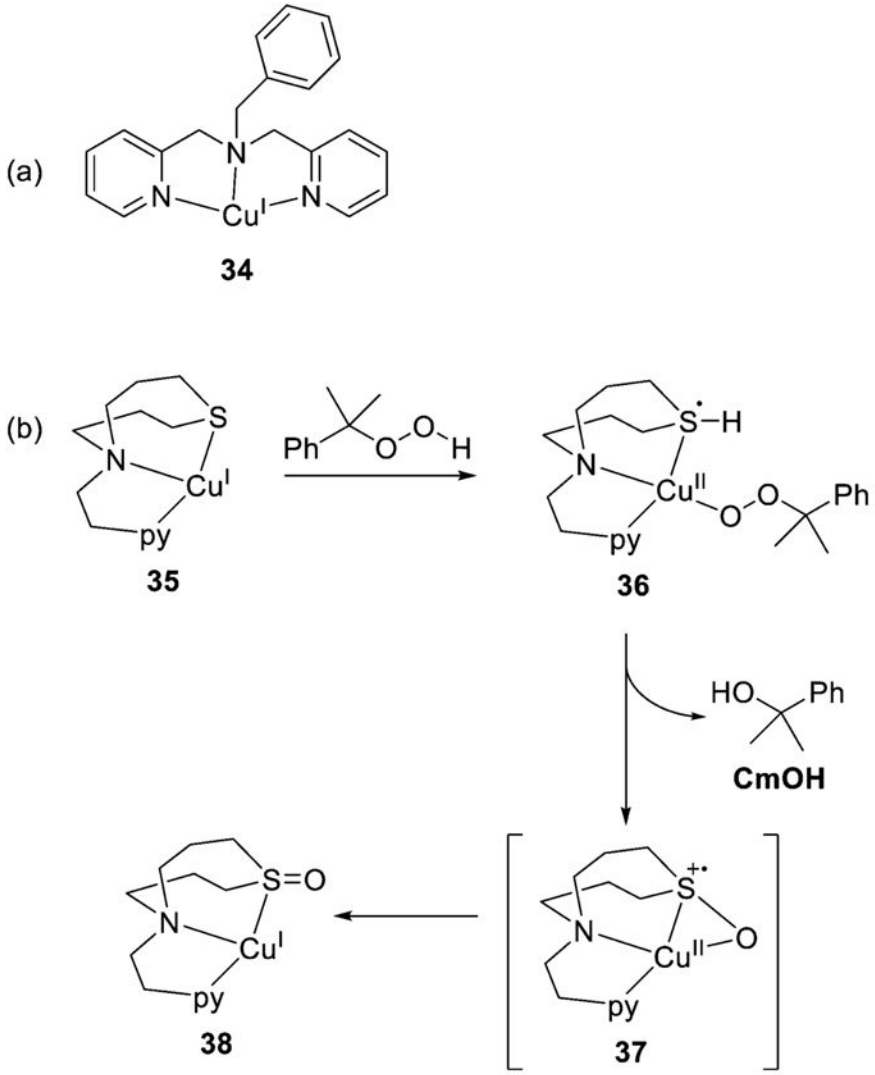

Figure 29.

Copper(I) complexes (a) **34** (supported by **L18a**) which proceeds via a 2:1 stoichiometry (not shown) and (b) the proposed pathway for reaction of cumyl hydroperoxide with **35** (supported by **L69**) to yield CmOH and the Cu(I) complex of the oxidized ligand **38** (refs 191 and 192).

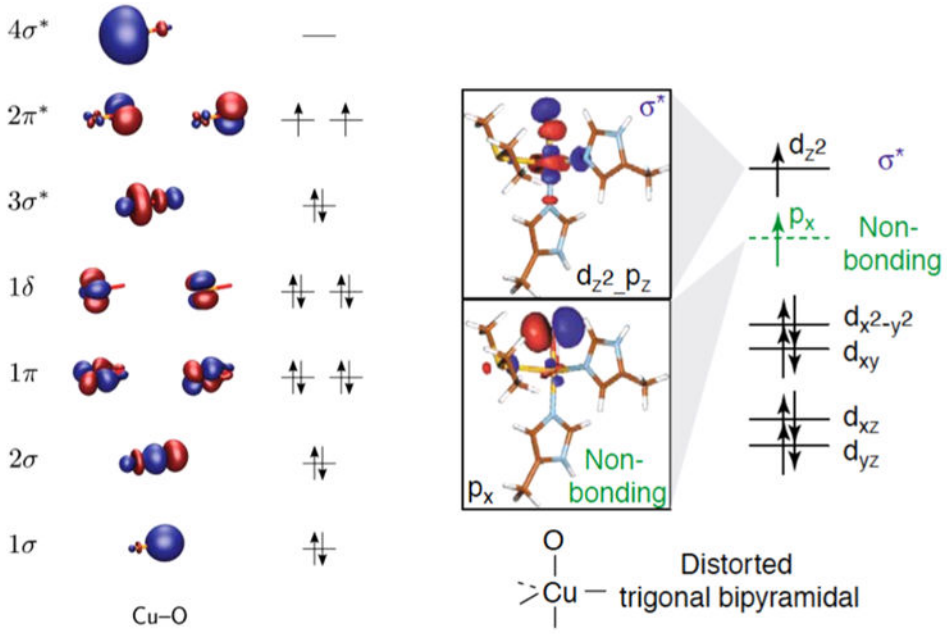

Figure 30.

(left) Qualitative molecular orbital (MO) scheme for $[CuO]^+$. Reprinted with permission from ref 57. Copyright 2011 AIP Publishing). (right) Orbital scheme for $[CuO]^+$ unit in PHM. Reprinted with permission from ref 17. Copyright 2005 Elsevier Ltd.

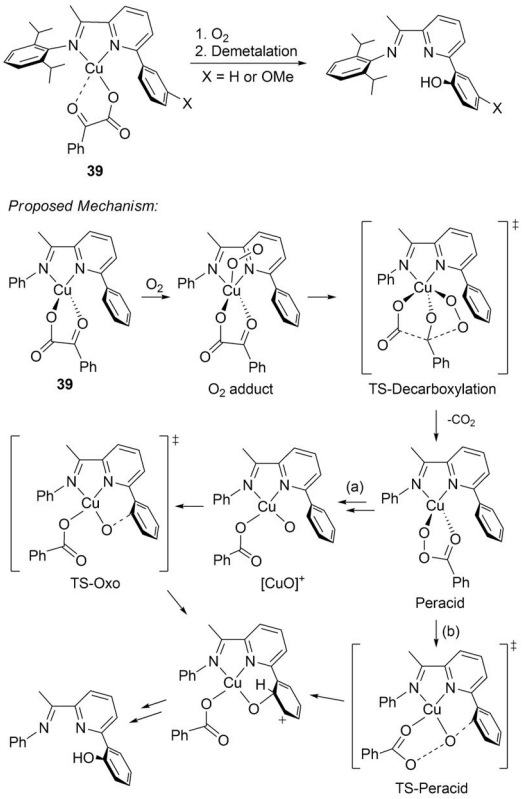

Figure 31.

Reaction of **39** (supported by **L17**) that results in hydroxylation of the ligand and the mechanism proposed on the basis of DFT calculations. Adapted from ref 228.

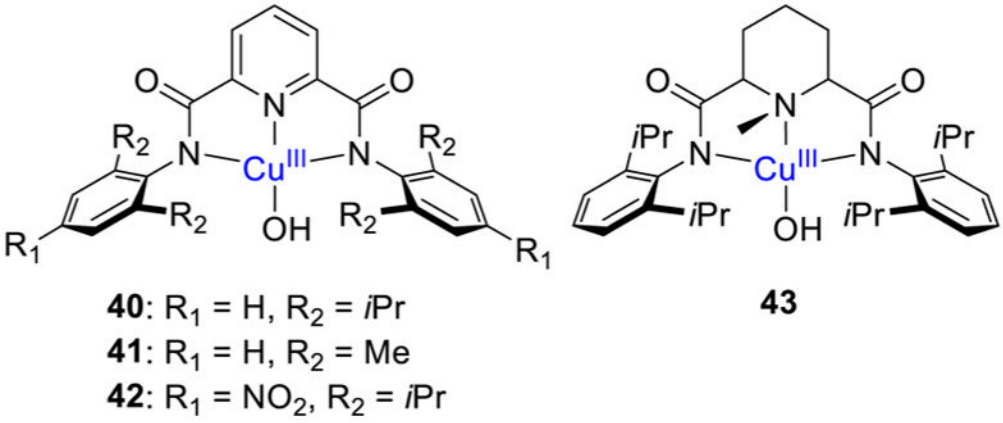

Figure 32.

Complexes with a $[CuOH]^{2+}$ core supported by **L28a–c** and **L25**, respectively (refs 237–239).

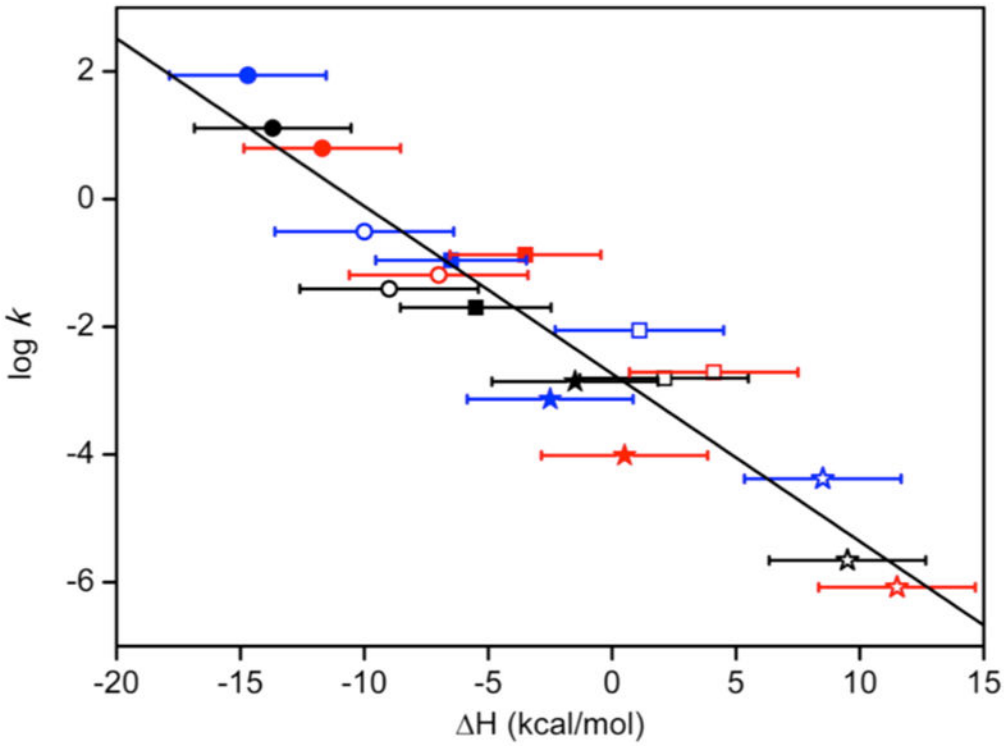

Figure 33.

Plot of log(*k*) vs Δ*H* (equivalent to the ΔBDE between the aqua complexes and the C–H bonds of the substrates) for reactions of **40** (black), **43** (red), and **42** (blue) with the substrates DHA (filled circles), cyclohexene (open circles), diphenylmethane (filled squares), THF (open squares), toluene (filled stars), and cyclohexane (open stars) at −25 °C in 1,2-DFB. Reprinted from ref 239. Copyright 2016 American Chemical Society.

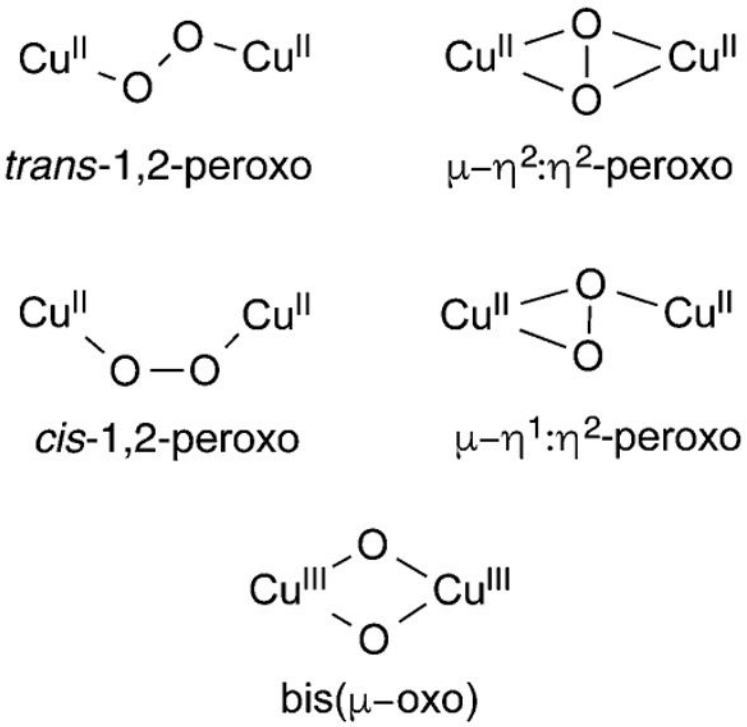

Figure 34.
Isomeric cores of 2:1 Cu:O_2 complexes.

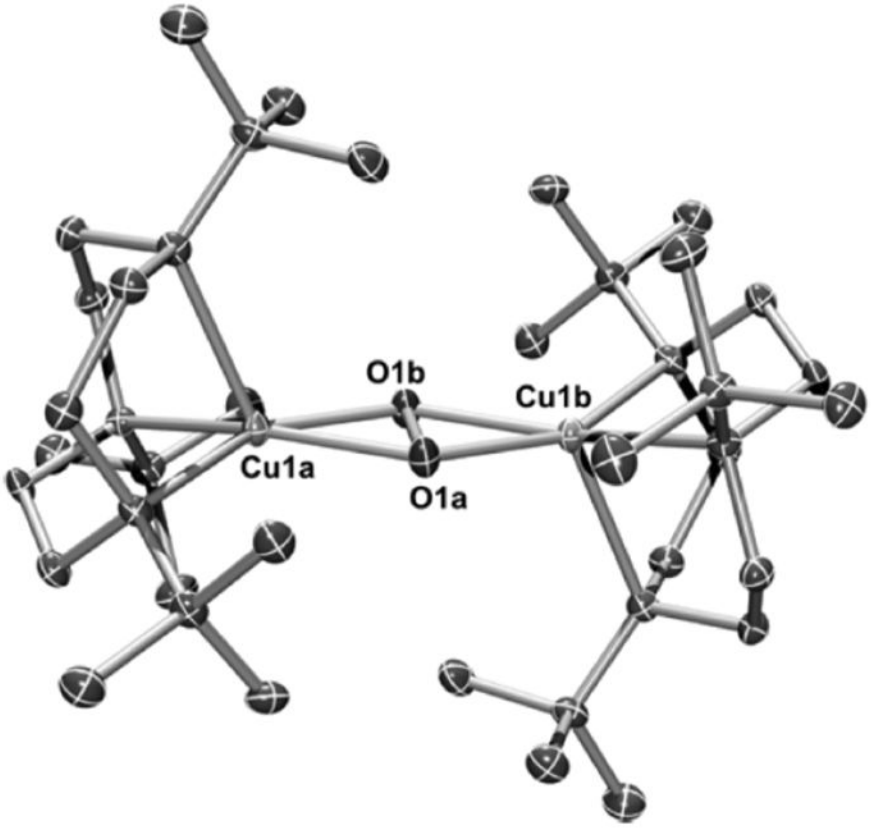

Figure 35.

X-ray crystal structure of the (μ-η^2:η^2-peroxo)dicopper complex dication supported by **L20c**. Selected interatomic distances (Å): O1a-O1b = 1.475(4), Cu···Cu = 3.6349(8). Reprinted from ref 250. Copyright 2016 American Chemical Society.

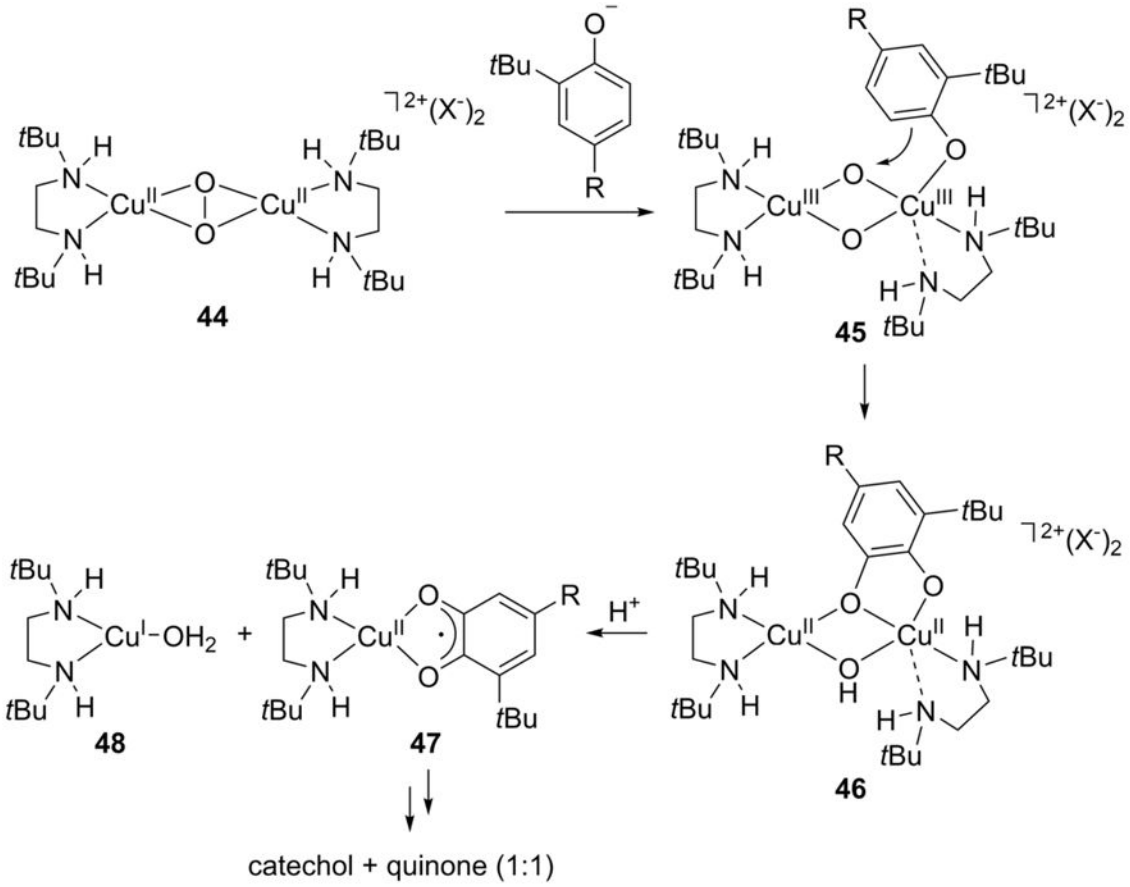

Figure 36.

Reaction of (μ-η^2:η^2-peroxo)dicopper complexes **44** (supported by **L1a**) with 2,4-di-*tert*-butylphenolate, with proposed mechanism based on spectroscopy and theory (refs 251–253).

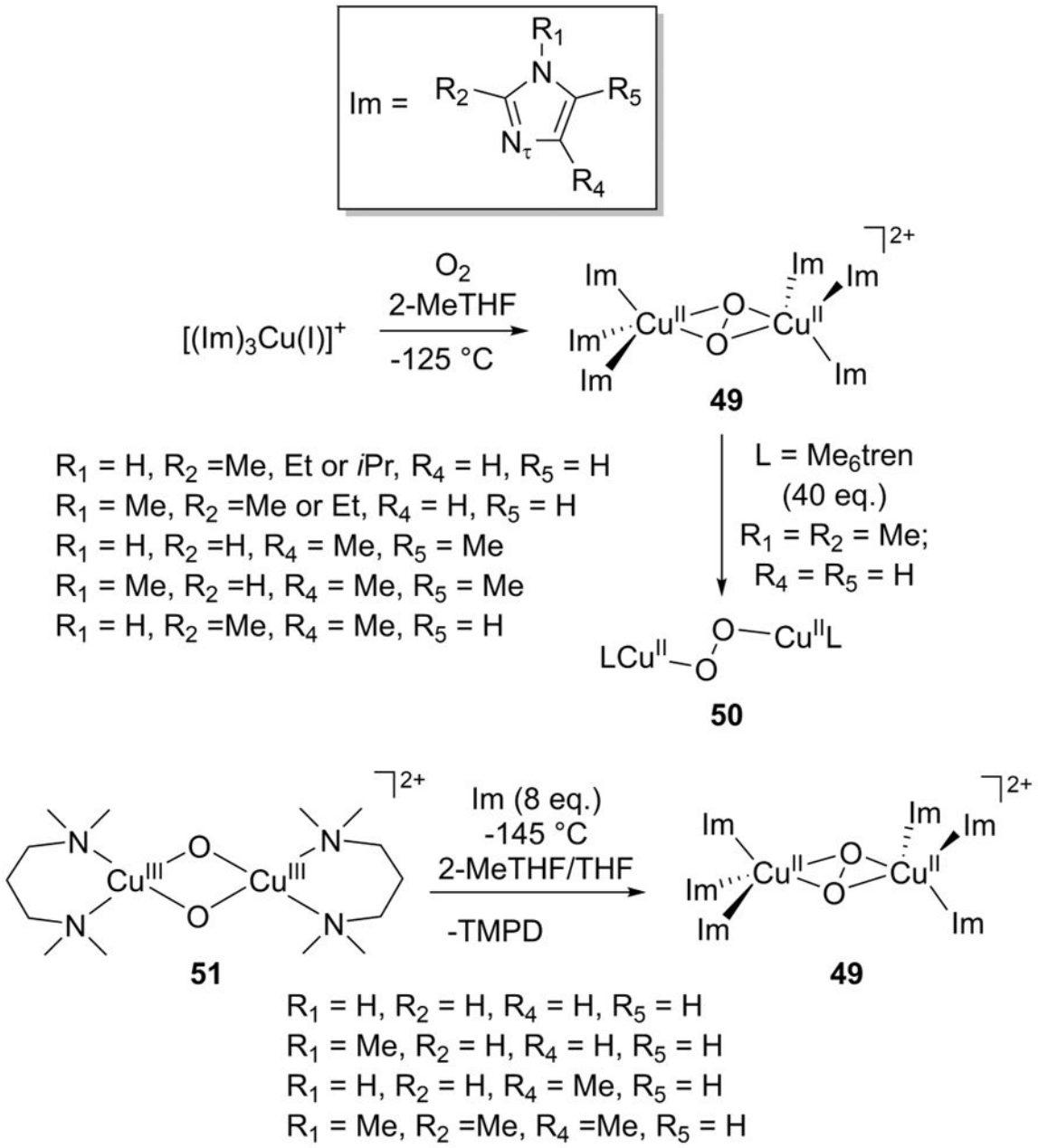

Figure 37.
Synthesis of (μ-η^2:η^2-peroxo)dicopper complexes with simple imidazole ligands (refs 257–259).

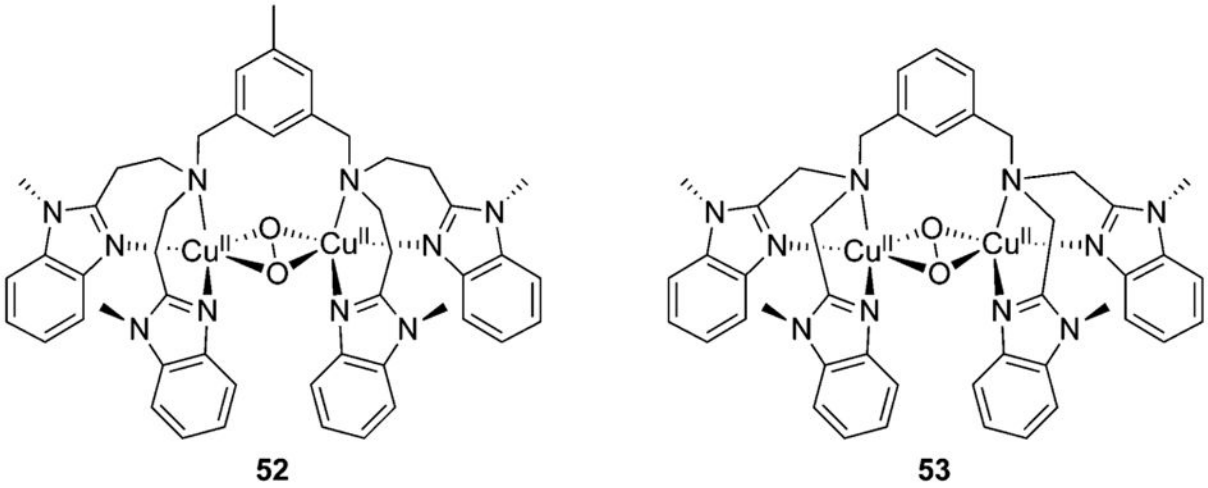

Figure 38.
Proposed (μ-η^2:η^2-peroxo)dicopper complexes supported by **L58c** (**52**; ref 268) and **L58a** (**53**; refs 272 and 273).

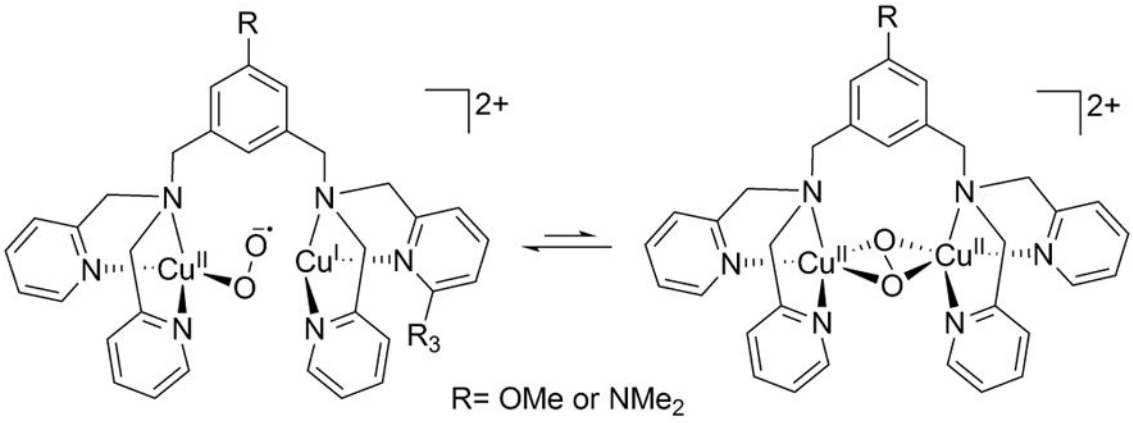

Figure 39.

Ligand hydroxylation reactions of (μ–η^2:η^2-peroxo)-dicopper complexes supported by **L58f–h** (**54**; refs 275 and 277) or **L58i** (R_3 = Me, R = H, OMe, *t*Bu, and NO_2) (**55**; ref 281).

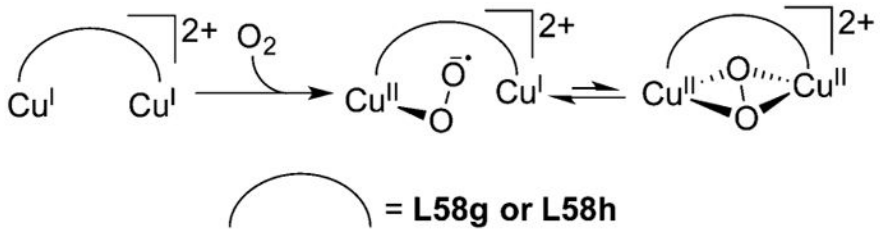

Figure 40.
Proposed formation of an intermediate $Cu^{I}Cu^{II}(O_2^{-\bullet})$ species (ref 280).

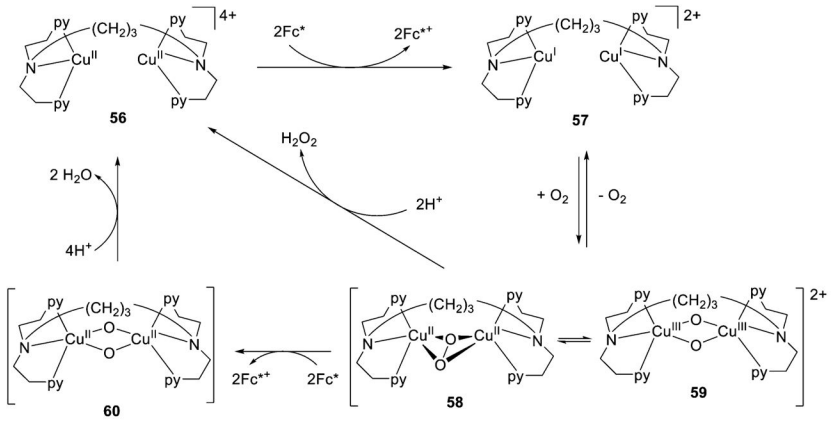

Figure 41.

Proposed mechanisms for the catalytic reduction of O_2 to H_2O by **56** (**L51a**) in the presence of exogenous Fc* as a reductant (ref 288).

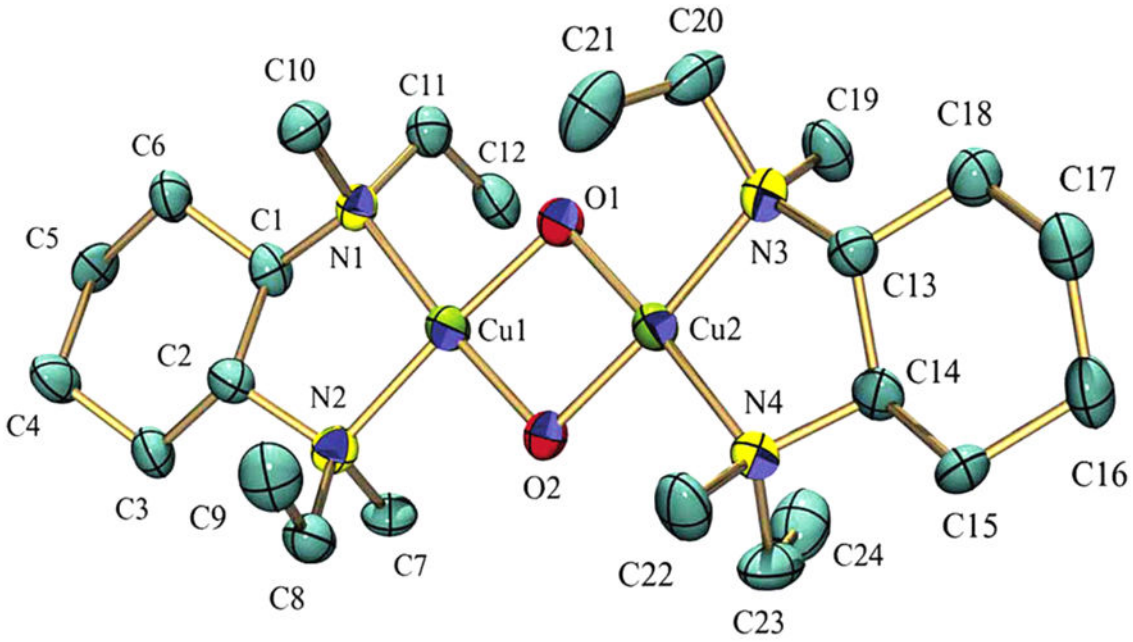

Figure 42.

X-ray crystal structure of the bis(μ-oxo)dicopper complex supported by **L6c**. Reprinted from ref 292. Copyright 2005 American Chemical Society. Selected interatomic distances (Å): Cu(1)–O(1), 1.809(6); Cu(1)–O(2), 1.808(6); Cu(2)–O(1), 1.795(5); Cu(2)–O(2), 1.799(6); Cu(1)···Cu(2), 2.744(1); and O(1) ···O(2), 2.334(1).

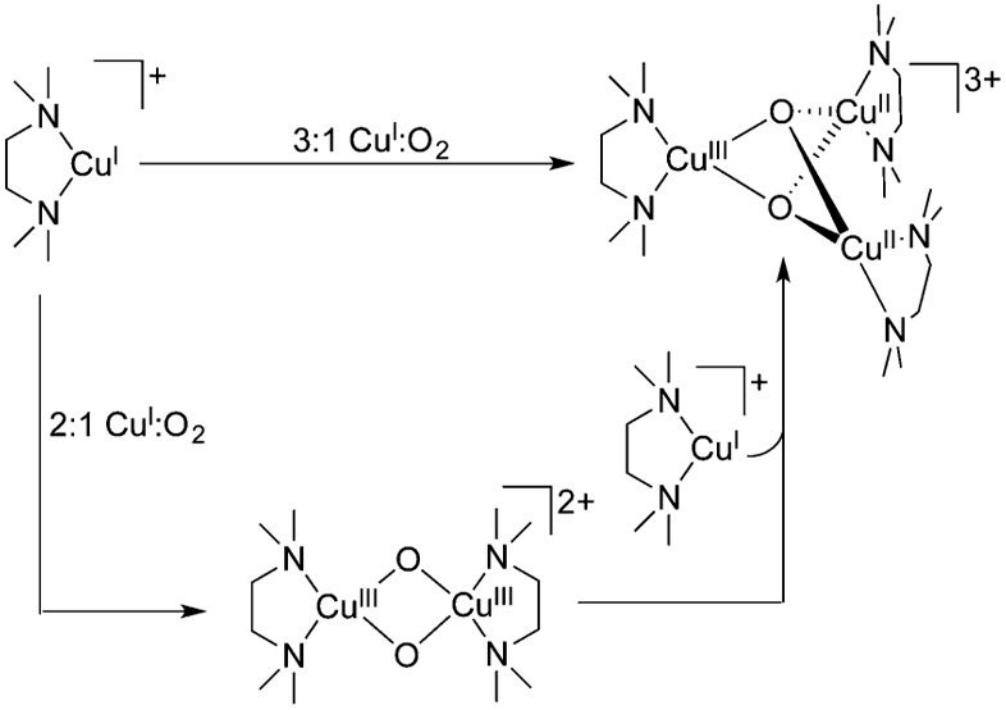

Figure 43.

Controlled formation of di- and tricopper complexes, $[(\mathbf{L1c})Cu_2O_2]^{2+}$ and $[(\mathbf{L1c})Cu_3O_2]^{3+}$, via selective addition of dioxygen (refs 291 and 294).

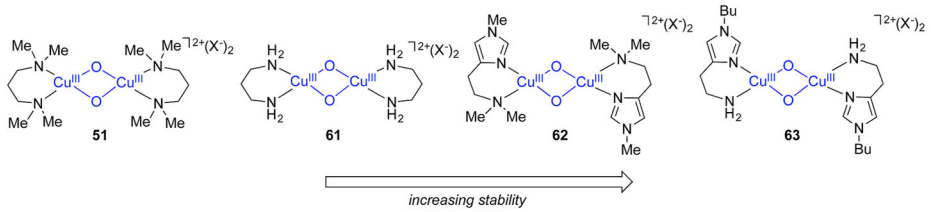

Figure 44.
Stability order of bis(μ-oxo)dicopper complexes. Adapted from ref 296.

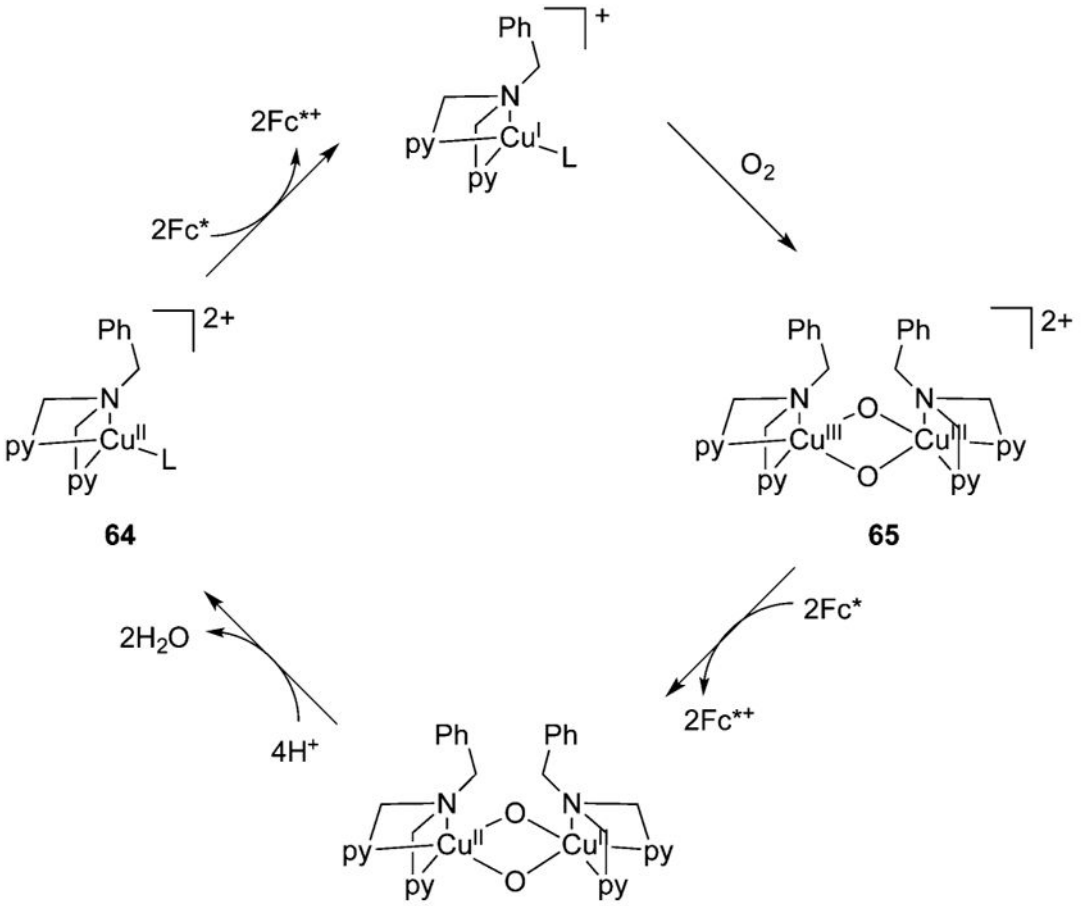

Figure 45.

Proposed mechanism for the reduction of O_2 to H_2O invoking the intermediacy of the bis(μ-oxo)dicopper (**65**) complex supported by **L18a** (ref 288).

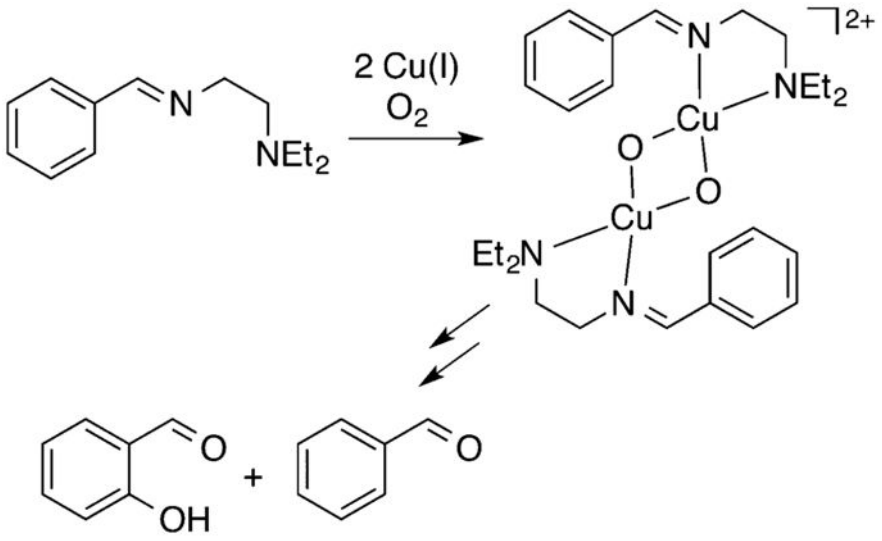

Figure 46.
Proposed pathway for hydroxylation of an appended arene of the **L7** ligand (ref 301).

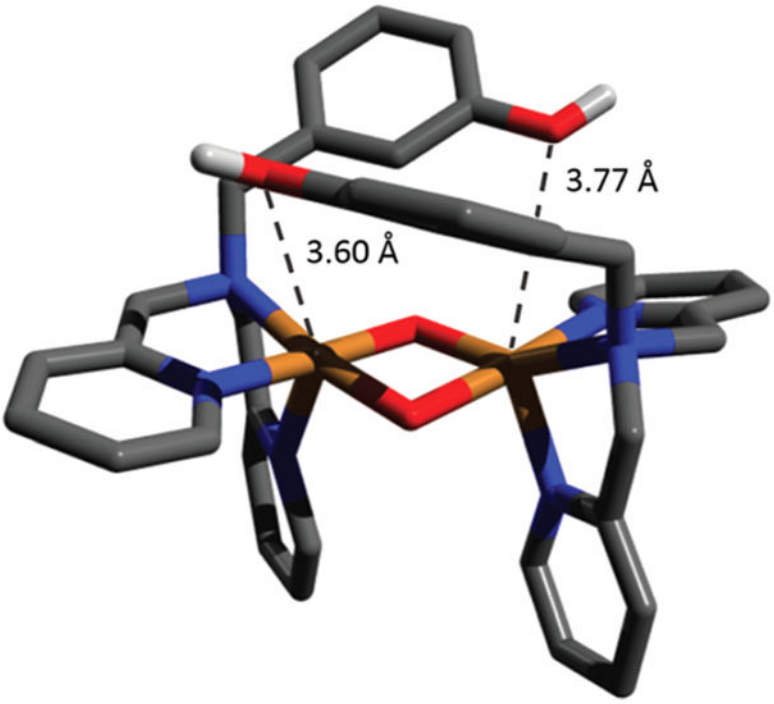

Figure 47.

DFT geometry-optimized structure for the bis(μ-oxo)-dicopper intermediate proposed in the oxidation of the appended phenol in **L80a**. Reprinted with permission from ref 302. Copyright 2015 the Royal Society of Chemistry.

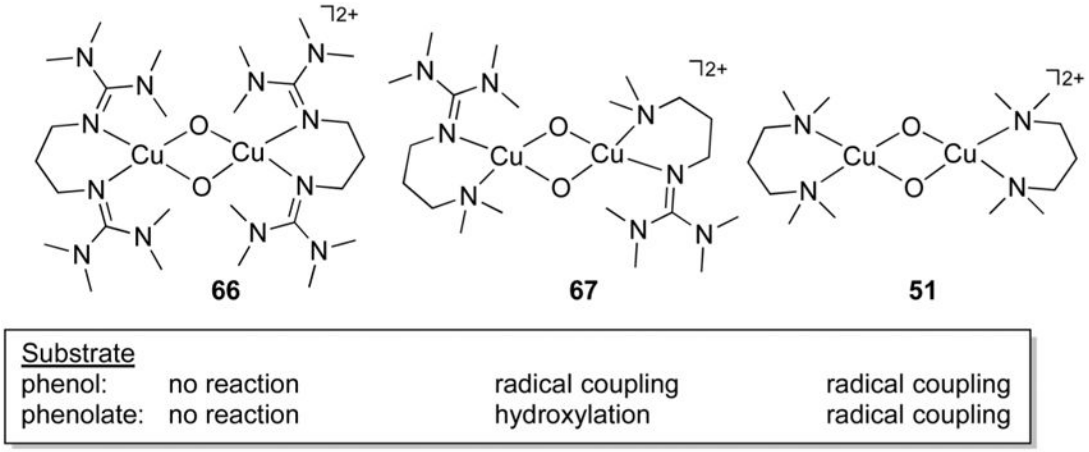

Figure 48.

Comparison of the reactivity of set of bis(μ-oxo)dicopper complexes **51** (**L10a**), **66** (**L14**), and **67** (**L27**) with 2,4-di-*tert*butylphenol (“phenol”) and 2,4-di-*tert*-butylphenolate (“phenolate”) (ref 306).

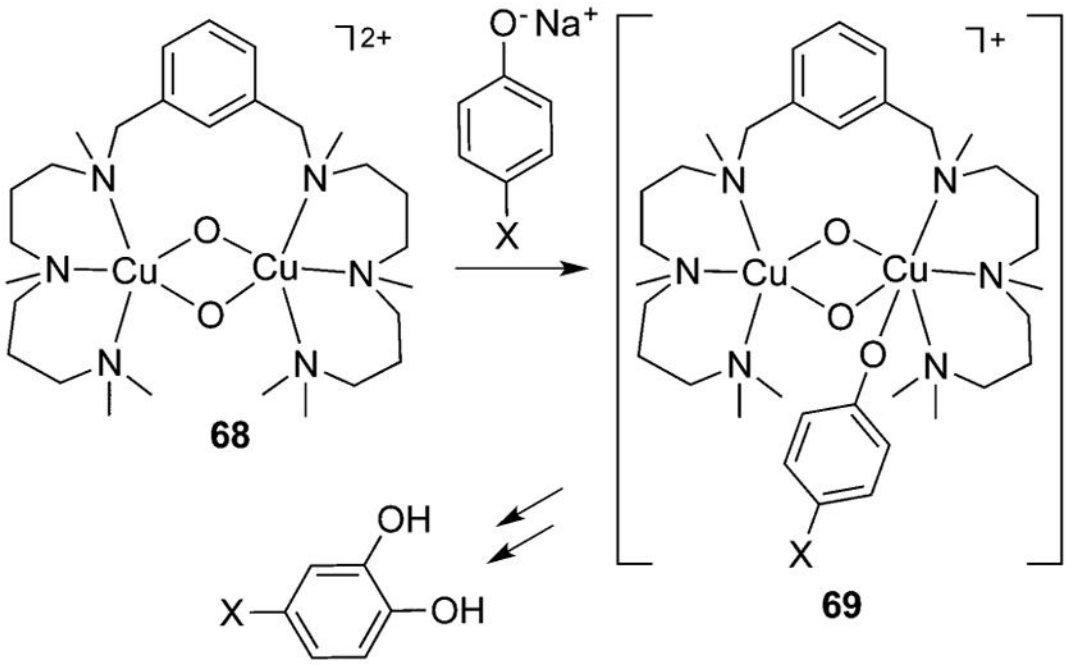

Figure 49.
Reaction of **68** (**L48**) with phenolates (**69**) identified for X = Cl (refs 309 and 310).

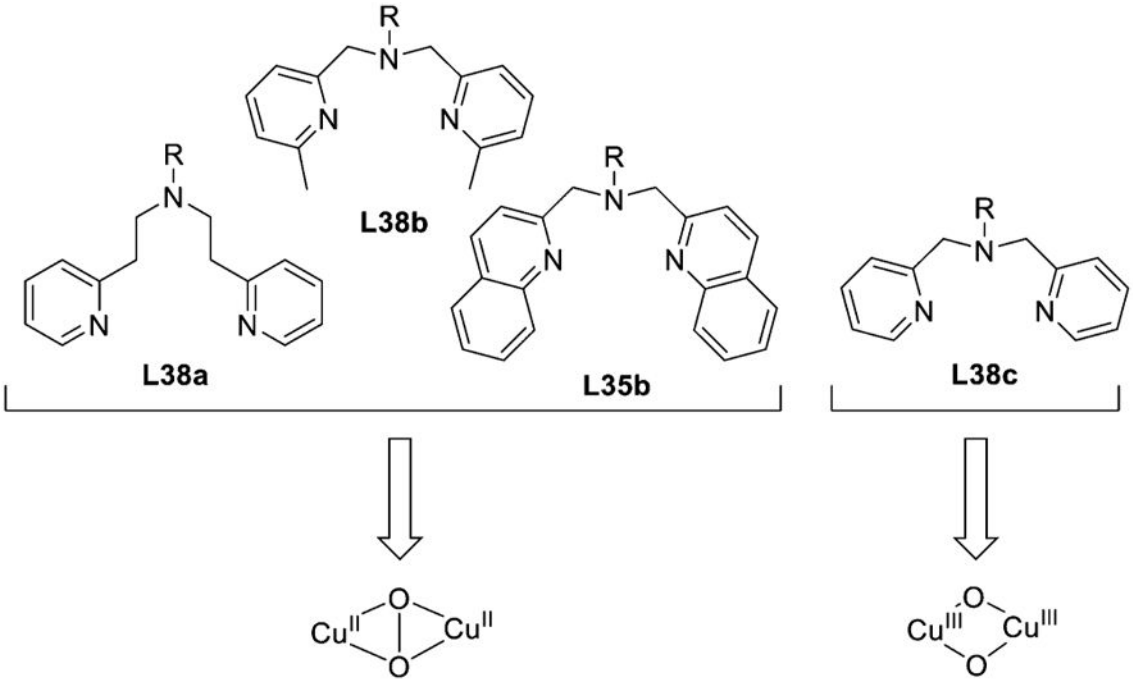

Figure 50.

Comparison of results of oxygenation of Cu(I) complexes of the indicated ligands (R = CH_2CH_2Ph), which yield either the indicated (μ-η^2:η^2-peroxo)- or bis(μ-oxo)dicopper cores (refs 314–317).

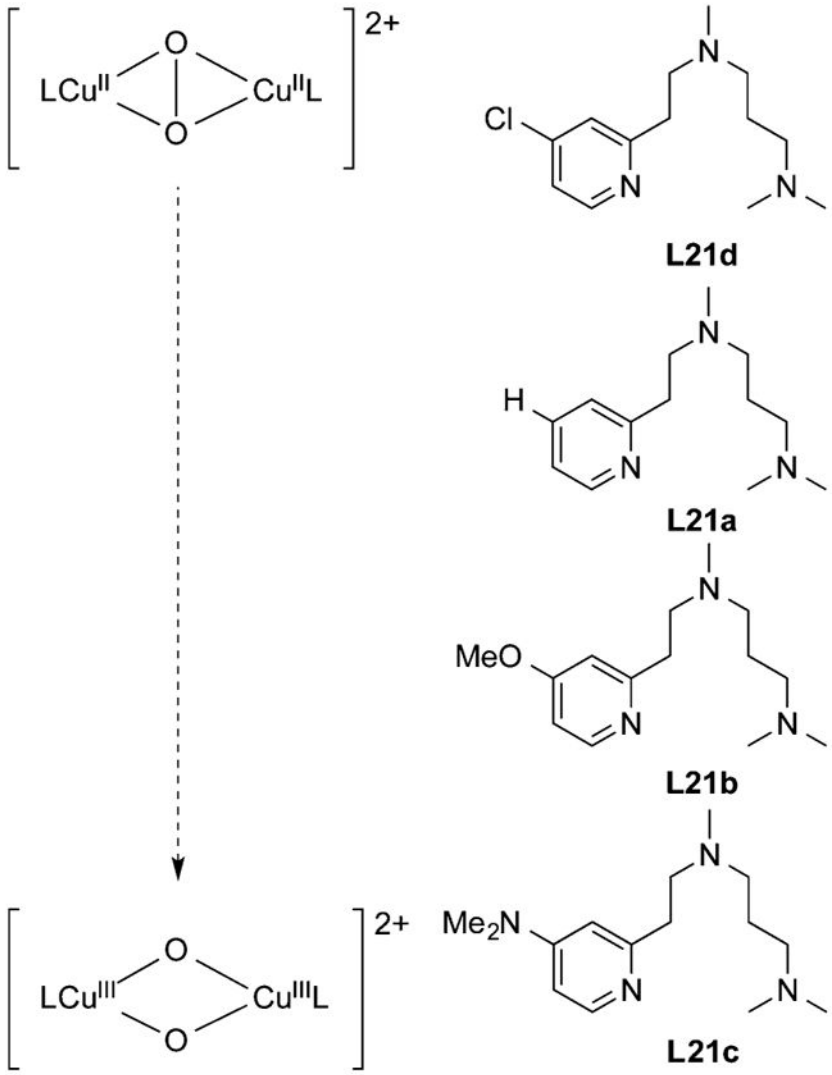

Figure 51.

Variation in ratio of isomers formed as a function of the substituent in the **L21** supporting ligand (ref 320).

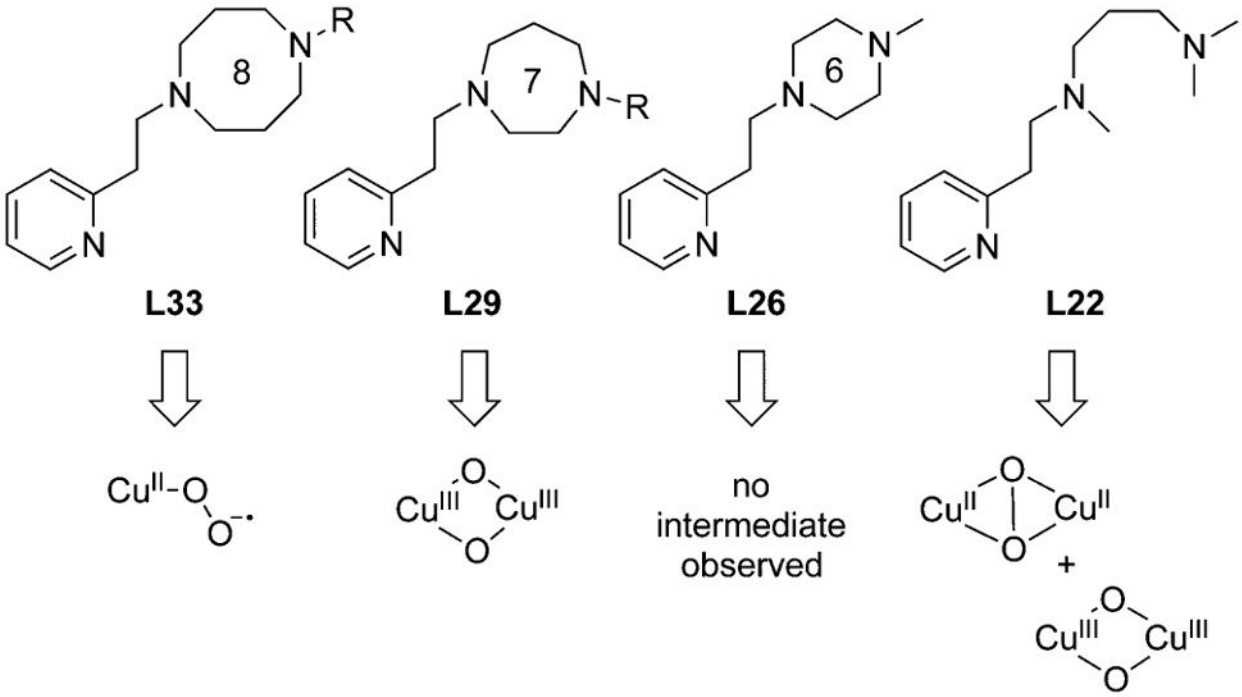

Figure 52.
Results of the reactions of the Cu(I) complexes of the indicated ligands with O_2 (ref 326).

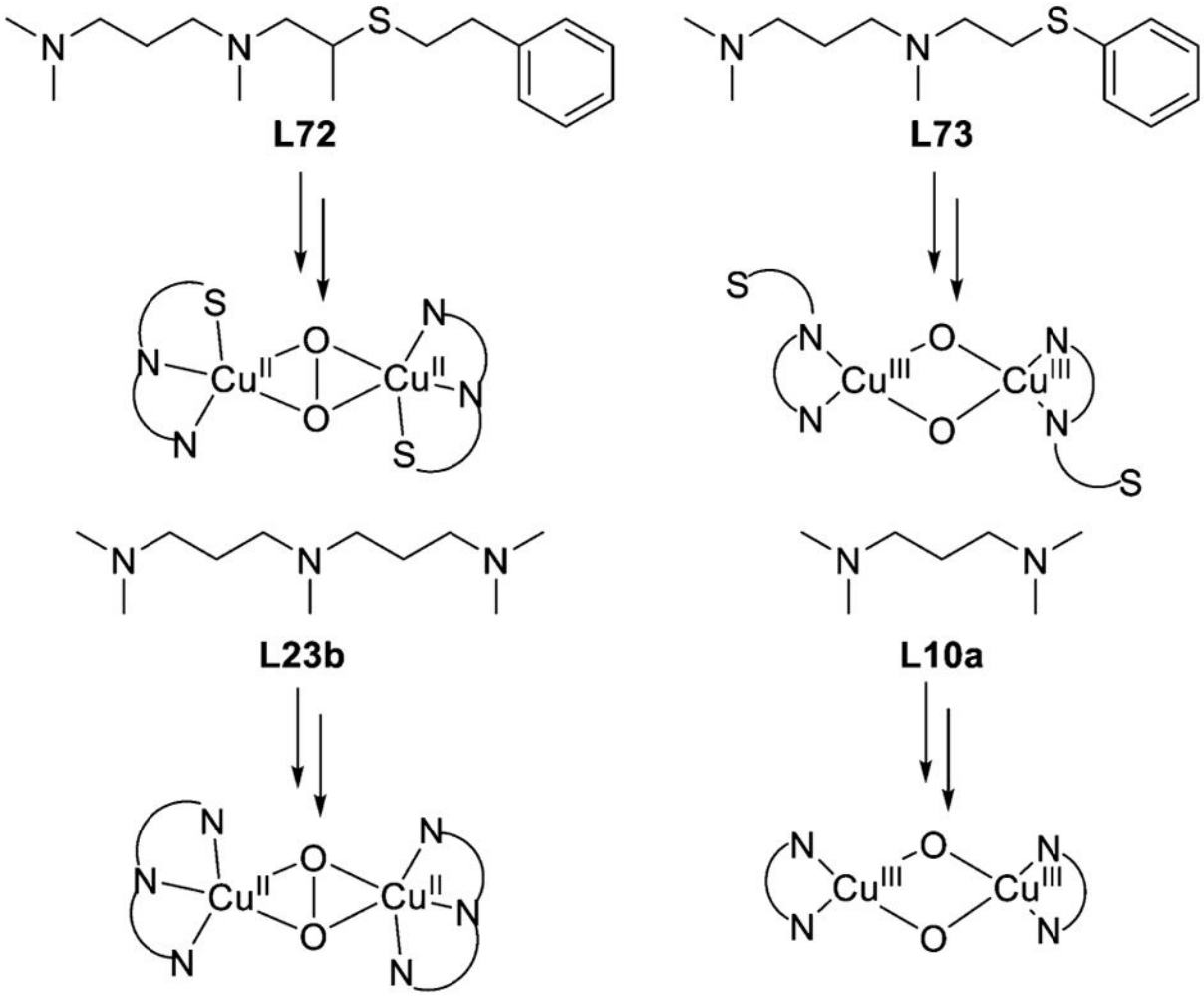

Figure 53.
Comparison of the results of oxygenations of Cu(I) complexes of the indicated ligands (refs 262, 324, 330, and 331).

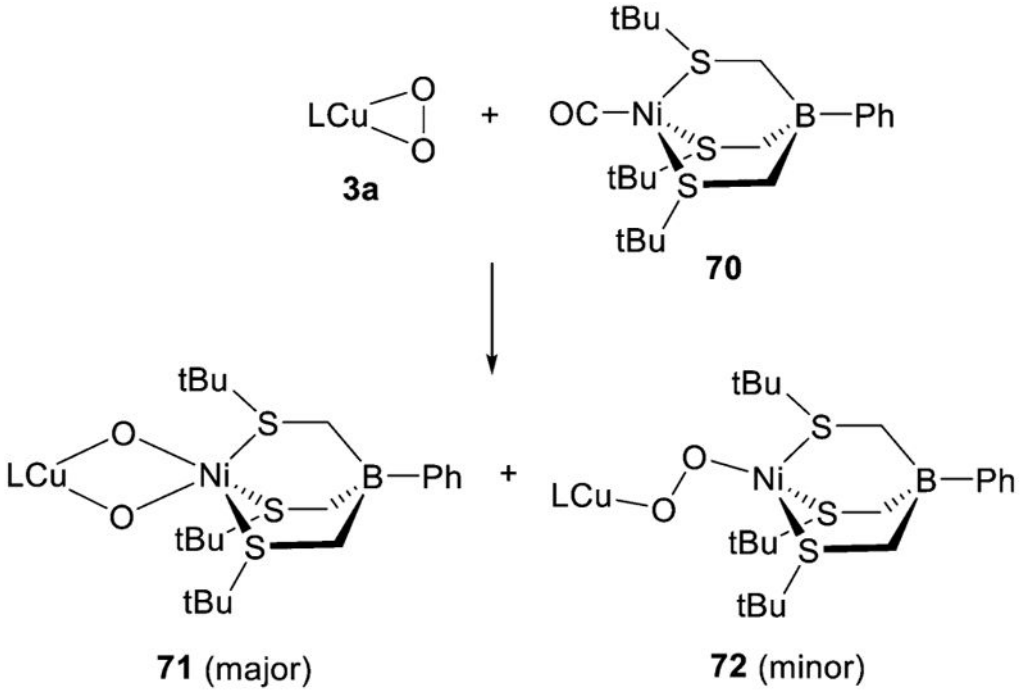

Figure 54.

Synthesis of Cu-containing heterobimetallic complexes using **3a** (**L2d**,**e**) and **70** (**L81**) as the starting materials (ref 167).

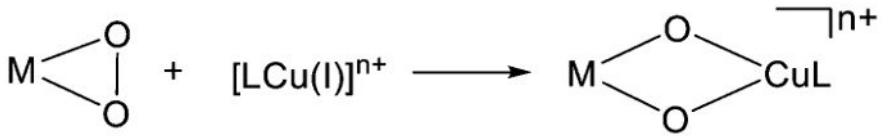

Figure 55.
General scheme showing the synthesis of Cu-containing heterobimetallic complexes using 1:1 M:O_2 adducts as starting materials (see Table 6 for specific M and L combinations).

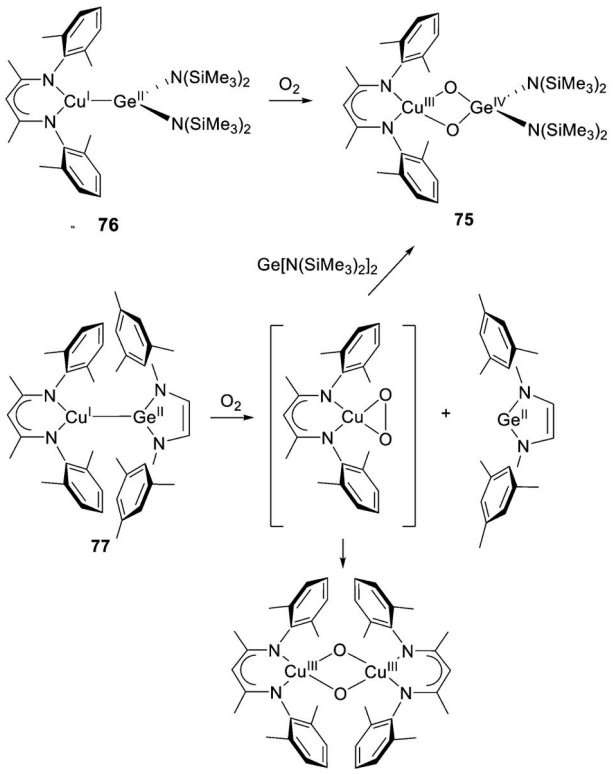

Figure 56.
Course of oxygenations of Cu(I)–Ge(II) complexes (ref 168).

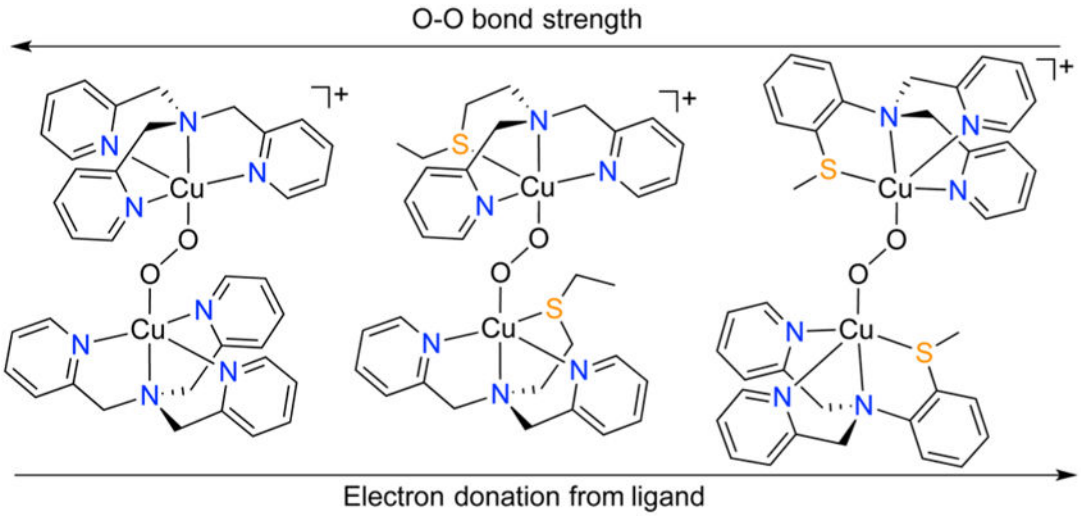

Figure 57.

Relationship of O–O bond strength and electron donation between complexes $[(\mathbf{L41a})Cu_2O_2]^+$ (left), **78** (**L67**) (middle), and $[(\mathbf{L82})Cu_2O_2]^+$ (right) (ref 342).

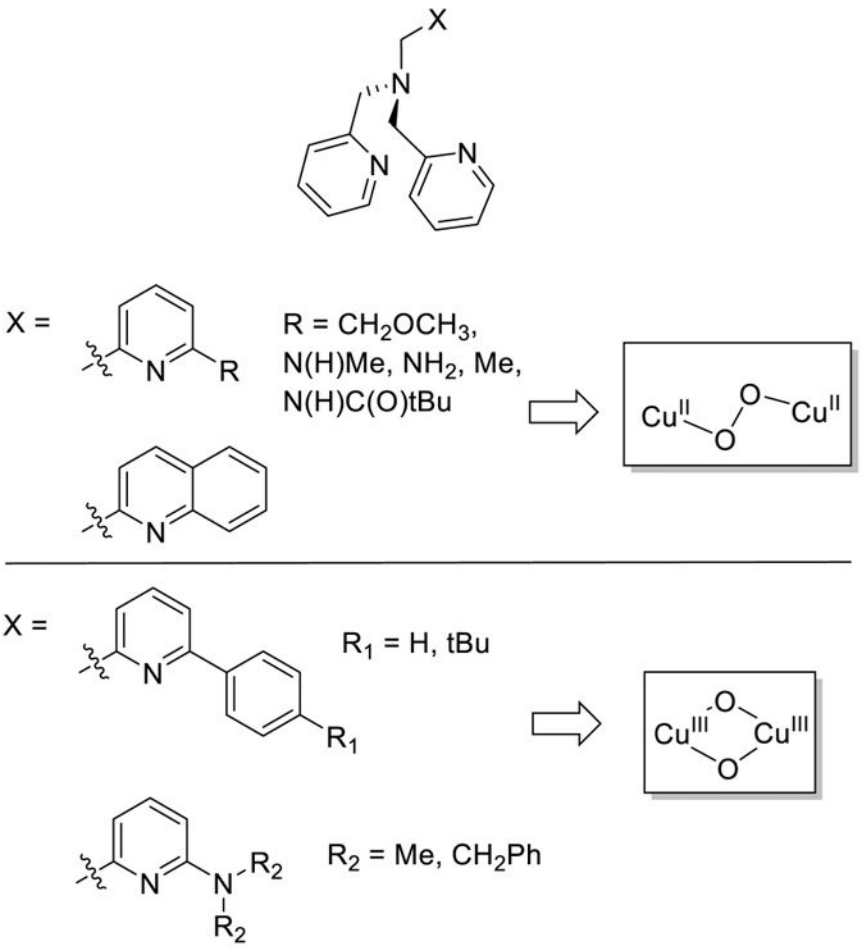

Figure 58.

Ligand derivatives that yielded indicated copper–oxygen cores upon reaction of their Cu(I) complexes with O_2 (refs 341, 343, and 348).

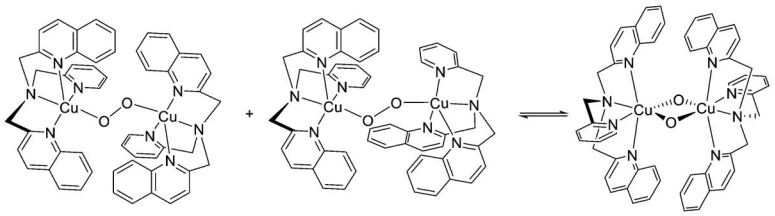

Figure 59.

Proposed equilibrium between C_i (left) and C_1 (right) isomers of (*trans*-1,2-peroxo)dicopper complexes with bis(μ-oxo)dicopper isomer (ref 345).

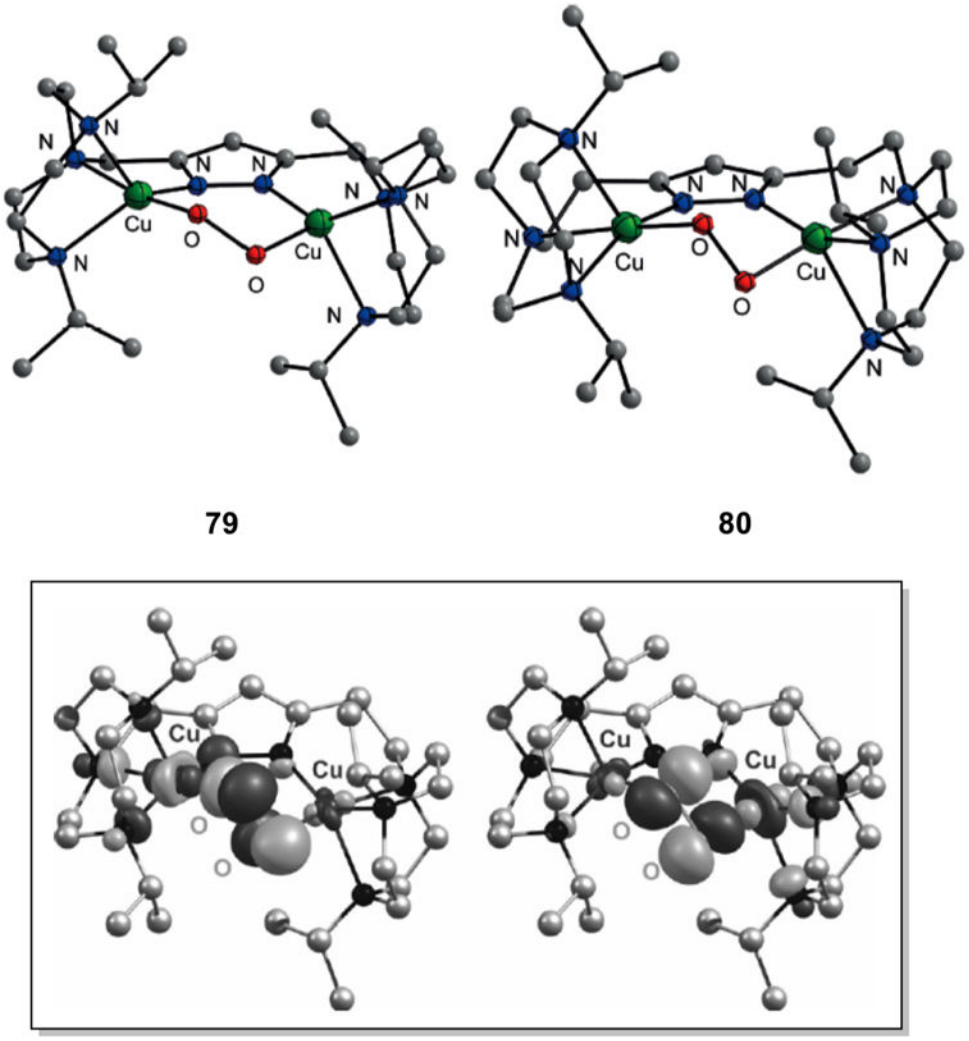

Figure 60.

(top) X-ray crystal structures of the (1,2-peroxo)dicopper complexes **79** and **80** and (bottom) orthogonal molecular orbitals in **80** that give rise to its S = 1 ground state. Reprinted with permission from ref 38 (top) and ref 354 (bottom). Copyright 2015 Wiley-VCH.

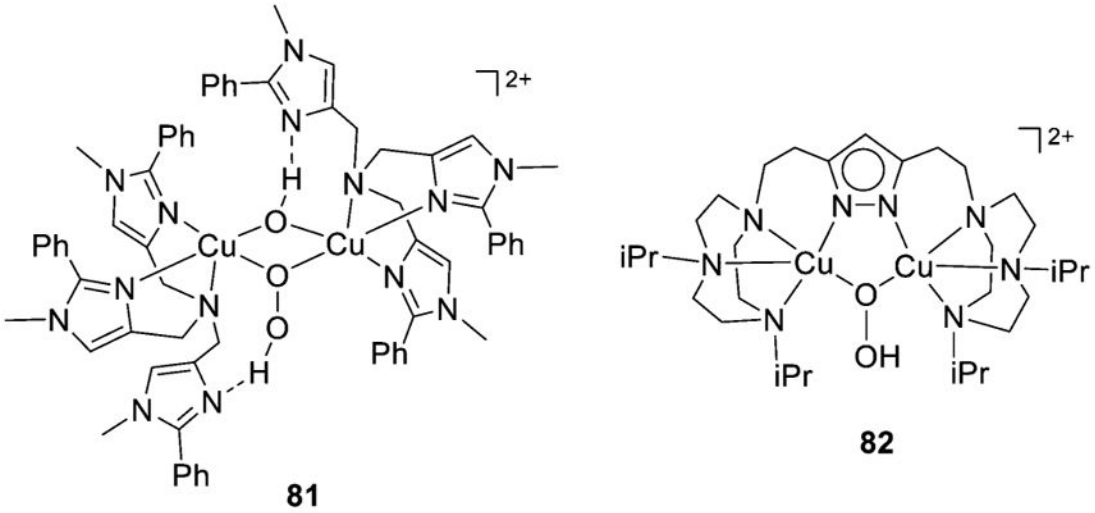

Figure 61.

(1,1-Hydroperoxo)dicopper complexes supported by **L40f** and **L65b**, respectively, that have been structurally characterized by Xray crystallography (refs 357 and 359).

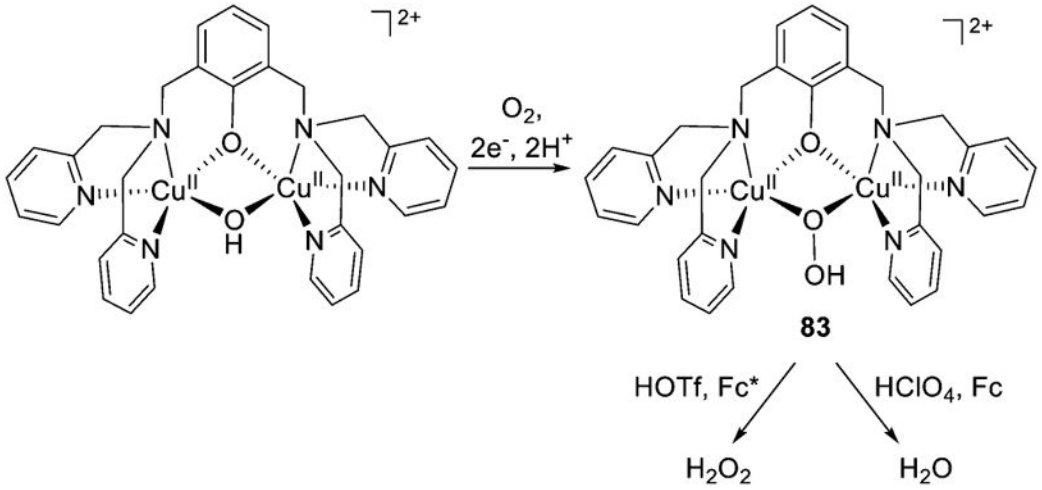

Figure 62.
Oxygen reduction reactions involving intermediate **83** (refs 362 and 363).

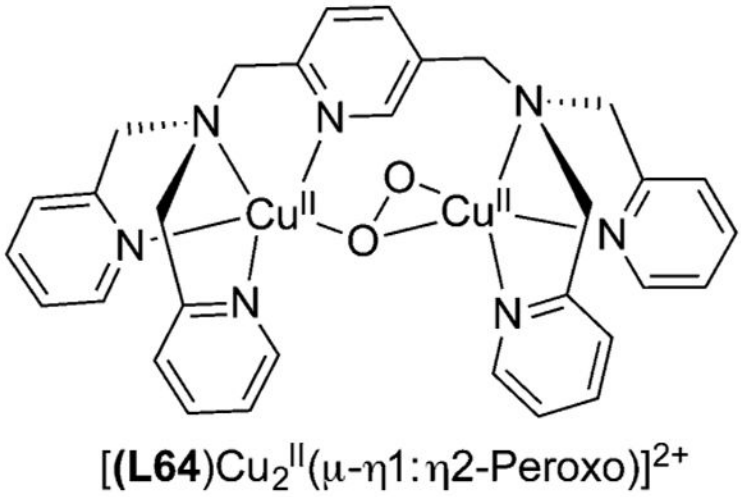

Figure 63.
Proposed structure of a (μ-η^1:η^2-peroxo)dicopper complex supported by **L64** (ref 364).

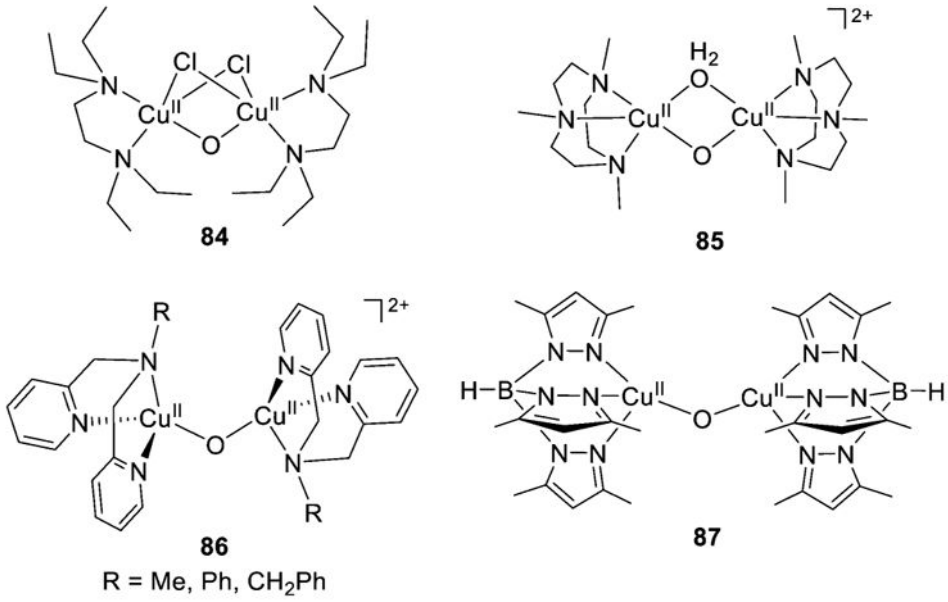

Figure 64.
Examples of (μ-oxo)dicopper(II) complexes (references cited in text).

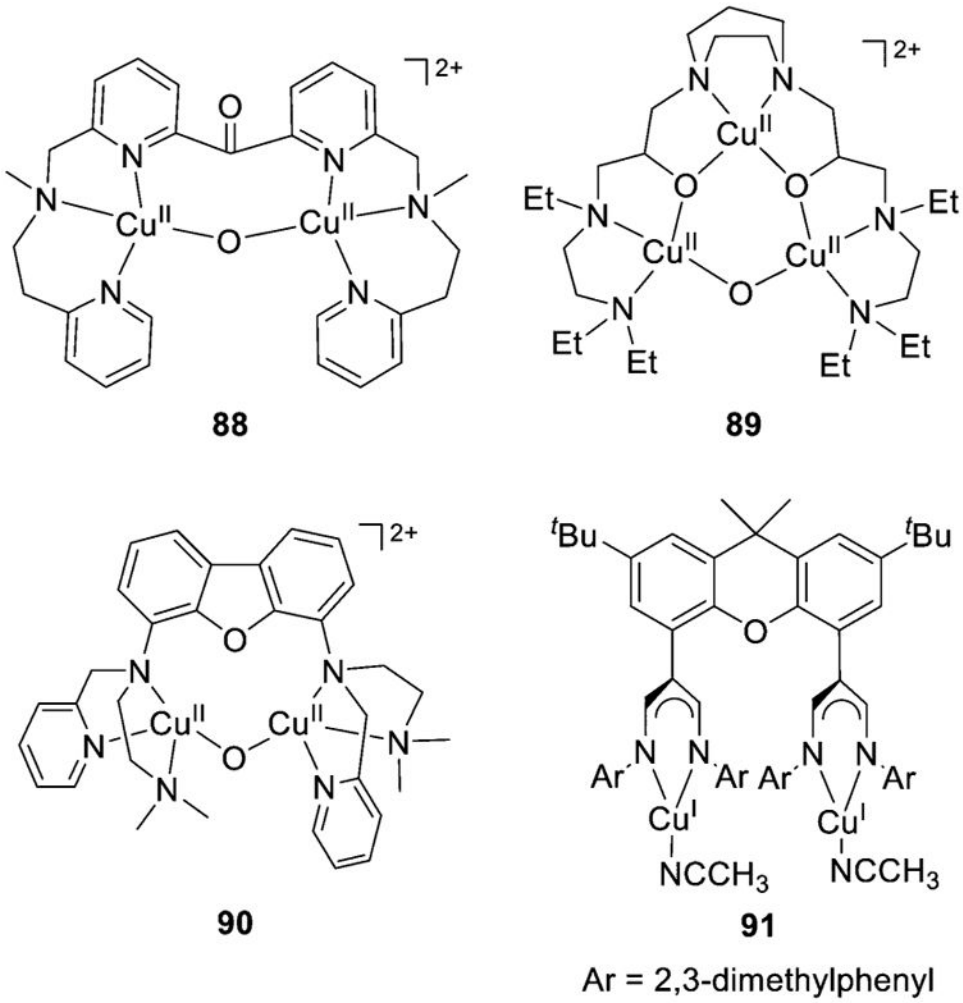

Figure 65.
Examples of (μ-oxo)dicopper(II) complexes (refs 372–375).

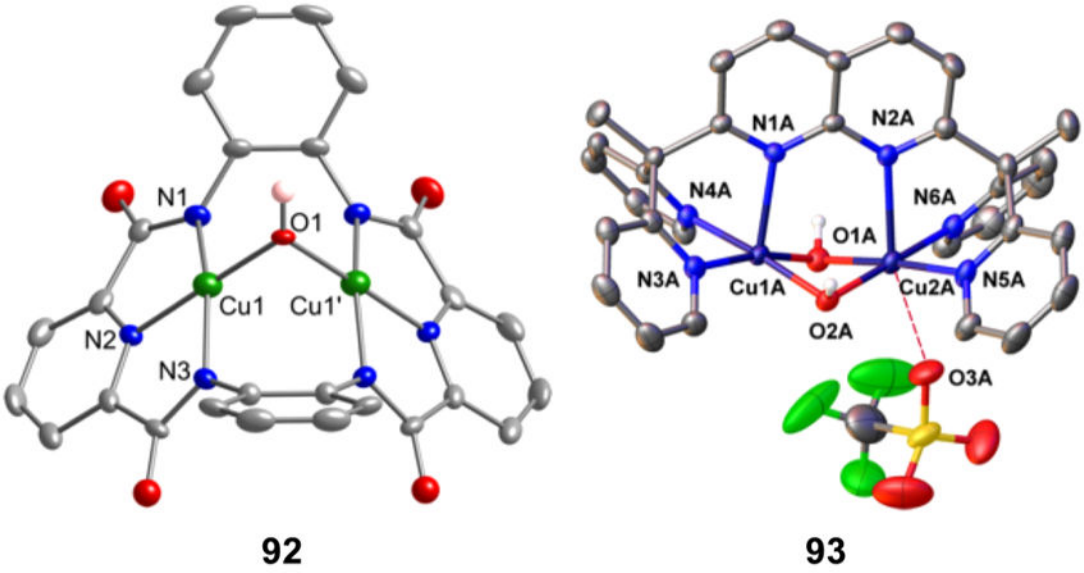

Figure 66.

X-ray crystal structures of hydroxo-bridged dicopper(II) complexes **92** (**L59**) and **93** (**L55**) that served as starting materials for the preparation of higher valent species. (left) Only anion shown; Cu–Cu = 2.6596(15) Å. Reprinted from ref 378. Copyright 2014 American Chemical Society. (right) Cation and one counterion shown; Cu–Cu = 2.7511(12) Å. Reprinted from ref 379. Copyright 2016 American Chemical Society.

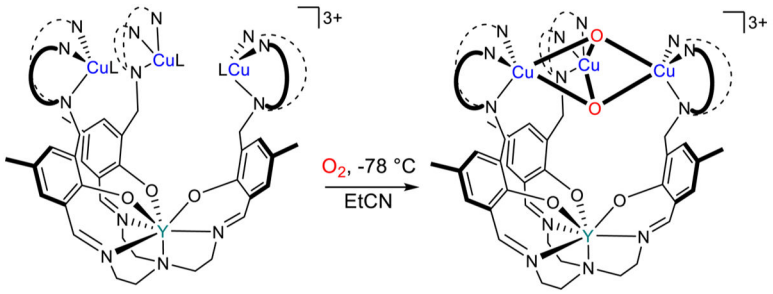

Figure 67.

Oxygenation of a tricopper(I) complex of a templated, preorganized ligand (**L61a,b**). Adapted from ref 386.

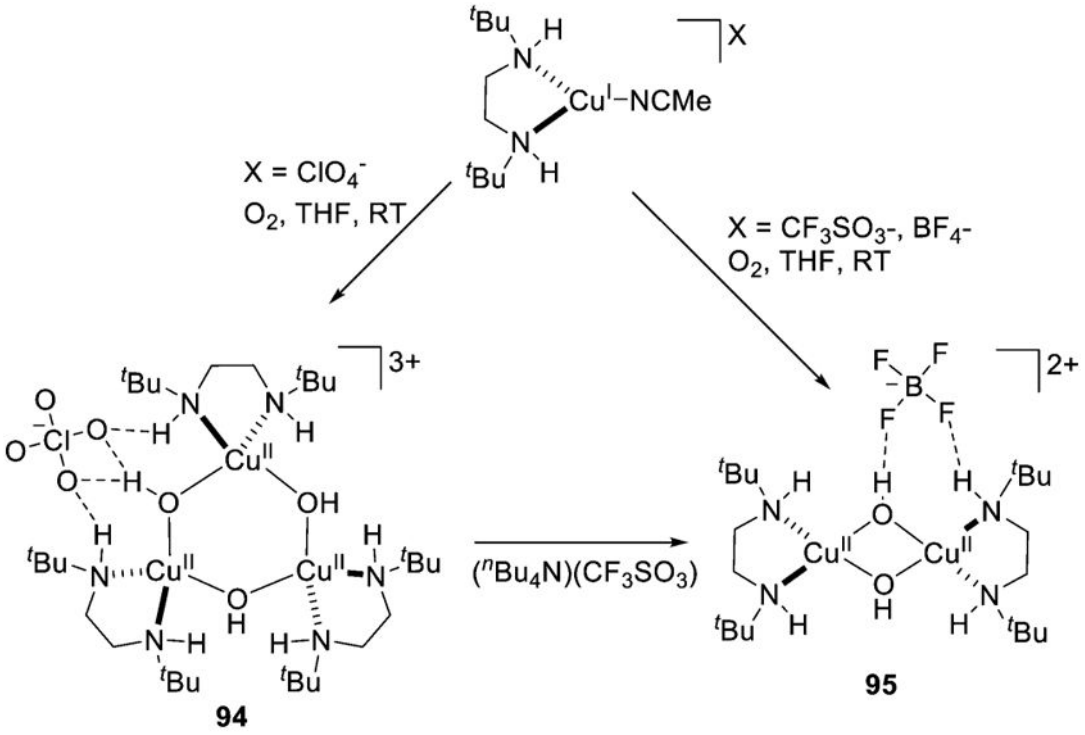

Figure 68.
Results of room temperature oxygenation of Cu(I) complexes of **L1a** (ref 396).

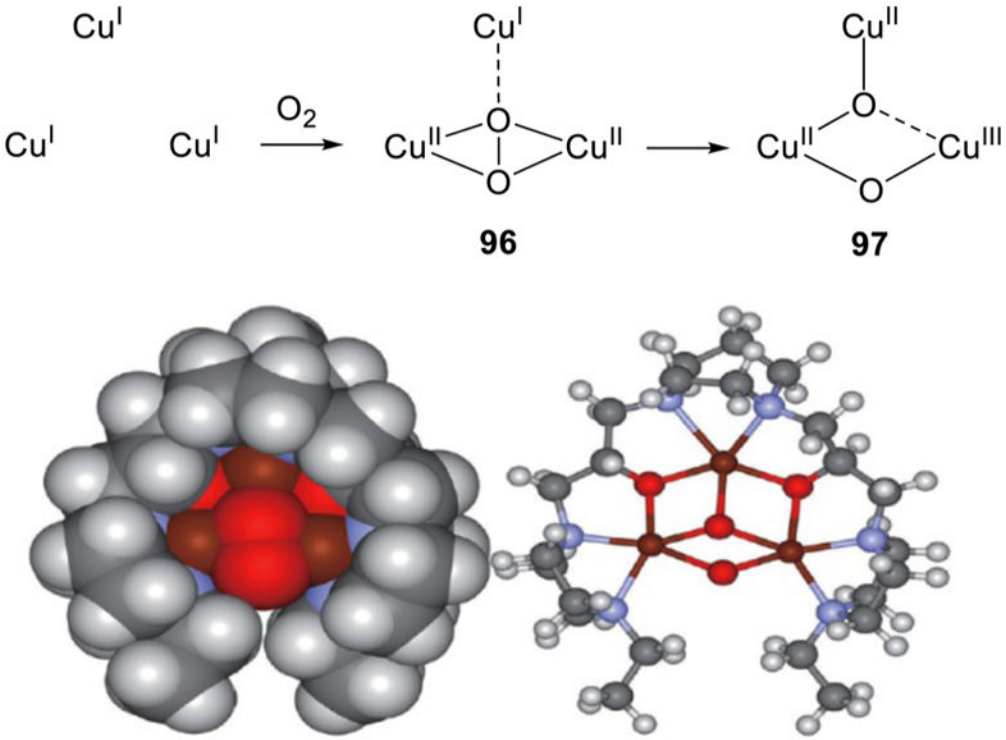

Figure 69.

(top) Proposed mechanism for generation of the hypothesized reactive intermediate in hydrocarbon oxidations by complexes of ligands **L79a**–**f**. Supporting ligands not shown. (bottom) Space-filling and ball-and-stick drawing of calculated structure for intermediate **97** supported by **L79f**. Reprinted with permission from ref 403. Copyright 2013 Wiley-VCH.

*Corresponding Author: wtolman@umn.edu.

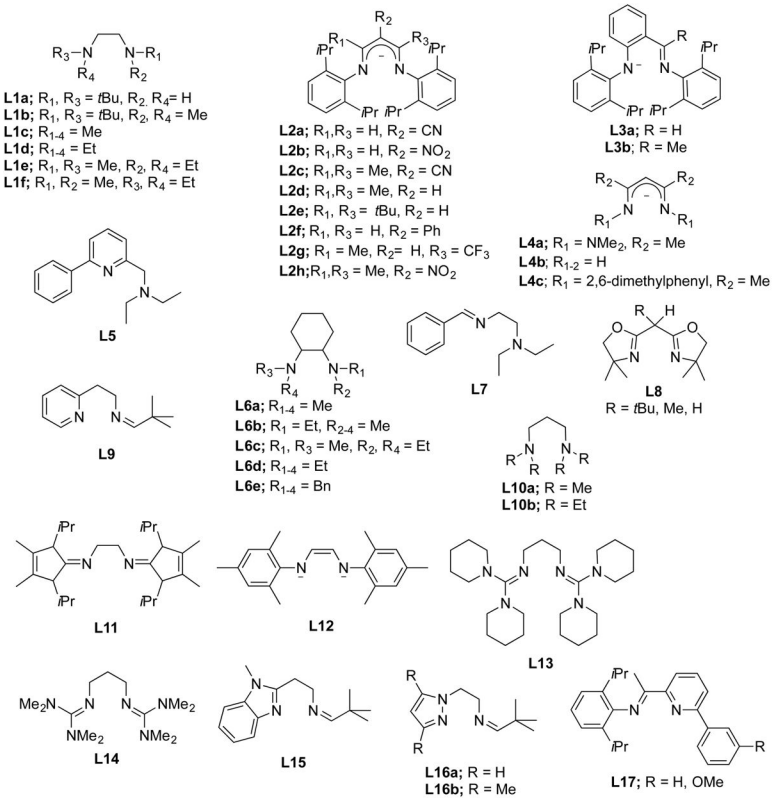

Chart 1.
Ligands Containing Two Nitrogen Donors

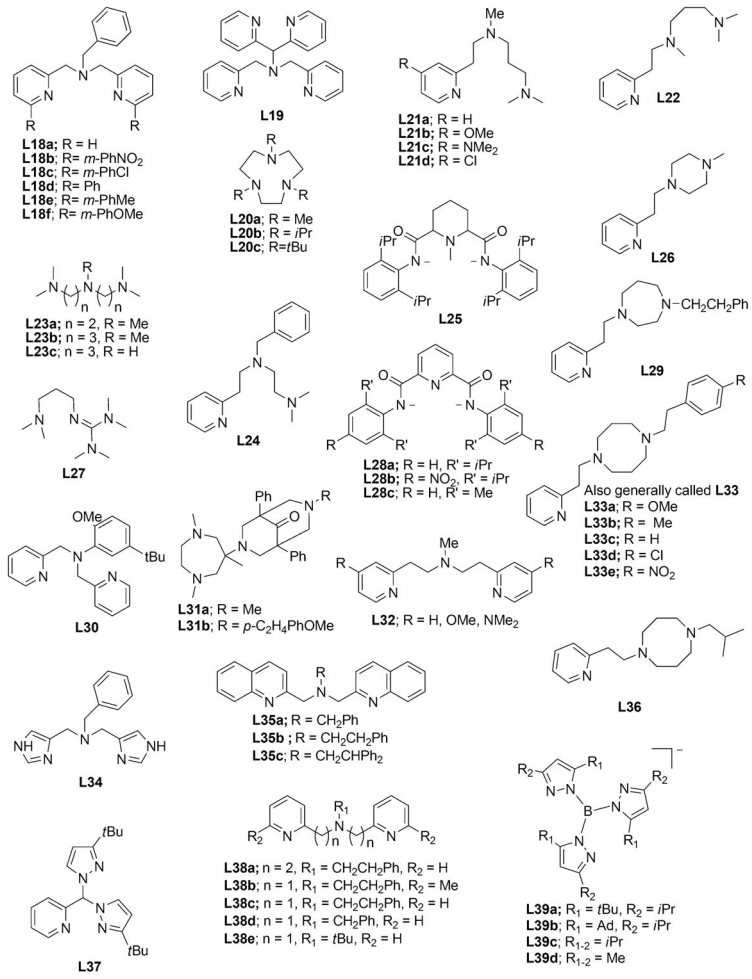

Chart 2.
Ligands Containing Three Nitrogen Donors

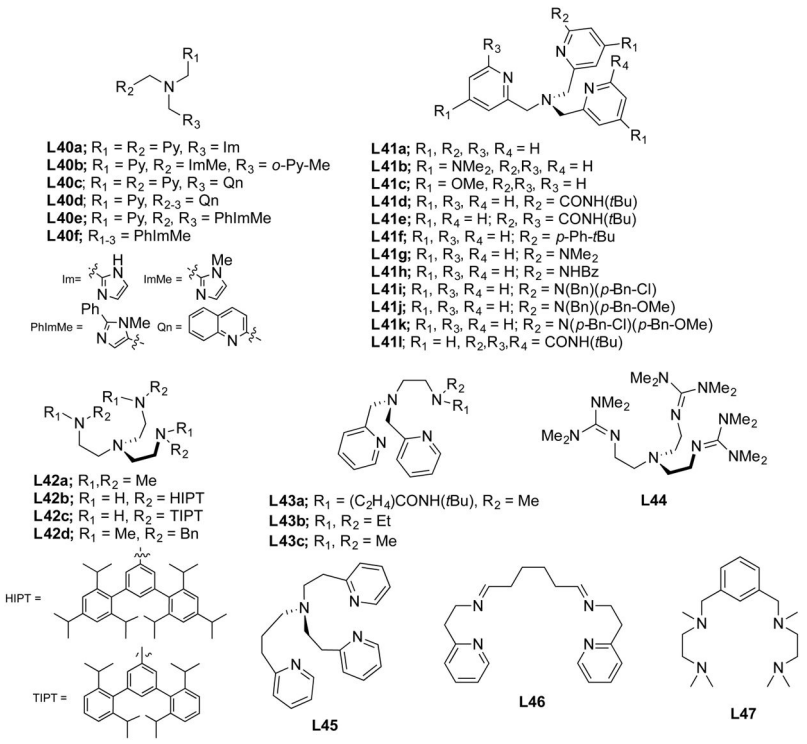

Chart 3.
Ligands Containing Four Nitrogen Donors

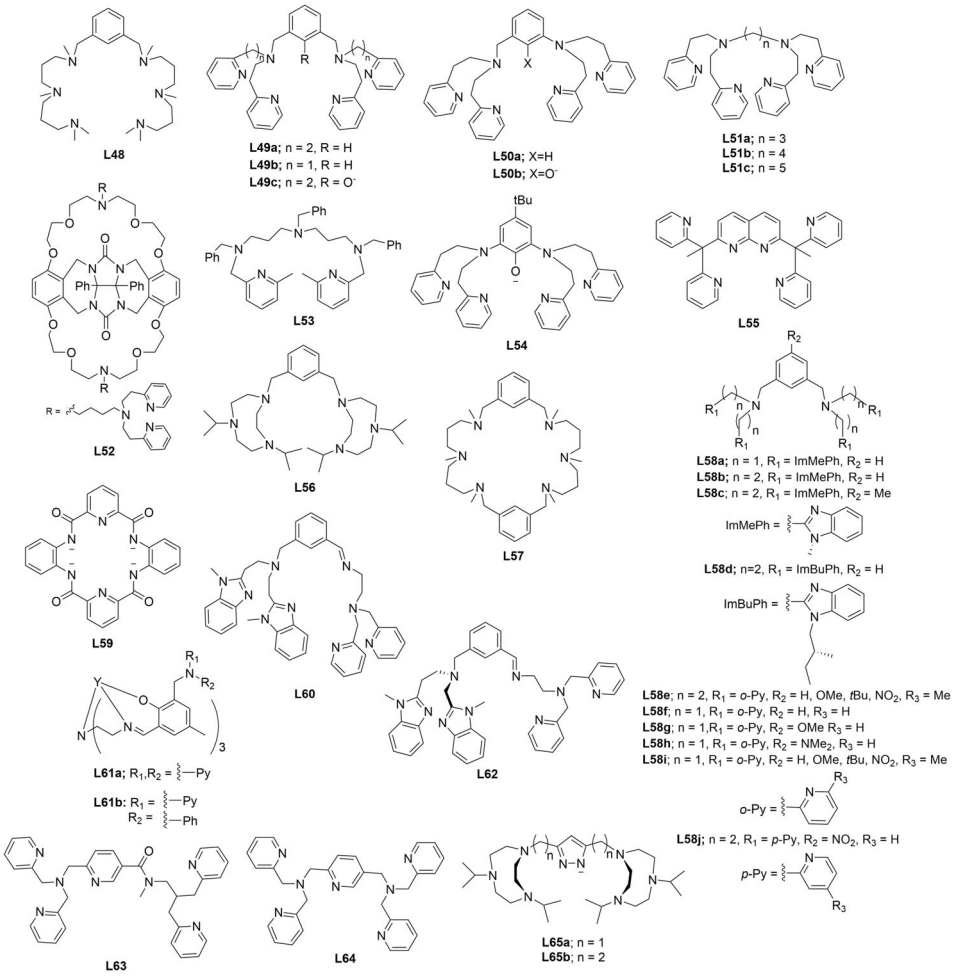

Chart 4.
Ligands Containing Five or More Nitrogen Donors

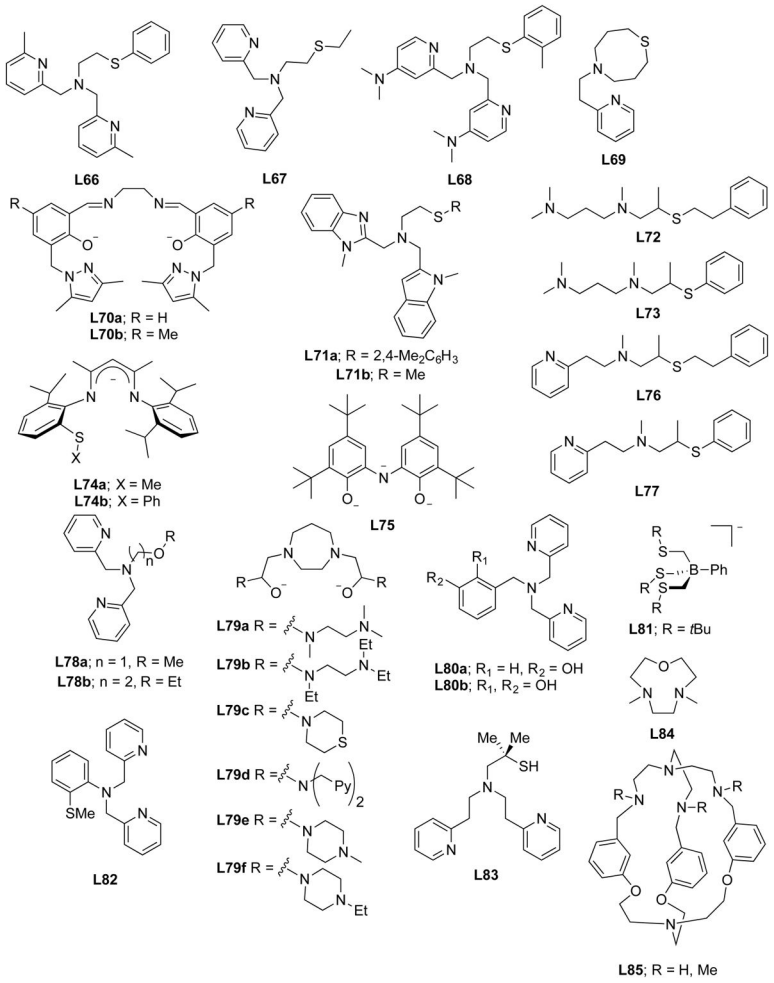

Chart 5.
Ligands Containing a Mixture of Nitrogen, Sulfur, and Oxygen Donors

Table 1

Selected Spectroscopic Properties of 1:1 Cu:O_2 Complexes

O_2^{n-} hapticity	ligand	UV–vis	Raman (exp, cm^{-1})		Raman (calc, cm^{-1})	ref
		λ_{max} (nm) (ε, M^{-1} cm^{-1})	ν(O–O) (Δ^{18}O)	ν(Cu–O) (Δ^{18}O)	ν(O–O) (Δ^{18}O)	
η^1	**L42a**	412 (480)	1122	–	–	144
η^1	**L44**	444 (3500)	1117 (28)	435 (20)	1218 (32)	126, 132, 133
η^1	**L44 + CF_3CO_2H**	382 (2600)	1149 (65)	–	–	123, 134
η^1	**L42b**	434 (3850)	1096 (67)	459 (17)	–	129, 135
η^1	**L42d**	416 (5400)	1120 (61)	474 (20)	–	145
η^1	**L41b**	418 (4300)	1121 (63)	472 (20)	–	136
η^1	**L41c**	409 (4250)	1121 (63)	474 (18)	–	127
η^1	**L41d**	410 (3700)	1130 (63)	482 (20)	–	130
η^1	**L68**	418	1117 (61)	460 (20)	–	137
η^1	**L41a**	–	–	–	1251 (33)	132
η^1	**L45**	–	–	–	1279 (29)	132
η^1	**L28a**	627 (1700)	1104 (60)	–	1182 (66)	128
η^1	**L33c**	397 (4200)	1033 (65)	457 (15)	–	131
η^1	**L75**	423 (1800)	964 (55)	–	–	146
η^2	**L39a**	352 (2330)	1112 (26)	–	1124 (31)	132, 147
η^2	**L39b**	–	1043 (59)	554 (20)	1040	138, 148
η^2	**L2d**	385 (2400)	968 (51)	–	–	149
η^2	**L2e**	–	961 (49)	–	1013 (28)	132, 150
η^2	**L2g**	415 (1780)	977 (49)	–	–	139
η^2	**L3b**	390 (7600)	974 (66)	–	1041	123, 140
η^2	**L74a**	~395	970(45)/992(67)	489 (14)	–	141
η^2	**L74b**	~395	970(45)/992(67)	494 (14)	–	141

Table 2

Selected Interatomic Distances in 1:1 Cu:O_2 Complexes

O_2^{n-} hapticity	ligand	distances (exp, Å)		distances (calc, Å)		ref
		Cu–O	O–O	Cu–O	O–O	
η^1	PHM enzyme	2.11	1.23	–	–	54
η^1	LPMO enzyme	–	–	1.98	–	142
η^1	**L44**	1.927(2)	1.280(3)	-	1.29	126, 132
η^1	**L41a**	–	–	–	1.28	132
η^1	**L45**	–	–	–	1.27	132
η^2	**L39a**	1.84(1)	1.22(3)	–	1.33	132, 147
η^2	**L39b**	–	–	1.88	1.36	138
η^2	**L4b**	–	–	1.890	1.366	143
η^2	**L2e**	1.821(5)	1.392(12)	1.86	1.38	132, 138, 151
η^2	**L3b**	1.826(2)	1.392(3)	–	–	140

Table 3

Selected Kinetic Parameters for the Formation of 1:1 Cu:O_2 Adducts

ligand (solvent)	k_{on} (M^{-1} s^{-1})	$\Delta H^{\ddagger}_{on}$ (kcal mol^{-1})	$\Delta S^{\ddagger}_{on}$ (cal mol^{-1} K^{-1})	k_{off} (M^{-1} s^{-1})	$\Delta H^{\ddagger}_{off}$ (kcal mol^{-1})	$\Delta S^{\ddagger}_{off}$ (Cal mol^{-1} K^{-1})	ref
L2d (THF)	$(1.560 \pm 0.019) \times 10^{3}$[a]	4.3 ± 0.5	−23.9 ± 2.4	–	–	–	151
L23a (acetone)	4.1×10^{7}[b]	−1.6 ± 0.2	−31 ± 1	2.4×10^{-2}[b]	10.5 ± 0.5	−11 ± 2	164
L42a (EtCN)	$(9.5 \pm 0.4) \times 10^{4}$[b]	4.1 ± 0.1	−12.4 ± 0.7	$(7.0 \pm 0.3) \times 10^{-2}$[b]	14.8 ± 0.1	18.2 ± 0.7	144
L44 (MeTHF)	$(2.1 \pm 1.0) \times 10^{6}$[c]	2 ± 1	−17 ± 6	$(5.2 \pm 2.0) \times 10^{2}$[c]	11 ±2	10 ± 8	160
L41a (THF)	$(1.5 \pm 0.02) \times 10^{8}$[c]	1.82	−10.8	240 ± 6[c]	13.9	25.1	163
L41d (MeTHF)	$(6.6 \pm 3.5) \times 10^{5}$[c]	2.2 ± 0.2	−23 ± 2	–	–	–	160
L43c (THF)	$(6.9 \pm 0.02) \times 10^{7}$[c]	7.67	19.1	470 ± 0.02[c]	15.9	37.5	161
L40a (THF)	$(1.8 \pm 0.03) \times 10^{8}$[c]	5.59	8.39	1600 ± 0.05[c]	15.4	35.9	161
L36 (THF)	$(7.6 \pm 0.2) \times 10^{-1}$[b]	5.83 ± 0.31	−26.3 ± 1.7	$(1.1 \pm 0.1) \times 10^{-3}$[b]	8.10 ± 0.26	−3 ± 1	162

[a] At 223 K.

[b] At 183 K.

[c] At 193 K.

Table 4

Selected Thermodynamic Parameters for the Formation of 1:1 Cu:O_2 Adducts

ligand (solvent)	K_{eq} (M^{-1})	$\Delta H°$ (kcal mol^{-1})	$\Delta S°$ (cal mol^{-1} K^{-1})	ref
L42a (EtCN)	$(1.35 \pm 0.04) \times 10^{6}$ [a]	−10.73 ± 0.05	−30.6 ± 0.2	144
L44 (MeTHF)	$(6.3 \pm 1.9) \times 10^{3}$ [b]	−9.6 ± 0.5	−32.0 ± 2.6	160
L41a (THF)	$(6.5 \pm 0.02) \times 10^{5}$ [b]	−11.6	−33.5	163
L43c (THF)	$(1.5 \pm 0.06) \times 10^{5}$ [b]	−8.22	−18.5	161
L40a (THF)	$(1.1 \pm 0.03) \times 10^{5}$ [b]	−9.82	−27.2	161
L36 (THF)	$(7.0 \pm 0.1) \times 10^{2}$ [a]	−2.27 ± 0.07	0.614 ± 0.382	162

[a] At 183 K.

[b] At 193 K.

Table 5

Selected Spectroscopic Data for $[CuOOH]^+$ and $[CuOOR]^+$ Complexes

copper core	ligand	UV–vis	Raman (exp, cm^{-1})[a]				Raman (calc, cm^{-1})	ref
		λ_{max} (nm) (ε, M^{-1} cm^{-1})	ν(O–O)	ν(Cu–O)	ν(C–O)/ν(C–C)	ν(O–C–C)/ν(C–C–C)	ν(O–O)	
$[CuOOH]^+$	**L83**	325 (6414)	822 (41), 836 (45)	–	–	–	–	203
	L38e	350 (3400)	834 (42)	–	–	–	–	204
	L41e	375 (700)	860 (45)	–	–	–	–	205
	L70b	374 (2589)	880 (11)	–	–	–	896	193
	L40b	~380	851 (46), 835 (46)	–	–	–	–	206
	L43a	381 (1000)	853 (46)	–	–	–	–	207
	L43b	372 (1000)	848 (45)	–	–	–	–	207
	L39a	604 (1180)	843 (26)	624 (17)	–	–	–	208
	L66	357 (4300)	881 (49)	–	–	–	–	209
	L45	332 (4240)	851 (56)	–	–	–	–	196
	L33c	375 (1650)	831 (43)	–	–	–	–	174
	L35a	345 (5000)	900 (50)	580 (25)	–	–	953	179
	L42a	375 (1250)	846 (48)	509 (25)	–	–	854	190
	e-His-Gly-His	366 (2600)	–	–	–	–	–	202
	L85	380 (2000)	–	–	–	–	–	187
$[CuOOR]^+$[b]	**L39c**	572 (3815)	844 (26)	652 (19)	802 (26)/755 (6)	555 (10)/540 (4)	–	208
	L39a	603 (5410)	843 (26)	645 (16)	809 (28)/756 (4)	551 (8)/536 (7)	–	208
	L39a[c]	610 (5000)	884 (24)	640 (27)	834 (37)/754 (15)	471 (6)	–	208
	L18b[d]	420 (1350)	855 (30)	545 (20)	823 (20)/792	(7) –	901	180
	L18d	465 (1100)	885 (30)	608 (11)	841 (33)	529 (5)/485 (9)	–	185
	L42a	440 (280)	887 (82)	–	839 (34)	–	845	190
	L69	465	887 (89)	610 (7)	827 (33)	–	–	192
	L42c	396 (5400)	831 (43)	604 (15)	–	569 (11)/541 (10)	833	194
	L41a[e]	332 (950)	–	–	1740 (C=O)	–	–	210
	L39c[e]	–	–	–	1640 (C=O)	–	–	210

[a] $D^{18}O$ indicated in parentheses.

[b] R = *Cm*, except where indicated.

[c] R = *t*Bu.

[d] 2-Hydroxy-2-peroxypropane complex **13**.

[e] R = acyl.

Table 6

Properties of Heterobimetallic LCu-(μ-O)$_2$-M Complexes

compound	L	M	solvent	UV–vis λ_{max} (nm) (ε, M^{-1} cm^{-1})	Raman (exp, cm^{-1}) ν($CuMO_2$) (^{18}O)	ref
73a	**L4c**	$Pd(PPh_3)_2$	THF	448 (5900)	660 (631)	334
73b	**L4c**	$Pt(PPh_3)_2$	4:1 CH_2Cl_2:THF	450 (5600)	628, 613 (594)	334
73c	**L10a**	$Pd(PPh_3)_2$	CH_2Cl_2	472 (2800)	610 (580)	334
73d	**L10a**	$Pt(PPh_3)_2$	CH_2Cl_2	483 (2700)	595 (569)	334
73e	**L6a**	$Pd(PPh_3)_2$	CH_2Cl_2	463 (3500)	640, 616 (600)	334
73f	**L6a**	$Pt(PPh_3)_2$	CH_2Cl_2	457 (3600)	647, 616 (603)	334
73g	**L20b**	$Pd(PPh_3)_2$	CH_2Cl_2	458 (2500)	630	334
73h	**L20b**	$Pt(PPh_3)_2$	CH_2Cl_2	462 (3000)	628 (601, 585)	334
71	**L2d**	Ni(**L81**)	THF	499 (8300)	625 (595)	167
74	**L23b**	Ni(**L2d**)	THF	895 (5000)	625 (595)	335
75	**L4c**	$Ge(N(SiMe_3)_2)_2$	toluene	440 (4400)	578 (559, 546)	168

Table 7

Properties of (1,2-Peroxo)dicopper Complexes

structure	ligand	solvent	UV–vis	Raman (exp, cm^{-1})		ref
			λ_{max} (nm) (ε, M^{-1} cm^{-1})	ν(O–O) (Δ^{18}O)	ν(Cu–O) (Δ^{18}O)	
trans	**L41a**	EtCN	525 (11,300), 615 (5800)	832 (44)	561 (26)	341
trans	**L41a**	MeTHF	525 (11,500), 615 (5800)	827	561	342
trans	**L78a**	THF	540 (9550), 610 (6500)	848 (47)	550 (26)	341
trans	**L42a**	acetone	552 (13,500), 600	825 (48)	–	144
trans	**L28a/L41a**	DMF/THF	624 (8300), 550	832 (44)	–	128
trans	**L31a**	MeTHF	618, 520, 450	811 (45), 801 (35)	547 (25)	200
trans	**L31a**	acetone		816 (48), 804 (36)	550 (20)	
trans	**L67**	MeTHF	445 (2150), 521 (8640), 615 (10,850)	817 (46)	545 (26)	342
trans	**L82**	MeTHF	442 (1500), 530 (8600), 605 (10,400)	828 (48)	547 (23)	343
trans	**L40a**	MeTHF	445 (2500), 535 (11,000), 610 (8100)	822 (46)	539 (26)	344
trans	**L40d**	THF	545, 620	835 (42), 821 (44)	542 (21), 504 (16)	345
trans	**L60**	acetone	478 (7800), 575–700(sh)	832 (45)	520 (22)	346
cis/*trans*	**L65b**	EtCN	506 (4800), 600 (2800)	803 (54)	512 (22)	354
cis	**L65a**	acetone	500 (3000)	799 (45)	437 (19)	353
trans	**L30**	CH_2Cl_2	508 (2000), 630 (1250)	837 (45)	571 (26)	348
trans	**L30**	toluene	513 (8300), 628 (5200)	–	–	348

Table 8

Properties of (1,1-hydroperoxo)dicopper Complexes

ligand	solvent	UV–vis	Raman (exp, cm^{-1})		ref
		λ_{max} (nm) (ε, $M^{-1}cm^{-1}$)	ν(O–O) (Δ^{18}O)	ν(Cu–O) (Δ^{18}O)	
L54	EtCN	407 (2700), 488 (1600), 622 (600)	870 (50)	–	355
L40f	MeCN	356 (6300), 580 (240), 664 (sh ~190)	868 (45)	572 (16)	357
L40e	MeCN	341 (~7000), 581 (~170), 770 (sh ~80)	883 (50)	562 (23)	357
L58b	MeCN	342 (8600), 444 (850), 610 (400)	–	–	358
L65b	MeCN	416 (5700), 373 (3300)	860 (46)	–	359
L53	acetone	370 (3700), 650 (300)	881 (49)	–	356